The University Of Sheffield.

Regulation of TGFβ/Smad Signalling During Early Follicle Development in the Mouse Ovary

Isam Bahnan Basheer Sharum

A thesis submitted in partial fulfilment of the requirements for the degree of Doctor of Philosophy

Academic Unit of Reproductive and Developmental Medicine
Department of Oncology and Metabolism
and
Department of Molecular Biology and Biotechnology

The University of Sheffield

September 2016

Contents

Acknowledgements

I would like to emphasise my appreciation to my main supervisor, Dr Mark Fenwick, for providing the opportunity to conduct my study in this interesting field of science. Throughout the past four years, Dr Mark Fenwick supported me with his unceasing encouragement, guidance and knowledge not only in science but also in my social life. Thanks to being patient with the proofreading of many drafts of my writing, your suggestions and comments were greatly helpful and critical; without your support, this work would not have been achieved. All of knowledge and skills that I learnt from you will assist me with my career and future researches.

Many thanks to my co-advisers 'Professors Alireza Fazeli and Alastair Goldman' for their generous support and advice, I would definitely not have progressed with my research without all of your endless encouragement. Many thanks to all staff members in the Academic Unit of Reproductive and Developmental Medicine for providing the excellent environment, equipment and facilities for my research. A warm thankfulness to my personal tutor 'Dr Andrew Chantry' for his constant encouragement.

Certainly, I would like to express a great acknowledgement to the past and present students in the unit for their friendship and support. A particular gratitude to my colleague Sofia Granados Aparici for her friendship and supportive ideas throughout my study. To Dr Sarah Elliott and Dr Sarah Waite, your support and technical advices throughout my study are appreciative. I am very grateful to Dr Paul R. Heath from SITraN for providing working apparatuses represented by the Bioanalyser and confocal microscopy. Many thanks to the Biological Services Unit for providing training and animals. I would like to acknowledge Dr Colin Gray (Microscopy Core Facility) for providing training on using fluorescent and confocal microscopy. Thanks to Ms Orla Gallagher (Bone Analysis Laboratory) for giving training on tissue processing and hematoxylin and eosin staining protocol.

I would like to express my deepest gratefulness to my wife 'Azhar' for her support and endless love, and to my gorgeous children 'David, Dina and Dylan' for the happiness you bring to us. An enormous grateful to my parents and brothers, for their constant love and support. My sincere appreciation to all friends and families of City Church in Sheffield for offering their praying and kindness.

I have financially supported by the Higher Committee for Education Development in Iraq (HCED), thanks to Iraqi government for providing this opportunity to make my dream to come true.

List of Figures

List of Tables

Abbreviation

ALK	Activin receptor-like kinases
AMH	Anti-Müllerian hormone
bFGF	Basic fibroblast growth factor
BMP	Bone morphogenetic protein
CBP	CREB binding protein
CDK	cyclin-dependent kinase
c-Kit	Cognate tyrosine kinase receptor
COCX	Cumulus-oocyte complexes
Co-Smad	Common mediator of Smad
CYP17a	cytochrome p-450 17alpha-hydroxylase
CYP19a1	Cytochrome p450 family 19 subfamily a 1
d4,d8,d16	Ovaries at day4, day8 and day16
DAP	3,3′-Diaminobenzidine
DAPI	4',6-Diamidino-2-phenylindole, dilactate
DMSO	Dimethyl sulfoxide
dpc	Days post-coitus
dpp	Days post-partum
ECM	Extracellular matrix
ERK	Extracellular signal-related kinase
FBS	Fetal bovine serum
FGCs	Female germline stem cells
FOXL2	Forkhead box L2
FoxO	Forkhead box protein
FSH	Follicle stimulating hormone
FSHR	Follicle stimulating hormone receptor
GCs	Granulosa cells
GDF9	Growth differentiation factor 9
Gn	Gonadotrophin
GS domain	Glycin serine domain

HDACs	Histone deacetylases
IgG	Immunoglobulin G
I-Smad	Inhibitory Smad
JNK	c-Jun N-terminal kinase
KGF	Keratinocyte growth factor
FGF7	Fibroblast growth factor 7
KL	Kit ligand
SCF	Stem cell factor
LAP	Latency-associated protein
LH	Luteinizing hormone
LIF	Leukaemia inhibitory factor
LLC	Large latent complex
LTBP	Latent TGFβ-binding protein
MAPK	Mitogen-activated protein kinase
NEDD4-2	Neural precursor cell expressed, developmentally down-regulated4-2
NF-kB	Nuclear factor of kappa light polypeptide enhancer in B-cells
Notch4ICD	Notch4 intracellular domain
Oo	Oocyte
PGCs	Primordial germ cells
PI3K	Phosphatidylinositol-4, 5-bisphosphate 3-kinase
PML	Promyelocytic leukaemia tumour suppressor
PND	Postnatal days
Ppm1a	Protein phosphatase Mg2+/Mn2+ dependent 1a
PTEN	Phosphatase and tension homolog deleted on chromosome 10
qPCR	Quantitative polymerase chain reaction
RanBP3	Ran-binding protein-3
R-Smad	Receptor-regulated Smad
RT-PCR	Reverse transcriptase-polymerase chain reaction
SARA	Smad-anchor for receptor activation
SBE	Smad binding elements

SCF	Stem cell factor
SD208	2-(5-Chloro-2-fluorophenyl)pteridin-4-yl]pyridin-4-yl-amine
siRNA	Small interfering RNA
Ski/SnoN	Ski-related novel protein N
SLC	Small latent TGFβ complex
Smurf	Smad ubiquitination-related factor
Strap	Serine-threonine kinase receptor associated protein
TGFβ	Transforming growth factor beta
TGFβRI	TGFβ type I receptor
TGFβRII	TGFβ type II receptor
Tmepai	Trans-membrane prostate androgen induced RNA
Unrip	Unr-interacting protein

Publication and conferences

Published Paper

1. IB. Sharum, S. Granados-Aparici, F. Warrander, F. Tournant and MA. Fenwick. Serine threonine kinase receptor associated protein regulates early follicle development in the mouse ovary. Reproduction 2016 Vol. 153, issue 2, 221–231.

Poster presentations

1. IB. Sharum and MA. Fenwick. Expression and localisation of TGFβ/ Smad signals and identification of potential inhibitors during early follicle development. 2nd Annual symposium of the Academic Unit of Reproductive and Developmental Medicine, Jessop wing, Sheffield, 23 Nov. 2012.
2. IB. Sharum and MA. Fenwick. Regulation of Smad signalling during early follicle development. Medical School Research meeting 17-18 June 2013.
3. IB. Sharum and MA. Fenwick. Expression and localisation of TGFβ/ Smad signals, and identification of potential inhibitors during early follicle development. 3ed Annual symposium of the Academic Unit of Reproductive and Developmental Medicine, Jessop wing, Sheffield, 22 Nov. 2013.
4. S. Granados-Aparici, IB. Sharum, K. Hardy, S. Franks, S. Waite, N. Chapman and MA. Fenwick. Foxl2 and Smad transcription factors during early follicle development: localisation and regulation of target genes. Annual Conference Society of Reproductive and Fertility SRF, Edinburgh, 1-2 September 2014.
5. IB. Sharum, S. Granados-Aparici, A. Fazeli, AS. Goldman and MA. Fenwick. Role of Serine Threonine Receptor-Associated Protein (Strap) in early follicle development. 4th Annual symposium of the Academic Unit of Reproductive and Developmental Medicine, Jessop wing, Sheffield, 21 Nov. 2014.
6. IB. Sharum, A. Fazeli, AS. Goldman and MA. Fenwick. Expression and localisation of TGFβ/ Smad signals and identification of potential inhibitors during early follicle development. The First HCED Iraq Scholars Conference, 29th May 2015 London, UK, MBG INT Ltd, Robinson Books Level 3 (378.198 HCE) (ISBN: 9780993042744 0993042740).

7. S Granados-Aparici, IB Sharum, K. Hardy, S. Franks, S. Waite, N. Chapman and MA. Fenwick. Regulation of CyclinD2 by Smad3 and Foxl2 during early follicle development. Annual conference Society of Reproductive and Fertility SRF, Oxford, 21 July 2015.
8. IB. Sharum, S. Granados-Aparici and MA. Fenwick. Serine/Threonine Kinase Receptor Associated Protein (Strap) inhibits early follicle development in mouse ovaries. Annual conference Society of Reproductive and Fertility SRF, Oxford, 21 July 2015. ***This poster was awarded the first prize.**
9. ZN. Sari, IB. Sharum, S. Granados-Aparici and MA. Fenwick. Identification and regulation of Pmepa1 during early follicle development in the mouse ovary. Poster presentation, Fertility Conference Edinburgh 2017.

Oral presentations

1. IB. Sharum and MA. Fenwick. Regulation of Smad signalling during early follicle development in the ovary. Medical School, University of Sheffield 2013.
2. IB. Sharum and MA. Fenwick. Identification and regulation of transmembrane prostate androgen-induced protein (Tmepai) in Mouse Ovary. Three minutes thesis presentation. 5th Annual symposium of the Academic Unit of Reproductive and Developmental Medicine, Jessop wing, Sheffield, 20 Nov. 2015.
3. IB. Sharum and MA. Fenwick. Identification of Serine/ Threonine Kinase Receptor Associated Protein (Strap) as a negative regulator of early follicle development in mice ovary. Medical School, University of Sheffield 13th July 2015.

Abstract

The molecular events responsible for the activation and growth of gonadotropin-independent stages of follicles are not well understood. This study is interested on the role of TGFβ signalling based on preliminary findings from our laboratory suggesting that this pathway is important in this context. Specifically, nuclear expression of the TGFβ signalling mediators and transcription factor Smad2/3 were more evident in the granulosa cells of primordial follicles but appeared to be excluded from nuclei in cells of early growing follicles. The overall aim of this thesis was to identify factors that have the potential to inhibit the Smad2/3 pathway and potentially determine their impact on early follicle development in the mouse ovary. Therefore, the first part of the study evaluated the expression of a selected of candidate genes (known to inhibit Smad signalling) during early follicle development.

Many Smad inhibitors were detectable, although serine-threonine kinase receptor associated protein Strap was further evaluated as its protein expression in granulosa cells of small follicles coincided with Smad2/3 staining. Neonatal mouse ovary fragments and preantral follicle culture models were employed to evaluate the function of Strap. Inhibition of Strap caused a significant reduction in the proportion of primordial follicles, leading to an increase in the proportion and size of growing follicles, while Strap supplementation promoted the growth of preantral follicles. Therefore, it is indicated that Strap can regulate the early follicle development in a stage-dependent manner and its function can be employed to expand our knowledge regarding several reproductive disorders, such as premature ovarian failure.

The expression of another Smad inhibitor, Tmepai, was also assessed and was found to be specifically localised in small preantral follicles that had just initiated growth. Since this coincided with the aforementioned reduction in nuclear Smad2/3, attempts were then made to determine whether TGFβ signalling regulated its expression. Inhibition of TGFβRI in cultured preantral follicles caused a significant decrease in *Tmepai* expression level. Thus, it is suggested that Tmepai can regulate TGFβ signalling in a negative feedback mechanism and consequently a relevant role in follicle growth. Finally, considering that TGFβ requires processing for their activity, and considering the evidence in this thesis and elsewhere that TGFβ signalling is important throughout the early stages of follicle development, we looked at the expression of the latent TGFβ binding proteins (Ltbp) in mouse ovaries.

Transcripts of *Ltbp1-4* were expressed in the immature and adult ovaries. Ltbp1 protein appeared to be more evident in the ovary surface, while Ltbp4 mainly detected in blood vessels. These distinct expression patterns might indicate that each Ltbp member functions in a diverse way.

In conclusion, this thesis presents a series of studies that show the essential role of TGFβ/Smad2/3 signalling in the regulation of early follicle development in the mouse ovary. The expression of many Smad2/3 inhibitors indicates that Smad pathway is regulated by a complex mechanism. Strap can regulate early follicle growth in a stage-specific manner. Tmepai is detectable in follicles with specific growth stages and regulated through TGFβRI receptor. The extracellular modulator of TGFβ ligands (*Ltbp1-4*) are expressed in the ovary, where their relative proteins localised in distinct compartments of the ovary.

Chapter 1

Introduction

1.1. Background

The fundamental role of the ovary is not only the secretion of steroid hormones, which are necessary for sexual maturation, the establishment of pregnancy and metabolism, but also to provide fully-grown oocytes for permitting the successful propagation of the species (Knight and Glister, 2003). It is proposed that the population of primordial follicles, small quiescent structures, present at birth reflects the entire number of follicles that are accessible to females throughout their reproductive lifespan (Bristol-Gould et al., 2006; Kezele et al., 2002). The percentage of these follicles is decreasing with age due to the continuous process of activation and atresia (Hansen et al., 2008); for example, in mouse ovaries, the percentage of primordial follicles decreases from 84% on day4 after birth to 51% at the age of 42 days, and these data varies depending on strain (Canning et al., 2003).

Over the past decades, details regarding factors that potentially activate some of the primordial follicles to grow have been described (Broekmans et al., 2009; Pangas, 2012). Prior to that, the focus of many investigations was in relation to the regulation of follicle growth by endocrine signalling pathways of the hypothalamic–pituitary–ovarian axis (Findlay et al., 2000; McGee and Hsueh, 2000). However, more recently, advances in molecular and genetic protocols have revealed that molecular processes are involved in the earliest stages of follicle development (Pangas et al., 2008; Wang et al., 2013). Thus, it has been suggested that the early stages of follicle growth or maintenance are regulated by interactions of locally secreted factors (Kim, 2012; Komatsu et al., 2015). Data from numerous laboratories have highlighted the role of the TGFβ superfamily members and their canonical Smad pathway as one of these essential intra-ovarian factors (Ding et al., 2010; Fenwick et al., 2013; Li, 2015; Tomic et al., 2004). TGFβ superfamily proteins are extracellular ligands which are widely expressed in the body tissues and are implicated in multiple cell activities including proliferation, differentiation, migration, and degeneration during both prenatal and postnatal life (Rahimi and Leof, 2007). Three types of functionally different TGFβ signalling components, called Smads, have been described. These include the receptor-regulated Smads (R-Smad; Smad1/2/3/5/8), common Smad (Co-Smad; Smad4), and the inhibitory Smads (I-Smad*;* Smad6/7), reviewed by (Lonn et al., 2009; Shi and Massague, 2003).

TGFβ signalling is initiating by the interaction between a particular activated TGFβ ligand with its specific transmembrane receptors (type I and II serine/ threonine kinase receptors) for activation by phosphorylation (Groppe et al., 2008). Following this, the R-Smads are recruited to interact with the TGFβ ligand/receptors complex for phosphorylation, which then allows complex formation with a Co-Smad (Inman et al., 2002).

Translocation of the R-Smad/Co-Smad complex into the nucleus is essential for regulation the expression of the target gene through interaction with various coactivator/repressor transcription factors (Ross and Hill, 2008; Schmierer and Hill, 2007). TGFβ signalling can also be inhibited by the I-Smads, where Smad6 can inhibit Bmp and Amh signalling (Bai et al., 2000), while Smad7 can inhibit TGFβ, activin, Gdf9 and with less affinity for the Bmp pathway (Chen et al., 2009). In the ovary, different TGFβ ligands that signal via Smad2/3 are shown to be involved with follicle development including the TGFβ isoforms (TGFβ 1-3), Activin, and Gdf9, while, others such as Bmp and Amh signal through the Smad1/5/8 pathway (Kaivo-oja et al., 2006; Li et al., 2008b). Importantly, this implicates the Smad family as regional modulators of different stages of follicle growth (Li et al., 2008b; Tian et al., 2010). In the ovary, TGFβ can also exert its biological effects through non-Smad pathways, such as MAPK, PI3K/AKT, Rho (Hough et al., 2012; Mu et al., 2012).

TGFβ/Smad signalling is regulated at different cell levels including extracellular regulation by the latent TGFβ binding proteins Ltbps (Su et al., 2015) and intracellularly (in addition to the I-Smads) by various Smad inhibitors such as Strap (Reiner and Datta, 2011) and Tmepai (Bai et al., 2014). Dysregulation of TGFβ/Smad signalling is associated with many pathological and reproductive disorders such as cancer (Fink et al., 2003), polycystic ovary syndrome (Hatzirodos et al., 2011) and ovarian failure (Pangas et al., 2006). In other tissues, additional TGFβ signalling inhibitors and suppressors have been recognised to implicate the cell physiology and pathology, such as *Ski/ SnoN* (Deheuninck and Luo, 2009), *Ppm1a* (Dai et al., 2011) and *Smurf1/ Smurf2* (Inoue and Imamura, 2008). Although TGFβ/ Smad signalling is active in the ovary, the expression and effect of such inhibitors on follicle development have not been defined yet. Therefore, initially, it is important to determine whether such factors are detectable in the ovary and then to further investigate their functional impact on follicle growth. Understanding molecular events that regulate the TGFβ signalling in follicles might be helpful to understand initial activation of primordial follicles or mechanisms that operate to maintain the quiescent state. Clinically, these regulators might be applicable for treatment of several causes of female infertility. For example, *in vitro* activation of primordial follicles, prevention of early follicle depletion, or to maintain the quiescent state of primordial follicles during treatments of cancer. This chapter provides information on mechanisms and factors that are implicating in the early follicle development. Particular attention is focussed on the TGFβ/Smad signalling compartments, its extracellular and intracellular regulators.

1.2. Mouse models for studying the ovarian function

In women, exposure to various factors, such as anti-cancer treatments, some medicines, and environmental pollutants can negatively affect the function of the ovary and can promote exhaustion of the follicle reserve leading to a decrease in fertility (Tilly, 2003). The mouse has been widely used to understand both the physiological or pathological factors that affect follicle and ovary development in women. For example, genetically modified mice were generated to study ovarian cancer in women (Fong and Kakar, 2009), also female mice were utilised to determine how dietary intakes can affect both the ovary function and reproductive lifespan (Nehra et al., 2012). Unlike ovaries from larger mammals, the small size of rodent ovaries has been widely exploited for the purposes of whole organ culture (Drummond et al., 2003; Eppig and O'Brien, 1996). In addition, postnatal mouse ovaries have been considered as a valuable system to investigate the role of different factors that implicated in the regulation of the primordial follicle development since the majority of follicles at this time are non-growing (Jin et al., 2010). It has been shown that ovary culture conserves the physiological interactions not only among follicles of different stages of development but also between follicles (Abdi et al., 2013). Over the last two decades, genetically modified mouse/ovary models have been extensively used to understand an essential information on the molecular mechanisms regulating primordial follicle growth (Reddy et al., 2008; Zheng et al., 2012).

Likewise, preantral follicle cultures have been developed where encapsulation of cultured follicle with materials such as alginate hydrogel and fibrin-alginate gel provides support of follicle growth by maintaining the crosstalk between oocytes and the surrounding cells (Jin et al., 2010; Pangas et al., 2003). In addition, whole ovary culture and co-culture systems have been described (Morgan et al., 2015). More recently, ovary fragments culture model have been used to identify the effect of exogenous treatments on early follicle development (Komatsu et al., 2015). Studies have also highlighted the usefulness of an *in vivo* ovary transplantation model to study follicle growth where mouse ovaries are maintained under the kidney capsule to recapitulate normal environmental conditions of follicle growth compared to *in vitro* culture models (Wang et al., 2013).

1.3. Follicle formation

Follicle formation requires three essential steps, firstly, formation and migration of primordial germ cell during embryogenesis, secondly, the formation of oogonia clusters in the ovary, and thirdly, the formation of individual primordial follicles (Pepling, 2006) . In the mouse ovary (Figure 1.1), the ovarian primordial germ cells (PGCs) originate around 6.5-7.5 days post coitus (dpc) of embryonic life in the extraembryonic mesoderm (Lawson and Hage, 1994; Saitou and Yamaji, 2012). PGCs migrate between 10-11 dpc to the genital ridge where they continue to multiply by mitosis to produce oogonial clusters (germ cell cysts) (McLaren, 2000). Then, oogonia embark on the early stages of meiosis, at approximately 13.5 dpc, to form oocytes (Pesce et al., 2002). From 17.5dpc to the 5th day after birth (continued arrested until ovulation), most oocytes become arrested at the diplotene phase of meiotic prophase I. From this stage, cyst breakdown occurs and oocytes become enclosed by a number of flattened precursor granulosa cells to generate primordial follicles (Hirshfield, 1991; McGee and Hsueh, 2000; Pepling and Spradling, 2001).

Kit ligand (Stem Cell Factor, SCF) is detectable in prenatal mouse ovaries from 16.5dpc and it is proposed that Kit signalling has an essential impact on the rate of cyst breakdown by preventing apoptosis of oocytes during the assembly of primordial follicles (Jones and Pepling, 2013). Culturing neonatal rodent ovaries with Kit protein supplemented media promotes primordial follicle formation, whereas immunoneutralisation by Kit antibody reduces the number of follicle formations (Wang and Roy, 2004).

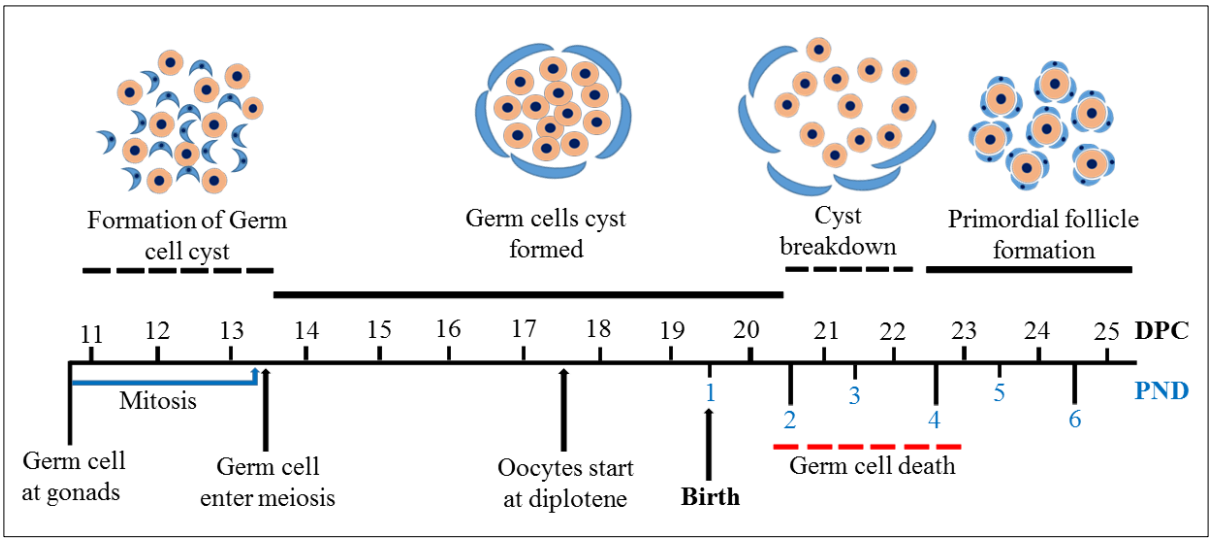

Figure 1.1. Overview of primordial follicle formation in the mouse ovary. The generation of germ line cyst occurs when the primordial germ cells (circle shapes) reaches the genital ridge after 10.5 days post-coitus (dpc). Some germ cells inside the germ cyst initiate meiosis at 13.5 dpc; then, at 17.5 dpc, a portion of oocytes become arrested at the diplotene stage. Breakdown of germ cysts and invasion of pre-granulosa cells (blue shapes) occurs shortly after birth, thus, each individual oocyte forms a primordial follicle; however, a substantial of oocytes loss occurs around this time, adapted from (Pepling, 2006).

An additional group of growth factors called neurotrophins are also essential for primordial follicle formation. For example, mutation of neurotrophic tyrosine kinase receptor type 1 (NTRK1) in mouse ovaries revealed a reduction in the number of primordial follicles with a high proportion of oocytes still enclosed in germ cell cysts (Dissen et al., 2001; Kerr et al., 2009). Other examples of growth factors that signal through NTRK2 receptors are brain-derived neurotrophic factor (BDNF) and neurotrophin 4 (NT4). Inhibiting the function of either BDNF or NT4 in cultured mouse ovaries causes an increase in the percentage of degenerative oocytes (Spears et al., 2003). Interestingly, a mutation in the signalling receptor (NTRK2) led to a decrease in the number of oocytes accompanied by a reduction in primordial follicle formation (Kerr et al., 2009).

TGFβ superfamily members are also involved in primordial follicle formation; for instance, in mice, deletion of bone morphogenetic protein 15 (*Bmp15*) or growth differentiation factor 9 (*Gdf9*) caused incomplete cyst breakdown manifested by substantial increases in the population of follicles containing more than one oocyte (Yan et al., 2001). Similarly, overexpression of inhibinα, an activin antagonist, also leads to increased numbers of the primordial follicle with multiple oocytes, suggesting the importance of activin in follicle formation (McMullen et al., 2001). In the rat ovary, incubation of immature ovaries with TGFβ1 led to a reduction in the formation of primordial follicles; however, populations were increased in ovaries treated with

either connective tissue growth factor CTGF, or with a combination of TGFβ1 and CTGF. These outcomes indicated the essential role of CTGF in both primordial follicle formation and the size of primordial follicle pool (Schindler et al., 2010). In endothelial cells, CTGF is identified as an extracellular protein that can directly associate with signalling molecules cooperates in various functions such as tissue healing and extracellular matrix formation (Brigstock, 2002). *In vitro* and *in vivo* studies showed that steroidal hormones, such as oestrogen and progesterone can impair both cyst breakdown and oocytes degeneration indicating the importance of maternal endocrinal system in primordial follicle formation (Chen et al., 2007; Kezele and Skinner, 2003).

Before the formation of individual follicles, a high proportion of oocytes undergo apoptosis (Hirshfield, 1991; Kim, 2012). Apoptosis of primordial germ cells or oocytes is characterised by morphological changes including nuclear condensation, loss outer membrane integrity, shrinking, and subsequently cellular death (Pesce and De Felici, 1994). It is suggested that genetic abnormalities or unsuccessful generation of some cellular compartments of the germ cell, such as the mitochondria, might explain oocyte death during cyst breakdown (Hunt and Hassold, 2002). It has also been proposed that oocyte degeneration not only acts as a nursing resource for the remaining oocytes (Lei and Spradling, 2016), but also, to provide space for somatic precursor granulosa cells to enclose each individual oocyte (Pepling and Spradling, 2001). In addition, others have proposed the importance of the programmed cell death as a mechanism to eliminate inadequately formed cells, which might affect the well-formed cells (Tingen et al., 2009). Primordial germ cells and oocytes can degenerate either before or after being enclosed by somatic cells (pre-granulosa cells). Degeneration of either structure prior to primordial follicle formation is called attrition; however, the term atresia is generally referred to the degeneration of the completely formed follicle (Hsueh et al., 1994).

In mice, the primordial follicles initially form in the ovarian medulla from 17.5 dpc; however, according to the mouse strain, the process of primordial follicle formation in the ovarian cortex might be delayed until the postpartum period between 5^{th} to 8^{th} dpc (Pepling, 2012). In humans, the period of primordial follicle formation is initiated from the 4^{th} month of gestation and ends by the time of parturition, where a portion of primordial follicles start to grow while the majority remain quiescent (Gougeon, 1996). In humans, a constant reduction in the population of small follicles from approximately 500,000 at birth to less than 1,000 follicles at menopause (Hansen et al., 2008). In mice, it has indicated that ovaries at 6dpp contain more than 10,000 primordial follicles and this number declines to less than 3,000 at the age of 45 days (Bristol-Gould et al., 2006).

Another study on four different mouse strains aged between d4 and d42, revealed significant difference between groups in the population of primordial follicles and also the rate of follicle loss at both time points, suggesting that the number of primordial follicles in the ovary and rate of follicle atresia are largely dependent on the strain (Canning et al., 2003).

1.4. Regeneration of oocytes

It is generally accepted that the population of primordial follicles at birth is the only source of follicles for the entire reproductive lifespan and new oocytes/follicles cannot be generated after this time (Kezele et al., 2002; Kezele and Skinner, 2003; McGee and Hsueh, 2000). In mice ovary, attempts were applied to extend the reproductive lifespan by increasing the population of primordial follicles; however, it has found that even in this context, the ovary was able to minimise the size of the artificially increased ovarian reserve (Flaws et al., 2001; Tingen et al., 2009). However, within the last decade, several reproductive biologists have challenged this concept and indicated the possibility of oocyte generation from stem cells that can develop into primordial follicles, reviewed by (Oktay and Oktem, 2007; Zhang et al., 2013). Initially, a study has proposed that mouse primordial follicles can develop (77 follicles/ovary each day) in postnatal ovaries from oogonial stem cells; the study stated that these cells are located in the ovary epithelium and are positive for Ddx4, a marker of germline cells and oocytes (Johnson et al., 2004). The authors later altered their assumptions about the positive staining of oogonial stem cells for Ddx4, stating that these cells were originally derived from the blood and bone marrow rather than ovary (Johnson et al., 2005).

More recently, female germline stem cells (FGCs) were obtained from postnatal mouse ovaries (5dpp) processed by a long series of cultivation, purification, and isolation. Then, FGCs were transplanted into ovaries of infertile adult female mice where these cells underwent oogenesis and offspring were successfully obtained (Zou et al., 2009). Similar outcomes were presented after isolating oogonial stem cells OSCs obtained from adult mouse ovarian cortical tissue from women, where oocytes of 35-50μm were generated (White et al., 2012).

Despite these findings, other have tried to confirm the possibility of postnatal oogenesis after exposure to radiotherapy; however, both adult and postnatal ovaries from the treated mice failed to show any signs of follicle renewal (Kerr et al., 2012). The concept of neo-oogenesis would be tremendously significant, since nowadays, infertility due to the ovarian ageing is more prevalent among women. The main reasons for this are related to social aspects such as development of careers and increased education level. In addition, increased patient survival after anti-cancer treatments, or due to pathological, physiological, and genetics causes, which

promotes premature ovarian failure (Jeruss and Woodruff, 2009) means that the primordial population of these women would be further compromised.

1.5. Follicle classification

Follicles can generally be categorised into three sections (Figure 1.2). Firstly, gonadotropin (Gn)-independent, lasts from the generation of primordial follicles to the secondary phase in which follicle growth is modulated via various intra-ovarian growth factors (Edson et al., 2009; Orisaka et al., 2009). Secondly, 'gonadotrophin- responsive' ranges from the secondary to the small antral, where the follicles will react to the hormonal effects, but do not depend on them for development (Picton et al., 2003; Scaramuzzi et al., 2011). Thirdly, during the gonadotrophin- dependent stage, follicle growth (from small antral to large antral) is supported by FSH and the LH surge and the interaction between somatic cells and oocyte (Eppig, 2001; Orisaka et al., 2009).

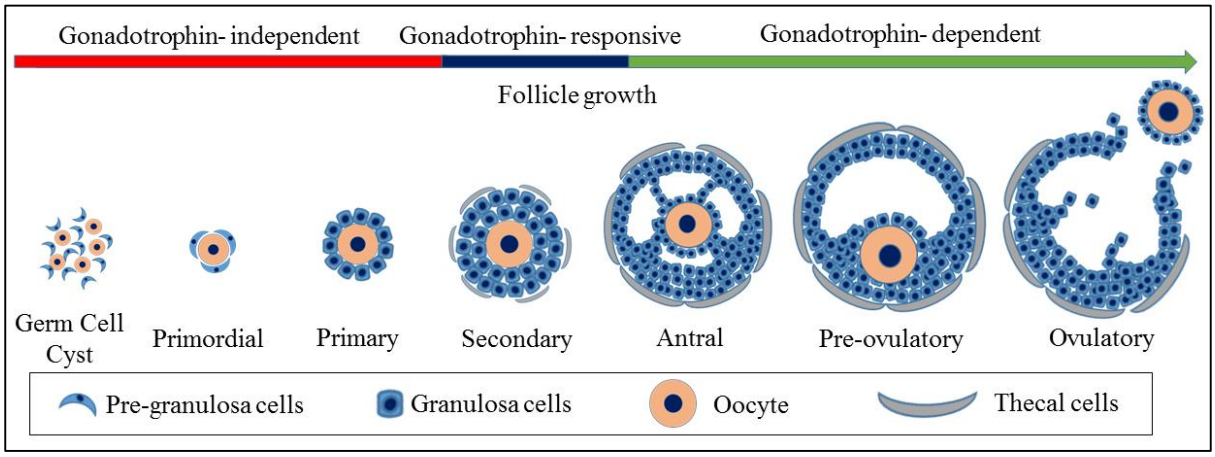

Figure 1.2. Stages of mammalian follicle development. Throughout the gonadotrophin-independent stage, primordial follicles originate from primordial germ cells surrounded by pre-granulosa cells. Development of primordial follicles into the primary stage is thought to be regulated by growth factors, manifested by increased oocyte size, morphological changes of flattened pre-granulosa cells into cuboidal and granulosa cell proliferation. The progression of primary follicles to secondary follicles includes further growth of the oocyte, proliferation of the granulosa cells to form a second layer, and development of the theca cells. Development of the later stages is largely dependent on gonadotrophin including follicle stimulating hormone FSH and luteinizing hormone LH where follicle are recognised by a larger size, more granulosa cell layers, and the development of antrum, after which, follicles either ovulate or undergo atresia, adapted from (Edson et al., 2009).

1.6. Primordial follicle activation

Activation of the primordial follicle to initiate the growth process is an essential step of follicle development. Even though many studies focused on this process, the mechanisms or factors that regulating follicle activation are still not well understood (Edson et al., 2009; Kim, 2012). Activation of primordial follicles is thought to be continuous and irreversible, and follicles that initiate growth either continue growing towards ovulation or degenerate by atresia (Edson et al., 2009; Scaramuzzi et al., 2011). The transition from primordial to primary growth stage is characterised by an increase in oocyte size, morphological change of granulosa cells from flattened to cuboidal and increases the number of granulosa cells.

Before puberty, a portion of the primordial follicles are activated to grow; however, these follicles later undergo atresia because of insufficient levels of pituitary gonadotropins (Hirshfield, 1992). In mouse ovaries, the majority of non-growing primordial follicles are distributed in the marginal region underneath the ovarian surface, while growing follicle are mainly localised in the medulla of the ovary (Byskov et al., 1997; Da Silva-Buttkus et al., 2009) (Figure 1.3).

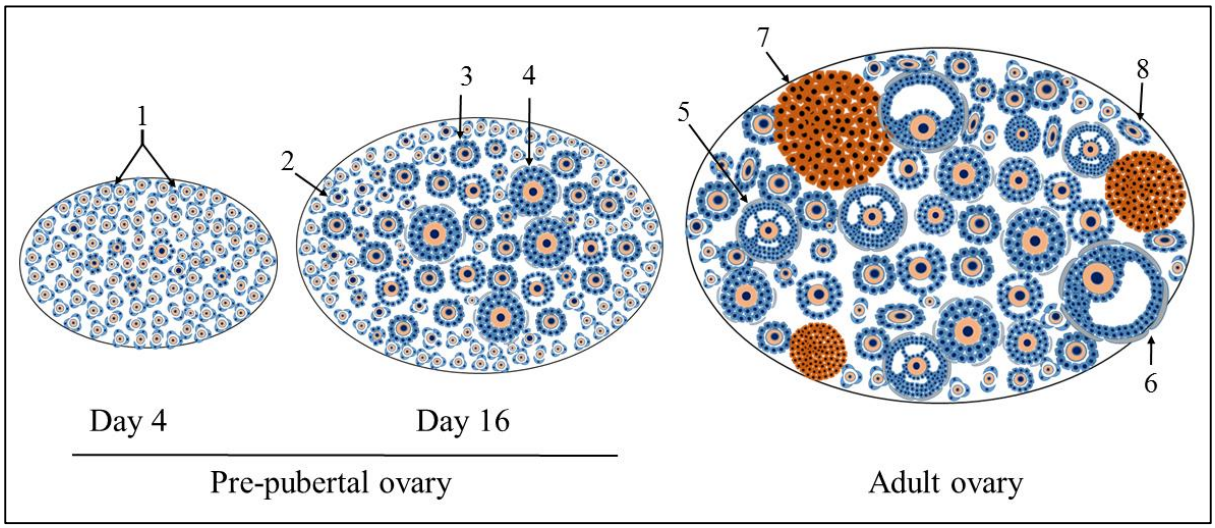

Figure 1.3. Distribution and types of follicles in pre-pubertal and adult mouse ovaries. The majority of follicles in the day 4 ovary are primordial follicles (1) with several transitional follicles (2) that have initiated growth. By day 16, more primordial follicles are activated to grow to the primary (3) and secondary (4) stages, mostly located in the medulla, while the peripheral region of the ovary is still dense with primordial follicles. In the adult ovary, due to the advances in follicle growth, other ovary structures can recognise including small (5) and large (6) antral follicles, corpora lutea (7) and atretic follicles (8) are evident, while the population of primordial follicles is noticeably reduced.

Many hypotheses and mechanisms have been proposed to explain why particular primordial follicles are activated to grow while others remain in a dormant state; for example, it has been proposed that primordial follicles located close to growing follicles are more likely to be activated than others situated among a group of non-growing follicles. This statement indicates a significant growth inhibitory effect of primordial follicles on each other (Da Silva-Buttkus et al., 2009). Others suggested that oocytes of growing follicles might produce growth factors that stimulate or enhance the growth of the adjacent primordial follicle, such as *Gdf9* (Pangas, 2012), and bone morphogenetic proteins *Bmp15* (*Gdf9b*) (Knight and Glister, 2006). In contrast, some of the TGFβ superfamily members were suggested to have an inhibitory impact on the activation of primordial follicles preventing them from growing, such as Anti-Mullerian Hormone (Amh), which is secreted from granulosa cells of growing preantral follicles (Durlinger et al., 2002). Despite this evidence, it should also be noted that in cultured neonatal mouse ovaries, where the source of Amh secretion is absent, a portion of primordial follicles still remain dormant (Jin et al., 2010). In humans, treatment of ovary fragments with human recombinant Activin A protein (50ng/ml) demonstrated a considerable decrease in the proportion of the activated primordial follicle relative to untreated control, with no impact on follicle atresia (Ding et al., 2010).

Other TGFβ superfamily members have also been directly implicated in primordial follicle activation; for example, treatment of immature (2dpp) mouse ovaries with rhBmp7 protein revealed an increased transition rate of primordial follicles into primary staged follicles accompanied with upregulation of *Fshr* expression supporting further follicle growth (Lee et al., 2004). Similarly, in postnatal rat ovaries, treatment with Bmp4 protein resulted in increased primordial to primary transition with a corresponding increase in ovary size. In contrast, massive oocyte degeneration, decreased primordial to primary transition and small ovary size after immunoneutralisation of Bmp4 (Nilsson and Skinner, 2003).

The bi-directional interaction between the granulosa cells and the oocyte is essential for the process of primordial follicle activation (Eppig, 2001; Kezele et al., 2002). For example, *in vitro* studies revealed that kit ligand (KL) and its receptor c-kit, has a key role in primordial follicle activation; treatment of cultured neonatal rodent ovaries by KL antibody caused inhibition of primordial follicle activation (Reynaud et al., 2001; Wang and Roy, 2004). It has been identified that granulosa cells are responsible for the production of KL, which can promote oocyte growth (Kezele and Skinner, 2003). KL increases the expression of androgens by stimulating the growth of both stromal and theca cells (Parrott and Skinner, 2000).

KL also activates the cell proliferative kinase pathways, such as PI3K/AKT, which are important component regulators of oocyte growth by inactivation of Foxo3a (Accili and Arden, 2004). *Foxo3a* is a member of forkhead box (Fox) subfamily that has a critical role in female fertility. During primordial follicle assembly, Foxo3 is expressed in the nucleus of the oocyte; however, as the follicle starts to grow, Foxo3 translocate into the cytoplasm, indicating that the nucleocytoplasmic translocation of Foxo3 is associated with follicle growth (John et al., 2008). Mice lacking Foxo3a in their oocytes exhibited loss of their reproductive efficiency followed by infertility manifested by enlarged ovaries due to the increased number of activated follicles accompanied with early depletion of primordial follicles from the ovary (Castrillon et al., 2003). Interestingly, during the process of primordial to primary follicle transition, pre-granulosa cells change their morphology from a flattened or squamous to cuboidal shape (Hirshfield, 1991).

Forkhead box protein L2 (*Foxl2)* is mainly expressed in pre-granulosa cells of primordial follicles being significantly decreased in granulosa cells of growing follicle (Uda et al., 2004). This transcription factor also belongs to the Fox family and is not only essential for granulosa cell differentiation and proliferation, but also in the determination of female gender (Uhlenhaut and Treier, 2011). *Foxl2* null mice exhibits primordial follicles with a normal morphology; however, as these follicles start to grow their pre-granulosa cells fail to cuboidalise while oocytes continue to grow prematurely and become surrounded by several undeveloped granulosa cells indicating that Foxl2 is a regulator of granulosa cell growth (Schmidt et al., 2004). The role of PI3K pathway on primordial follicle development and apoptosis was determined using genetically modified ovary models; for example, the basic level of PI3K is essential to keep the quiescent state of primordial follicles (Zheng et al., 2012).

In mouse ovaries, stimulation of PI3K pathway by blocking the inhibitory effect of PTEN, a PI3K pathway inhibitor, leads to premature activation of a high proportion of primordial follicles followed by early ovarian failure, indicating that PTEN is a negative regulator of primordial follicle activation (Reddy et al., 2008). However, suppression or inhibition of the PI3K pathway causes pathological conditions manifested by a high apoptosis rate in primordial follicles, suggesting that the PI3K pathway participates in cell survival and disruption of this pathway might cause premature ovarian failure and infertility (Reddy et al., 2009) (Figure 1.4).

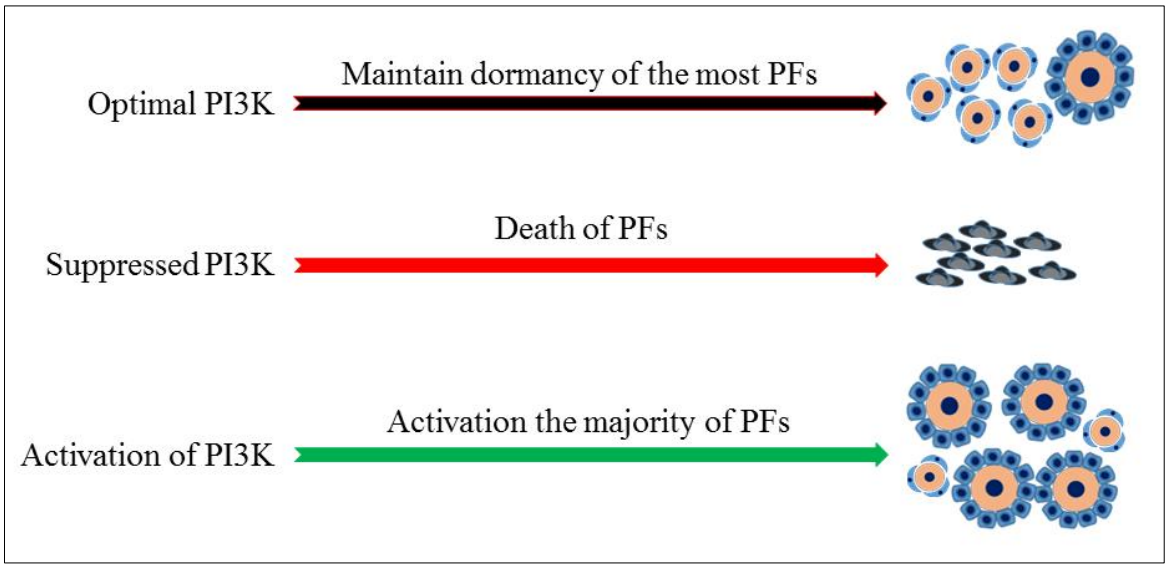

Figure 1.4. Effect of modulated PI3K pathway on primordial follicle growth and survival. In the ovary, the optimal level of PI3K signalling is required to maintain the majority of primordial follicles (PFs) in an inactive state. Inhibition of PI3K signalling causes substantial death among primordial follicles. In contrast, activation of PI3K signalling causes massive activation of primordial follicle growth and depletion of the primordial follicle pool. Adapted from (Reddy et al., 2009).

In rat ovaries, basic fibroblast growth factor (bFGF) has been localised in the oocytes of growing follicles (Ergin et al., 2008) and in granulosa and theca cells of growing follicles in human ovaries (Yamamoto et al., 1997). Throughout the process of primordial to primary follicle transition, bFGF function in the activation of stromal, granulosa and theca cell development. Supplementation of bFGF to cultured neonatal rat ovaries led to decreases in the number of primordial follicles accompanied with a significant increase in the population of growing follicles (Nilsson et al., 2001b). In the immature rat ovary culture, leukaemia inhibitory factor (LIF) was also found to cause a considerable increase in the percentage of growing follicles and a decline in the percentage of primordial follicles, particularly in the presence of insulin. By contrast, immunoneutralisation using anti-LIF antibodies revealed a moderate reduction in follicle activation (Nilsson et al., 2002). However, in mice, a recent study indicated that treatment of the cultured ovary fragments with anti-LIF antibodies enhanced follicle growth, while supplementation of rLIF protein caused inhibition the growth of growing follicles (Komatsu et al., 2015). Keratinocyte growth factor (KGF), also called fibroblast growth factor 7 (FGF7), is expressed in oocytes of primordial follicles, granulosa cells, and stroma cells in human ovaries (Abir et al., 2009). FGF7 exerts positive growth effects on the adjacent pre-granulosa and granulosa cells and therefore enhances the process of primordial to primary follicle transition (Nilsson and Skinner, 2003) (Figure 1.5).

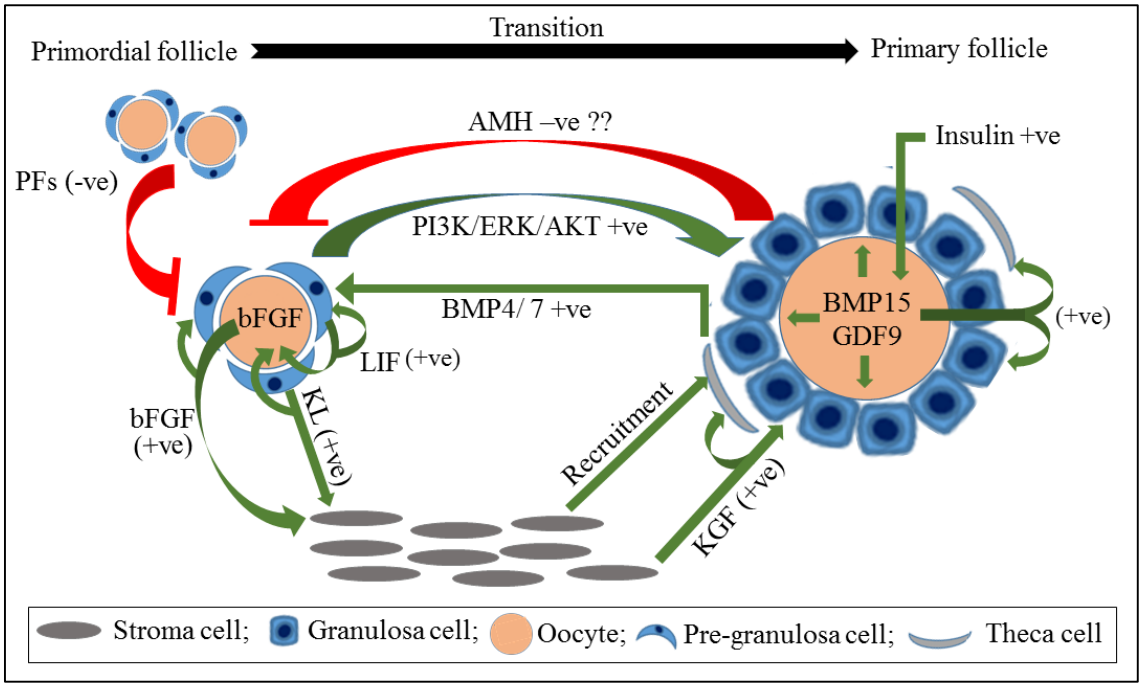

Figure 1.5. Several factors influencing primordial follicle activation and transition. Primordial follicle (PF) activation and transition to the primary stage are regulated by the cooperative interaction of various growth factors produced either by the oocyte (bFGF, GDF9 and Bmp15), the surrounding pre/granulosa cells (LIF, KL and AMH), stroma cells (KGF) or from circulation (Insulin). Neighbouring primordial follicles influence activation of the primordial follicle. Several pathways function to enhance cell proliferation such as PI3K, AKT and ERK resulting in increased primordial follicle activation. Adapted from (Knight and Glister, 2006).

1.7. Overview of the transforming growth factor TGFβ superfamily

TGFβ superfamily proteins are extracellular ligands extensively expressed throughout the body and are implicated in many physiological activities including proliferation, differentiation, migration, and cell degeneration during both pre-and postnatal life (Rahimi and Leof, 2007). TGFβ superfamily members are structurally related and consist of more than 40 members including TGFβ (β1, β2 β3), Activin (A, B and AB), Inhibin (A and B), Growth differentiation factor (Gdf9), Bone Morphogenetic Proteins (Bmps1-15), Anti-Müllerian Hormone (Amh), Nodal and Lefty (Drummond et al., 2003; Pangas, 2012). Briefly, all of the TGFβ ligands can signal through a heteromeric serine/threonine kinase receptor complex, which in turn activates the cytoplasmic Smad mediators by phosphorylation (Shi and Massague, 2003; ten Dijke and Hill, 2004). Activated Smads interact with another type of Smad (Smad4) to enhance their translocation to the nucleus where target gene transcription occurs (Brown et al., 2007; Moustakas and Heldin, 2008). The third type of Smad (I-Smads) can attenuate or inhibit the signalling pathway at different levels (Goto et al., 2007; Yan and Chen, 2011).

In the ovary, modulation of TGFβ signalling is associated with activation of primordial follicles (Ding et al., 2010), impaired follicle growth (Li, 2015) or the development of pathological phenotypes (Pangas et al., 2008).

1.7.1. Functional role of the TGFβ superfamily in the ovary

Over the last two decades, many studies have investigated the role of the TGFβ superfamily in the regulation of follicle growth (Knight and Glister, 2006; Pangas, 2012). In mice, knockout of TGFβ1 delayed sexual maturity and disruption ovarian function (Ingman et al., 2006). In cows, TGFβ1-3 proteins are expressed in oocytes of primordial and growing follicles, TGFβ2 and β3 in granulosa cells of all developmental follicle stages, while TGFβ1 is exclusively localised in the granulosa cells of primordial to early antral follicles (Nilsson et al., 2003).

Bmp proteins, such as Bmp4 and Bmp7 are thought to be essential for the primordial to the primary follicle transition in rodents (Ding et al., 2013; Shimasaki et al., 2004). Immunostaining of juvenile rat ovaries indicated that Bmp4 is detectable in precursor theca cells (Nilsson and Skinner, 2003). Passive immunisation of mice with anti-Bmp4 (50μg) for 7 days revealed a significant reduction in primordial to primary follicle transition accompanied with reduced ovary size (Tanwar et al., 2008). In neonatal rat ovaries, *in vitro* treatment with anti-Bmp4 IgG demonstrated similar outcomes with less activation of primordial follicles and a significant increase in oocyte apoptosis. Conversely, treatment with exogenous Bmp4 protein caused a significant increase in the population of growing follicles with a concomitant decrease in the proportion of primordial follicles (Nilsson and Skinner, 2003).

Treatment of neonatal mouse ovaries with rhBmp7 also promoted activation and transition of quiescent primordial follicles to the primary stage (Lee et al., 2004). By comparison, Bmp6 is detectable in the oocyte and granulosa cells of growing follicles and has been shown to influence FSH–induced steroidogenesis, but the effect of this protein on early follicle development has not been investigated (Otsuka et al., 2001). In both neonatal and mature ovaries, Bmp15 (Gdf9b) and Gdf9 proteins are detectable in oocytes of all follicle stages that have initiated growth (McGrath et al., 1995).

Deletion of *Gdf9* from mouse ovaries exhibited inadequate granulosa cell proliferation, insufficient oocyte development, and failure of theca cell formation (Elvin et al., 1999). More recently, natural homozygous mutations of *Bmp15* and *Gdf9* in ewes revealed loss of fertility manifested by defective follicle development and anovulation. Surprisingly, ewes carrying heterozygous mutations (i.e. one copy) exhibited increased ovulation rate (Hanrahan et al., 2004).

In immature female rats, the effect of *in vivo* treatment with exogenous Gdf9 protein caused an increase in the number of primary and small preantral (i.e. growing) follicles with a significant reduction in the population of primordial follicles indicating that *Gdf9* is essential for the transition of primordial to primary follicle stage (Vitt et al., 2000).

Anti-Müllerian hormone (Amh) is believed to inhibit the transition of primordial follicles. Treatment of neonatal mouse ovaries with exogenous Amh protein prevented the majority of primordial follicles from growing (Durlinger et al., 2002). However, this statement has been challenged by incubation of postnatal mouse ovaries, which is free from the source of Amh as the majority of follicles are primordial, at the end of culture, different stages of follicle growth were determined including primordial follicles (Jin et al., 2010).

Activin is expressed in granulosa cells of growing follicles and is formed by a combination of two β subunits (either βA or βB). Thus, three isoforms of activin have been identified included activin A (βA- βA), B (βB- βB), or AB (βA -βB) (Knight and Glister, 2001). Generally, activin has a role in the progression of oocyte growth, granulosa cell proliferation in preantral follicles and enhancement of antrum formation in late stage pre-antral follicles (Zhao et al., 2001). Activin signalling is antagonised by the presence of follistatin, an extracellular binding protein, which can bind to activin thereby obstructing the association between activin and its specific receptors (Thompson et al., 2005).

Similarly, overexpression of inhibin (the product of an α and β subunit) can block activin signalling by associating with the type II activin receptors (Zhu et al., 2012). Inhibin null mice demonstrated a significant increase in the proliferation of granulosa cells with an elevated incidence of ovarian tumour. Furthermore, these effects were accompanied with enhanced activin signalling (Matzuk et al., 1992). Interactions between TGFβ signals that regulating early follicle development are illustrated in Figure 1.6.

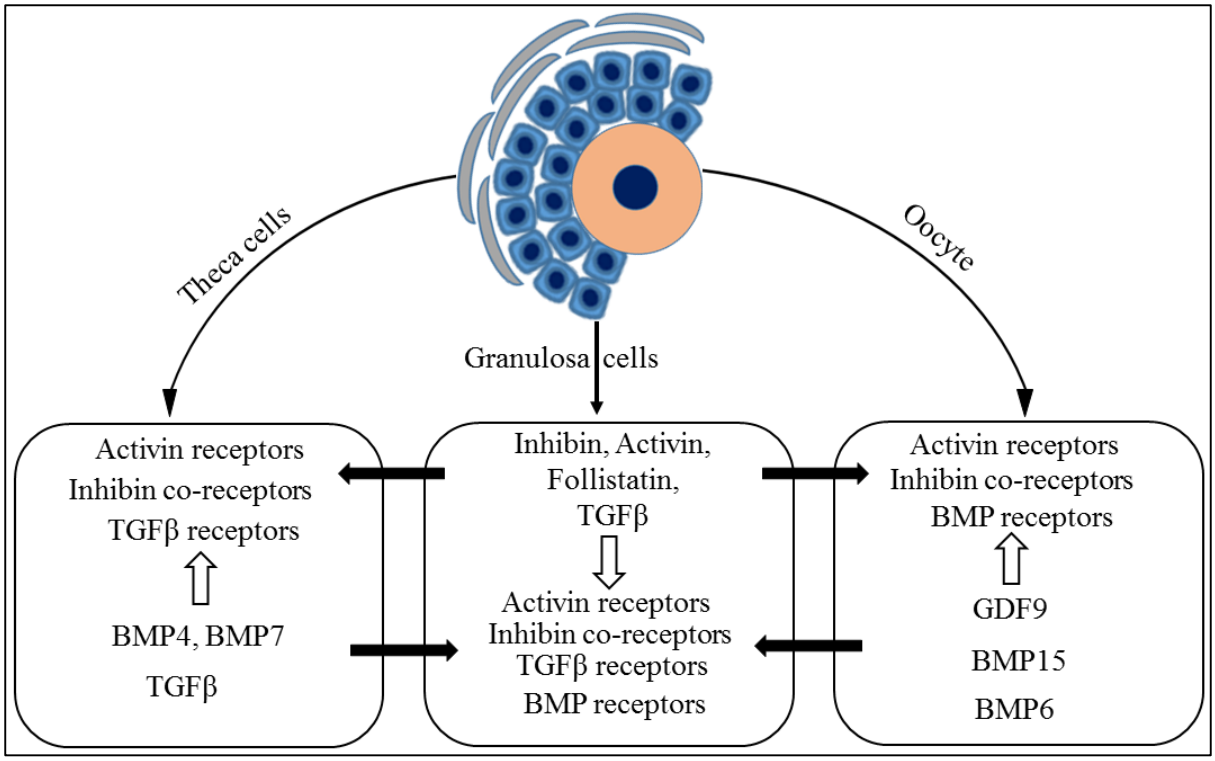

Figure 1.6. A model for TGFβ signalling in the follicle. Different TGFβ superfamily members are implicated in the regulation of follicle growth. These members and their receptors are detectable in different follicle compartments including oocytes, granulosa cells, and theca cells. Follicle growth is regulated in part through the interaction of these factors with their specific receptors in an autocrine (white arrows) and paracrine (black arrows) manner. Adapted from (Knight and Glister, 2003).

1.7.2. Synthesis and structure of TGFβ

Intracellularly, TGFβ proteins (TGFβ1-3) undergo several processes before secretion to the ECM as biologically non-functional structures. TGFβ members are produced as a single precursor pro-TGFβ (pre-pro-TGFβ). Two of these monomers then associate by their interaction between three conserved disulphide bonds forming a dimeric pro-TGFβ (Annes et al., 2003; Gray and Mason, 1990). A fundamental stage of TGFβ synthesis is the proteolytic breakdown of pro-TGFβ by the endopeptidase, furin convertase, which splits the pro-TGFβ protein to produce a non-covalently linked structure called the small latent TGFβ complex (SLC) (Blanchette et al., 1997; Dubois et al., 1995). A particular glycoprotein (Emilin1) which interacts with elastic fibres in the ECM can antagonise furin function. Emilin1 knockout in mice caused increased TGFβ signalling in blood vessels and hypertension was revealed (Zacchigna et al., 2006). The SLC consists of a latency-associated peptide (LAP) and the mature TGFβ as a dimer. LAP is essential to enable the passage of TGFβ through the cell membrane to ECM (Brown et al., 1990).

Extracellularly, the SLC binds to the large latent TGFβ-binding protein (Ltbp) by two disulphide bonds (covalent binding) between LAP (cysteine 33 residues) and the third 8-Cys repeat of the Ltbp form a large latent complex (LLC) (Hyytiainen et al., 2004) (Figure 1.7).

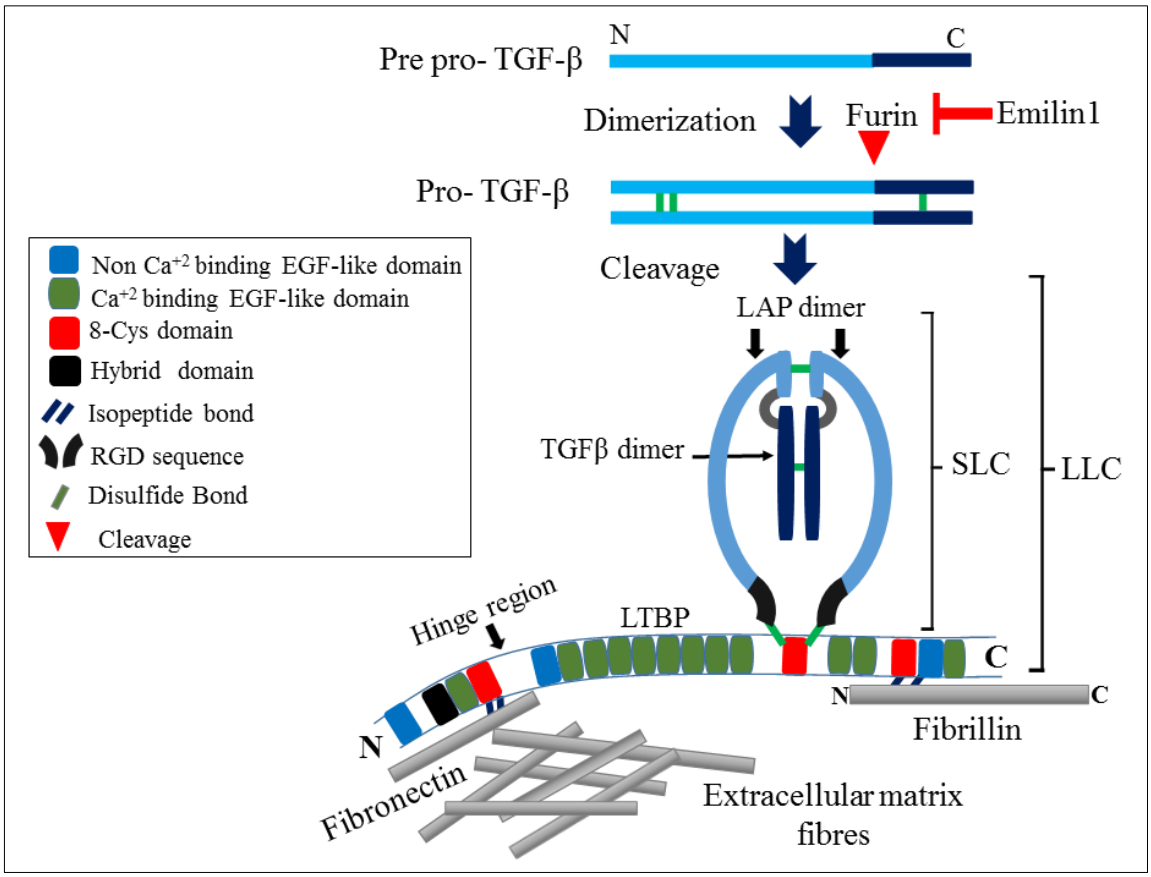

Figure 1.7. Schematic illustrating synthesis and structure of the latent TGFβ complex. TGFβ members are produced as a precursor protein (pre-pro- TGFβ). Two pro-TGFβ are connected with each other by disulphide bond before being cleaved by furin to produce the small latent TGFβ complex (SLC). In the ECM, Emilin1 antagonise furin function. SLC is composed of two parts, latency-associated peptide (LAP) and mature TGFβ, connected together by non-covalent bonds. SLC associates with the latent TGFβ binding protein by a disulphide bond to form the large latent complex (LLC). The LLC is stored in the extracellular matrix by its association with other structures such as fibrillin and fibronectin. Adapted from (Hayashi and Sakai, 2012).

TGFβ ligands can be secreted either in the form of LLC or SLC (Hyytiainen et al., 2004; Saharinen et al., 1996). However, secretion of small latent TGFβ complexes associated with Ltbp (LLC) and also the free Ltbp isoform from cells occurs more readily than unbound small latent TGFβ complexes (SLC) (Miyazono et al., 1991). After secretion, TGFβ signalling cannot be initiated as LAP covers the epitopes of the mature TGFβ preventing access to its particular receptor (Annes et al., 2003).

Ltbp1 and Ltbp3 can create covalently linked complexes with all TGFβ members (TGFβ1-3) while Ltbp4 can only bind to TGFβ1 and Ltbp2 cannot associate with any TGFβ members (Penttinen et al., 2002; Saharinen and Keski-Oja, 2000). However, more recently, a study indicated a possible association between Ltbp2 and the microfibrils proteins, fibrillin1 and 2, suggesting that Ltbp2 is important for elastic fibre assembly in the ECM (Hirai et al., 2007). In the ECM, the LLC associate with the elastic microfibrils by binding of the C- terminal region of Ltbp1, 2, 4 to the N- terminal region of fibrillin1 and 2 (Isogai et al., 2003). In addition, for further anchoring of the LLC complex to the ECM, the N-terminal domain of LTBP1 and 4 connects to other components of the ECM, such as fibronectin (Dallas et al., 2005; Nunes et al., 1997).

1.7.3. Activation TGFβ ligands

All TGFβ members are secreted and stored as inactive structures (LLC/SLC complex) in the ECM because LAP prevents the interaction between epitopes of mature TGFβ and TGFβ receptors (Annes et al., 2003). Thus**,** activation of latent TGFβ (Figure 1.8) is an essential stage that regulates TGFβ bioavailability, which requires releasing of active TGFβ by disrupting the association between LAP and mature TGFβ (Hyytiainen et al., 2004). Different mechanisms and factors have been reviewed in relation to the activation process (Koli et al., 2001; Saharinen et al., 1999). However, it is difficult to evaluate whether these mechanisms/ factors function as principal activators or if they simply act to enhance the activation process. For example, plasmin has the potential to release the active TGFβ from LAP but also acts to enhanced the dissociation of LLC from the ECM by its proteolysis effect on the hinge region of Ltbp (Annes et al., 2003; Taipale et al., 1992). Several other proteases are essential to release the bioactive TGFβ, such factors include elastase, mast-cell chymase, and BMP1-like metalloproteinases, which act by directly targeting the complex of Ltbp and LAP (LLC), as well the interaction of Ltbp and the ECM (Ge and Greenspan, 2006).

Additionally, structures termed 'ligand traps', which are structurally diverse ligand-interacting proteins, function as obstacles to prevent the contact between TGFβ ligands and their receptors. Examples of such ligand traps include noggin, chordin, gremlin, follistatin and DAN/Cerberus (Fenwick et al., 2011; Shi and Massague, 2003).

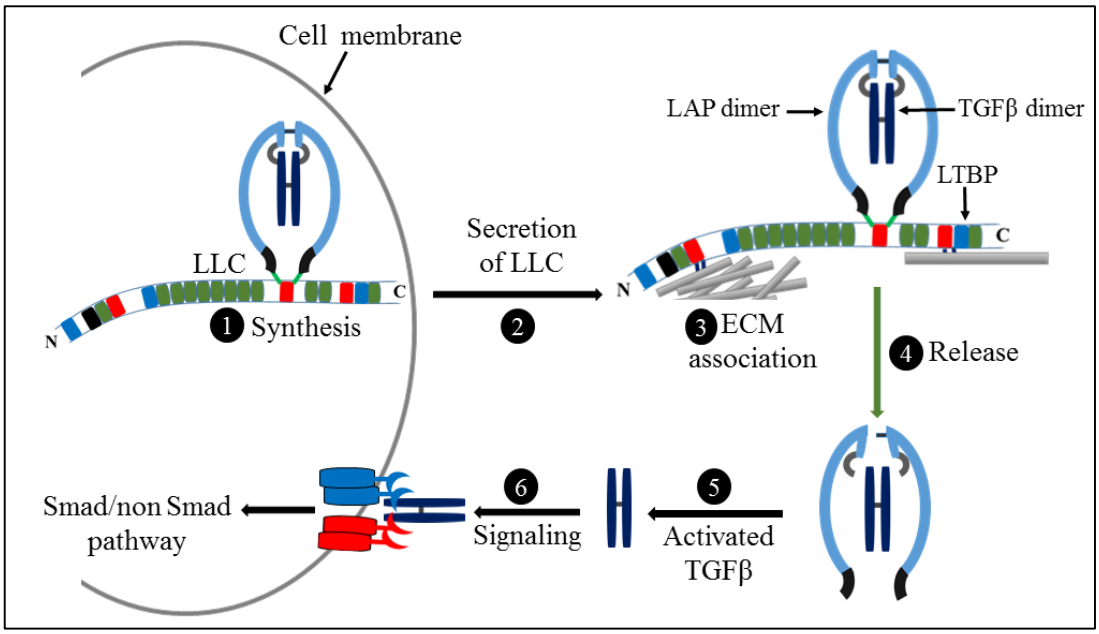

Figure 1.8. Schematic model for secretion and activation of latent TGFβ complex. The majority of inactive TGFβ is secreted from cells in the form of LLC (associated with Ltbp). This complex binds to the ECM via the N-terminal of Ltbp. The first step of activation by a protease is through cleavage of Ltbp from ECM at the hinge region, a protease sensitive part. The following step includes releasing of the mature TGFβ from LAP by another proteolytic agent. Subsequently, TGFβ can interact with the specific signalling receptors for activation of the signalling pathway. Adapted from (Koli et al., 2001).

In vivo, active TGFβ is also released from LAP or latent TGFβ complex in response to tissue destruction and remodelling (Kyriakides and Maclauchlan, 2009). For example, thrombospondin type 1 motif (TSP1) and matrix metalloproteinase (MMP2, and MMP 9) are proteases that promote TGFβ activation during tissue damage and healing (Bourd-Boittin et al., 2011; Yu and Stamenkovic, 2000). *In vitro*, in addition to protease treatment, activation of TGFβ can be achieved by the exposure to high temperature, extreme changes in pH, or by disruption of the ECM (Bourd-Boittin et al., 2011; Brown et al., 1990). The absence of binding between Ltbp and ECM elements, fibrillin and/or fibronectin, leads to increased of TGFβ activity and Smad signalling, while the lack of, or regulation of latent TGFβ activators and/or Ltbp causes a reduction in the activation process (Loeys et al., 2010).

The released/activated TGFβ ligand initiates signalling by binding and assembling receptor complexes, which leads to phosphorylation of internal factors (Shi and Massague, 2003).

1.7.4. TGFβ superfamily receptors

The biological effect of all TGFβ superfamily ligands is mediated by cell membrane receptors classified as activin receptor-like kinases type I (Alk1- Alk 7) and serine/ threonine kinase receptors type II (TGFβRII, BmprII, ActrII, ActrIIb, and AmhrII) (Moustakas and Heldin, 2009; Schmierer and Hill, 2007). These receptors consist of three distinct regions including an extracellular ligand-interacting cysteine-rich domain, a transmembrane domain, and an intracellular cytoplasmic domain, which has serine/ threonine kinase activity (Groppe et al., 2008) (Figure 1.9). Alk4, Alk5 and Alk7 have a high affinity for TGFβ and activin signalling; that is, factors that activate Smad2 and Smad3 (Feng and Derynck, 1997), while Alk1, Alk2, Alk3, and Alk6 are generally activated by Bmps and Amh, which lead to signalling via Smad1, Smad5, and Smad8 (Persson et al., 1998). Activated serine/threonine kinase receptors can activate the canonical Smad pathway and also Smad-independent pathways; for example, mitogen-activated protein kinases MAPK (Javelaud and Mauviel, 2005).

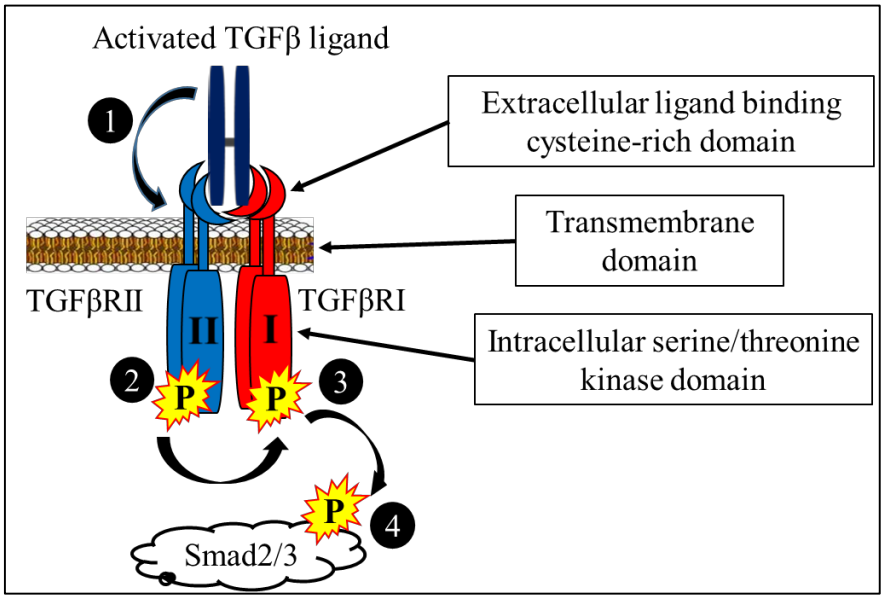

Figure 1.9. Diagram illustrating activation of the TGFβ pathway. At the level of the cell membrane, TGFβ receptors consist of an extracellular TGFβ ligand binding cysteine-rich domain, which connects to a short transmembrane domain and the long intracellular Ser/Thr kinase domain, which can interact with R-Smads. TGFβ signalling is initiated upon stimulation of the phosphorylated (yellow stars) TGFβRII receptor by the activated TGFβ ligand (1). Once stimulated (2), the TGFβRII receptor activates the serine/threonine kinase activity of TGFβRI by phosphorylation (3). Then, the activated TGFβRI recruits and phosphorylates the R-Smads transcription factors (4).

Additionally, beta glycan receptor III (TGFβRIII) is a co-receptor that has the potential to associate with some TGFβ ligands to enhance interaction with signalling receptors (TGFβRI and TGFβRII); however, TGFβRIII cannot mediate internal signalling as it lacks an internal kinase domain (Esparza-Lopez et al., 2001). Other studies have demonstrated the expression of TGFβRIII receptor caused suppression of TGFβ signalling and inhibition of metastasis in models of breast and prostate cancer (Elderbroom et al., 2014; Turley et al., 2007). The inhibitory effect of TGFβRIII on TGFβ/ Smad signalling was further evaluated using cell lines where both TGFβRI and TGFβRII independently associates with TGFβRIII, preventing the interaction of Smads with the activated TGFβRI receptor (Tazat et al., 2015).

1.8. Smad family

The Smad family consists a family of eight closely related proteins which mediate the signal transduction of TGFβ superfamily proteins (Shi and Massague, 2003). Smads were first identified through genetic studies on the fruit fly *Drosophila melanogaster* where an intracellular protein termed "Mad" was found to mediate decapentaplegic signalling (Mothers Against Dpp), a TGFβ superfamily member (Sekelsky et al., 1995). Then, after the identification of an orthologous gene in *Caenorhabditis Elegans* (Small body size), the names of the two genes were combined to "Smad" (Derynck et al., 1996). Functionally, Smads have been categorised into three subgroups: Firstly, receptor-activated Smads (R-Smad) including Smad1/2/3/5/and 8. Secondly, Smad4 is the common mediator Smad (Co-Smad) that interacts with activated R-Smad to facilitate nuclear import and has an essential role in the association with transcriptional factors. Thirdly, Inhibitory Smads (I-Smad) include Smad7 that exclusively blocks the Smad2/3 pathway (inhibit TGFβ1-3, GDF9 and Activin signalling), and Smad6 which primarily inhibits the Smad1/5/8 pathway (inhibit BMPs and AMH signalling) (Kimura et al., 2000; Miyazono et al., 2001; Shi and Massague, 2003).

Smad proteins, consist of 400 - 500 amino acid residues in length and have three precise domains including a Mad homology domain-1 (MH1) at the N-terminus, which is required for nuclear translocation, DNA binding and regulation of transcription (Moustakas et al., 2001). The MH1 domain, binds particular sequences (5'-AGAC-3') of DNA called Smad binding elements SBE (Dennler et al., 1999). However, Smad2 is unable to bind DNA because the MH1 domain in this protein contains an additional 30 amino acid sequence enriched with serine/ threonine known as TID (Yang et al., 2009). The next domain is the central linker which contains numerous of essential peptides including prolines and serine/ threonine that serve as sites of phosphorylation for signalling pathways other than TGFβ, such as mitogen-activated

protein kinases (MAPK)/ Extracellular signal-regulated kinases (ERK) and c-JUN NH(2)-terminal kinase JNK (Mori et al., 2004; Wicks et al., 2000). The linker of Smad3 contains a site called a transactivation domain (TA), which is essential to promote transcription and the physical association with coactivators (Prokova et al., 2005).

The third domain is a Mad homology domain-2 (MH2), located in the C-terminus and is responsible for the interaction of R-Smad with other Smads/receptors and also with co-activators and co-repressors. The MH1 domain is absent in the I-Smads but is evident in the structure of Co-Smad and R-Smad, while MH2 domain is present in all three Smad sub-types (Shi and Massague, 2003; ten Dijke and Hill, 2004; Xu et al., 2007).

1.8.1. Expression of Smads in the ovary

In rat ovaries, both Smad2 and Smad3 are expressed in small follicles, in particular in primordial follicles, indicating a possible influence of TGFβ signalling during these early stages (Xu et al., 2002a). In the mouse ovary, Smad4 is expressed in oocytes of non-growing (primordial) and growing follicles (Pangas et al., 2006). Likewise in primate ovary, Smad2/3 and Smad4 have been detected in oocytes and pre/granulosa cells of primordial and primary follicles at the mid and late gestation period, respectively (Billiar et al., 2004). In mice, the Smad6 protein was shown to be strongly expressed in the oocyte of small quiescent follicles; however, in growing follicles, the staining was relatively weaker in the oocyte, granulosa, and theca cells, suggesting that the reduction in Smad6 expression in growing follicles is to permit TGFβ signalling through Smad1/5/8 (Gueripel et al., 2004). Unlike Smad6, the staining pattern of the Smad7 protein in the mouse ovaries was shown to be increased in both granulosa cells and oocytes of multi-layered follicles (Quezada et al., 2012), where staining for Smad2/3 are decreased (Fenwick et al., 2013).

More recently, a detailed analysis of Smad2/3 staining in the mouse ovary in our laboratory has identified that these proteins appear to be localised in the nuclei of granulosa cells of primordial follicles, possibly indicating their crucial role in the maintenance of the primordial follicle phenotype. In addition, Smad2/3 becomes excluded from the nuclei of granulosa cells of primary/ pre-antral follicles that have initiated growth, suggesting that the exclusion of Smad2/3 from the nucleus of granulosa cells is a key molecular event in follicle activation (Figure 1.10; Fenwick et al. unpublished). This observation underpins the general hypothesis that TGFβ signalling plays an important role in small follicles and that modulation of the Smad pathway is a key aspect of early follicle development. This will be explored in more detail throughout this thesis.

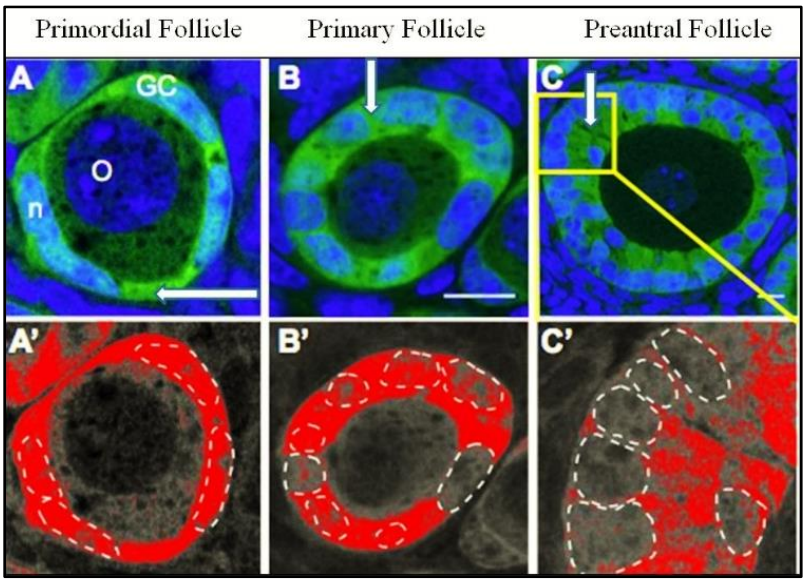

Figure 1.10. Localisation of Smad2/3 in granulosa cells of small follicles in the mouse ovary. Smad2/3 are localised (green) in the cytoplasm of granulosa cells (GC). Nuclei (n) were counterstained with DAPI (Blue). Nuclear exclusion of Smad2/3 during follicle activation and growth is highlighted by the grey scale image (A'-C') of the green channel, where saturated pixels are coloured red. By comparison with earlier follicle stages (A: primordial and B: transitional), the staining pattern of Smad2/3 in nuclei of granulosa cells of the primary follicle (C) was largely reduced.

1.8.2. Functional role of Smad pathway in the ovary

Mutations in specific Smad genes have provided important information on the role of these factors in the regulation of ovarian function and fertility (Pangas and Matzuk, 2004; Tomic et al., 2002; Xu et al., 2002a). In reviewing the literature, the role of *Smad2* and *Smad3* in the regulation of the early follicle development is not clearly understood (Li et al., 2008b). In one model, *Smad3* null mice were affected by colorectal cancer accompanied with rapid loss of body weight (Zhu et al., 1998), while *Smad2* null mice die during embryonic period (7.5 to 12.5 dpc) with extensive development of malignant tumours (Hamamoto et al., 2002). *Smad3* deficient mice exhibit a reduced number of growing follicles accompanied with a high percentage of primordial follicles, more atretic follicles, and degenerative oocytes, indicating that Smad3 is essential for primordial follicle growth (Tomic et al., 2002). A reduction in *Smad3* also impairs follicle differentiation at the later stages of follicle development as reduced levels of oestrogen receptor *beta* and inhibin *alpha* subunits were evident in these mice. Moreover, deletion of *Smad3* results in a decline in the ability of granulosa cells of growing follicles to respond to FSH stimulation (Gong and McGee, 2009). It has been suggested that *Smad*3 might substitute for *Smad2* and vice versa when individual genes are mutated in mice (Li et al., 2008b). Therefore, double conditional mutants in granulosa cells (under the control of the cell-specific Amhr2 promoter) were generated.

This study revealed that the absence of both *Smad2* and *Smad3* in granulosa cells causes early ovarian failure and infertility manifested by a massive decrease in the population of primordial follicle, increase the percentage of atretic follicles, anovulation, and defects in cumulus differentiation, indicating their essential role in ovarian function and maintenance of female fertility (Li et al., 2008b). Interestingly, conditional deletion of *Smad1, 5* and *8* in the granulosa cells revealed a considerable prevalence of granulosa cell tumours accompanied with upregulation of Smad2 and Smad3 signalling. This suggests that the Smad2/3 pathway might be implicated in the progression of the ovarian tumours while Smad 1/5/8 may function as tumour suppressors (Pangas et al., 2008).

Deletion of *Smad1* and *Smad5* individually results in embryonic death. However, these studies showed that S*mad1* null embryos exhibited major defects in allantois development and a considerable reduction in the establishment of primordial germinal cells (Tremblay et al., 2001). Similarly, *Smad5* knockout mice exhibited a defective proliferation of primordial germinal cells (Chang and Matzuk, 2001). *Smad8* knockout mice are fertile; however, signs of vascular thickness and hyperplasia were observed (Huang et al., 2009). Knockout of *Smad4* in granulosa cells causes defective cumulus cell differentiation, disordered oocytes growth and early luteinisation (Pangas et al., 2006).

1.8.3. Nucleocytoplasmic translocation of Smads

TGFβ signalling involves the translocation of Smads between the cytoplasm and nucleus through the nuclear pores (Brown et al., 2007). Nuclear pores contain essential nucleoproteins (importins) that associate with the activated R-Smad in an energy-dependent manner to enhance their translocation into the nucleus (Moustakas and Heldin, 2008).

The MH1 domain in both R-Smads and co-Smad contains a specific site termed the nuclear localisation signal (NLS), which can associate with specific importin proteins, for example, importin α specifically interacts with Smad4, importin β with Smad1 and Smad3, while importin 7 and 8 can specifically interact with Smad2, 3, and 4 (Xu et al., 2007; Yao et al., 2008). The association between R-Smads and Smad4 is thought to be essential for nuclear translocation of R-Smads (Shi and Massague, 2003). However, in some cell lines, Smad2 and Smad3 are detectable in the nucleus in response to stimulation by TGFβ1 even in the absence of Smad4 (Fink et al., 2003).

Another study suggested that the shuttling (import and export) of Smad2 and Smad3 between the cytoplasm and nucleus is enhanced by the interaction of the MH2 domain with some proteins found in nuclear pores such as CAN/Nup214 and Nup153 (Xu et al., 2002b). In addition, to enhance the exclusion process, the linker domain of Smad4 and the MH2 domain of Smad1 and Smad3 contain nuclear export signals (NESs) that can associate with exportin proteins (Inman et al., 2002).

Several exportin proteins have been identified; for instance, exportin1 is required for the exclusion of Smad1 and Smad4, while exportin4 is specific for Smad3 (Dai et al., 2009). Locations of these factors in the structure of Smads are shown in Figure 1.11. Another mechanism for the exclusion of Smad2 and Smad3 from the nucleus is by protein phosphatase 1A, magnesium-dependent alpha (Ppm1a), which acts to dephosphorylate Smad2 and Smad3 leading to dissociation with Smad4 (Lin et al., 2006). The dephosphorylated Smad2 and Smad3 are exported from the nucleus by another exportin factor called RAN-binding protein3, RANBP3 (Dai et al., 2011). Upon a persistent stimulation of TGFβ, R-Smads constantly translocate between the cytoplasm and the nucleus. This occurs because the excluded inactive R-Smads can be re-phosphorylated as long as the receptor (TGFβRI) remains active (Inman et al., 2002; Xu et al., 2002b).

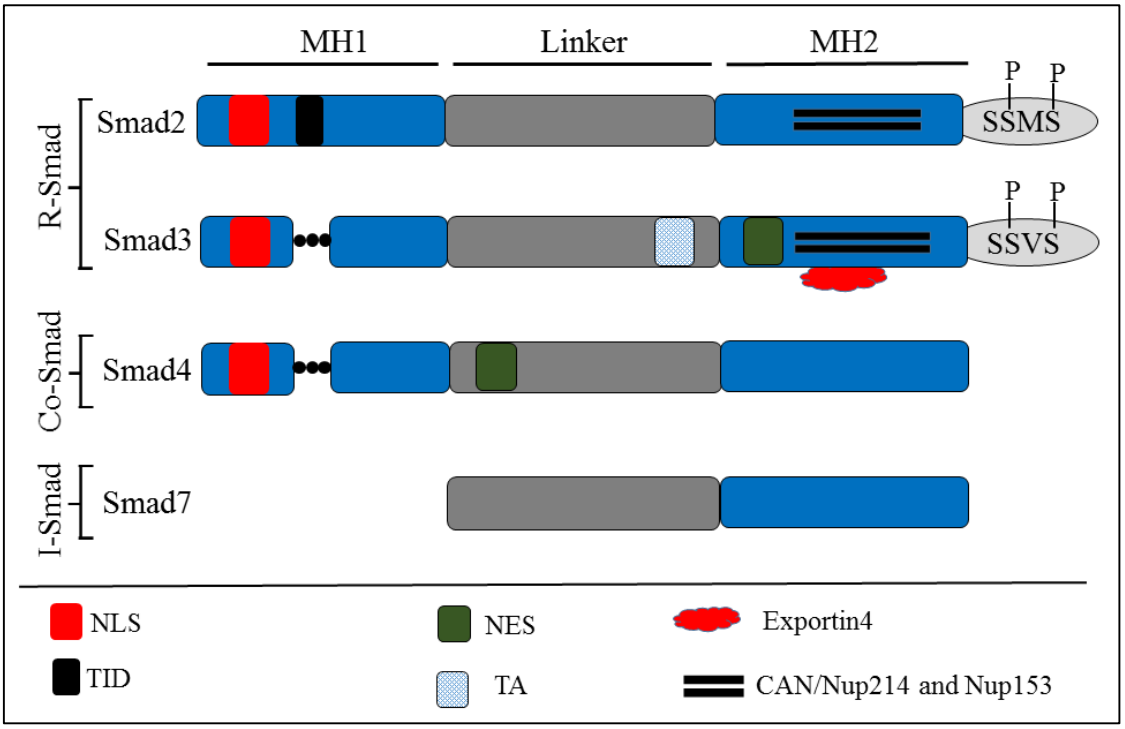

Figure 1.11. The structure of different Smad proteins showing some of the functional sites. The R-Smad and co-Smad proteins contain two well-recognised domains, the Mad homology domain-1 (MH1) and -2 (MH2), while the I-Smad lacks for the MH1 domain. The MH1 domain of Smad2 contains a group of amino acids sequence (TID, black shape) enriched with serine/threonine that prevent Smad2 from interaction with DNA. In addition, nuclear localisation signals (NLS, red shapes) are included in the MH1 domain of both R-Smad and Co-Smad, where Co-Smad also contains another functional structure called nuclear export signals (NES, green shape). The MH1 and MH2 domains are joined by a medially situated structure, which is enriched with proline and is essential for the activation of a non-Smad pathway called the linker domain. The linker of the Smad3 includes a site for the association with coactivators called transactivation domain (TA, white block), while the Smad4 linker contains a nuclear export signal (NES), which associate with exportin1 to enhance nuclear translocation. Upon the TGFβ stimulation, the TGFβRI becomes activated which then activates by phosphorylation (P) of Smad2 and Smad3 at their MH2 C-terminal serine residues (SSMS or SSVS motif, respectively). The MH2 domain of Smad2 and Smad3 also can interact with CAN/Nup214 and Nup153, which are essential for the nucleocytoplasmic translocation of Smads. Smad3 also include a site that can associate with the exportin4 that promotes the nuclear exclusion. Adapted from (Brown et al., 2007; Inman et al., 2002).

1.9. TGFβ/Smad signalling pathway

Signalling via R-Smads is thought to be a common signalling pathway for most TGFβ members (Drummond et al., 2003; Pangas and Matzuk, 2004). The intracellular signal for TGFβ1-3, GDF9, Nodal, and Activin are mediated through the phosphorylation of Smad2 and 3, while the BMPs and AMH utilise Smad1, 5, and 8 reviewed by (Kaivo-oja et al., 2006) (Figure 1.12).

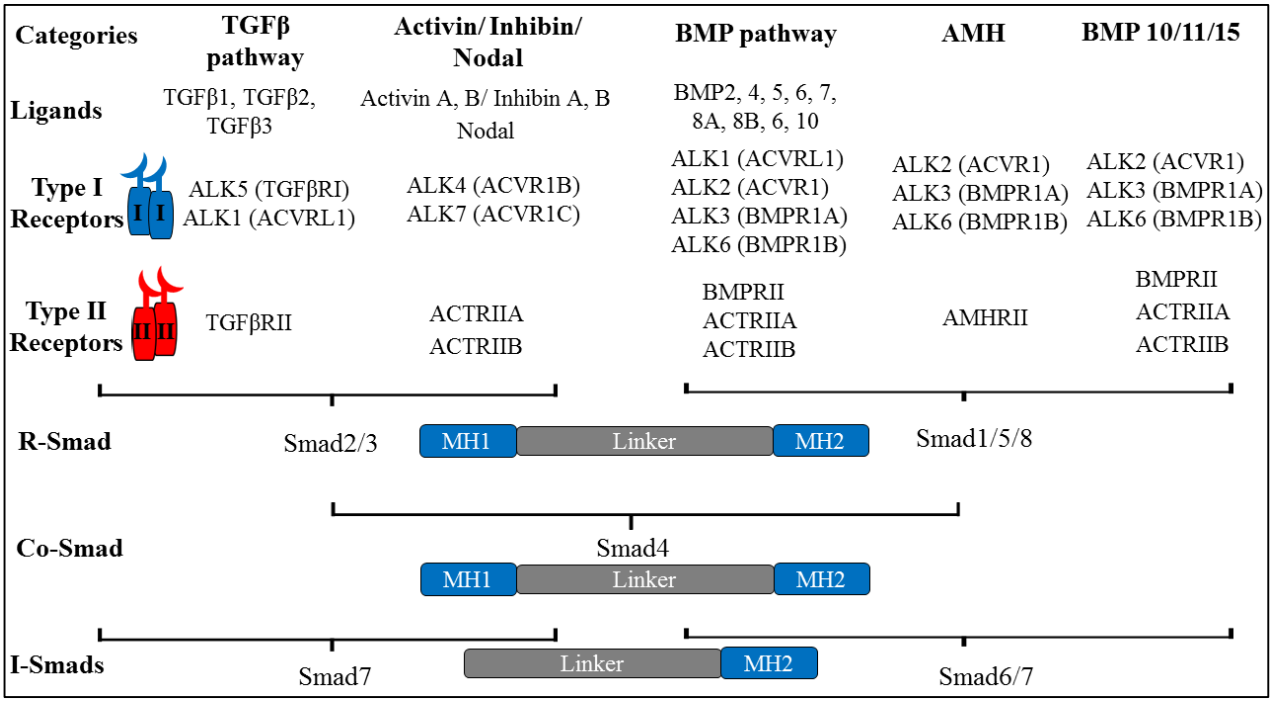

Figure 1.12. Simplified schematic model of TGFβ superfamily and signalling components in the ovary. Adapted from (Akhurst and Hata, 2012; Moustakas and Heldin, 2009).

As shown in Appendix I, TGFβ signalling is initiating through extracellular activation of TGFβ ligands followed by their association with the serine/ threonine kinase type II receptor, which undergoes auto-phosphorylation (Groppe et al., 2008). Then, the activated TGFβRII receptor recruits TGFβRI by phosphorylation on its glycine-serine motif to form a stabilised oligomeric receptor complex (Schmierer and Hill, 2007). Intracellularly, the MH2 domain of inactive Smad2 and Smad3 (but not Smad1 or Smad5) interact with an accessory protein called Smad anchor for receptor activation (SARA) that promotes recruitment and trapping of Smad2/3 to the activated TGFβRI receptor complex. Inhibition of SARA causes downregulation of TGFβ signalling in some models (Qin et al., 2002; Tsukazaki et al., 1998). However, others argued that TGFβ could signal through Smad2/3 pathway even in the absence of SARA, suggesting that SARA is not essential for Smad2/3 activation (Bakkebo et al., 2012; Goto et al., 2001).

TGFβ1-3 can stimulate the expression of a cytoplasmic protein termed PML (Promyelocytic leukaemia tumour suppressor) which essential for the interaction and binding of SARA to Smad2/3, thus PML participates in the regulation of TGFβ /Smad2/3 signalling (Lin et al., 2004). Consequently, the type I receptor kinase is able to activate the R-Smad by phosphorylation in their two serine residues located at their C-terminus SSXS motif (Miyazono et al., 2001). Dissociation of SARA and TGFβ receptors from the complex occurs after the activation of Smad2 and Smad3 (Wu et al., 2000). Unlike R-Smads, Smad4 is not activated by type I receptors, as the C-terminus of Smad4 does not include the phosphorylation site (two serine residues). However, the C-terminal domain of the Smad4 is essential for the interaction with the MH2 domain of the activated R-Smads to form a heteromeric complex (Shi and Massague, 2003).

Then, the heteromeric complex (activated R-Smad and Co-Smad) translocate into the nucleus where it cooperates with different transcriptional coactivators or corepressors to modulate genes responsible for cell proliferation, differentiation or apoptosis (Schmierer and Hill, 2007; Shi and Massague, 2003; ten Dijke and Hill, 2004). Several transcriptional coactivators have been identified such as SMIF, CBP/p300, and ARC105; while examples of corepressors include c-Myc, p53, c-Ski, SnoN and FoxH1/FAST (Ross and Hill, 2008). According to the R-Smad pathway used by different TGFβ ligands, Smad6/ or Smad7 is stimulated to inhibit or suppress of TGFβ signalling (Li, 2015). Smad7 is a specific negative regulator of TGFβ (1-3), Gdf9, and Activin (Quezada et al., 2012; Yan and Chen, 2011), whereas both Smad6 and Smad7, inhibit Bmp and Amh signalling (Bai et al., 2000; Kimura et al., 2000).

1.10. Non-Smad pathway

In addition to the Smad-dependent signalling, TGFβ can also signal through the non-Smad pathway via the activated TGFβ receptors (ten Dijke and Hill, 2004). Several non-Smad pathways have been well reviewed including P38, JNK, PI3K, ERK, NF-KB and AKT (Mu et al., 2012; Zhang, 2009). Crosstalk between both Smad-dependent and independent pathways is possible to coordinate cell growth by regulation of Smad transcription and nuclear translocation (Derynck and Zhang, 2003). The mechanism of their interaction is representing by the ability to phosphorylate the serine and threonine residues in the linker region of R-Smads.

For example (Figure 1.13), activated ERK pathway can target the nuclear Smad2 and Smad3 at their linker region to prolong the process of transcription of the targeted genes (Hough et al., 2012). In the ovary, non-Smad pathways have been identified to promote follicle development including PI3K (John et al., 2008; Zheng et al., 2012) and AKT (Altomare et al., 2004).

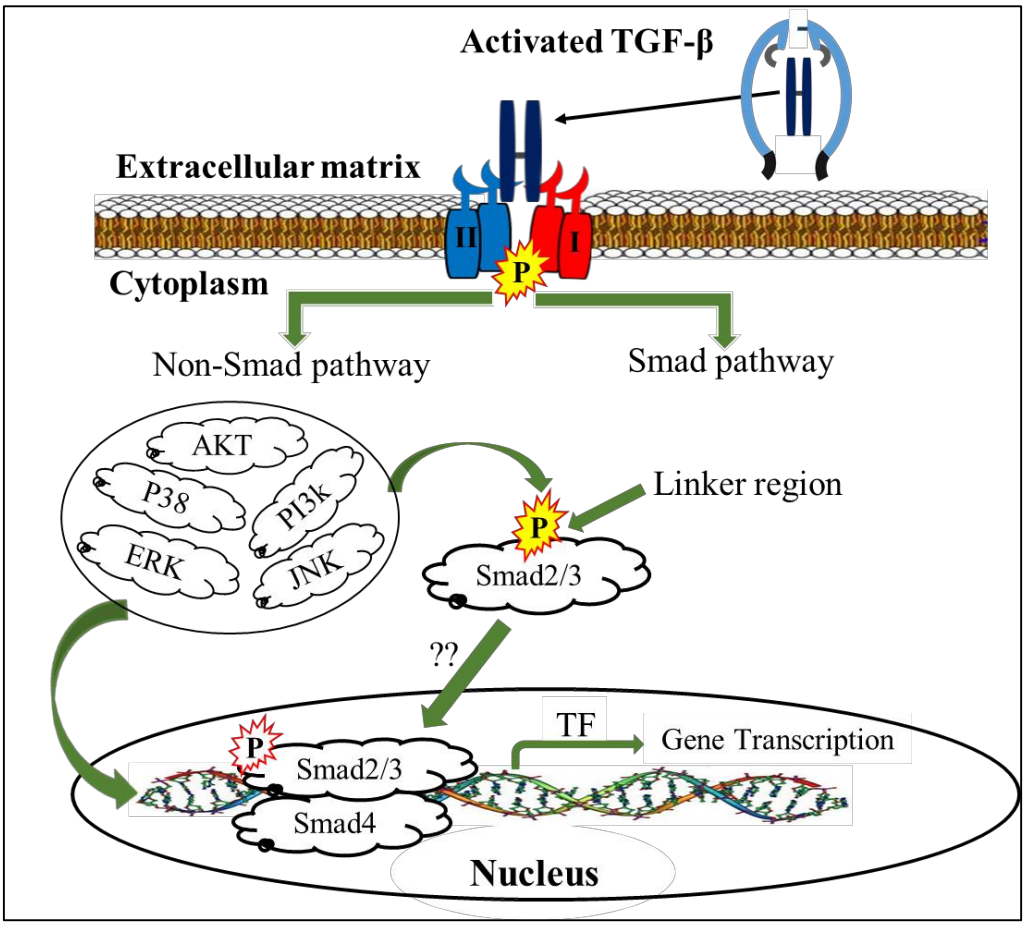

Figure 1.13. Non-Smad pathway. In addition to Smad signalling, activated TGFβ receptors can induce the activation of various non-Smad pathways such as P38, JNK, PI3K, ERK, and AKT. After activation, these pathways regulate gene transcription in the nucleus. However, both Smad2 and Smad3 may also phosphorylated by non-Smad pathways at the Smad linker region. This process can either enhance or prevent nuclear translocation of Smad2/3, prolong the activity of Smad in the nucleus and prevents nuclear exclusion.

1.11. Intracellular regulation of the TGFβ signalling

The TGFβ/Smad signalling pathway can be modulated at different cellular levels including extracellularly (as previously described), at the cell membrane level, and/or intracellularly where various inhibitory factors have been identified (Table 1.1) (Lin et al., 2006; Moustakas and Heldin, 2009; Schmierer and Hill, 2005; Wrighton et al., 2009). TGFβ signalling is regulated at the receptor level by different processes such as dephosphorylation, ubiquitination, sumoylation, degradation or acetylation (Dai et al., 2011; Inoue and Imamura, 2008; Lonn et al., 2009). As described earlier, regulation through the interaction of TGFβ signalling components with other pathways is possible. Activated TGFβ or Bmp signals are also capable of inducing a self-regulatory feedback mechanism by upregulation of the inhibitory Smad7 or Smad6/7, respectively (Moustakas and Heldin, 2009). In addition to blocking the activation process of Smad1/5/8 by activated TGFβRI (Goto et al., 2007), Smad6 functions to inhibit Bmp signalling by competition with Smad4 to prevent the formation of a heteromeric complex with activated R-Smad. In the nucleus, Smad6 also acts as a transcriptional co-repressor by association with transcription factors, homeobox (Hox) c-8 (Bai et al., 2000).

In order to block the stimulated TGFβRI and to prevent the generation of hetero-complex between Smad2/3 and Smad4, the exclusion of Smad7 from the nucleus into the cytoplasm is induced via an interaction with Smad ubiquitination-related factor Smurf1/Smurf2 (Liu et al., 2002). In the nucleus, Smad7 can inhibit the complex between nuclear R-Smads and DNA leading to dissociation of the nuclear *Smad2/ Smad3* and *Smad4* complex, thereby influencing translocation between nucleus and cytoplasm (Zhang et al., 2007).

Furthermore, through proteasomal and lysosomal pathways, the Smurf protein can enhance degradation and induce dissociation of the TGFβRI and Smad2/3 complex and also promote expression of Smad7 (Zhang et al., 2001). Interaction of Gadd34–Pp1c with Smad7 can antagonise TGFβ signalling by dephosphorylating of the activated TGFβRI (Shi et al., 2004). The two major co-repressors *Ski/SnoN* can interfere with the formation of the heteromeric complex by associating with Smad4. This process leads to a considerable reduction in the binding sites in the heteromeric complex. Moreover, it recruits histone deacetylases (HDACs) to the nuclear Smad complex, which results in suppression of transcription of target genes (He et al., 2003).

The role of the nuclear protein phosphatases (Ppm1a) is also important in two sequential events during Smad2/3 nuclear export (Dai et al., 2011). Ppm1a can interact with nuclear phosphorylated Smad2/3 and eliminate their C-terminal SSXS phosphorylation site (Lin et al., 2006). Elimination of the phosphate group from these R-Smads causes dissociation of the heteromeric complex and eventually exclusion of Smad proteins from the nucleus (Schmierer and Hill, 2005). This process is followed by dephosphorylation of Ran-binding protein-3 (RanBP3) by Ppm1a to stimulate its functional activity in the targeting and exclusion of inactive Smad2/3 from the nucleus (Dai et al., 2011) (Figure 1.14).

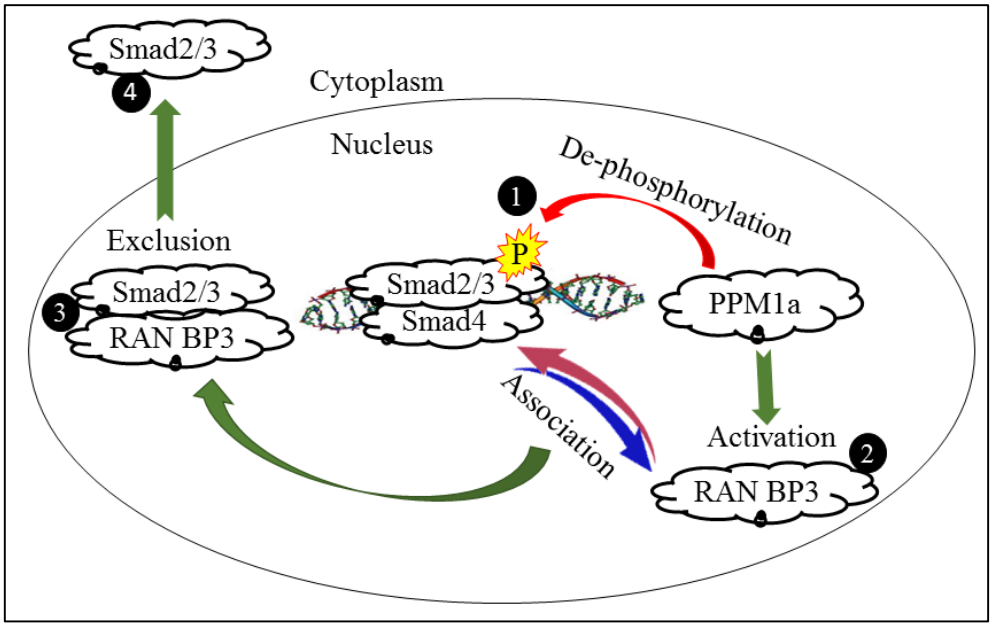

Figure 1.14. Diagram illustrating the mechanism of Smad2/3 nuclear export by Ppm1a and RanBP3. In addition to its ability to dephosphorylate of nuclear R-Smad (1), Ppm1a also interacts (2) with RanBP3 to stimulate its association with dephosphorylated Smad 2/3 in the nucleus (3); eventually, the export activity of RanBP3 promotes the exclusion of Smad2/3 from the nucleus.

Serine/threonine kinase receptor associated protein (Strap) has a dual role in antagonising TGFβ signalling mainly by its interaction with Smad7, but not Smad6, to recruit phosphatases to the receptor complex. At the level of the cell membrane, Strap function to block phosphorylation of Smad2/3 and receptor activation (Datta and Moses, 2000; Wrighton et al., 2009). FK506-binding protein is another TGFβ signalling inhibitor, which functions by interfering with the glycine-serine (GS) rich motif of the TGFβRI receptor to prevent its association with the TGFβRII receptor. FK506-binding protein forms a complex with Smad7 preventing phosphorylation of R-Smad by the activated TGFβRI (Yamaguchi et al., 2006). Trans-membrane prostate androgen induced RNA (Tmepai) specifically antagonises Smad2/3 pathway and its expression is induced by TGFβ signalling (Singha et al., 2014).

The inhibitory effect of this protein is achieved either by direct association with the activated TGFβRI or by competing with the accessory binding protein (SARA) for association with Smad2 and Smad3. In cell lines, knockout of *Tmepai* caused prolonged TGFβ signalling, indicated that expression of Tmepai is regulated by a self-regulatory mechanism (Watanabe et al., 2010). Another protein, NEDD4-2 inhibits TGFβ signalling by three mechanisms; firstly, by forming a complex with Smad7, which then promote association with the TGFβRI resulting in receptor degradation. Secondly, it is able to associate with Smad2 and Smad3 leading to degradation of Smad2, but not Smad3; however, Smad3 is then unable to interact with the receptor. Thirdly, upregulation of *NEDD4-2* can inhibit the transcriptional activity stimulated by TGFβ or Bmp signalling (Kuratomi et al., 2005). *Notch*4 intracellular domain (*Notch4ICD*) is another protein that acts to prevent complex formation by the interaction with Smad2, Smad3, and Smad4, but it binds more efficiently to Smad3 (Sun et al., 2005). The inhibitory actions of the above TGFβ signalling inhibitors are summarised in Table 1.1.

Table 1.1. Direct/ indirect inhibitory mechanisms of various TGFβ signalling regulator.

Smad inhibitors	Interaction with receptors	Heteromeric complex formation	Interference with transcription	De-phosphorylation	References
Smad 6	+	+	+	-	(Bai et al., 2000)
Smad 7	+	+	+	-	(Liu et al., 2002; Lonn et al., 2009)
Ppm1a	-	-	-	+	(Schmierer and Hill, 2005)
Gadd34	+	-	-	-	(Shi et al., 2004)
Smurfs	+	-	+	-	(Zhang et al., 2001)
Ski/SnoN	-	+	+	-	(He et al., 2003)
Strap	+	+	-	-	(Wrighton et al., 2009)
Fkbp12	+	-	+	-	(Yamaguchi et al., 2006)
Mapk1	-	+	-	-	(Kretzschmar et al., 1999)
Tmepai	+	+	-	-	(Watanabe et al., 2010)
Nedd4-2	+	-	+	-	(Sun et al., 2005)
Notch	-	+	-	-	(Kuratomi et al., 2005)

1.12. Conclusion and aims

Primordial follicles are relatively quiescent structures that contribute to the reproductive lifespan in females. Periodically, some of these small follicles are recruited to leave the quiescent state and develop further to terminate by either ovulation or atresia. It has been suggested that primordial follicle maintenance, activation and growth are regulated by various growth factors within and between neighbouring follicles. Among these factors, the TGFβ superfamily that signals through Smad proteins has an essential influence on the regulation of primordial follicle activation. However, the mechanism that operates to regulate TGFβ/Smad signalling during follicle development is not well understood.

In other TGFβ responsive cells, a range of different internal inhibitory factors is regulated TGFβ signalling. However, in the ovary, the expression and role of these inhibitors in early follicle development are almost entirely unknown. In the mouse ovary, recent observations from our lab have revealed that R-Smad proteins are detectable in a stage-specific manner; in particular, the exclusion of Smad2/3 proteins from the nucleus of granulosa cells appears to coincide with the initiation of primordial follicle growth.

Therefore, we hypothesised that inhibitors of the TGFβ pathway may also be detectable in the ovary and these could have a functional relevance in the process of early follicle development. The initial aim of this study is to determine the expression of candidate inhibitory factors during early follicle development. Based on findings from the first aim, the study will evaluate the role of specific TGFβ inhibitory factors in culture models of early follicle development using various tools for modifying the expression of the target gene.

Chapter 2
Materials and Methods

2.1. Animals and ovary dissection

Mouse ovaries and follicles from the C57BL/6 genetic background were utilised for all studies in this thesis. All tissue donor mice were housed and maintained in the Biological services unit at the University of Sheffield. Prior to dissection, mice were killed by Schedule 1 procedures (Cervical dislocation and exsanguination) according to the Animals and Scientific Procedures Act, 1986 and associated codes of practice

Ovaries were dissected from neonatal, prepubertal and adult female mice before being transferred in isolation media containing Leibovitz's media L15 (Gibco) with 1% (w/v) bovine serum albumin BSA (Sigma). Ovaries were cleanly dissected using acupuncture needles (AcuMedic) or insulin needles under aseptic conditions in the laminar flow hood fitted with a dissecting microscope (Leica) with a heated stage at 37ºC. Ovaries were dissected free from the ovarian bursa, oviduct and periovarian fat in drops of isolation media. Ovaries were prepared for either culture, preantral follicle isolation and culture, RNA extraction, or fixation according to the procedures below.

2.2. Culture protocols

All instruments, chemicals and buffer/solution recipes used in this study are listed in Appendix II-IV.

2.2.1. Ovarian fragments culture

Culture media were prepared immediately prior to each particular experiment before ovaries were dissected. The utilised culture media (MEM-α media; Gibco) was supplemented with 10% fetal bovine serum (FBS; ThermoFisher), penicillin (75µg/ml; Sigma PENK), streptomycin sulphate (100µg/ml; Sigma≠56501) and insulin-transferrin-sodium selenite (ITS; 5µg/ml, 5µg/ml, 5ng/ml, respectively; Sigma- I1884). Culture media in all experiments was filter sterilised through a 0.2 µm pore, 25 mm diameter filter (Corning Costar-Sigma-Aldrich). Culture plates of 24-wells (Corning Costar- Sigma-Aldrich) were utilised and 1ml of media was added to each of the selected wells before being incubated at 37ºC with 5% CO_2 at least for 30 minutes, to equilibrate the temperature and pH.

Ovaries from d4 old mice were used for all fragments culture where each ovary was dissected into 6-8 pieces using blunt acupuncture needles in drops of isolation media. Equivalent sized fragments (3-5 pieces) were transferred into each well for maintenance in a culture similar to (Maiani et al., 2012). In all groups, at 72 hours of incubation, half of the culture media (500µl) was carefully removed and were replaced with an equivalent volume of fresh media.

Cultured ovary fragments were imaged using an inverted light microscope (Olympus CKX41 with a Nikon camera DS-Fi1), where images were used to identify the effect of treatments on follicle growth by measuring oocyte diameters using ImageJ (http://imagej.nih.gov/ij/). At the end of culture, fragments either were fixed for immunostaining or were collected for RNA extraction.

2.2.2. Preantral follicle culture

Ovaries from d16 mice were cleanly dissected in isolation media in a laminar flow hood fitted with a dissecting microscope (Leica) with a heated stage at 37ºC in accordance with previously published protocols (Fenwick et al., 2013). Preantral follicles were mechanically isolated using blunt acupuncture needles (AcuMedic) in drops of isolation media in a 75mm dish. Approximately 15-25 preantral follicles per ovary were carefully selected under the microscope for culturing. Only rounded follicles with relatively similar size and (visually) undamaged basement membrane were selected. The selected follicles were rinsed in a drop of clean pre-warmed isolation media before being transferred to a 96-well plate (Nunclon) using a modified curved glass pipette fixed to a mouth pipette. Each individual preantral follicle was carefully transferred to a single well (1 follicle/well) containing 100µl of culture media.

The culture media (MEM-α media; Gibco) was supplemented with BSA 0.1% (w/v) (Sigma), penicillin (75µg/ml; Sigma PENK), streptomycin sulphate (100µg/ml; Sigma) and insulin-transferrin-sodium selenite (ITS; 5µg/ml, 5µg/ml, 5ng/ml, respectively; Sigma). Preantral follicles from each single ovary were cultured in a single plate; therefore, each plate represents a single subject. Cultured follicles were incubated at 37°C with 5% CO_2, and were imaged under a light microscope (Olympus CKX41 with a Nikon camera DS-Fi1) at 0, 24, 48, 72 hours of treatment. In all experiments, at 48 hours of culture, 50µl of media was replaced with fresh media for each group. At the end of culture, follicles from each treatment were collected for fixation in formalin 10% (Sigma- Aldrich) or snap frozen in liquid nitrogen until processing for RNA extraction.

2.3. RNA extraction (whole ovaries, fragments and follicles)

After dissection, whole ovaries were rinsed in drops of clean isolation media, transferred into Eppendorf tubes by a glass pasture pipette, immediately snap freezing in liquid nitrogen and stored at -80ºC until processing. To facilitate tissue lysis, ovaries from d8 and d16 were dissected into 3-4 fragments and then fragments were re-collected into an Eppendorf tube and processed for RNA extraction.

Adult ovaries were also dissected to four fragments, and each fragment was processed individually. Cultured ovary fragments and follicles were processed without prior mechanical fragmentation. Total RNA was extracted from all samples using Qiagen RNeasy Micro Kits (QIAGEN, Crawley, UK) according to manufacturer's instructions. Briefly, 75µl of Buffer RLT (β-ME -RLT) was added to each Eppendorf tube containing ovary samples and vortexed for 5 minutes. To improve capturing of low concentrations of RNA, 5µl of carrier RNA (4ng/µl) was added to each sample and vortexed for 2 minutes. Then, to precipitate the RNA, 75µl of 70% ethanol was added to each sample and well mixed by pipetting before being transferred into RNeasy Mini Spin Columns. After centrifugation (15 seconds at 8000xg), samples were washed with 350µl Buffer RW1 and centrifuged at 8000xg (10.000 rpm) for 15 seconds.
To prevent genomic DNA contamination, 80µl DNase I (Qiagen; Crawley, West Sussex, UK) was directly added to the membrane for 15 minutes at room temperature. Samples were washed again in buffer RW1 followed by 500µl Buffer RPE to remove traces of salts, then columns were briefly centrifuged. Membranes were washed with 80% ethanol, (500µl) and were centrifuged at the maximum speed for 5 minutes. Nuclease-free water (14µl) was added to the membrane and centrifuged at the maximum speed for 1 minute to elute the RNA sample. Purified extracted RNA samples were stored at -20^{o}C, until being tested for integrity and concentration.

2.4. cDNA synthesis

Extracted total RNA from ovaries, ovary fragments and cultured follicles were tested for concentration and integrity using a Bio-analyser (Agilent; G2938B). The Bioanalyser assess RNA sample through the fluorescent evaluation of electrophoretic separation of the RNA and outcomes are presented as an electropherogram and gel image. Only high-quality RNA samples were selected for cDNA preparation to be used for both gene qualification (RT-PCR) and quantification (qPCR). Samples were considered to be good quality if the RNA integrity number (RIN) was between 8-10 and the RNA electrophoresis revealed the absence of degradation products. RNA samples with a RIN number less than 8 and/or presence of degradation in the electrophoresis gel were excluded, Figure 2.1.

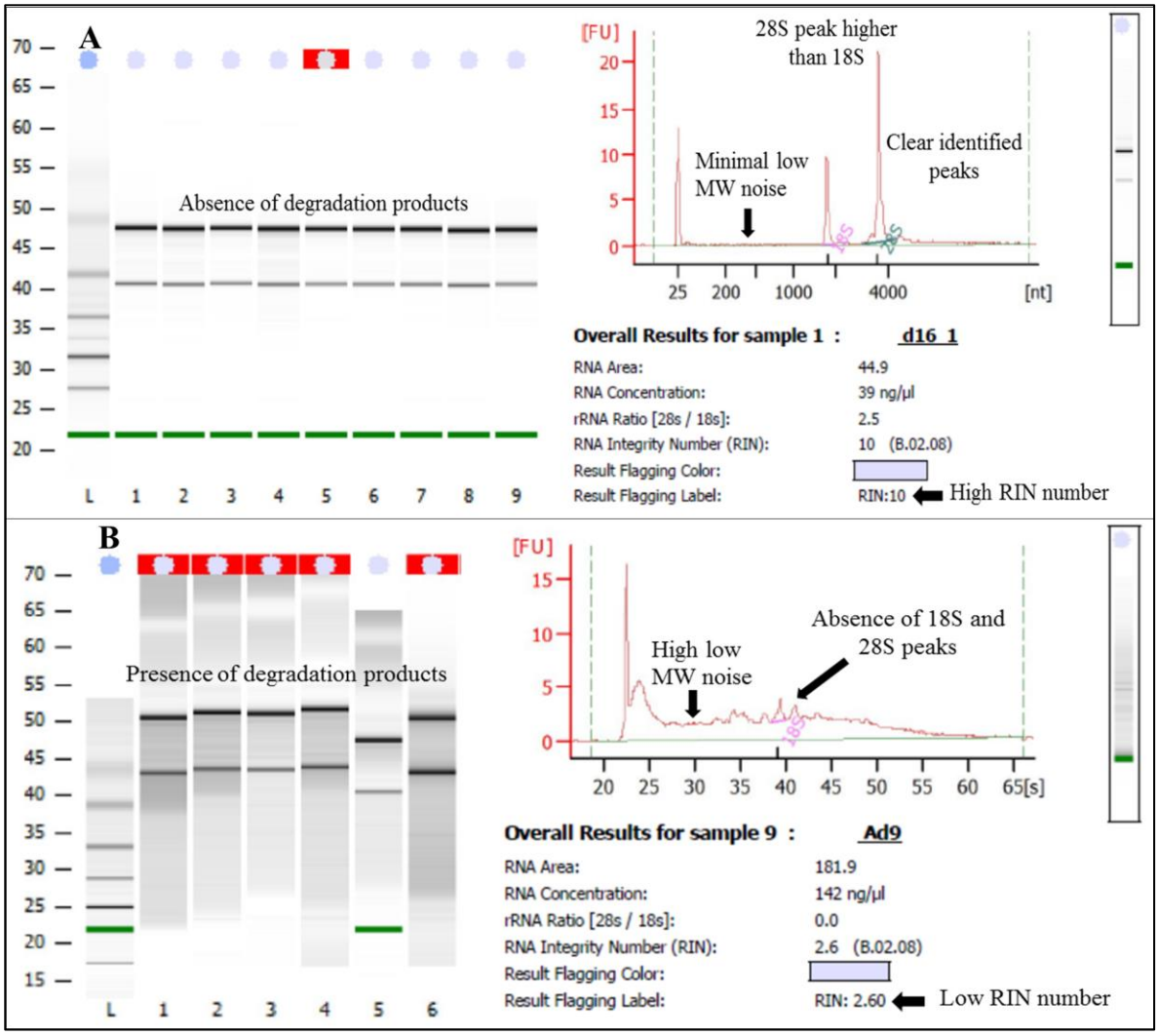

Figure 2.1. Examples of extracted RNA samples assessed by the Agilent Bio-Analyser. To consider whether the RNA sample is of sufficient quality for gene analysis, several criteria were followed. For high quality samples (A), the RNA electrophoresis gel reveals clear well-defined 18S and 28S bands and the absence of degradation products. The RNA integrity number (RIN), as determined from the electropherogram, is between 8-10. Low-quality samples (B) revealed degraded products, which are reflected by a low RIN number.

For each specific experiment, equal quantities of total RNA was converted to cDNA using the Superscript III First strand synthesis system (Invitrogen, 18080-051) in according with the manufacturer's instructions. The RNA mixture was prepared on ice by adjusting the volume of each sample to 8µl with nuclease-free water (Qiagen). Then, 1µl of random hexamers (50ng/µl) and 1µl of 10mM deoxynucleotides triphosphates (dNTPs; Invitrogen) were added to the RNA mixture. Random hexamers were added to prepare the single-stranded RNA for extension by reverse transcriptase and to increase the sensitivity of cDNA synthesis. To inactivate the DNase, reaction mixes were mixed by pipetting and were incubated in a thermal cycler (Geneflow) for 10 minutes at 65°C, with a final holding at 4°C.

Samples were placed on ice for 1 minute before adding 10µl of cDNA synthesis mix consisting of 2µl of 10x reverse transcriptase buffer, 4µl of 25mM MgCl2, 2µl of 0.1M DTT, 1µl of recombinant ribonuclease inhibitor (RNase OUT 40U/µl; Invitrogen P/N51535) and 1µl of 200U/µl reverse transcriptase. The reaction mixture (20µl) was incubated at 25°C for 10 minutes, followed by 50 minutes at 50°C, 85°C for 5 minutes, and then 4°C. To increase the volume, 20µl of nuclease-free water was added to each prepared ovary cDNA, then aliquoted into four tubes, and stored at -20°C.

2.5. Primer design

Primers were designed to detect mouse (*Mus Musculus*) transcripts for each candidate genes using the sequences available from the databases from the National Centre for Biotechnology Information NCBI (*http://www.ncbi.nlm.nih.gov/nucleotide/*).

Transcript sequences were entered into the Primer3 Plus online software at (*http://www.bioinformatics.nl/cgibin/primer3plus/ primer3plus.cgi/*). All primers used in the present study were designed to include between 19-21 nucleotide, melting temperature (TM) ranged 55-56ºC, primer GC content between 40-60% and with minimum self and pair complementarity. To reduce the likelihood of genomic DNA amplification, primers were designed to span an intron. Primer specificity was checked using the basic local alignment tool (BLAST) available through NCBI (*http://www.ncbi.nlm.nih.gov/tools/primer-blast/*).

Primers were reconstituted in nuclease-free water to obtain a stock concentration of 100µM and tubes were heated at 65ºC for 15 minutes. In order to prepare a working solution for each primer pair, a volume of 20µl from each primer set was added to 60µl of nuclease-free water, briefly mixed and stored at -20°C. For RT-PCR and qPCR, primers were used at a final concentration of 500nM.

2.6. Polymerase chain reaction (PCR)

All cDNA samples were qualified by PCR using primers designed to detect the ubiquitously expressed control gene, *Gapdh*. PCR mixtures were prepared on ice in a reaction volume of 25µl. Each PCR mixture consisted of 1µl of cDNA (cDNA concentration was normalised for each individual experiment) as a template, 12.5µl of 2x Taq Red PCR Mix (Bio-Line), 0.5µl (500nM) of premixed forward and reverse primers, and the volume was completed by 11µl of nuclease-free water. For the negative control, nuclease-free water (1µl) was added instead of cDNA template; *Gapdh* primers was utilised as a positive control for the PCR reactions.

Samples were cycled in a thermal cycler (GeneFlow) by initial denaturation at 95°C for 3 minutes, followed by 32 cycles of denaturation at 95°C for 15 second, annealing at 58°C for 15 seconds, extension at 72°C for 10 seconds, with a final hold at 4°C.

2.7. Agarose gel and electrophoresis

A 2% agarose (w/v) (Bioproducts) was prepared in 1X TAE (Tris (Hydroxymethyl) aminomethane; BDH Prolabo) by heating in the microwave for 2-3 minutes. To visualise DNA bands, 0.01% (v/v) gel red nucleic acid stain (Biotium) was added to the cooled agarose solution before being poured into the gel cassette where it was kept to set at room temperature for 20 minutes. The gel was covered in 1X TAE buffer. DNA hyper ladder 5µl (Bioline, BIO-33057) and 12.5µl of amplified PCR products were loaded into the gel wells. A non-template (negative) control was included in each experiment. Samples were run at 80 volts for an hour and 45 minutes. Bands were visualised and imaged by an ultraviolet transilluminator (Geneflow).

2.8. Quantitative polymerase chain reaction (qPCR)

Relative expression levels of candidate gene transcripts were determined by qPCR using an Applied Biosystems 7900HT Fast instrument (Applied Biosystems Inc.). For each sample, two technical replicates were prepared in a 384-well plate (Applied Biosystems). Each single reaction mix (20µl) included nuclease-free water, 2X SensiFAST SYBR Hi ROX Mix (Bioline) or KAPA SYBR Green (KAPA Biosystems) and ROX dye (KAPA Biosystems), and 500nM of premixed forward and reverse primer. The equivalent concentration of ATP synthase subunit beta *Atp5b* (1µl) (Primerdesign) or *Hprt1* were used as housekeeping genes. For each gene, an equal concentration of cDNA was added (1µl) to 19µl of reaction mix using automated pipettes. Control groups (non-template) were included in each qPCR experiment where nuclease-free water was added instead of cDNA. qPCR plates were sealed by the optical adhesive cover (Applied Biosystems) and centrifuged (Fisher Scientific-Accuspin 3R) at 500rpm for 1 minute. Thermal cycles were initiated by denaturation for 2 minutes at 95°C, followed by cycles of 5 seconds at 95°C, annealing for 10 seconds at 58°C, and extension at 72°C for 12 seconds. Melt curve data were collected for all PCR products to confirm consistency and specificity. For each technical replicates, the average cycle number at threshold (CT) were recorded. Then, ΔCT values were determined by subtracting the average CT value of the internal reference gene *Atp5b* or *Hprt1* from the averaged values of targeting gene.

To calculate the ΔΔCT values, ΔCT values of the treatment groups were averaged and the number was subtracted from the ΔCT of the control group. The fold changes in gene expression were calculated using the equation $2^{-\Delta\Delta CT}$ (Livak and Schmittgen, 2001).

2.9. Tissue processing protocols

2.9.1. Fixation, embedding and sectioning of whole ovaries

Freshly dissected mouse ovaries (all ages) were immediately immersed in 10% neutral buffered formalin solution (v/v, Sigma) for 24 hours, and then transferred into 70% ethanol (v/v) until being processed in paraffin blocks. Ovaries were dehydrated by immersing in 70% ethanol, 90% ethanol (v/v) followed by three changes in 100% ethanol for 20 minutes each. Tissue was cleared in Histochoice solvent- clearing agent (Sigma) for 60 and 30 minutes, respectively. Ovaries were transferred to embedding molds and melted paraffin was poured in molds for 60 minutes at 60ºC before applying the plastic cassette and allowing the blocks to cool on ice. Paraffin blocks were sectioned at 5µm using a manual processing microtome (Reichert-Jung). Sections were mounted on positively charged slides in a water bath at 45ºC and were dried overnight at 37ºC.

2.9.2. Fixation, embedding and sectioning of cultured follicles

At the end of culture, follicles from each group (5-7 follicles) were fixed in a single well of a 96-well plate using 10% neutral buffered formalin (Sigma) for 30 minutes. After washing with PBS, follicles were placed in a drop of preheated (60ºC) 1% (w/v) low gelling temperature agarose (Sigma). As the agarose semi-congealed, a drop of nuclear fast red stain (Sigma) was applied to aid visualisation of the follicles. Each gel was cut into small cube containing follicle samples (Figure 2.2). Agarose cubes were submerged in Eppendorf tubes containing 70% ethanol prior to processing in paraffin embedding as described in 2.9.1. Embedded follicles were sectioned at 5µm and sections were mounted on positively charged slides.

Figure 2.2. An example of preantral follicles embedded in agarose.

2.9.3. Immunofluorescence staining in ovary and follicle sections

Immunofluorescence staining was performed to support PCR data of some candidate genes and to localise their proteins to specific cells and follicle types in the ovary. Several troubleshooting of some staining problems were stated in Appendix V. Ovary or follicle sections were dewaxed (2x5minutes) in Histochoice (Sigma), rehydrated in a graded series of ethanol solutions of 100%, 95%, and 70% (3 minutes each), and washed in distilled water (5 minutes). To unmask the antigen, sections were microwaved in 0.1 M citrate buffer (pH 6.0) for 20 minutes. Sections were washed in PBS (2x5 minutes each) before blocking with CAS (CAS-Block; Invitrogen) for 15 minutes at room temperature. Primary antibodies were diluted in the blocking solution at an appropriate concentration that was previously optimised by titrating.

Antibodies were applied to sections and incubated overnight at 4ºC in a humidified chamber. Negative controls were included for each staining, where equivalent concentrations of non-immune mouse IgG or Rabbit IgG (Vector) were used to determine non-specific staining. For double labelling (colocalisation), both primary antibodies or non-immune mouse IgG and Rabbit IgG (controls) were prepared in the same tube and were incubated together. After the overnight incubation, sections were washed in PBS three times for 10 minutes. Fluorescent secondary antibodies (Invitrogen) were diluted 1:200 in PBS, added to the sections and incubated in dark humidified chamber at room temperature.

For double labelling, both specific secondary antibodies were prepared and applied at the same time. After 45 minutes of incubation, slides were washed in PBS twice for five minutes each. A coverslip was mounted to each slide after addition of 30µl of Prolong Gold anti-fade reagent with DAPI (Invitrogen). Slides were allowed to dry in the dark for at least 1 hour before storing at 4ºC prior to imaging. Stained ovary sections were imaged using Leica inverted SP5 confocal laser scanning microscope (Leica Microsystems, Wetzlar, Germany). Images presented in this study were taken from sections stained in the same run, using the same laser and gain settings. Stained follicles were imaged with either an Olympus IX73 inverted microscope supplemented with Photometrics-CoolSNAP HQ camera, or with an inverted Widefield fluorescence microscope (Leica DMI4000B).

The double labelling protocol was often assessed by colocalisation of Smad2/3 (0.25µg/ml, Santa Cruz sc-133098) and Ddx4 (5µg/ml; Abcam, ab13840) proteins in d8 ovary section as a reliable and consistent positive control (Figure 2.3). In addition, positive control staining was also included for preantral follicle staining, see Appendix VI.

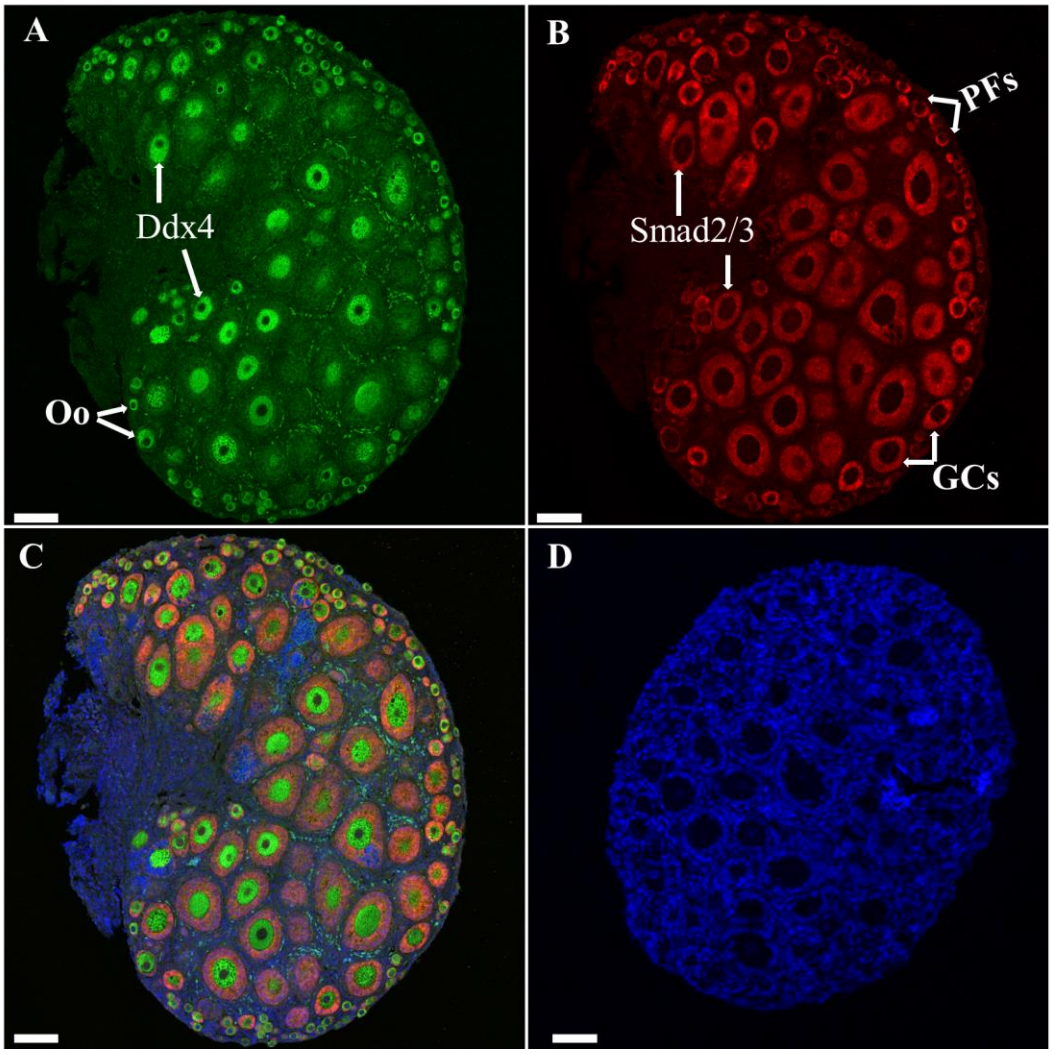

Figure 2.3. Immunofluorescent colocalisation of Smad2/3 and Ddx4 in the ovary. In order to evaluate the protocol of double staining used in this study, Ddx4 and Smad 2/3 were used as positive control of staining in day8 ovary sections. Ddx4 (A-green) was specifically localised in the oocytes (Oo); while Smad 2/3 (B-red) were detected in the granulosa cells (GCs) with high intensity of staining in primordial follicles (PFs). Merged image (C) revealed the specific localisation of both proteins. Negative control ovary sections (D) were treated with a mixture of non-immune Rabbit and Mouse IgG. Both stained and control sections were treated with Alexa Donkey anti-Mouse 555 and Donkey anti-Rabbit 588 secondary antibodies. Nuclei (blue) were stained with DAPI. Scale bar 100µm.

2.9.4. Immunofluorescent staining of cultured ovary fragments

At the end of culture, media was removed, and cultured fragments were double washed (two minutes each) with PBS. Ovary fragments were fixed in neutral buffered formalin (Sigma) for 30 minutes, followed by washing twice with PBS for two minutes each. To enhance cell permeability, fragments were treated with 0.25% (v/v) Triton (Sigma) in PBS for 10-15 minutes, followed by three further washes of PBS for three minutes each.

To reduce nonspecific binding, fragments were incubated in CAS-Block (Invitrogen) for 20 minutes at room temperature. A mixture of Rabbit anti-Ddx4 (5µg/ml; Abcam, ab13840) and Mouse anti-Amh (1:400; MCA2246; AbD Serotec, Oxford, UK) was added to wells overnight at 4ºC. After washing in PBS (3x5 minutes), Alexa Fluor 555 Donkey anti-Mouse IgG and Alexa Fluor 488 Donkey anti-Rabbit (both 1:400) secondary antibodies were added for 45 minutes. Ovary fragments were washed in PBS (2x2 minutes each) and were counterstained with 10µg/ml DAPI (Thermo Scientific) for 10 minutes. Then, the DAPI solution was replaced with PBS. Stained tissues were imaged with an Olympus IX73 inverted microscope.

2.9.5. Haematoxylin- Eosin staining

Hematoxylin and eosin staining was utilised for the staining of d4, d8, d13, d16 and adult ovary sections. The purpose of staining was either for follicle classification or to show the histological tissue characteristic in these ages. The protocol of staining included dewaxing the slides in Histochoice (2x5 minutes, Sigma), followed by a series of rehydrating steps in different concentrations of ethanol (99%, 95%, and 70% for 5 minutes each). After one minute of washing under tap water slides were submerged in Gills haematoxylin II stain (Surgipath) for 90-120 seconds and were rinsed under tap water to remove extra staining for three minutes. Then, slides were submerged in aqueous eosin 1% (Diagnostics) for five minutes followed by 30 seconds washing in tap water. Sections were dehydrated in 70% ethanol and 95% ethanol for 10 seconds each, followed by two steps in 99% ethanol for 30 seconds each. To clear sections and remove ethanol, sections were submerged two times in Histochoice (Sigma) for 1 and 3 minutes, respectively. Finally, sections were mounted with DPX (Merck) and coverslipped. Stained sections were imaged with an Olympus CKX41 microscope and Nikon DS-Fi1 camera.

2.10. Identification rate of follicle growth

2.10.1. Measurement of the cultured preantral follicles

Preantral follicles were imaged by inverted light microscopy (Olympus CKX41 with a Nikon camera DS-Fi1) at 0h, 24h, 48h and 72h. Images were utilised for estimation of follicle diameters where two measurements were taken from the basal lamina of the granulosa cells (basement membrane) (Figure 2.4). The vertical and horizontal measurements were averaged and were presented as follicle diameter.

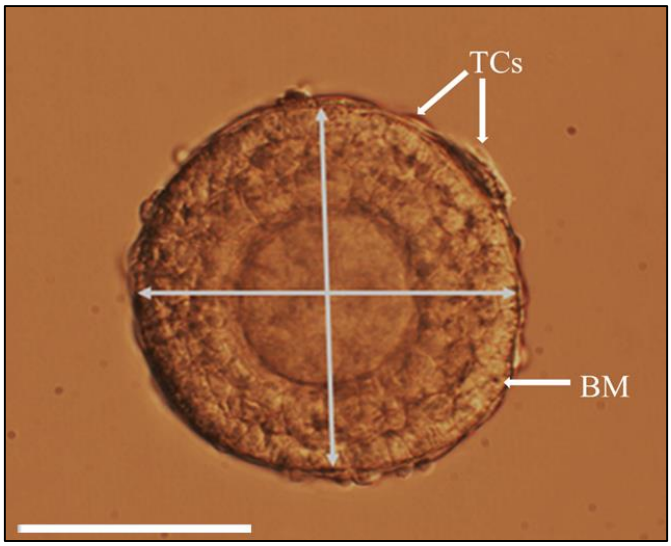

Figure 2.4. Light microscopy image of cultured preantral follicle showing a method of follicle measurement. ImageJ software was utilised to measure follicle diameter by averaging the vertical and horizontal diameter taken from the basement membrane (BM). Theca cells (TCs) were excluded from measurement. Scale bar 100µm.

2.10.2. Oocyte measurements in cultured ovary fragments

In order to identify the effect of different treatments on follicle growth, cultured fragments were imaged using an Olympus CKX41 with a Nikon camera DS-Fi1. The accurate measurement of oocyte size was determined with the ImageJ software after calibration certificates using a stage micrometre (Graticules PYSER-SGI). In order to identify oocyte diameter, a vertical and horizontal line was recorded for each oocyte (Figure 2.5). The two measurements were averaged and were presented as the diameter of the oocyte. Only round, clearly identifiable oocytes were measured, while atretic or misshapen oocytes were not included.

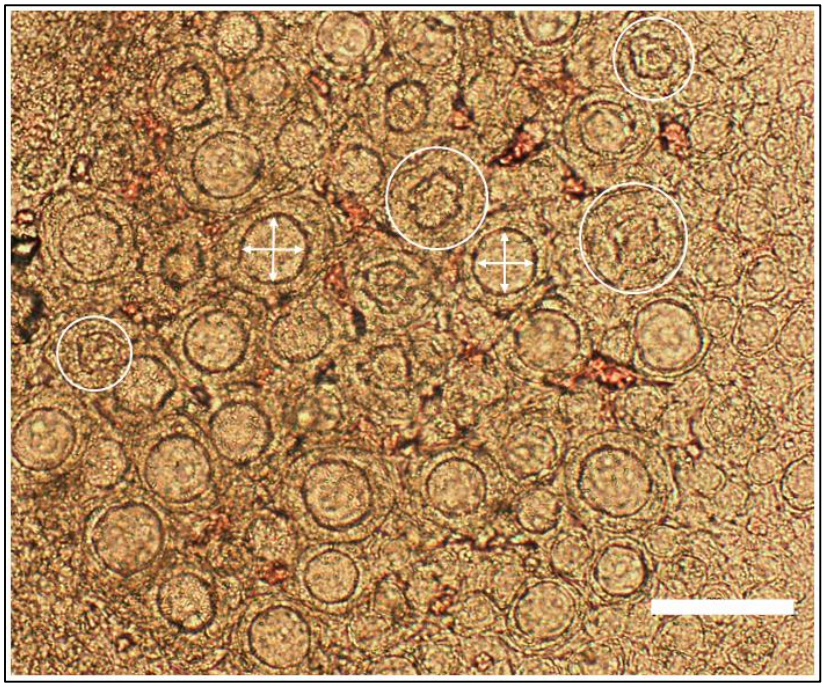

Figure 2.5. An example of a light microscopy image of a cultured ovary fragment showing the method of oocyte measurement. Both vertical and horizontal lines (white arrows) were estimated from the external surface of the oocytes using ImageJ software. The two measurements were averaged and the estimated number was presented as the diameter of a single oocyte. Atretic oocytes (white circles) were excluded from measurements. Scale bar = 200μm.

2.11. Classification of oocytes

Haematoxylin and eosin stained sections from immature mouse ovaries at d4 (n=5), d8 (n=8), d13 (n=5) and d16 (n=7) were used to stage oocytes and apply this information to classify oocytes from cultured ovary fragments. For all ages, one stained section was used for the measurement of oocyte diameters using ImageJ software (Appendix VII). Oocyte diameters were estimated only in follicles that had a clearly identifiable oocyte nucleus. In addition to the oocyte diameter, oocytes were classified by considering the morphology and number of granulosa cells layers contained within the follicle. An oocyte that was surrounded by a monolayer of flat cells was considered non-growing. Oocytes surrounded by one layer of granulosa cells that included both cuboidal and flat cells were scored as transitional. Large oocytes with at least one complete layer of cuboidal granulosa cells were classified as growing (Figure 2.6-A).

Data were plotted and presented as mean ±1 SD where each single point represents a single oocyte (n=992 non-growing, n=292 transitional, n=331 growing). Classification of oocytes was based on the mean ±1SD above and below the transitional group specified by the shaded area on the graph (Figure 2.6-B). Thus, oocytes were categorised according to the diameter either as non-growing (<18.3µm), transitional (18.3-25.7µm) or growing (>25.7µm).

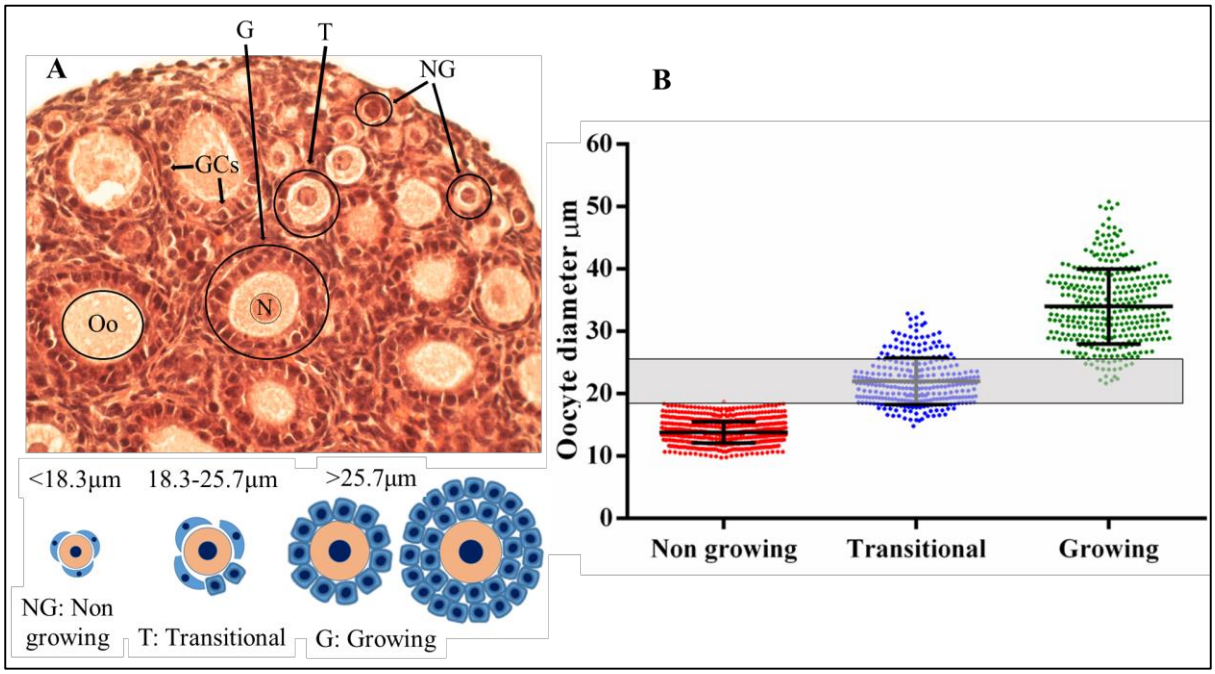

Figure 2.6. Classification of oocytes from H&E stained mouse ovaries. Paraffin-embedded ovary sections from immature mouse ovaries at d4 (n=5), d8 (n=8), d13 (n=5), and d16 (n=7) were stained with haematoxylin and eosin. Only oocyte (Oo) that had a clearly recognised nucleus (N) and pre/granulosa cells (GCs) were included (A). Any oocyte smaller than one standard deviation from the mean of the transitional category was defined as non-growing (NG: <18.3µm), and conversely any oocyte larger than one standard deviation from the mean of the transitional category to be defined as growing (G: >25.7µm). Any oocyte diameter between these boundaries was defined as transitional (T: 18.3µm-25.7µm). Across all ages, 992 non-growing, 292 transitional and 331 growing preantral follicles were measured. These criteria were used to classify oocytes in treated ovarian fragment cultures.

Chapter 3

Identification and expression of receptor-regulated Smads and candidate Smad inhibitors during early follicle development.

3.1. Introduction

The mammalian ovary is a multifunctional structure containing follicles at different growth stages (Hirshfield, 1991). The earliest stage of follicle development is the quiescent primordial follicle where a relatively small sized oocyte is surrounded by a single layer of flattened granulosa cells (McGee and Hsueh, 2000). Even though the primordial follicle represents a fundamental unit of the ovary that determines the length of the reproductive lifespan (Kim, 2012; Zheng et al., 2014) factors responsible for maintaining their quiescent state or regulating early follicle growth remain unclearly defined; many studies have revealed that these two processes are controlled by various local signalling pathways including the TGFβ pathway (Kezele et al., 2002; Kim, 2012; Wang et al., 2014).

In the ovary, several studies have investigated the role of the TGFβ superfamily and its respective mediator elements in follicle development (Li et al., 2008b; Pangas, 2012). The TGFβ superfamily regulates a variety of cellular function, such as cell survival and apoptosis, and comprises more than 30 structurally related members including TGFβ, Activin/Inhibin, Nodal, Bmp, Gdf9, and Amh (Shi and Massague, 2003; ten Dijke et al., 2000). Canonical TGFβ signalling is initiated by the interaction between TGFβ ligands with a receptor complex leading to the activation of R-Smads by phosphorylation (Bakkebo et al., 2012; Derynck and Zhang, 2003). In order for translocation into the nucleus, phosphorylated R-Smads associate with the common mediator Smad4 (Inman et al., 2002).

In many instances, the Smad signalling pathway activates a self-regulatory mechanism by inducing the expression of inhibitory factors (Quezada et al., 2012; ten Dijke and Hill, 2004). In other tissues, many factors are identified as intracellular Smad inhibitors, which attenuate or inhibit TGFβ/Smad signalling at different levels through various molecular mechanisms (Lonn et al., 2009). For example, Strap and Smad7 cooperate to inhibit signalling at the receptor level by preventing the interaction of Smad2/3 with the activated receptors (Datta and Moses, 2000). SnoN, Smurf1, and Smurf2 have the potential to inhibit Smad2/3 phosphorylation and interfere with their nuclear translocation (Inoue and Imamura, 2008; Moustakas and Heldin, 2009), while Ppm1a can inhibit transcription by dephosphorylation of R-Smads (Dai et al., 2011) (Figure 3.1).

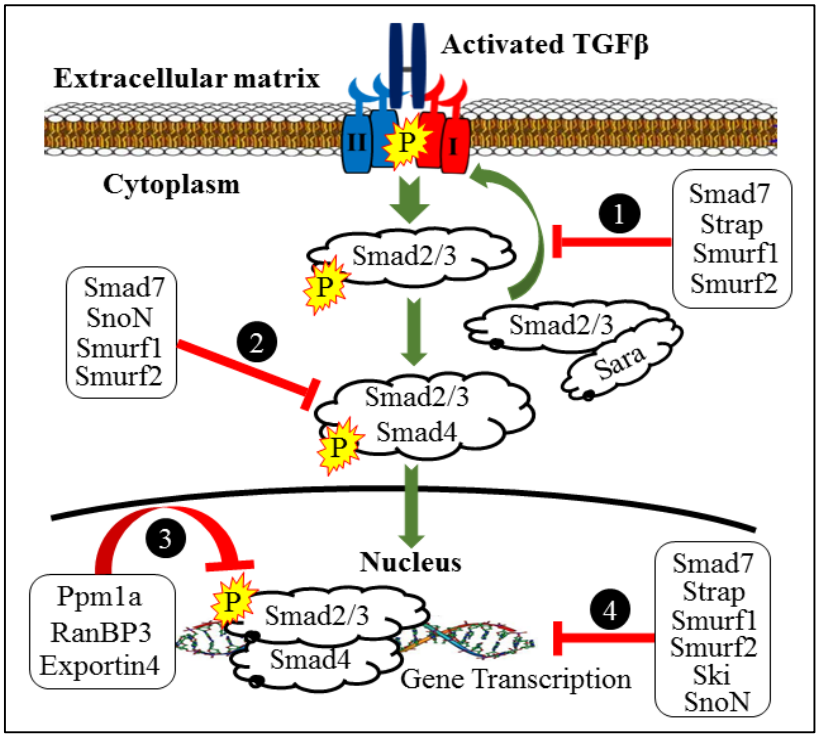

Figure 3.1. Intracellular negative regulatory mechanisms of TGFβ/Smad2/3. Inhibition or attenuation of TGFβ/ Smad2/3 signalling is achieved at different cell levels and mechanisms. Some of the Smad inhibitors have the potential to antagonise signalling at more than one level. Mechanisms of signalling include preventing the interaction of Smad2/3 with the activated receptor complex (1), inhibition of the heteromeric complex formation between Smad2/3 and Smad4 (2), dephosphorylation of activated Smad2/3 and enhancing their exclusion from the nucleus (3), or by inhibition of gene transcription by interrupting the association between Smads and DNA (4).

In the ovary, R-Smad elements are differentially localised in granulosa cells of both the quiescent and growing follicles (Billiar et al., 2004; Fenwick et al., 2013), and their role in the follicle development has been investigated using various culture models (Ding et al., 2013; Li et al., 2008b; Tomic et al., 2004). However, the negative regulatory mechanism for R-Smads and its impact on follicle development are yet to be defined. Thus, we hypothesise that Smad inhibitors, particularly those regulate the Smad2/3 pathway, might also be detectable in the ovary and be associated with early follicle development. This study was carried out using mouse ovaries and isolated follicles at different developmental stages to achieve several aims including the expression of nine candidate Smad2/3 inhibitors (selected from the literature as being important in other tissues) in isolated follicles and oocyte samples. Secondly, to determine the expression profile of these candidates in ovaries containing different proportions of primordial and early preantral follicles. Finally, to determine the relationship between key R-Smad inhibitors and Smad2/3 during early follicle development.

3.2. Materials and Methods

3.2.1. Instruments and chemicals

All instruments, chemicals, and buffer recipes used in this chapter listed in Appendix II-IV.

3.2.2. Tissue collection (ovaries and follicles)

Mouse ovaries from d4, d8, d16 and adults mice were used in this chapter for mRNA and protein expression. Ovaries were dissected as described in 2.1. In order to identify the histological features of each age group, ovary sections (5µm) were stained with haematoxylin and eosin (section 2.9.5). In addition, isolated follicles at different stages of development ranged from primordial to large antral follicles, and oocyte samples (Appendix VIII) were used for RNA extraction and gene analyses. These follicles were mechanically isolated from neonatal, juvenile and adult mouse ovaries and immediately stored at -80ºC.

3.2.3. RNA extraction, cDNA synthesis and RT-PCR/qPCR

Total RNA was extracted from ovaries and follicles using Qiagen RNeasy Micro Kits (Qiagen; Crawley, West Sussex, UK), as described in 2.3. For follicle and oocyte samples, since these samples consist of a small amount of starting materials, the extracted RNA was concentrated first by vacuum centrifugation for 6.5 minutes before being stored at -20ºC. For each sample, the entire volume of extracted RNA was reverse transcribed and utilised for cDNA synthesis. Follicle and oocyte cDNA samples were diluted 1x with RNase/ DNase free water. All samples were subjected to 32 cycles of amplification to detect *Gapdh* as an indicator of cDNA quality. RNAs extracted from all ovary samples were tested for integrity and concentration using the Bioanalyser (Agilent).

Similar criteria shown in chapter 2 (Figure 2.1) were followed to identify a high-quality RNA for cDNA synthesis. For all ovary samples (n=7ovary/age group, 6 for the adult group), equal quantities (50ng/µl) of analysed RNA were used for the preparation of cDNA according to the methods described in section 2.4. All ovary cDNA samples were diluted 2x with a volume of 20µl of RNase/DNase free water before being utilised for gene expression. All cDNA samples were checked for quality using RT-PCR prior to their use in qPCR reactions (Figure 3.2).

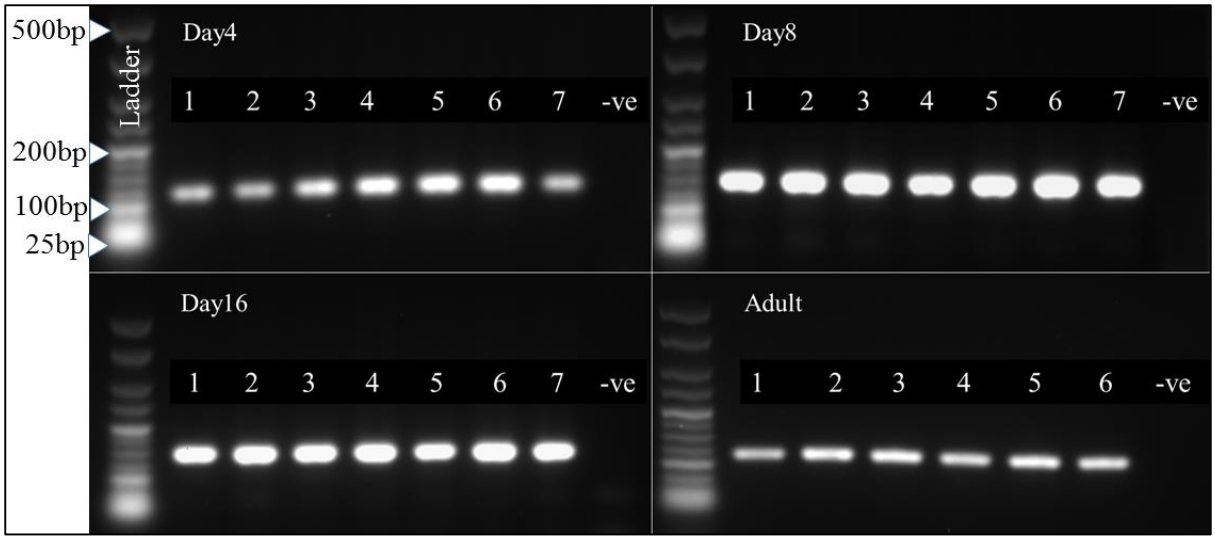

Figure 3.2. Qualification of ovary cDNA samples by RT-PCR. Agarose gel images showing the expression of *Atp5b* (120bp) in day4 and adult ovaries and expression of *Gdf9* (139bp) in days8 and 16 samples. For negative control (-ve), RNase/ DNase free water was added rather than cDNA.

Primers used to determine the expression of *Smads* and candidate Smad inhibitory factors by RT-PCR and qPCR are presented in Table 3.1. In addition, primers for seven positive control genes, which are known to be expressed in specific follicle cells and oocytes, were also designed and related to the follicle samples. For example, *Amh*, and its receptor (*Amhr2*) is not detectable in oocytes and primordial follicles, while its expression is largely increased in granulosa cells of early growing to the preantral stage with a noticeable decline in later advanced stages (Durlinger et al., 2002; Weenen et al., 2004). Conversely, *Gdf9* is exclusively expressed in the oocyte, thus, it should be expressed by all follicle samples, but not in isolated granulosa cells (Hanrahan et al., 2004). *Cyp17a* is a specific marker of theca cells (Vitt et al., 2000), while *Kl1* and *Kl2* are expressed in granulosa cells of all growing follicles (Parrott and Skinner, 2000). Similar protocols described in chapter 2 were followed for RT-PCR reaction mix preparation/ PCR running (2.6), gel electrophoresis (2.7), and qPCR reactions (2.8) using specific annealing temperatures as listed in Table 3.1.

Table 3.1. Oligonucleotide primer sequences used to amplify mRNAs of candidate genes by RT-PCR and qPCR. Primers were designed and prepared as previously described in 2.5.

Gene	Primer sequences (5' →3')	Annealing Temperature	Product size (bp)
Amh	F: GGGGCACACAGAACCTCT R: GCACCTTCTCTGCTTGGTTG	60	124
Amhr2	F: ACAGCATGACCATATCGTTCG R: GAGTCAAGTAGTGGCATAAGGAG	56.4	122
Cyp17a	F: GATCGGTTTATGCCTGAGCG R: TCCGAAGGGCAAATAACTGG	57	81
Exportin 4	F: TAACTTAGGGCGGCAAAGGA R: TAAAACGACATCAGCTGCCG	59	193
Fshr	F: ACAACTGTGCATTCAACGGAAC R: GACCTGGCCCTCAACTTCTT	58.4	187
Gapdh	F: CTGCCGTCTAGAAAAACC R: GGTATGACAACGAA	58	120
Gdf9	F: TCACCTCTACAATACCGTCCGG R: GAGCAAGTGTTCCATGGCAGTC	59	139
Kl1	F: GATTCCAGAGTCAGTGTCAC R: CCAGTATAAGGCTCCAAAAGCAA	58	192
Kl2	F:TTGTCAAAACCAAGGAGATCTGCG R: CTTTGCGGCTTTCCCTTTCTC	58	471
Ppm1a	F: GTGAGAACATCCCCAGC R: TCGGTTGACGCAGAATCA	58	167
Ranbp3	F: AACTCCAGGCTCAGCATTCT R: GAGCATCAAGTCAGCTCAGC	59	154
Ski	F: ACACAGCACAACGTCTCTAC R: CAAGCAGAGAACCAGCTACG	57.5	171
Smad 1	F: ACCTGCTTACCTGCCTCCT R: GCCTGAACATCTCCTCTGCT	59	114
Smad 2	F: CGTCCATCTTGCCATTCAC R: GTCCATTCTGCTCTCCACCA	60	102
Smad 3	F: GTCAAAGAACACCGATTCCA R: TCAAGCCACCAGAACAGAAG	85.5	154
Smad 4	F: CGGCGATTGTGCATTCTCAG R: CCTGGAAATGGTTAGGGCGT	60	209
Smad 5	F: CCTTGCTCATCTCCCTGTCT R: CCGTGAATCTCCTTTCTGTG	85.8	173
Smad 9	F: GTCTGACCTTGCAGATGGCT R: TAGGTGCCAGGCTGAGAGAT	60	235
Smad7	F: AGTCAAGAGGCTGTGTTGCTGT R: CATTGGGTATCTGGAGTAAGGA	60	130
Smurf1	F: CAGACAGCAACATCGTCAGG R: CAGGTGAATGGTGAACAGCC	58	164

Smurf2	F: AGTGTAACTCAGCCTGGTGG R: GAAAGCAGCGTCTCCTTAGC	59	164
SnoN	F: GCACCTGTGACTCAACCTTG R: CTCCAGCTTCTGTCTTGCCT	59	152
Strap	F: GGCTACTTTCTGATCAGCGC R: CTGAGACCGCATCCCATACT	59	187

3.2.4. Tissue processing and staining

Mouse ovaries at specific ages (d4, d8, d16 and adult) were dissected, processed for paraffin embedding and sectioned for staining. Protocols described in chapter 2 were followed for localisation and colocalisation of different proteins (Table 3.2) by immunofluorescence staining (2.9.3). For negative control, equivalent quantities of non-immune Rabbit and/or Mouse IgG (Vector) were used to determine non-specific staining in ovary sections.

Table 3.2. Primary and secondary antibodies used for immunofluorescent staining

Primary antibody	Company	Dilution and/ or concentration	Secondary antibody (Invitrogen)
Rabbit anti- Ppm1a	Abcam Ab154489	1:200 1.25µg/ml	Alexa fluor 488 Donkey anti-Rabbit
Rabbit anti- Smad 1/5/8	Santa Cruz sc-6031-R	1:400 0.5µg/ml	Alexa fluor 488 Donkey anti-Rabbit
Mouse anti-Smad2/3	Santa Cruz sc-133098	1:800 0.25µg/ml	Alexa fluor 555 Donkey anti-Mouse
Rabbit anti-Smad2/ 3	Cell Signalling ≠5678	1:400	Alexa fluor 488 Donkey anti-Rabbit
Mouse anti- Strap	Santa Cruz sc-136083	1:300 0.3µg/ml	Alexa fluor 555 Donkey anti-Mouse

3.2.5. Statistical analysis

Data (CT values) from qPCR were normalised relative to the expression of the internal housekeeping gene (*Atp5b;* PrimerDesign, Southampton, UK). Fold changes relative to d4 ovaries were calculated using the $2^{-\Delta\Delta CT}$ method, as described in 2.8. One-way ANOVA with Bonferroni post-hoc test was used to compare gene expression in d8 and d16 ovaries relative to d4. Results were presented as mean ± SEM and difference were considered statistically significant if $P<0.05$.

3.3. Results

Follicle stages presented in ovaries of immature (d4, d8 and d16) and adult mice were determined with haematoxylin and eosin staining, where primordial follicles are obviously decreased with age (Figure 3.3)

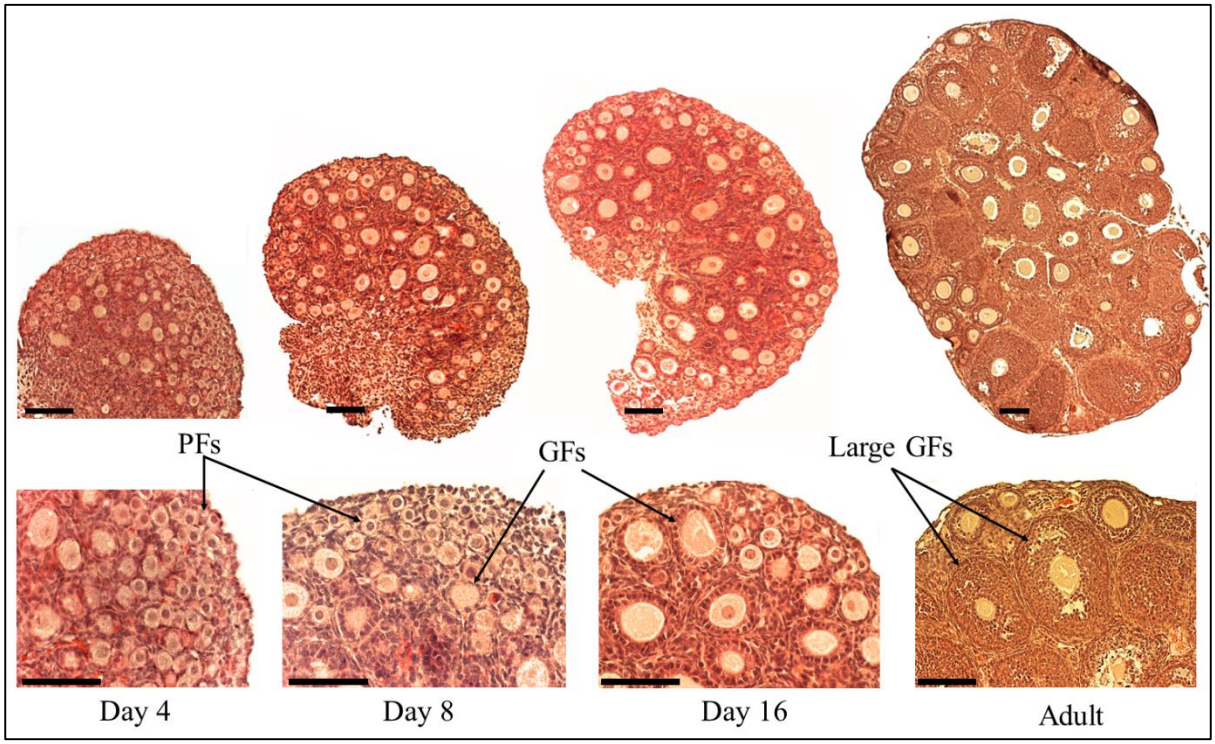

Figure 3.3. Haematoxylin and eosin staining of ovary sections from d4, d8, d16 and adult mice. In the d4 ovary, the non-growing primordial follicles (PFs) constitutes the majority of the follicle population. At d8 several follicles are activated to grow (GFs), while at d16 more growing and multi-layered follicles have developed. In d8 and d16 ovaries, growing follicles are located in the middle of the ovary, while primordial follicles are generally situated closely to the ovary surface. In the adult ovary, the population of primordial follicles is markedly decreased and more advanced stages of follicle growth (large GFs), including antral follicles, are evident. Scale bar 200µm.

3.3.1. Expression of control genes in follicle samples.

Seven factors, which are essential for follicle development and growth, were used as positive controls for isolated tissue samples taken from the ovary. These samples were assayed to confirm the initial follicle staging during isolation. *Kl and Kl2* isoforms were similarly expressed in all stages of growing follicles from primary to the large antral follicle and with a light band in cumulus oocyte complex COCX sample (a mature oocyte surrounding by somatic cumulus cells). *Amh*, a granulosa cell-specific gene and its receptor, *Amhr2*, were detectable in all growing stages but was absent in the primordial follicles, large antral, and oocyte samples. *Gdf9*, an oocyte-specific gene, was detected in all samples where multiple oocytes were present. The large pre-antral and large antral follicle samples only contained two and one

oocytes, respectively, and this was insufficient to detect *Gdf9* mRNA. *Fshr* was expressed in all growing follicles except the large antral follicle and oocytes. The androgen biosynthesis enzyme, *Cyp17a*, which is normally expressed in theca cells, was only detectable in the advanced stages of the growing follicles, particularly in the large pre-antral follicles. These results (Figure 3.4; Appendix IX) provide confirmation of the initial staging of the follicle and oocyte samples, as PCR expression generally reflected the known cell and follicle stage-specific expression.

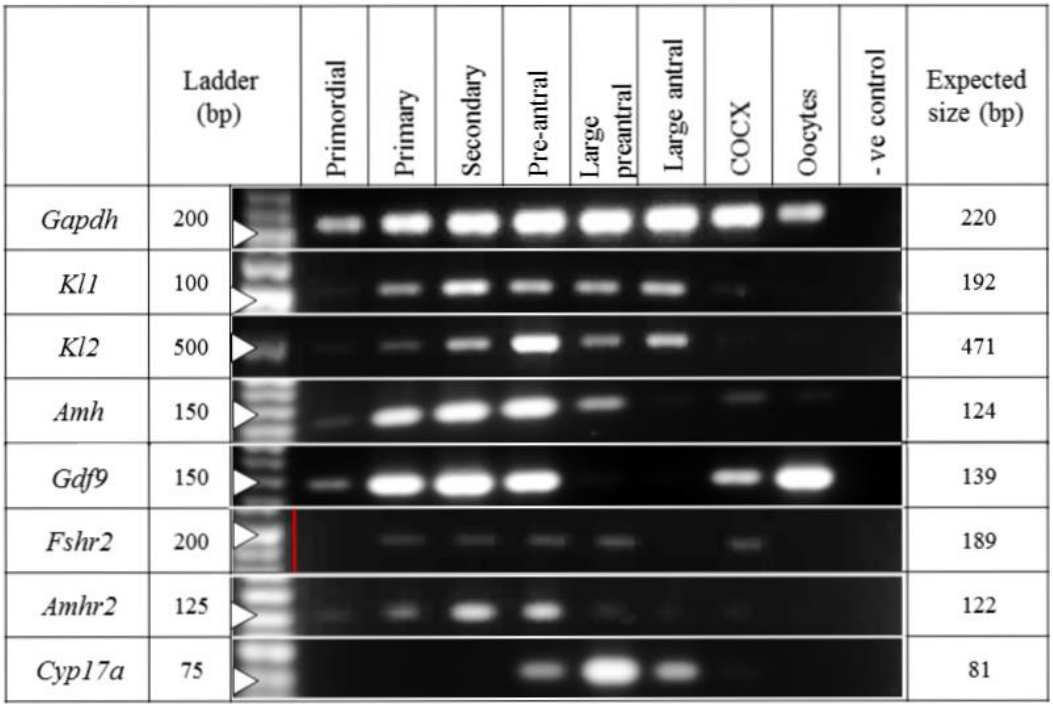

Figure 3.4. Expression of mRNA of control genes in follicles and oocytes samples. Follicle samples were mechanically isolated from mouse ovaries. The non-growing primordial follicles were obtained from a postnatal d4 ovary where the ovary was cut into small fragments. Oocytes (n=12) and growing follicles including primary, secondary and preantral stages (n= 5 follicles each) and were isolated from d 16 ovary. Large preantral, antral follicles and COCX (n= 2, 1, 6, respectively) were isolated from mature mouse ovaries. After isolation, all follicle and oocyte samples were immediately snap frozen and stored at -80ºC for RNA extraction. The red line in *Fshr2* gel represents to a pasted ladder. For negative control (-ve), RNase/ DNase free water was added rather than cDNA.

3.3.2. Expression R-Smad mRNA in follicle samples

Transcripts for the R-Smad (*Smad 1, 2, 3 and 5*) were expressed in all stages of follicle growth and oocyte samples by RT-PCR. However, by comparison with *Smad1* and *Smad5*, expression of *Smad2* and *Smad3* were stronger in the primary and secondary follicle samples. Weak bands were detected for all R-Smad transcript in primordial and COCX samples (Figure 3.5).

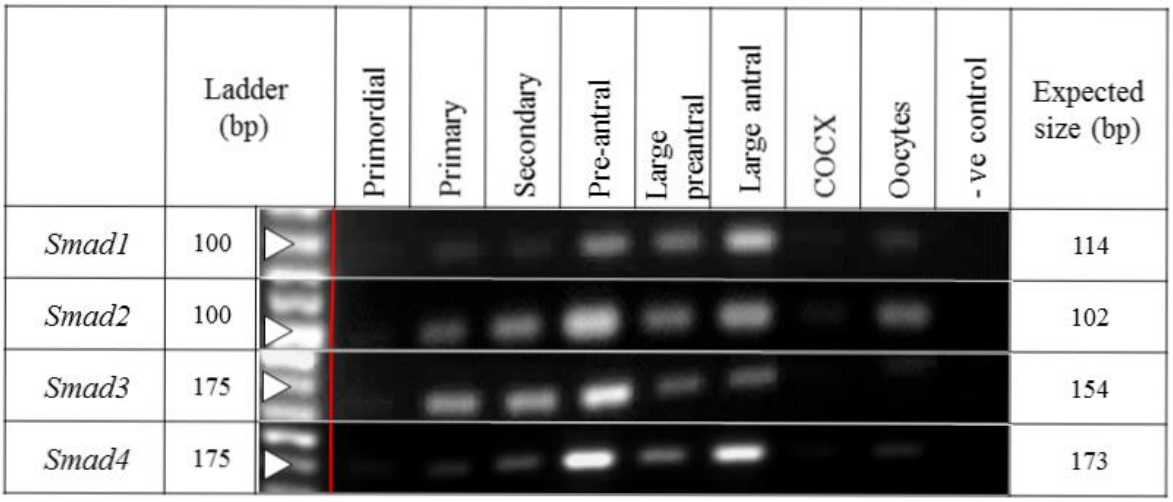

Figure 3.5. Expression of R-Smad transcripts in follicle and oocyte samples using RT-PCR. *Smad2* and *Smad3* were detectable with stronger bands in the earlier stages of follicle development relative to *Smad1* and *Smad5*. Red lines in gels represent to pasted ladders. Negative controls consist of RNase/ DNase free water instead of cDNA.

3.3.3. Expression and quantification of R/Co-Smad transcripts in ovary samples

Transcripts for *Smad1, 2, 3, 4, 5 and 8* were detected in cDNA derived from immature and adult ovary samples (Figure 3.6). *Smad1* and *Smad2* were weaker in d4 and d8 ovary samples, while the intensity was increased in d16 and adult samples. In d4 ovary, *Smad3* produced the strongest band compared with other Smads. *Smad8* expressed with weak bands in immature ovaries, while a strong band was revealed in adult ovary sample. *Smad4* was expressed with a band in d4 ovary, while the intensity was obviously increased in d8, d16 and adult ovaries. In general, expression bands of *Smad3* and *Smad5* were more constant than *Smad1*, *Smad2* and *Smad8* in all ovary samples.

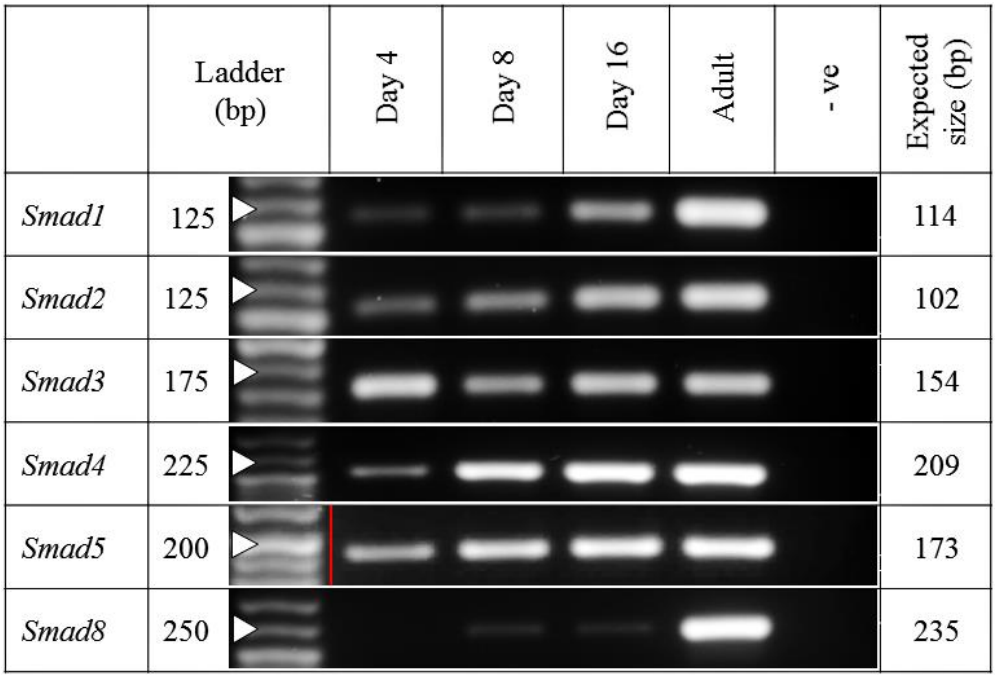

Figure 3.6. Expression of R-Smad and co-Smad transcripts by RT-PCR in mouse ovaries. The intensity of *Smad1* and *Smad2* bands appeared to increase with age, while the intensity of *Smad3* and *Smad5* were more consistent in ovary samples. *Smad4* expressed with a small band in d4, but with stronger and consistent bands in older age groups. In contrast to adult sample, *Smad8* lightly expressed in immature ovary samples. The red line in *Smad5* gel represents to a pasted ladder. Negative controls (-ve) were included where RNase/ DNase free water was added rather than cDNA.

In addition, qPCR was performed to identify the relative mRNA expression of *Smad1, 2, 3, 4, 5* and *Smad8* in ovaries of different ages (Figure 3.7). Adult ovary samples were also assayed to provide more information on the expression levels of R-Smads in mature ovaries. However, since adult ovaries contain numerous antral follicles, atretic follicles and corpora lutea, structures which are mostly absent from juvenile ovaries, adult ovary samples were not considered comparable and were therefore excluded from statistical analyses of the qPCR data. *Amh* (positive control) transcript levels were significantly increased in the d16 ovary, which contains a high proportion of multi-layered growing follicles relative to d4 ovary ($P<0.001$). Expression *of Smad2, 4 and Smd8* remained constant with age; however, the level of *Smad3* mRNA was reduced in d16 relative to d4 ($P< 0.05$). In contrast to *Smad3* expression, the expression levels of both *Smad1* and *Smad5* were significantly increased in the d16 ovary relative to d4 ($P<0.01$ and $P<0.001$, respectively).

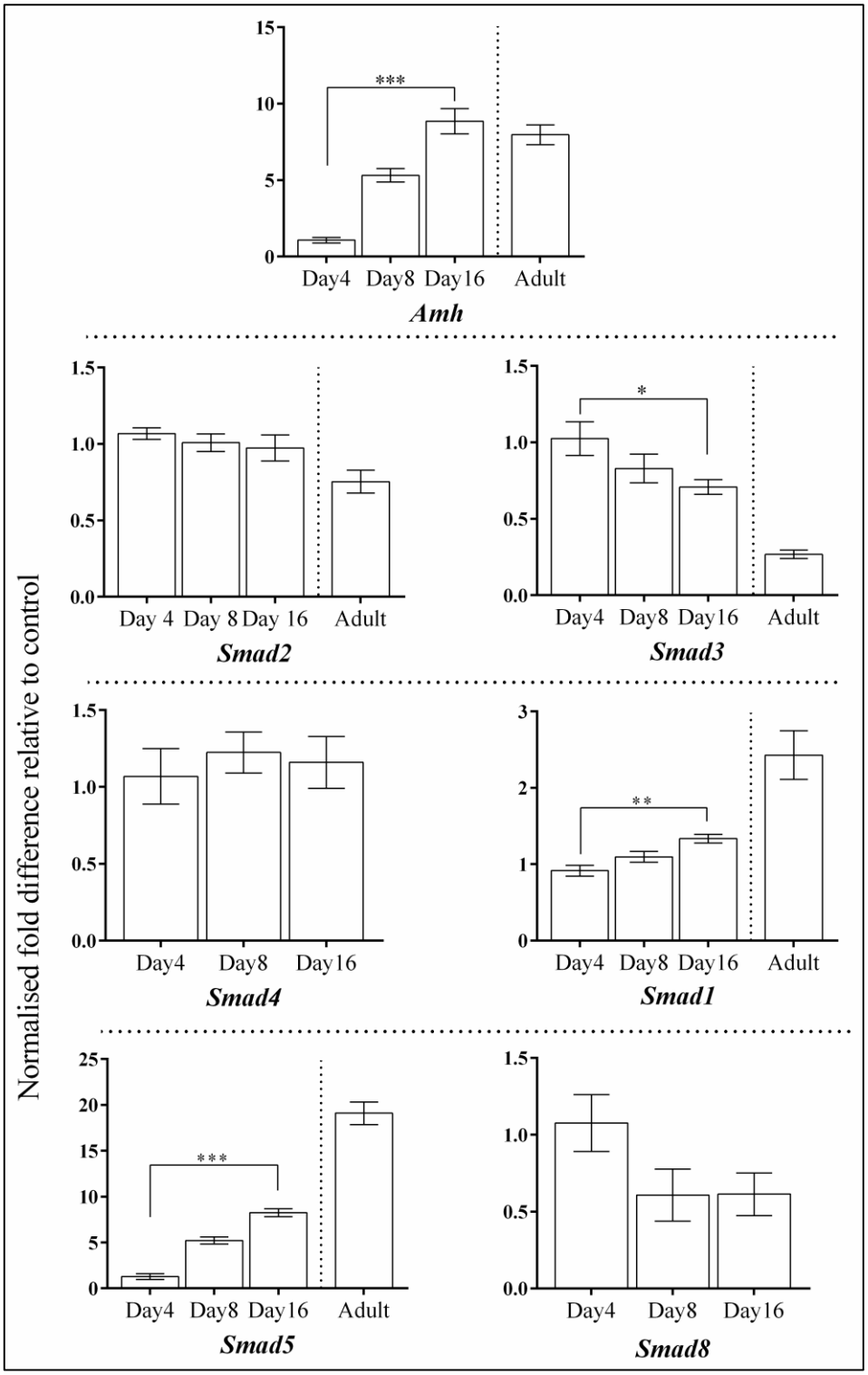

Figure 3.7. Relative mRNA expression of *R-Smads, Co-Smad* and *Amh* in mouse ovaries. qPCR was used to determine the relative expression of *R/Co-Smads* in d4, d8, d16 and adult ovaries. Data were normalised relative to the expression of the internal housekeeping gene, *Atp5b*, and expressed as fold changes relative to d4 ovary. Statistical differences were assessed using one-way ANOVA with Bonferroni post-hoc test, where adult samples were not included in statistics. Data were represented as mean ± SEM (n=6 for *Smad1, 2, 3, 5* and *Amh*; n=5 for *Smad4* and *Smad8*). Asterisks (*P<0.05, **P<0.001and ***P<0.001) indicate statistically different at P< 0.05.

3.3.4. Expression of Smad inhibitors in follicle and oocyte samples

As a first step for further investigations, the expression of nine candidate Smad2/3 inhibitors was analysed in follicle samples. With the exception of *Smad7* and *Smurf2*, all candidates were detectable in growing follicles from secondary to large antral stages. However, by comparison with other genes, *Strap, Ski* and *Ppm1a* transcripts were detectable in all follicle stages, but with lower intensity bands in primordial follicles. In the oocyte sample, six inhibitory factors were expressed including *Strap, Ski, Ppm1a, Exportin4, Smad7* and *Smurf1* (Figure 3.8; Appendix X).

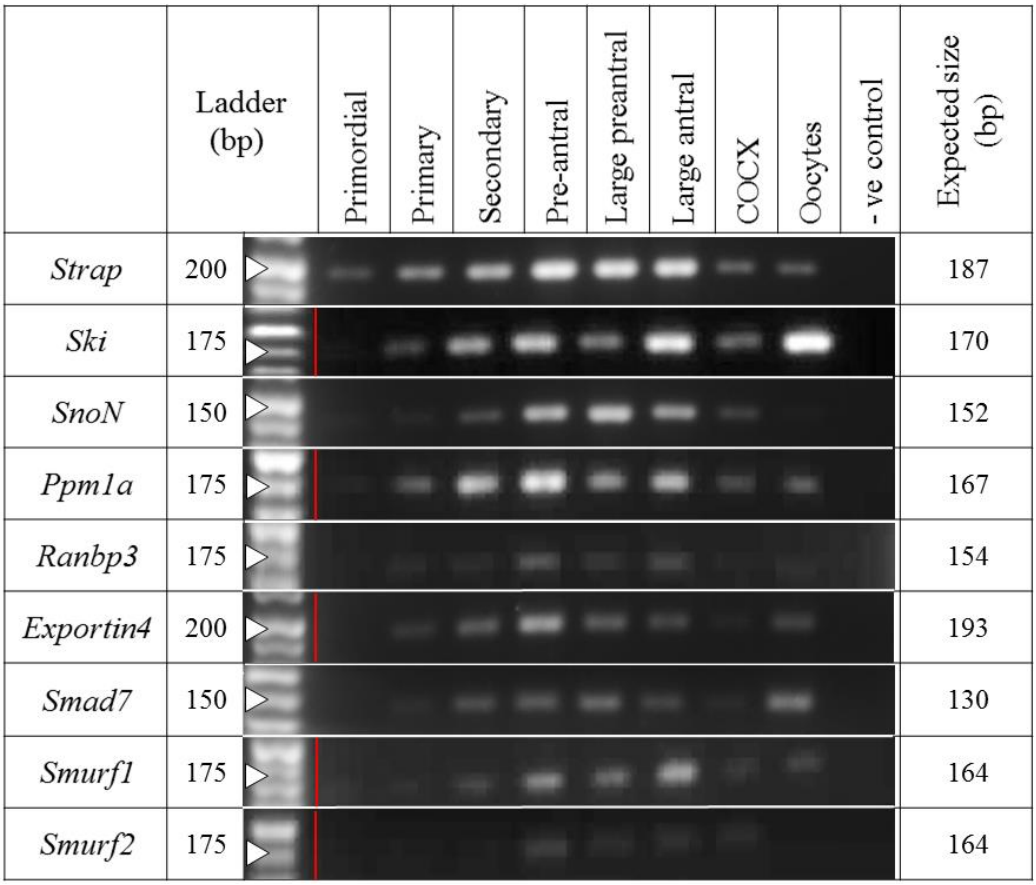

Figure 3.8. Expression of Smad inhibitor in follicles, cumulus-oocyte complexes and oocytes by RT-PCR. Red lines in gels represent to pasted ladders. For negative control (-ve), RNase/ DNase free water was added rather than cDNA.

3.3.5. Expression and quantification of Smad inhibitors in the ovary

Immature (d4, d8 and d16) and adult mouse ovaries, which contain different populations of primordial and growing follicles were utilised for the expression of candidate Smad inhibitors by RT-PCR. Transcripts for all of the inhibitors were detectable in the d4 ovary where the majority of follicles are primordial. Among other candidates, *Strap* and *Ski* were detected with higher intensity in all age groups. Generally, transcripts for all inhibitors in the adult and d16 ovaries were expressed with more obvious bands than in d8 or d4 ovary samples (Figure 3.9).

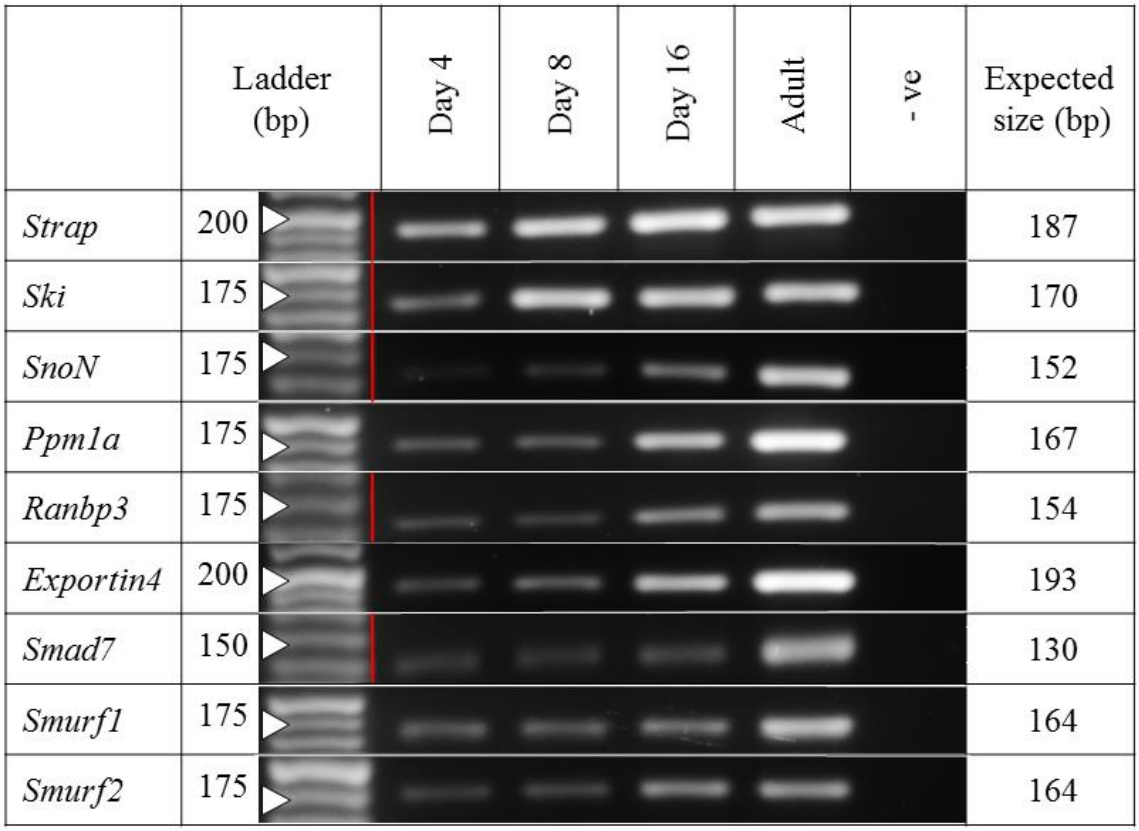

Figure 3.9. Expression of Smad inhibitors in postnatal and adult ovaries by RT-PCR. Red lines in gels represent to pasted ladders. For negative controls (-ve), RNase/ DNase free water was added rather than cDNA.

Data from qPCR revealed differential expression patterns of Smad inhibitors at various ovary ages. *Smad7*, *Smurf1* and *Smurf2* transcript levels were reduced in d16 ovaries relative to d4 ovaries ($P< 0.01$), while no significant difference in their expression was found in d8 ovary relative to d4 ($P>0.05$). Likewise, the expression level of *Ski* and *Strap* mRNA were significantly reduced in d16 ovaries relative to d4 ($P< 0.05$). No differences in expression levels were detectable for *SnoN, Exportin4, Ppm1a* and *RanBP3* in the different age groups (Figure 3.10).

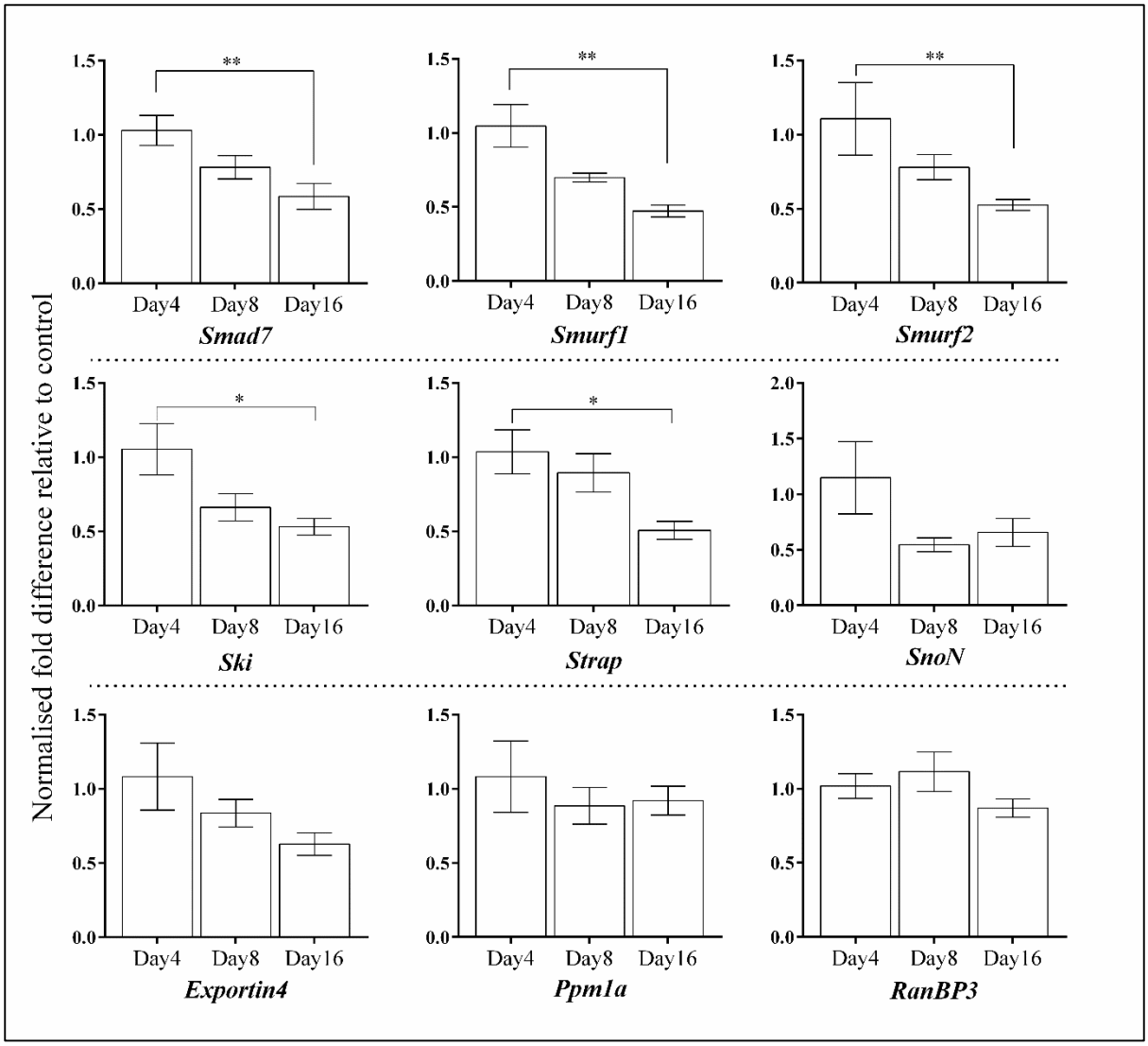

Figure 3.10. Expression levels of Smad inhibitors in mice ovaries at different ages. Data were normalised relative to the expression of the internal housekeeping gene, *Atp5b*, and expressed as fold changes relative to d4 ovary. Data were represented as mean±SEM. The biological replicates for *Smad7*, *Smurf1*, *Smurf2*, *SnoN*, *RanBP3* were six samples each, where five replicates were utilised for the expression of *Strap*, *Ski*, *Exportin4* and *Ppm1a*. Statistical differences were assessed using one-way ANOVA with Bonferroni post-hoc test. Asterisks (*P<0.05, **P<0.01) indicate statistically different at $P < 0.05$.

3.3.6. Localisation of R-Smads

Immunofluorescent localisation of R-Smad proteins was applied to identify the expression pattern of these proteins in ovary sections of d4, d8 and d16. Localisation of R-Smad proteins in these ovary sections was associated with the stage of follicle growth. For example, a high intensity of staining was observed for Smad2/3 proteins in the ovary section of d4, where the majority of follicles are primordial. Similarly, in d8 and d16 ovaries, Smad2/3 staining was expressed in primordial and small growing follicles located at the marginal region of the ovaries.

In multilayer follicles located at the ovary centre (secondary follicles), the staining intensity of Smad2/3 proteins appeared to be reduced. Conversely, Smad1/5/8 proteins were undetectable in primordial follicles, while the staining was more prominent in granulosa cells of multi-layered pre-antral follicles of d8 with more intensity in the d16 ovary. Follicles positive for Smad1/5/8 staining appeared to be more localised at the centre of ovary section.

High power imaging showed that Smad2/3 proteins are strongly localised in pre-granulosa and granulosa cells of primordial to primary follicle stages, respectively. In primordial and transitional follicles, weak staining for Smad2/3 proteins was detectable in the cytoplasm of oocyte and became undetectable in more advanced stages.

Smad2/3 and Smad1/5/8 expression overlapped in follicles that had begun to develop a second layer of granulosa cells. Smad2/3 and Smad1/5/8 were not localised in any other ovary compartments including theca cells, blood vessels, stroma or surface epithelium (Figure 3.11). In non-growing, primordial follicles, Smad2/3 was evident in the nucleus of the pre-granulosa cells while the intensity of nuclear staining was reduced in granulosa cells from transitional and larger growing follicles, where clear cytoplasmic staining was still evident (Figure 3.12).

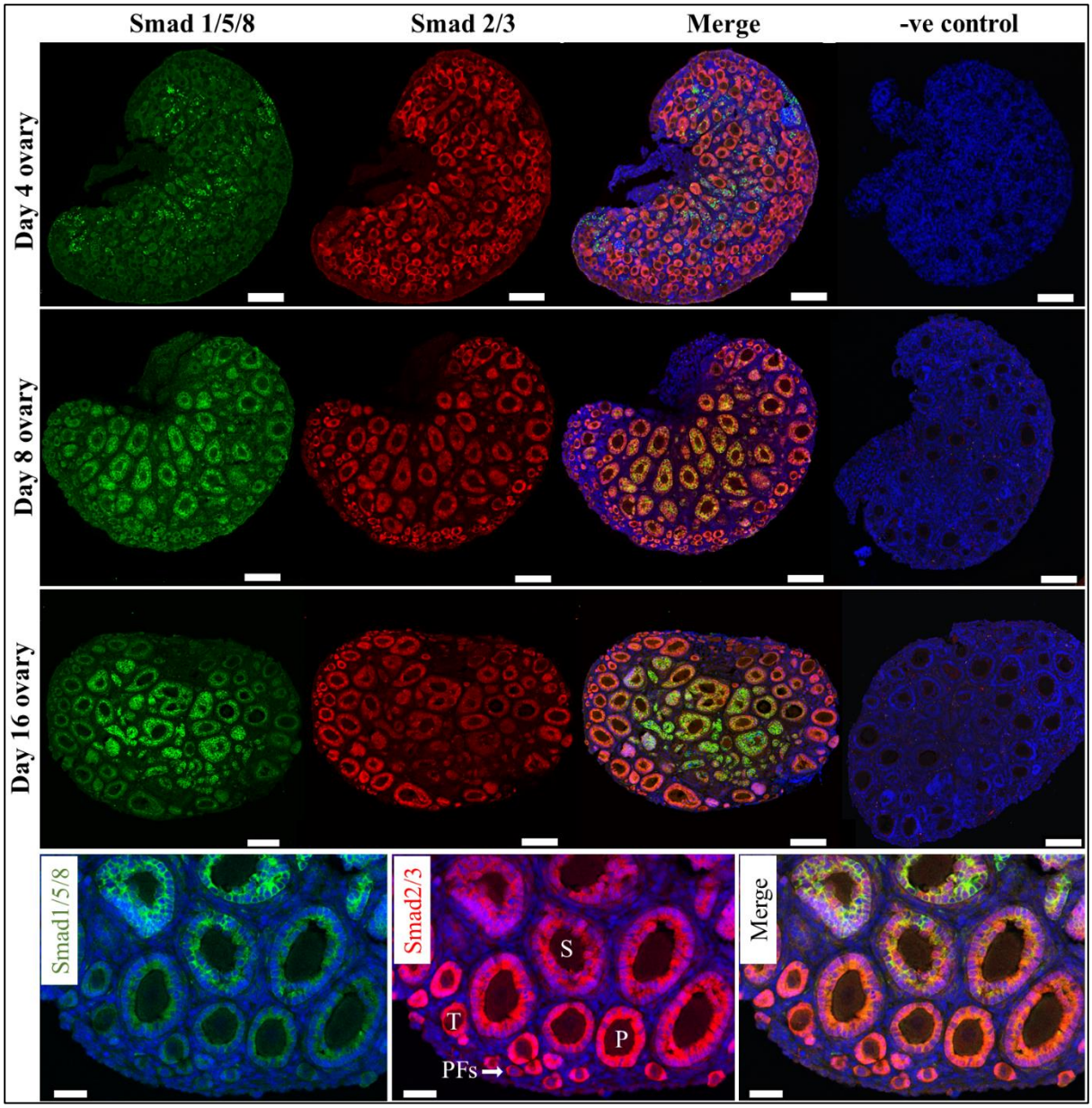

Figure 3.11. Localisation of R-Smad proteins in d4, d8 and d16 mouse ovaries. Smad2/3 proteins (red) were strongly detected primordial (PFs), transitional (T), and primary (P), while Smad1/5/8 (green) were localised in multi-layered follicles starting in secondary follicles (S). Higher power images (lower panels) represent a zoomed area from a d16 ovary. For the negative control, a mixture of equivalent quantities of non-immune Rabbit and Mouse IgG were applied to determine non-specific staining in ovary sections. Nuclei were counterstained with DAPI (blue). Scale bar 200μm (large panels), or 50μm (small panels)

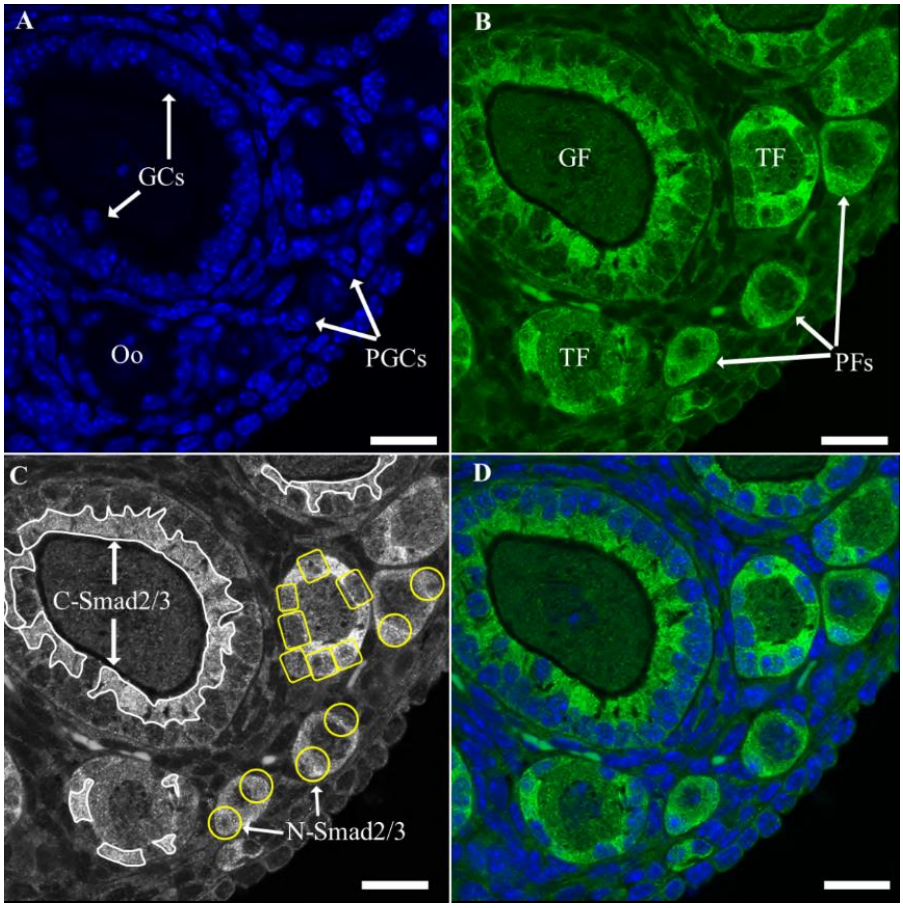

Figure 3.12. Immunofluorescent localisation of nuclear and cytoplasmic Smad2/3 in small follicles. Nuclei were counterstained with DAPI (blue) (A) and follicle stages are labelled in B. According to the stage of follicle growth, both nuclear (N-Smad2/3) and cytoplasmic (C-Smad2/3) were detectable (labelled in C) by high-power confocal microscopy in the d16 ovary. In primordial follicles (PFs), Smad2/3 were localised in the nuclei of pre-granulosa cells (PGCs, circle shapes). The nuclear exclusion of Smad2/3 into the cytoplasm (white margin shapes) occur as these follicles initiated to grow into transitional (TF, Square shapes) and complete exclusion was found in granulosa cells (GCs) of growing follicles (GF). Scale bar 25µm.

3.3.7. Localisation of Ppm1a and Strap protein in the ovary.

One of the objectives of the present study was to identify factors that have the potential to inhibit R-Smads particularly at the early stages of follicle development. RT-PCR revealed that *Strap* and *Ppm1a* are detectable in all follicle growth stages including primordial follicles (Figure 3.8) and in postnatal ovaries (Figure 3.9) where *Smad2* and *Smad3* mRNA and proteins were also detected. Thus, the aim of this section was to identify the staining pattern of Strap and Ppm1a proteins in immature (d4, d8 and d16) ovary sections. For the localisation of Ppm1a, numerous attempts were made to successfully label this protein by immunohistochemistry by changing different optimisation parameters; however, the signal to noise ratio was consistently low, thus, specific staining for Ppm1a protein was not achieved (data not shown).

In order to identify whether Strap is detectable and have the potential to interact with Smad2/3; these proteins were co-localised in ovary section of previously defined ages. Low power images revealed specific staining of Strap in all ovary ages. Moreover, Strap protein was detectable in all stages of small follicles. At low power microscopy, both Smad2/3 and Strap were co-localised in follicles located in the medulla and ovary margin of d4 ovary section, where the majority of follicles are primordial; while this pattern of staining was mainly observed towards the marginal aspect of d8 and d16 ovaries, where primordial and early follicle stages are located (Figure 3.13).

In primordial follicles, similar to Smad2/3, high-power confocal microscopy revealed that Strap protein is detectable in the cytoplasm of the oocyte and pre-granulosa cells. However, in d8 and d16 ovaries, as follicles initiated in the growing process, Strap protein was also detectable in granulosa cells of growing follicles. In the oocytes, Strap staining was reduced in the oocytes of follicles at the secondary stage. In all age groups, both Strap and Smad2/3 proteins were co-localised with the strongest staining in granulosa cells of transitional to primary follicle stages, whereas this pattern of staining was reduced in preantral follicles, where staining for Smad2/3 was largely reduced. Strap protein was also detectable in stroma and theca cells, but not in blood vessels or surface epithelium (Figure 3.14).

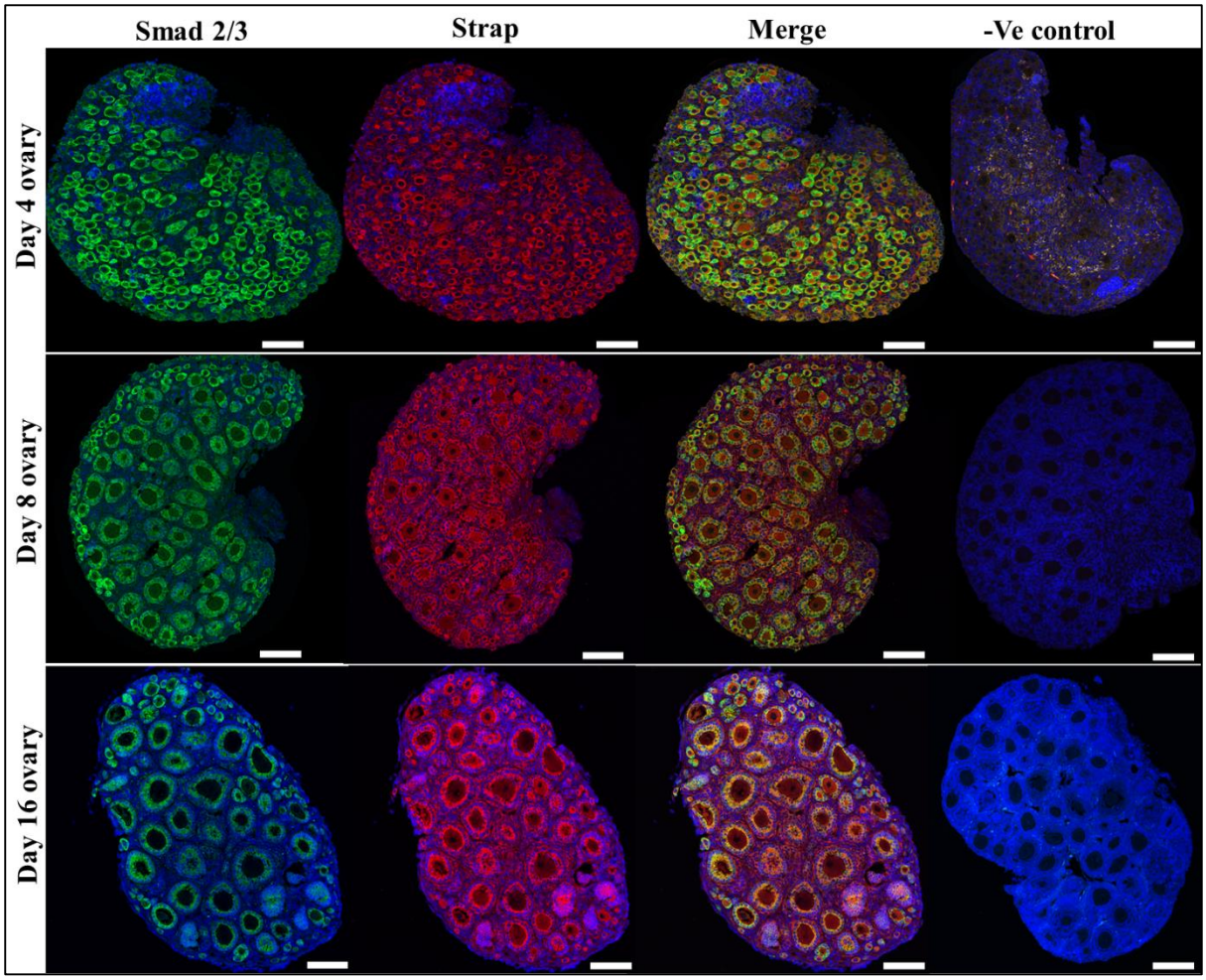

Figure 3.13. Colocalisation of Strap and Smad2/3 proteins in the immature mouse ovary. Ovaries from d4, d8 and d16 mice were stained for Strap (red) and Smad2/3 (green). Negative control sections were supplemented with a mixture of non-immune Rabbit and Mouse IgG. Nuclei were counterstained with DAPI (blue). Scale bar 200µm.

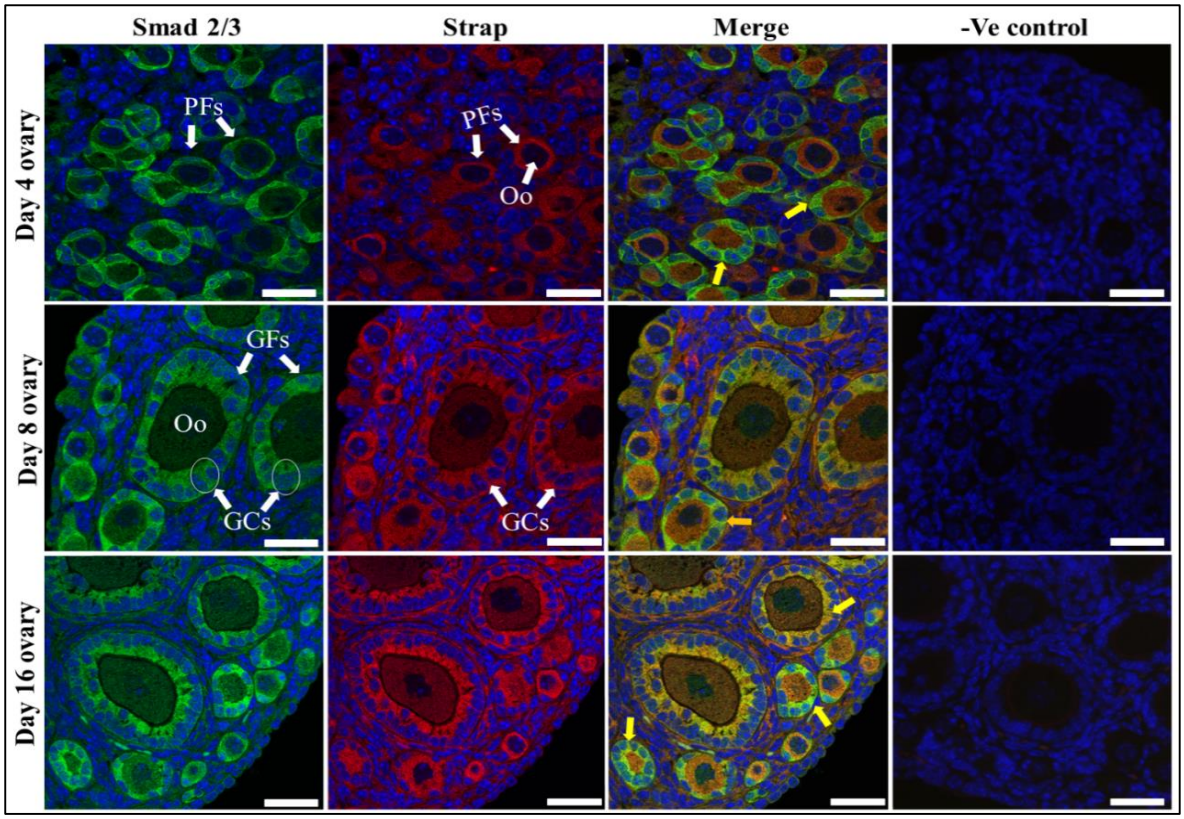

Figure 3.14. Co -localisation of Strap and Smad2/3 proteins in small follicles. In all age groups, positive detection of Strap (red) and Smad2/3 (green) proteins were co-localised in the cytoplasm of the oocyte (Oo) and pre-granulosa cells of the primordial follicle (PFs). As these follicles started to grow, Strap protein appeared to be mainly detectable in granulosa cells (GCs), where it colocalised (yellow arrows) with Smad2/3 (green). Negative control sections were supplemented with a mixture of non-immune Rabbit and Mouse IgG. Nuclei were counterstained with DAPI (blue). Scale bar 25µm.

3.4. Discussion

3.4.1. Expression of Smad inhibitors

In the ovary, a considerable amount of literature has identified the critical role of the intra-ovarian TGFβ/Smad signalling as a major regulatory mechanism of follicle activation, development and apoptosis (Fenwick et al., 2013; Knight and Glister, 2006; Li et al., 2008b; Pangas, 2012). Phosphorylation of the R-Smads through the activated receptors at the cell membrane level is a vital process for mediating the intracellular signals of the TGFβ superfamily (Groppe et al., 2008). Many Smad inhibitors have been identified to function and cooperate with I-Smads (Smad6 and Smad7) to regulate both the duration and strength of the TGFβ signalling through different mechanisms such as dephosphorylation, ubiquitination, sumoylation, degradation, and acetylation (Inoue and Imamura, 2008; Lonn et al., 2009). Factors that might influence the termination or attenuation of the Smad pathway in the early stages of follicle development have not been identified. Therefore, the purpose of this chapter was to analyse the expression of candidate Smad regulators in this context.

RT-PCR analysis confirmed the expression of all of the candidate genes in the whole ovary at the d4, d8 and d16 as well as in adult samples. To determine whether any of these candidate genes are associated with early follicle development, samples of isolated follicles at a range of stages also were screened by RT-PCR. All of the candidate factors were expressed in multi-layered follicles; however, the study identified three inhibitors, *Strap*, *Ski* and *Ppm1a,* which were clearly detectable in all follicle stages including primordial follicles and oocyte samples. The presence or absence of transcripts of Smad inhibitors in some follicle stages suggests that these factors might function in a stage-specific manner. In immature ovaries, data from qPCR revealed different expression between these Smad inhibitors at various ovary ages. For instance, relative to d4, transcripts level for *Smad7*, *Smurf1*, *Smurf2, Ski* and *Strap* were significantly reduced in the d16 ovary, while no statistical variation was determined in the expression of *Ppm1a*, *Exportin4*, *SnoN or RanBP3*.

Since changes in expression are associated with major changes in the follicle composition of these ovaries, and since RT-PCR showed the presence of certain candidates in isolated follicles, we can assume that factors such as Strap (and possibly Ski) play an important role in early follicle development. Potential mechanisms of these inhibitory factors to inhibit Smad signalling have been reviewed in section 1.11.

These findings may provide initial information that TGFβ-Smad signalling can negatively regulate by a complex of different factors that might have roles in follicle development. For example, the synergistic interaction between Ppm1a and Ranbp3/Exportin4 to enhance the exclusion of phosphorylated Smad 2/3 from the nucleus into the cytoplasm (Dai et al., 2011; Lin et al., 2006). In adult mouse ovaries, the expression of Ppm1a mRNA is stable; however, the expression is increased during oocyte maturation, suggesting a role of Ppm1a during advanced stages of follicle growth (Chuderland et al., 2012). The association between Smad7 and Smurf1/Smurf2 ubiquitin ligases to block TGFβ receptors at the cell membrane level is also an important mechanism for inhibiting R-Smad phosphorylation (Kuratomi et al., 2005; Liu et al., 2002). A similar interaction has been reported between Smad7 and Strap (Datta and Moses, 2000; Wrighton et al., 2009), and between Ski and SnoN (He et al., 2003).

Several studies have reported the localisation of these inhibitors in ovaries in different animal species. In adult rat ovaries, Ski protein was detected in granulosa cells of atretic follicles, but not in growing follicles, suggesting a role of Ski in follicle degeneration (Kim et al., 2006). In immature mouse ovaries, SnoN was localised in the stromal cells; however, in mature ovaries, SnoN protein was detected in theca cells of multi-layered follicles and atretic follicles (Xu et al., 2009). In mouse ovaries, Smad7 *mRNA* and protein were detected in granulosa cells of growing follicles and oocytes where upregulation of Smad7 in granulosa cells was associated with increased apoptosis rate (Quezada et al., 2012). Even though these factors have been broadly described as Smad2/3 inhibitors, however, it is still unknown whether both of these Smads are acting at the same time, or if they operate independently (Brown et al., 2007).

3.4.2. Expression of R/Co-Smad mRNA and protein

The initial aim of this chapter was to identify the expression of R/Co-Smads in mouse ovaries at different ages, as well as in isolated follicles at various developmental stages. Transcripts for all *R-Smads* were detected by RT-PCR throughout all stages of follicle development and in whole ovary samples from immature and adult mice, suggesting a relevant role in ovarian function. By RT-PCR, *Smad2 and Smad3* were more obvious in primordial to secondary follicle samples, whereas, *Smad1* and *Smad5* were more obvious in multi-layered follicle stages, including secondary to the large antral follicle. Expression of R-Smad transcripts has previously been reported in mature mouse ovaries (Tian et al., 2010), rats (Drummond et al., 2002), zebrafish (Wang and Ge, 2003) and in primate ovaries (Billiar et al., 2004).

Moreover, qPCR data revealed that expression levels of *Smad3*, but not *Smad2*, was significantly reduced in d16 relative to d4 ovaries; However, another study revealed no statistical variation in the expression of *Smad2* nor *Smad3* mRNA levels between growing and mature mouse oocytes (Tian et al., 2010). In this study, comparisons were performed between whole ovary samples at d4, where the majority of follicles are non-growing, with older ovaries (d8 and d16) containing both non-growing and growing and follicles. Relative to d4, mRNA expression of *Smad1* and *Smad5*, but not *Smad8*, were dramatically increased in the d16 ovary. Conversely, in another study in the rat, *Smad5* was significantly reduced in d12 ovaries relative to d4, while *Smad1* was reduced in d8 ovaries (Drummond et al., 2002), suggesting a possible species variation. As the Smad4 is essential for nuclear translocation of all R-Smads, it was not surprising that expression level of *Smad4* did not vary among various ovary ages (Brown et al., 2007; Moustakas and Heldin, 2008).

Similar to a previous investigation in mouse ovaries (Fenwick et al., 2013), colocalisation of Smad2/3 and Smad1/5/8 in ovary sections revealed that these proteins are precisely localised in granulosa cells in a stage-specific manner. In the current study, Smad2/3 proteins, but not Smad1/5/8, were also localised in oocytes of the earliest stages of follicle development. Similar protein expression was found in oocytes of baboon ovaries (Billiar et al., 2004) and in rats (Drummond et al., 2002). Another study in rat ovary indicated that Smad2 and Smad3 proteins are detectable with a high intensity of staining in granulosa cells of preantral and small antral follicles, but with less intensity in fully grown antral follicles (Xu et al., 2002a). In the present study immature mouse ovaries were utilised where follicle stages beyond the secondary stage were not present; however, by comparison with earlier stages, staining for Smad2/3 appeared to be reduced in the secondary stage.

Expression of Smad2/3 and Smad1/5/8 proteins was consistent with their mRNA expression in ovaries at different ages. For example, Smad2/3 proteins were specifically localised in pre-granulosa/granulosa cells of primordial and primary follicles, respectively, and staining intensity was reduced in multi-layered follicles; while Smad1/5/8 proteins were detectable in granulosa cells of multi-layered, preantral, follicles, but not in primary nor primordial follicles. Interestingly, Smad2/3 and Smad1/5/8 proteins co-localised in follicles that had developed a second layer of granulosa cells. This may indicate the cooperative influence of the two different canonical branches of the TGFβ superfamily as follicles initiate growth.

In primordial follicles, Smad2/3 proteins were localised in the nuclei of pre-granulosa cells and the intensity of staining was reduced in follicles that began to grow. A similar pattern of staining was observed in rat ovaries where nuclear translocation of these proteins was enhanced by TGFβ and activin treatments through phosphorylation (Xu et al., 2002a). In mammalian cells, the exclusion of Smad2/3 from the nucleus is essential for termination the TGFβ signalling (Dai et al., 2009). As mechanisms that promote follicle activation are still unclear, further work is required to identify factors responsible for the nuclear exclusion of Smad2/3.

Taken together, data from R-Smad mRNA and protein expression studies here suggests that the Smad pathway is active in the ovary. In particular, it supports evidence that Smad 2/3 are essentially implicated in the mediating of TGFβ and Gdf9 signalling during the earliest stages of follicle development (Dai et al., 2009; Yan et al., 2001). Concerning Smad1/5/8, the increased expression of *Smad1* and *Smad5* mRNA and Smad1/5/8 proteins in granulosa cells of multi-layered preantral follicles suggests their important role in mediating Bmp and Amh ligands (Durlinger et al., 2002; Kaivo-oja et al., 2006).

3.4.3. Localisation of Ppm1a and Strap proteins

Based on the mRNA expression of R-Smads and Smads inhibitors, both Ppm1a and Strap were selected for further investigation including protein localisation and colocalisation with Smad2/3 in immature ovary sections. Ppm1a protein was undetectable in immature mouse ovaries by immunofluorescence. In a previous study in adult mouse ovary, Ppm1a was localised in the oocyte and with less intensity in granulosa cells of growing follicles, where the intensity of protein was increased in mature oocytes (Chuderland et al., 2012). In this study, failure to detect Ppm1a might be due to either poor quality antibody or the fact that the expression of the protein in immature ovaries is very low.

Consistently with mRNA expression by RT-PCR, Strap protein was localised in follicles that ranged from primordial to preantral follicle stages. Strap and Smad2/3 proteins were colocalised in immature ovary sections at different ages to identify the specific follicle stage where these proteins are interact. This will provide useful evidence to identify both age and ovary tissue that can utilise for *in vitro* culture model. Colocalisation of Strap and Smad2/3 revealed a high intensity of staining in pre/ granulosa cells from primordial to primary stages. In addition, both were co-localised in the oocytes of primordial to transitional follicles. These results support data obtained by qPCR indicated that expression of both *Strap* and *Smad3* were significantly reduced with age.

In addition, the decreased intensity of colocalisation in growing follicles might explain by the reduction of Smad2/3 staining in more advanced follicle stages. The higher staining pattern in small follicles indicates the possible interaction between Strap and Smad2/3, which may inhibit the Smad2/3 pathway and consequently promote early follicle growth. Functionally, Strap can interact with Smad7 to form a stabilised complex on the phosphorylated TGFβ Type I receptor preventing phosphorylation of Smad2 and Smad3 (Wrighton et al., 2009). In addition, phosphorylated Strap has the potential to associate with inactive Smad2 and Smad3, but not Smad1/5/8, to inhibit their interaction with the Type I receptor (Datta and Moses, 2000). In contrast with the significant decline of *Strap* mRNA by qPCR, there was no obvious reduction in Strap staining in multi-layered follicles of d16 ovary sections; suggesting that Strap might have other cellular functions. For example, Strap can promote cell growth by stimulation of pathways which function to enhance cell proliferation such as PDK1/PI3K (Reiner and Datta, 2011) and Erk (Halder et al., 2006). Moreover, Strap also has an anti-apoptotic function by inhibition of the tumour necrosis factor alpha (TNF-α) (Seong et al., 2005). As these pathways are a part of a complex system that regulates early follicle growth (John et al., 2008; Reddy et al., 2009), Strap might also have an essential role in the development of the preantral follicle. A previous study conducted on the fish ovary, *Silver Crucian Carp*, indicated that Strap is only expressed in fully grown oocytes, but not in the early-developing oocytes (Wen et al., 2001). In the present study, Strap was only detected in the oocytes of primordial follicles; the difference in protein expression might relate to species variation.

For this chapter, several limitations were specified; for example, to some extent, the biological replicates of ovary samples for each age group assessed by qPCR were relatively small. More samples would increase the statistical power and would provide flexibility to omit samples that were subject to technical variation rather than repeating the experiment several times. In addition, the relatively low amounts of RNA that could be obtained from the isolated follicle and oocyte samples limited the number of genes that could be analysed by qPCR. Inconsistency between some RT-PCR gels and the qPCR data is attributed to the use of an individual ovary sample, while in qPCR at least five samples were utilised to quantify gene expression. In addition, gel images are a reflection of samples that have cycled 32 times, where is unknown whether samples were reached a plateau, or in other words, the gel images can only be used to determine the presence or absence of mRNA; while using of qPCR can show relative expressions.

In conclusion, this chapter provides useful information on the expression of R-Smads mRNA and proteins in different ovary ages. The study proposed that exclusion of Smad2/3 from the nucleus of pre-granulosa cells might be essential in the process of primordial follicle growth. In addition, nine Smad inhibitors were detected in the immature ovaries of different ages and follicles at various stages of development, which might indicate that Smad signalling is not only inhibited by I-Smads but also through different inhibitory factors. In particular, Strap was found to coincide with the expression of Smad2/3, raising the possibility that this candidate plays an important regulatory role in TGFβ/Smad signalling during primordial follicle activation and preantral follicle growth. The functional impact of Strap and other candidates on the regulation of the early follicle development has not yet been studied. Thus, future experiments will focus on the effect of Strap modulation on the primordial follicle activation and preantral follicle growth.

Chapter 4

Functional role of Serine-Threonine Kinase-Receptor Associated Protein (Strap) in regulation of early follicle growth

4.1. Introduction

Mechanisms that maintain the primordial follicle in a dormant non-growing state or that initiate growth are unclear. It is suggested that primordial follicle activation and the early stages of follicle development are largely regulated by interactions of locally secreted factors (Kim, 2012; Knight and Glister, 2006). Even though it is not fully understood, it has determined that TGFβ signalling participate in these two process; for example, incubation of human ovarian cortical tissue in a medium supplemented with a low concentration of exogenous activin caused inhibition of follicle activation, while higher concentration increased follicle activation (Ding et al., 2010). In addition, Gdf9, another TGFβ member, is also believed to be important for the transition of primordial to the primary follicle growth. In a study in rats, exogenous Gdf9 treatment caused an increased proportion of growing follicles with a dramatic decrease in the proportion of primordial follicles (Vitt et al., 2000).

In chapter 3, R-Smads and nine of their potential negative regulators were analysed for expression in immature ovaries and different stages of early follicle growth. In particular, the detection of Strap in granulosa cells of small follicle was found to coincide with the expression of Smad2/3 in the same cells. In addition, transcripts of *Strap* and *Smad3* followed the same expression pattern, being reduced in d16 ovaries relative to d4. In tissues other than ovary, Strap negatively regulates the Smad2/3 pathway by the stabilising Smad7, but not Smad6, to the activated TGFβ receptors complex preventing the interaction between the receptor complex and inactivating Smad2/3 (Datta et al., 1998; Datta and Moses, 2000). Another study indicated that Strap has the potential to interact with the activated cytoplasmic complex of Smad2/3 and Smad4 preventing its translocation into the nucleus (Halder et al., 2006). In addition to its Smad inhibitory function, Strap regulates a wide range of molecular mechanisms and genes involved in cell proliferation (Chen et al., 2004) and survival (Jung et al., 2010). For example, Strap can act as an anti-apoptotic factor by inhibiting tumour necrosis factors alpha (TNF-α) and has the potential to enhance phosphoinositide-dependent kinase-1 (PDK1) signalling (Seong et al., 2005). Dysregulation of strap expression is also associated with some pathological disorders including cancer; for example, upregulation of Strap results in persistent PDK1/PI3K signalling, indicating that Strap might normally operate to stimulate pathways that enhance cell proliferation (Reiner and Datta, 2011). Moreover, upregulation of Strap is associated with elevated Erk signalling accompanied with downregulation of $p21^{Cip1}$, a cell cycle suppressor protein, which together acts to enhance cell proliferation and consequently tumour progression (Halder et al., 2006).

With regards to canonical TGFβ signalling, even though TGFβ1-3, Gdf9, activin, and nodal are capable of signalling through the Smad2/3 pathway (Kaivo-oja et al., 2006; Li et al., 2008b), the functional impact of Strap, as a Smad inhibitor, on follicle activation and development is currently unknown. The hypothesis of this chapter is that Strap has a relevant functional role in the process of follicle activation and development through the inhibition of Smad2/3 pathway.

The aim of this part is to assess the impact of modification in Strap expression on early follicle development. To achieve this aim both ovary fragments and preantral follicle culture models will be utilised. The expression and/or function of Strap will be manipulated by different molecular protocols including the inhibition of Strap expression by Small interfering RNA (siRNA), inhibition of Strap bioactivity using anti-Strap antibodies or by enhancing Strap function by exogenous recombinant protein supplementation. The effects of these treatments on early follicle development are evaluated using morphological and gene expression criteria.

4.2. Material and Methods

Similar procedures and materials described in section 2.1 were followed for ovary dissection and manipulation.

4.2.1. Ovary fragments culture model

Immature d4 ovaries enriched with primordial follicles were fragmented and maintained *in vitro* in accordance with the procedure outlined in section 2.2.1. This approach was used as a model to evaluate the functional role of Strap on primordial follicle growth. Three different treatments were used in this model in accordance with the following:

4.2.1.1. Knockdown of *Strap* mRNA by siRNA treatment

Equivalent size ovary fragments (3-5 pieces) were cultured in 1ml of MEM-α media (Gibco) supplemented with 10% FBS (ThermoFisher), 100µg/ml Streptomycin sulfate (Sigma), 75µg/ml Penicillin (Sigma) at 37ºC with 5% CO_2. After 72 hours of incubation, media was replaced and supplemented with either 1µM Accell Mouse Strap siRNA (E-045977-00; Dharmacon), 1µM Accell green non-targeting siRNA (D-001950-01-05; Thermo Scientific), 1µM Accell non-targeting siRNA (D-001910-10-05; Thermo Scientific), or without siRNA (Figure 4.1). Doses were used according to the manufacture instruction.

After 96 hours of incubation, cultured fragments were imaged with an Olympus CKX41 with a Nikon camera DS-Fi1. Ovary fragments from one plate were used for immunofluorescent staining, as described in 2.9.4. Ovary fragments from the other two plates (with the exception of Accell green non-targeting siRNA treated group) were used to determine the effect of siRNA treatment on *Strap* mRNA levels between groups by qPCR. To increase the amount of the yield RNA, ovary fragments of each individual treatment/control groups were pooled in a single tube and were processed for RNA extraction.

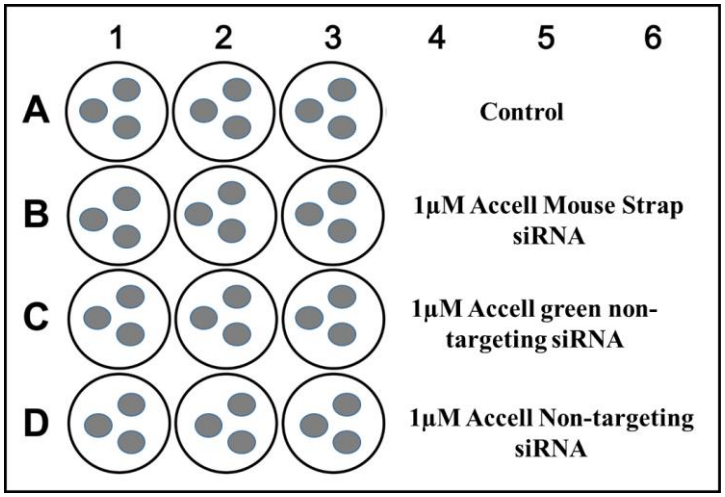

Figure 4.1. The layout of the ovary fragment culture with Strap siRNA. After 3 days in culture media, ovary fragments were incubated for additional 4 days with or without Strap siRNA treatment. Images were obtained at two-time points during culture to identify the effect of treatments on oocyte/follicle development. At the end of culture, plates (n=3) were utilised either for RNA extraction (n=2) or immunofluorescent colocalisation of Amh and Ddx4.

4.2.1.2. Inhibition of Strap protein by immunoneutralisation

Ovary fragments from d4 ovaries were prepared and cultured in 24-well plates as described in 2.2.1. Each well contained 1ml of MEM-α culture media (with supplements as described above) and either 1µg/ml or 10µg/ml of Rabbit anti-Strap IgG (AB1) (Sigma; AV48038) or the equivalent concentration of non-immune Rabbit IgG (Vector). Additional control wells without IgG were also included on each plate (Figure 4.2).

Cultured fragments were imaged with an Olympus CKX41 with a Nikon camera DS-Fi1 at 4 and 7 days after the addition of treatments. To determine the effect of treatments on follicle growth, images were used for oocyte measurements. After this, samples were fixed and were processed for immunostaining for Amh and Ddx4, as described in section 2.9.4.

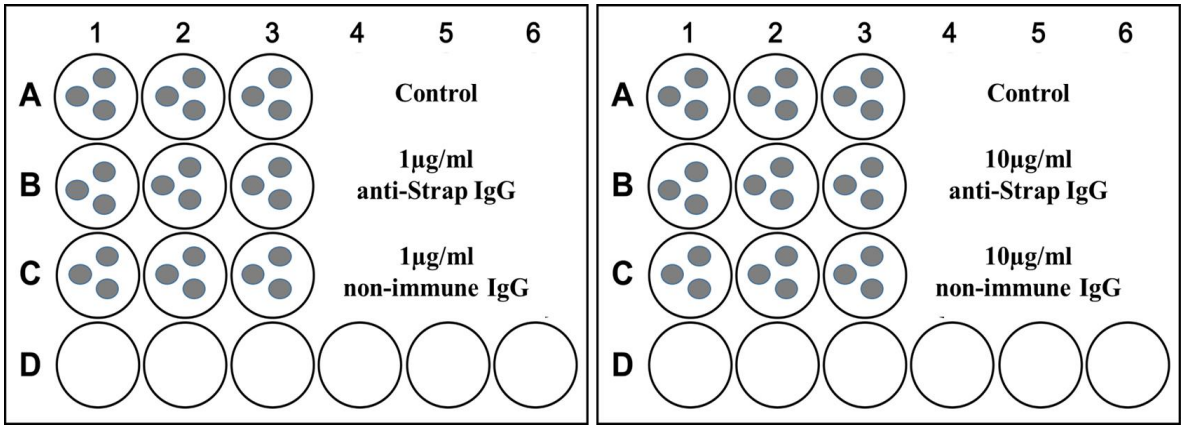

Figure 4.2. The layout of ovary fragment culture for Strap immunoneutralisation. Ovary fragments were incubated for 7 days in culture media with either 1µg/ml or 10µg/ml of Rabbit anti-Strap IgG, an equivalent concentration of non-immune Rabbit IgG or without any treatment (control). Fragments were imaged at 4 and 7 days of culture and images were used for oocyte measurements. At the end of culture (day 7), plates (n=3/each concentration) were utilised for immunofluorescent colocalisation of Amh and Ddx4.

4.2.1.3. Supplementation of Strap protein (rhStrap)

Recombinant Human Unrip full-length protein (Abcam; designated rhStrap) was utilised to enhance Strap function in the culture of d4 ovary fragments. Ovary fragments in control untreated group were incubated in 1ml of MEM-α medium (Gibco) with supplements as described above. Treated groups were cultured in 1ml of culture media that also included either 100ng/ml or 200ng/ml rhStrap (Abcam) (Figure 4.3). Controls also included an equivalent volume of rhStrap diluent L-Glutathione–Tris solution (Appendix IV). The cultures (plates, n=3) were incubated at 37ºC with 5% CO_2. Cultured ovary fragments were imaged with (Olympus CKX41 with a Nikon camera DS-Fi1) at 4 and 7 days of culture. At the day 7, cultures were terminated and samples were fixed for immunofluorescent staining according to section 2.9.4.

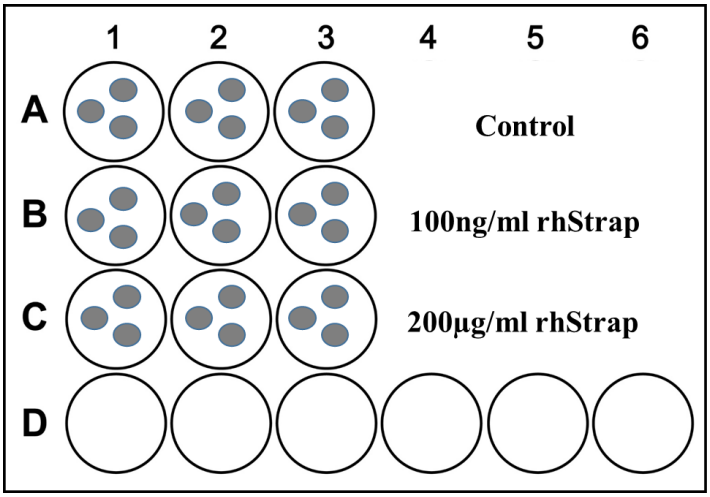

Figure 4.3. The layout of ovary fragment culture for rhStrap supplementation. Ovary fragments were incubated for 7 days in culture media with either 100ng/ml or 200ng/ml rhStrap or with diluent only (control). Fragments were imaged at 4 and 7 days of culture and images were utilised for oocyte measurement. At the end of culture (day 7), plates (n=3) were utilised for immunofluorescent colocalisation of Amh and Ddx4.

4.2.2. Preantral follicle culture model

Preantral follicles were mechanically isolated from d16 ovaries and used to identify the effect of *Strap* siRNA or rhStrap treatments on follicle growth.

4.2.2.1. *Strap* siRNA treatment

4.2.2.1.1. Preparation of siRNA media for *Strap* knockdown

The aim of this experiment was to determine the effect of *Strap* mRNA knockdown on preantral follicle growth. Preantral follicles were mechanically isolated from d16 ovaries and cultured in 96-well plates (4 plates), as previously described 2.2.2. According to the manufacturer's guidelines, it was recommended that cells/tissues exposed to Accell siRNA could be maintained in culture media without supplements, and/or with the proprietary basal culture medium (Accell delivery medium). Therefore, an initial experiment was carried out to determine whether these variables would have an impact on basal preantral follicle growth. Results of this experiment specified that growth supplements to be added to the Accell delivery used for *Strap* siRNA treatment (Appendix XI). For the main experiment, each plate included four lines of treatment where a single line consisted of five individual follicles cultured in 100µl of media. Groups consisted of the following (i) Accell delivery media only (control), (ii) 1µM Accell Mouse Strap siRNA (E-045977-00; Dharmacon), (iii) 1µM Accell non-targeting siRNA (D-001910-10-05; Thermo Scientific) and (iv) 1µM Accell green non-targeting siRNA (D-001950-01-05; Thermo Scientific).

All groups were supplemented with 0.1% (w/v) BSA (Sigma), 75µg/ml penicillin (Sigma), 100µg/ml streptomycin sulphate (Sigma) and insulin-transferrin-sodium selenite ITS (5µg/ml, 5µg/ml, 5ng/ml, respectively; Sigma) (Figure 4.4).

Seven plates (n=7) were prepared and cultured at 37°C with 5% CO_2. Half of the culture media was refreshed after 48 hours of incubation. Follicles were imaged at regular time points (0h, 24h, 48h, and 72h) using light microscopy (Olympus CKX41 with a Nikon camera DS-Fi1). To identify the effect of treatments on follicle growth, images were utilised for the estimation of follicle diameter by ImageJ software, as described in 2.10.1. The experiment was applied twice where follicles from the first one (n=20 follicles/group/4 plates) were utilised for RNA extraction, while follicles from the second experiment (n=21/group/3 plates) were utilised for paraffin embedding.

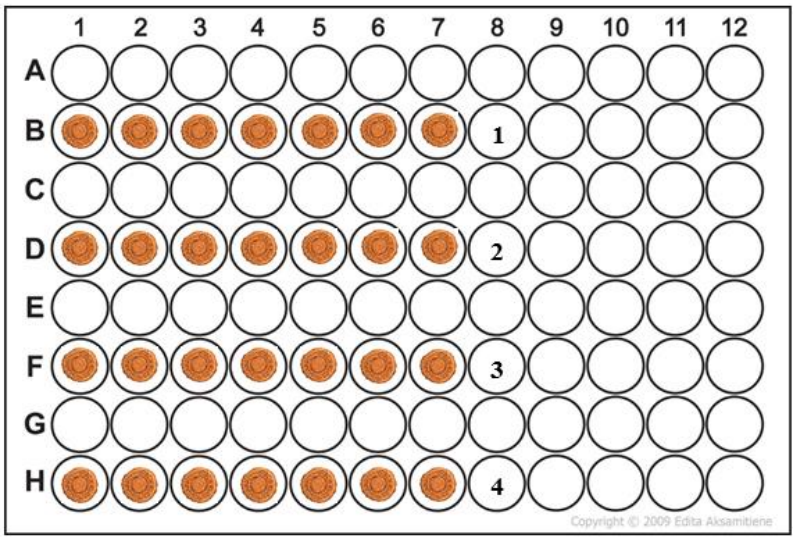

Figure 4.4. The layout of Strap siRNA treatment in the preantral follicle culture. Lines of treatment included an untreated control group (1), 1µM Accell Mouse Strap siRNA group (2), 1µM Accell Non-targeting siRNA group (3) and 1µM Accell green non-targeting group (4). Each well contained a single preantral follicle in 100µl of a particular reagent media. Cultured follicles were imaged at 0h, 24h, 48h and 72h to identify the effect of treatments on follicle growth. Each plate was filled according to the above layout with follicles from an individual d16 ovary and this was repeated 4 times (n=4).

4.2.2.1.2. RNA extraction, RT-PCR and qPCR of cultured ovary fragments and preantral follicles

At the end of incubation (72 hours), cultured follicles (n=5) from each treatment line were collected in a single Eppendorf tube (4 tubes/ group), snap frozen in liquid nitrogen and stored at -80ºC for RNA extraction according to section 2.3. After extraction, RNA samples were evaluated for integrity and concentration using an Agilent 2100 Bioanalyser (Agilent), as shown in chapter 2 (see Figure 2.1). An equal amount (10ng/µl) of RNA from each sample was reverse transcribed into cDNA (section 2.4) and was assessed by RT-PCR for the expression *Strap* and *Amh* in order to confirm the RT reaction was successful.

To identify the effect of siRNA treatments on *Strap* transcript levels, *Strap* was quantified by qPCR. In addition, *Amh* was also assessed as a positive control gene, since Amh is known to be expressed in granulosa cells of healthy preantral follicles (Weenen et al., 2004). Primer sequences for these genes are provided in Table 3.1. Reaction mixtures (20µl) consisting of 2x Kapa SYBR Green (10µl) and ROX dye, 0.4 µl (Kapa Biosystems Ltd., London, UK), 0.5µl (500nM- final concentration in reaction) of each primer set, 8.1µl nuclease-free water and 1µl cDNA (or nuclease-free water for non-template sample) was added into wells of 384-well plate. Thermal cycles were started by initial denaturation for 3 minutes at 95°C, followed by a denaturation step for 40 cycles of 3 seconds at 95°C, annealing for 20 seconds at 58°C, and extension at 72°C for 10 seconds.

Cultured ovary fragments (with the exception of Accell green non-targeting siRNA treated group) were collected, pooled together (fragments of 6 wells/group) to obtain sufficient RNA from each group and used for cDNA synthesis, using similar protocols mentioned above. Four technical replicates from each group were used to identify changes in *Strap* mRNA levels. qPCR reaction mix (20µl) were prepared using 2X SensiFAST SYBR Hi ROX Mix (Bioline). Thermal cycles included an initial denaturation for 2 minutes at 95°C, followed by cycles of 5 seconds at 95°C, annealing for10 seconds at 59°C, and extension at 72°C for 12 seconds.

For both experiments, CT values were normalised against mouse *Hprt1* (*Atp5b* for ovary fragments) and fold changes relative to control were estimated using the equation $2^{-\Delta\Delta CT}$ method (Livak and Schmittgen, 2001).

4.2.2.1.3. Staining of cultured preantral follicles

An additional experiment was performed to confirm results of Strap knockdown on preantral follicle growth. A single plate was set up as above and cultured follicles were utilised for histological assessment. At the end of culture (72h), follicles from each group (5-7 follicles) were fixed in 10% neutral buffered formalin, embedded in low gelling temperature agarose, embedded in paraffin, and sectioned as described in 2.9.2. Follicle sections from control and Accell green non-targeting siRNA groups were compared to determine if follicles took up siRNA. These sections were dewaxed in Histochoice (Sigma), rehydrated in a graded series of ethanol solutions of 100%, 95%, and 70% (3 minutes each), and washed in distilled water (5 minutes). Then, sections were mounted in ProLong Gold antifade reagent with DAPI (Invitrogen) and coverslipped.

Sections were imaged by inverted Widefield fluorescence microscope (Leica DMI4000B). To determine the effect of Strap protein expression after siRNA treatment, immunofluorescent staining was performed on follicle sections for protein localisation using 0.3µg/ml Mouse anti-Strap (Santa Cruz, sc- 136083) according to protocols described in section (2.9.3) and labelled with Alexa fluor 555 Donkey- anti-Mouse IgG (Invitrogen).

4.2.2.2. rhStrap treatment

The aim of this experiment was to identify the effect of rhStrap supplementation on cultured preantral follicle growth. Follicles were mechanically isolated from d16 ovaries (n=7) in drops of isolation media using acupuncture needles. Follicles were transferred into 96-well plates (Nunclon) where each well contained 100µl media with supplements, as described in 2.2.2. A single follicle was placed into each well, and for each plate, eight wells contained media with 200ng/ml rhStrap (Abcam; ab132509), and other eight wells contained media without rhStrap (control).

The product of rhStrap contains 0.31% Glutathione (Sigma- Aldrich) and 0.79% Tris HCL (Sigma- Aldrich), thus, equal quantities of diluent were prepared (Appendix III) and were added to control media only. Follicles were maintained for 72 hours at 37°C and 5% CO_2 and imaged regularly using inverted light microscopy (Olympus CKX41 with a Nikon camera DS-Fi1) to be used for growth assessment. Unhealthy follicles that lost their morphology at any stage of culture were excluded from measurement (Figure 4.5).

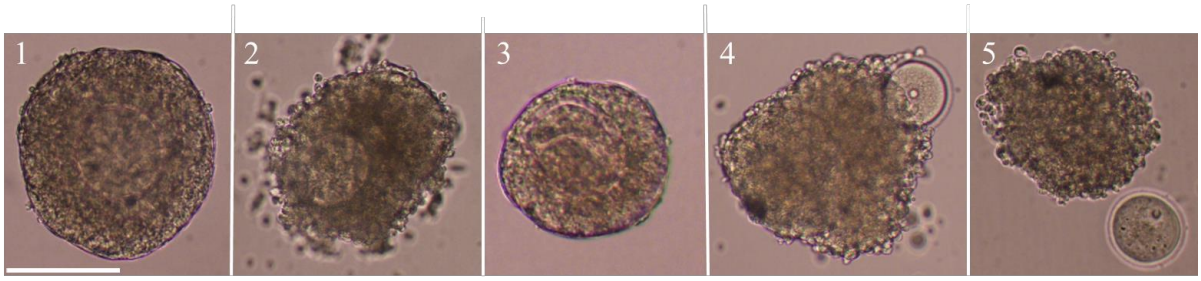

Figure 4.5. Examples of cultured follicles excluded from measurement. Only follicles with normal morphology (1) were measured for growth assessment. Follicles that were exhibited morphological features of deformity, such as abnormality in the basal lamina and extrusion of cells (2), a misshapen or obviously deformed oocyte (3), partial or complete extrusion of the oocyte (4-5, respectively) were omitted from growth assessment, scale bar =100μm.

4.3. Statistical analyses

The impact of Strap knockdown on preantral follicle growth was analysed by Kruskal-Wallis and Dunn's multiple comparisons test. The effect of Strap siRNA treatment on *Strap* and *Amh* mRNA levels were assessed by qPCR and data were analysed using ANOVA with Bonferroni's multiple comparisons test. Changes in preantral follicle growth rates between control and rhStrap protein treated group were evaluated at 24h, 48h and 72h relative to 0h using two-way ANOVA with Bonferroni's multiple comparisons test.

For cultured ovarian fragments, the effect of treatments on oocyte growth at d4 and d7 of culture was analysed using a Kruskal-Wallis and Dunn's multiple comparisons test. To identify differences in proportions of oocyte growth stages (non-growing, transitional, growing) between treatments and control groups, data from three plates (n=3) were analysed using ANOVA with a post-hoc Bonferroni multiple comparisons test. All analyses were performed using Prism (v6.0d; Graphpad) with differences considered significant if $P<0.05$.

4.4. Results

4.4.1. Effect of *Strap* siRNA treatment on the early follicle growth

4.4.1.1. Ovary fragments model

In order to identify the effect of *Strap* mRNA knockdown on follicle activation, immature d4 ovaries containing a high proportion of primordial follicles were cultured. In addition to the untreated control group, ovary fragments were cultured with either1µM Accell Mouse Strap siRNA or 1µM Accell Non-targeting siRNA. After four days in culture, light microscopy images of the cultured fragments were utilised to obtain oocyte diameters, where only clearly identified oocytes were measured.

The median diameter of all oocytes in the Strap siRNA treated group was significantly greater than in control and non-targeting siRNA-treated group (25.54µm vs 23.23µm and 23.75µm, respectively; $P<0.05$). The same effect was also observed when only oocytes classified as "growing" were considered (i.e. all oocytes >25.7µm), where the median diameter of growing oocytes in the *Strap* siRNA group was greater than in control and non-targeting siRNA-treated group (36.04µm, 32.66µm and 31.95µm, respectively; $P<0.05$) (Figure 4.6).

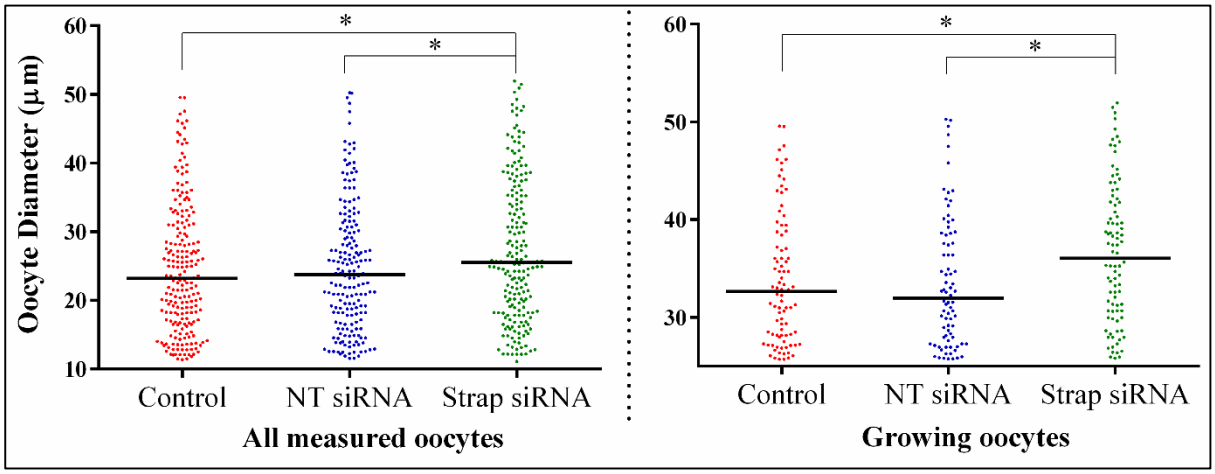

Figure 4.6. Effect of *Strap* siRNA treatment on oocyte size in cultured ovaries. Ovary fragments from d4 ovaries were cultured for 96 hours in either siRNA targeting *Strap* mRNA, non-targeting (NT) siRNA or without any treatment (control). All measured oocytes included oocytes that classified as non-growing (<18.3µm), transitional (18.3- 25.7µm) and growing oocytes (>25.7µm) from three cultured plates incubated under similar conditions. Differences between groups were evaluated using Kruskal-Wallis and Dunn's multiple comparisons test *$P<0.05$.

When the proportions of oocytes in each category (non-growing, transitional, and growing oocytes) were considered by treatment, there was a reduced proportion of non-growing oocytes in the *Strap* siRNA treated group, relative to control and non-targeting groups (24.87%, 30.51%, and 29.56%, respectively; P<0.001). In contrast, the percentage of growing oocytes was significantly increased in *Strap* siRNA group relative to control and non-targeting groups (46.27%, 41.78%, and 43.01%, respectively; P<0.001). However, statistical analysis showed no significant difference in the proportion of transitional oocytes between groups (Figure 4.7).

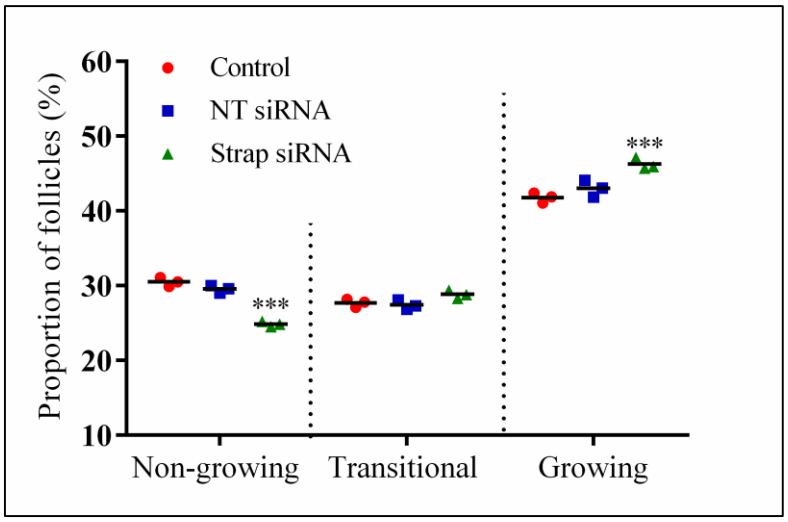

Figure 4.7. Effect of *Strap* siRNA treatment on the proportion of oocytes in ovary fragment cultures. The proportion of oocytes treated with strap siRNA, non-targeting siRNA (NT) or control after 96 hours in culture. Data are presented as mean proportions of oocytes in each stage from three cultured plates (n=3). Data were evaluated using ANOVA with a post-hoc Bonferroni multiple comparisons test. *** P<0.001.

The next aim was to relate results of the oocyte measurements with the *Strap* mRNA expression levels between treated and control groups. Incubation of d4 ovary fragments for 96 hours with *Strap* siRNA caused a significant decrease in the expression of *Strap* mRNA relative to non-targeting siRNA group and reduced by a half relative to its expression in control group (Figure 4.8).

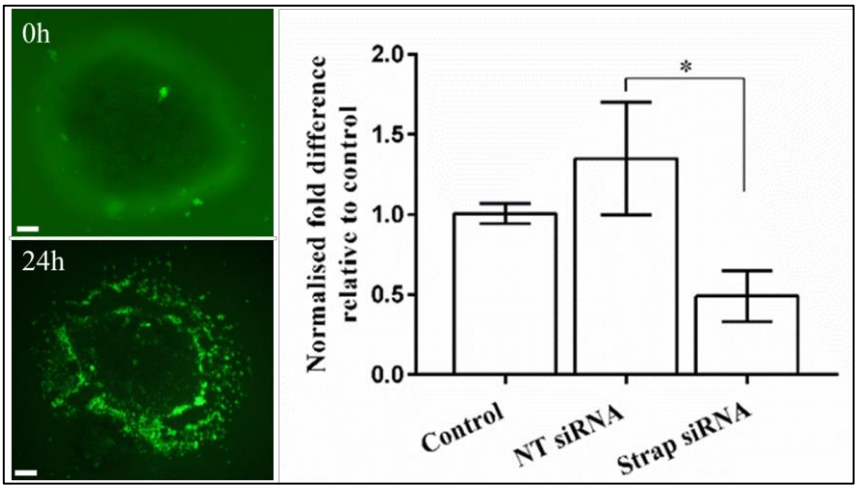

Figure 4.8. Effect of *Strap* siRNA on the expression of *Strap* in ovary fragments. Fluorescent images represent an individual ovary fragment treated with non-targeting green siRNA at 0h and after 24h of culture. Image after 24h confirms the uptake of siRNA by the cultured fragment. A significant reduction in the expression of *Strap* level was revealed relative to non-targeting siRNA (NT siRNA) and its expression was reduced by approximately 50% relative to control. Expression of *Strap* mRNA was determined in relation to the internal reference gene *Atp5b* and expressed as fold change relative to a control group using the formula $2^{-\Delta\Delta CT}$. Fold changes (mean ±SEM) are shown for four technical replicates (n=4). *P<0.05, One-way ANOVA and Bonferroni's multiple comparisons test. Ovary fragment was imaged at the same setting of gain and exposure with an Olympus CKX41 with a Nikon camera DS-Fi1. Scale = 200µm.

Cultured fragments from one plate were used for immunofluorescent colocalisation of Ddx4 (oocyte marker) and Amh (to identify granulosa cells of growing follicles). In addition to the importance of using this staining protocol to recognise growing follicles, it also provides additional evidence that the ovary fragments culture model was able to maintain primordial follicle activation and early preantral follicle development. Although not quantified, Amh staining was more detectable in the *Strap* siRNA treated group than control and non-targeting siRNA groups, further supporting an increase in the proportion of growing follicles with *Strap* knockdown (Figure 4.9).

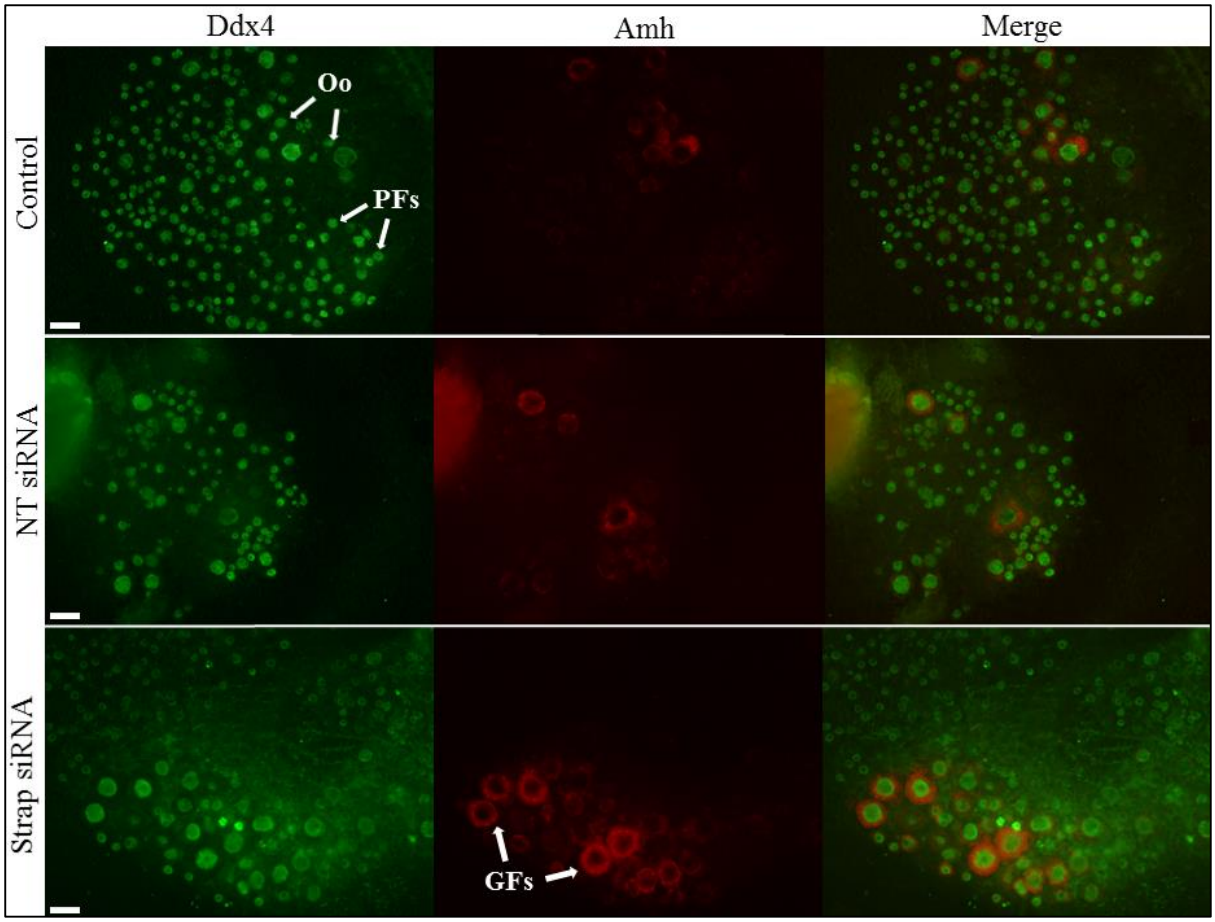

Figure 4.9. Immunofluorescent staining of cultured ovary fragments with or without siRNA. After 96 hours of culture, control, non-targeting (NT) siRNA, and Strap siRNA ovary fragments were stained with both Ddx4 and Amh. Ddx4 (green) was localised in oocytes (Oo), while Amh (red) was localised in granulosa cells of growing preantral follicles (GFs), but not in primordial follicles (PFs). Scale bar = 100 μm.

4.4.1.2. Effect of *Strap* siRNA treatment on preantral follicle growth

In order to identify the effect of *Strap* knockdown on preantral follicle growth, isolated preantral follicles were cultured in the presence or absence of 1μM *Strap* siRNA, 1μM Non-targeting siRNA or 1μM labelled non-targeting siRNA. The siRNA uptake by follicles was examined by fluorescent microscopy of sections of cultured follicles where, unlike control, follicles treated with Accell green non-targeting siRNA showed green staining in the cytoplasm of granulosa cells (Figure 4.10).

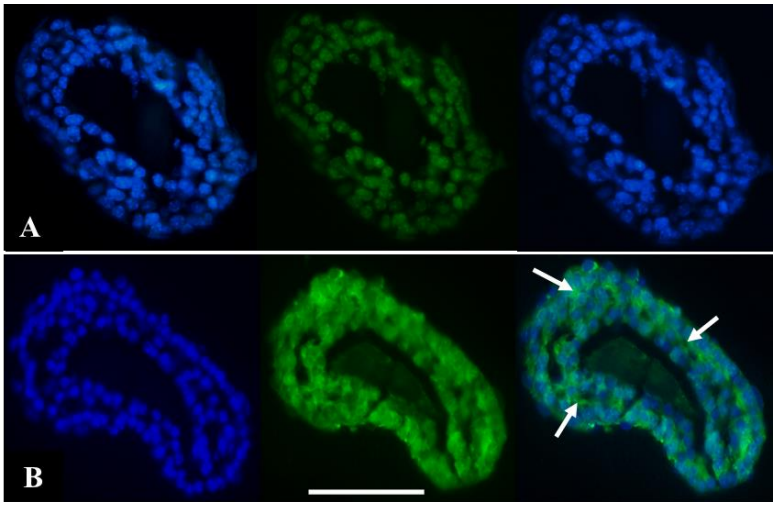

Figure 4.10. Follicle sections confirming cellular uptake of siRNA. After 72h in culture, follicle sections from Control (A) and Accell green non-targeting siRNA treated group (B) were utilised to confirm the uptake of siRNA (white arrows, green stain). Sections were dewaxed, mounted in DAPI and cover-slipped. Follicle sections were imaged at the same setting of gain and exposure with an inverted Widefield fluorescence microscope (Leica DMI4000B). Scale = 100µm.

Considering the effect of *Strap* siRNA on preantral follicle size, there was no significant difference in the mean follicle diameter between treatment groups at any time point (24h, 48h or 72h). However, within groups, the mean follicle diameter was significantly increased during the first 24 hours of incubation in both control and non- targeting siRNA groups ($P<0.01$, $P<0.05$, respectively), but not in the *Strap* siRNA treated group at the same incubation time ($P=0.1422$). Fluorescent microscopy of preantral follicles treated by Accell green non-targeting siRNA clearly showed the penetration and uptake of siRNA throughout the culture, consistent with the staining observed in sections of follicles at the termination of culture (Figure 4.11).

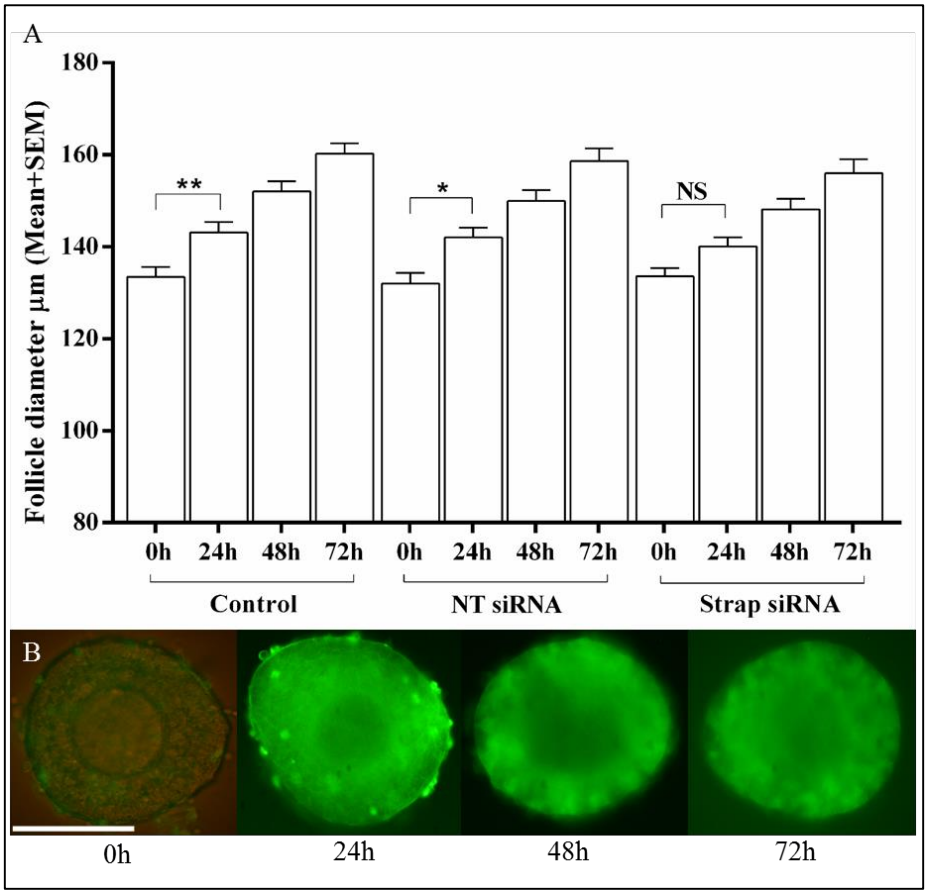

Figure 4.11. Effect of *Strap* siRNA treatment on preantral follicle growth. Follicle diameters were estimated at 0h, 24h, 48h and 72h (n= 20 follicles/group). Follicle diameters were presented as mean ± SEM and were analysed using ANOVA with a post-hoc Bonferroni multiple comparisons test. *P<0.05, ** P<0.01, NS non-significant. Fluorescent images taken throughout culture (B) show evidence of green non-targeting siRNA uptake by follicles in the culture at different time points. Scale bar 100µm.

To evaluate the effect of treatments on *Strap* expression, *Strap* transcript levels were assessed in cDNA (10ng/µl) from pooled follicles of each group. The expression level of *Strap* was significantly reduced relative to non-targeting siRNA group (P<0.05), however, the reduction was not statistically different when compared with the untreated control group. There was no significant difference in the expression of *Amh* among groups (Figure 4.12).

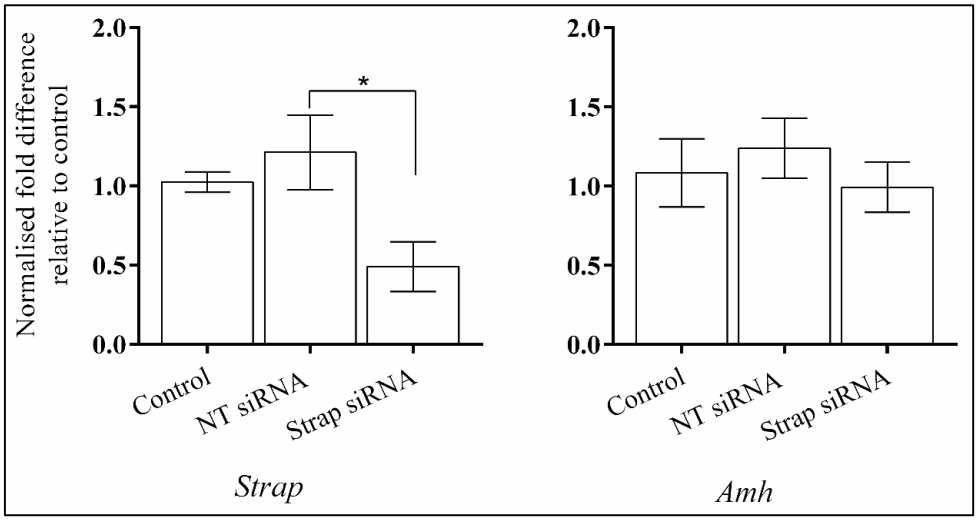

Figure 4.12. Expression of *Strap* and *Amh* in preantral follicles by qPCR. Each group is represented by four cDNA samples (n=4), where each sample was derived from five cultured preantral follicles after 72 hours of culture. Data were normalised relative to the expression of the internal housekeeping gene, Hprt1, and expressed as mean fold changes (± SEM) relative to controls. *P < 0.05.

For further evaluation of siRNA treatment, the expression of Strap protein was evaluated by immunofluorescent localisation in histological sections of cultured follicles. Images revealed a reduction in Strap staining in the siRNA treated follicles relative to non-targeting siRNA treated follicles (Figure 4.13). Collectively, these findings indicate that the Strap-specific siRNA treatment reduced the levels of both Strap mRNA and protein in the treated follicles in comparison to controls.

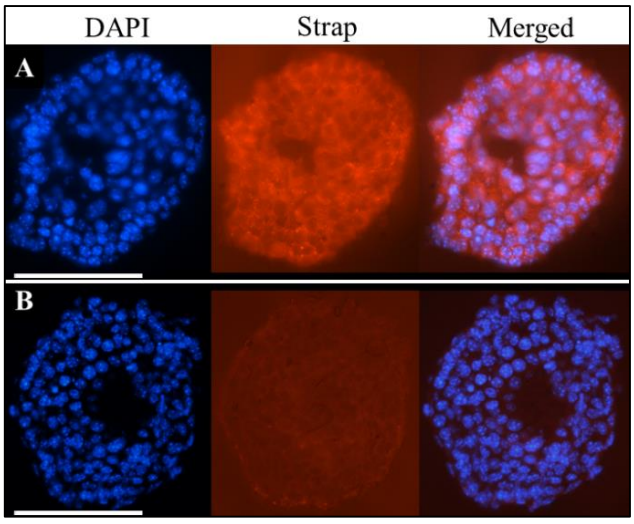

Figure 4.13. Immunofluorescent localisation of Strap protein in cultured preantral follicles. Paraffin-embedded sections of cultured follicles were stained for localisation of Strap (red) in a non-targeting siRNA follicle (A) and a siRNA treated follicle (B). Images were obtained with inverted Widefield fluorescence microscope (Leica DMI4000B). Scale bar =100μm.

4.4.2. Effect of immunoneutralisation of Strap protein in the ovary fragment model

The model of d4 ovary fragments was used to assess the impact of Strap protein inhibition on early follicle growth using specific antibodies. Ovary fragments were cultured in either 1µg/ml or 10µg/ml anti-Strap IgG. Control groups included treatment with an equivalent concentration of non-immune IgG and no IgG. Oocyte diameters were measured from images at 4 and 7 days of incubation. After 4 days in culture, fragments treated with 1µg/ml anti-Strap IgG showed no significant variation in the median oocyte diameter relative to control groups. Likewise, when only growing oocytes were considered at this time point, the median oocyte diameter in the anti-Strap group was not different to control nor non-immune IgG groups (33.64µm, 32.32µm and 30.99µm, respectively).

However, a slight, but significant increase in the median diameter of oocytes treated with 1µg/ml anti-Strap was found after 7 days when compared with control or non-immune IgG-treated group (25.18µm, 23.92µm and 24.03µm, respectively; $P<0.05$ vs control or non-immune IgG-treated). When only growing oocytes were considered at the 7 day time point, the median size of measured oocytes in the anti-Strap treated group was greater than the control and non-immune IgG group (36.56µm, 32.70µm and 31.68µm, respectively; $P<0.05$ and $P<0.01$ versus control and non-immune IgG, respectively) (Figure 4.14).

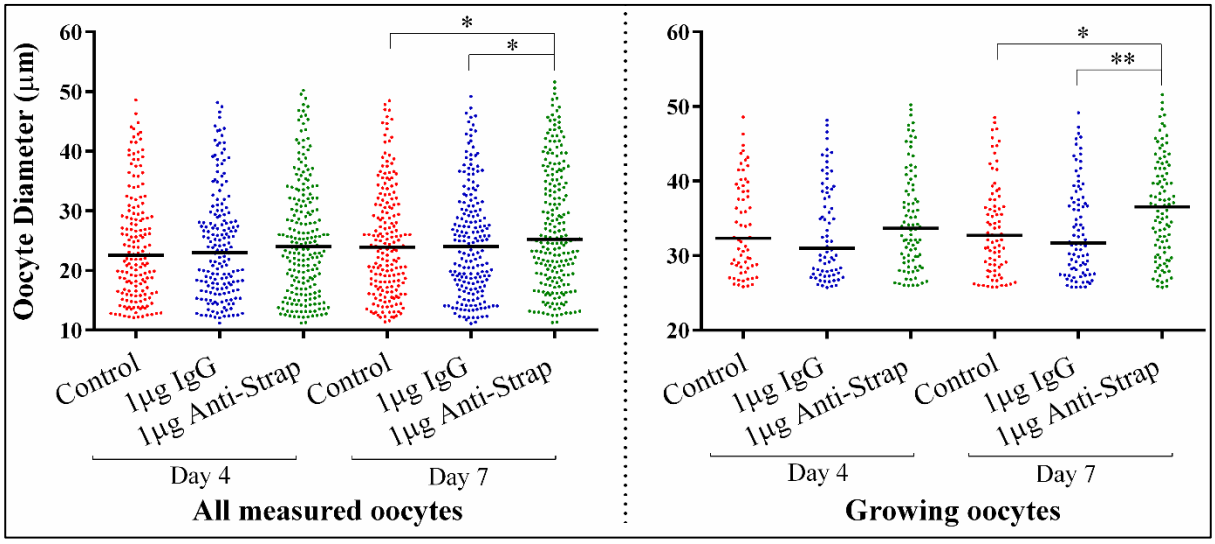

Figure 4.14. Effect of 1µg/ml anti-Strap IgG treatment on oocyte size. Day 4 ovary fragments were maintained for 7 days in 1µg/ml anti-Strap IgG or 1µg/ml non-immune IgG (1µg/ml IgG) or no IgG (control). Cultured fragments were imaged after 4 and 7 days of exposure to different treatments. All measured oocytes (non-growing, transitional and growing) or only growing oocytes (>25.7µm) are plotted. Variation in the median oocyte diameter between groups at both time points was evaluated using Kruskal-Wallis and Dunn's multiple comparisons tests. *P<0.05, **P<0.01.

When the proportion of oocytes in each category (non-growing, transitional, growing) was considered by treatment, there were no differences at 4 days in culture. However, at 7 days there was a reduced proportion of non-growing oocytes in the group treated with 1µg/ml anti-Strap relative to control and non-immune IgG group (22.76%, 29.62% and 28.57%, respectively; P<0.001vs control or non-immune IgG-treated).

The percentage of transitional staged oocytes was significantly increased in the 1µg/ml anti-Strap group relative to control and non-immune IgG groups (30.2%%, 27.5% and 27.0%, respectively; P<0.001 vs control or non-immune IgG-treated). The percentage of growing oocytes was also significantly increased in the 1µg/ml anti-Strap group relative to control and non-immune IgG groups (47%, 42.86% and 44.38%, respectively; P<0.001 vs control and non-immune IgG groups) (Figure 4.15).

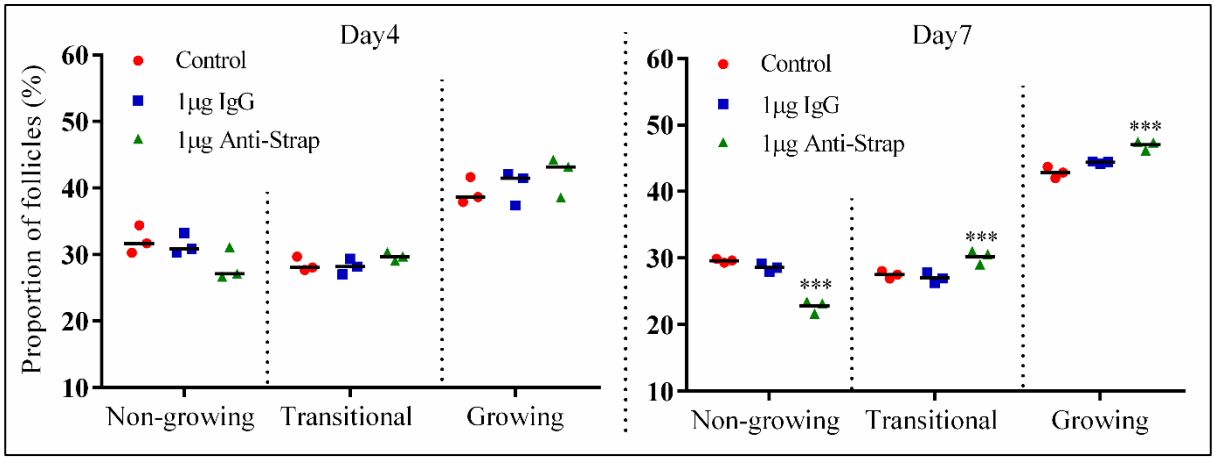

Figure 4.15. Effect of 1µg/ml anti-Strap on oocyte growth in the cultured fragments. Graphs show the proportion of oocytes treated with 1µg/ml anti-Strap, 1µg/ml non-immune IgG or control after 4 days or 7 days exposure. Data are presented as mean proportions of oocytes in each stage from three culture plates (n=3). Data were evaluated using ANOVA with a post-hoc Bonferroni multiple comparisons test. ***P<0.001 vs control and non-immune IgG group.

At the end of culture, Amh staining was more detectable in the 1µg/ml anti-Strap treated group than the other two control groups, consistent with an increase in the proportion of growing follicles with anti-Strap treatment (Figure 4.16).

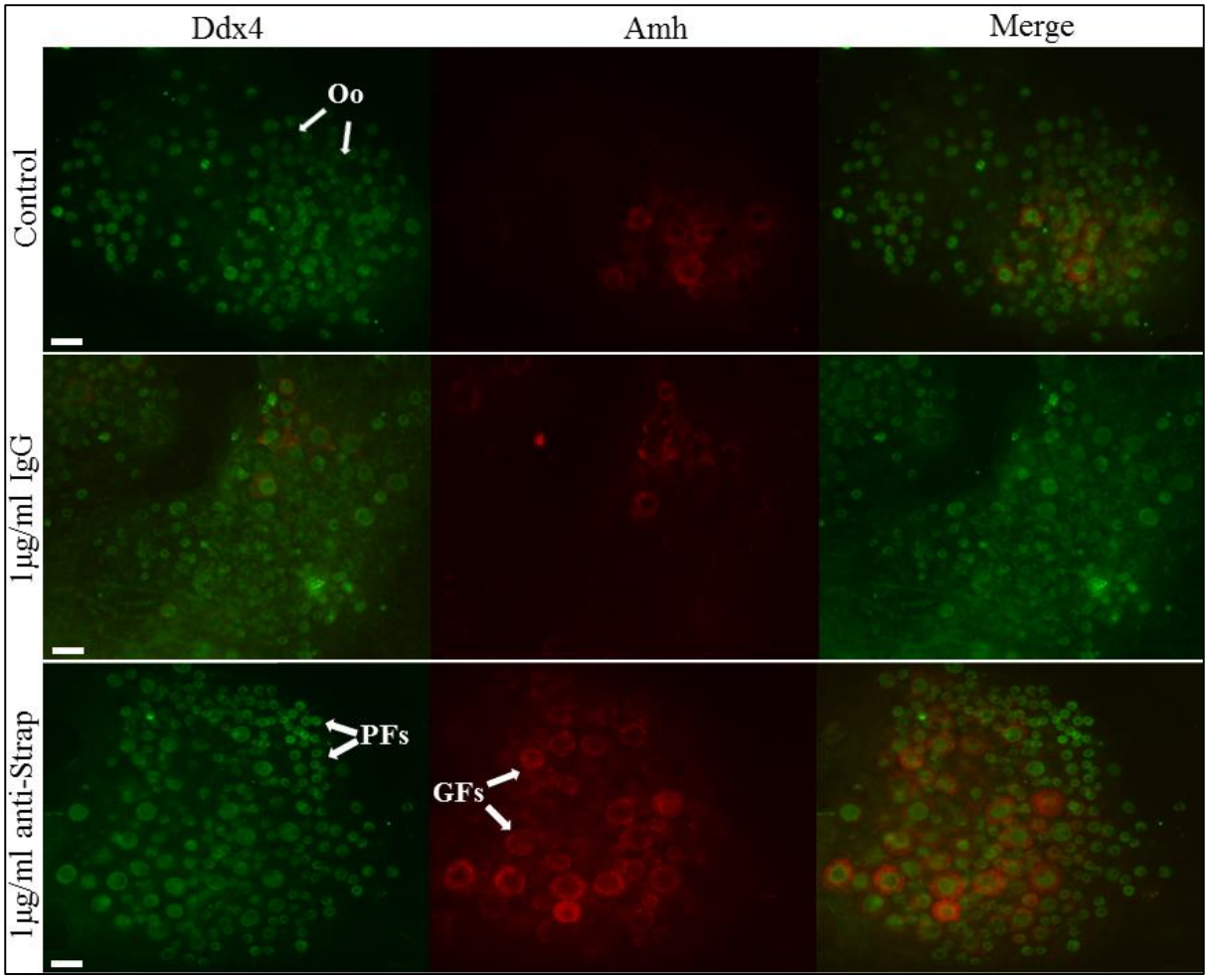

Figure 4.16. Immunofluorescent staining of ovary fragments treated with 1µg/ml anti-Strap IgG or non-immune IgG. After 7 days in culture, ovary fragments were stained for the detection of Ddx4 (green) and Amh (red). GFs: Growing follicles, Oo: oocytes, PFs: primordial follicles. Scale bar= 100µm.

To identify whether Strap function has affected early follicle development in a dose responsive manner, ovary fragments were treated with a higher concentration of anti-Strap IgG and non-immune IgG (10µg/ml each). In comparison with the low concentration treatment, the effect of 10µg/ml anti-Strap IgG was found to promote a significant increase in oocyte median diameter at 4 days, relative to control and non-immune IgG groups ($P<0.05$ each). Furthermore, after 7 days of treatment, this effect became more significant ($P<0.001$ vs control and $P<0.01$ vs 10µg/ml non-immune IgG).

When only growing oocytes were considered, the median size of measured oocytes from the 10µg/ml anti-Strap group was greater than control and non-immune IgG at 4 days (33.68µm, 31.07µm and 31.13µm, respectively; both P<0.05). The effect of 10µg/ml anti-Strap treatment on the median size of growing oocytes further increased after 7 days of exposure relative to control and 10µg/ml non-immune IgG (34.51µm, 31.36µm and 31.35µm, respectively; P<0.01 vs control and P<0.001 vs non-immune IgG) (Figure 4.17).

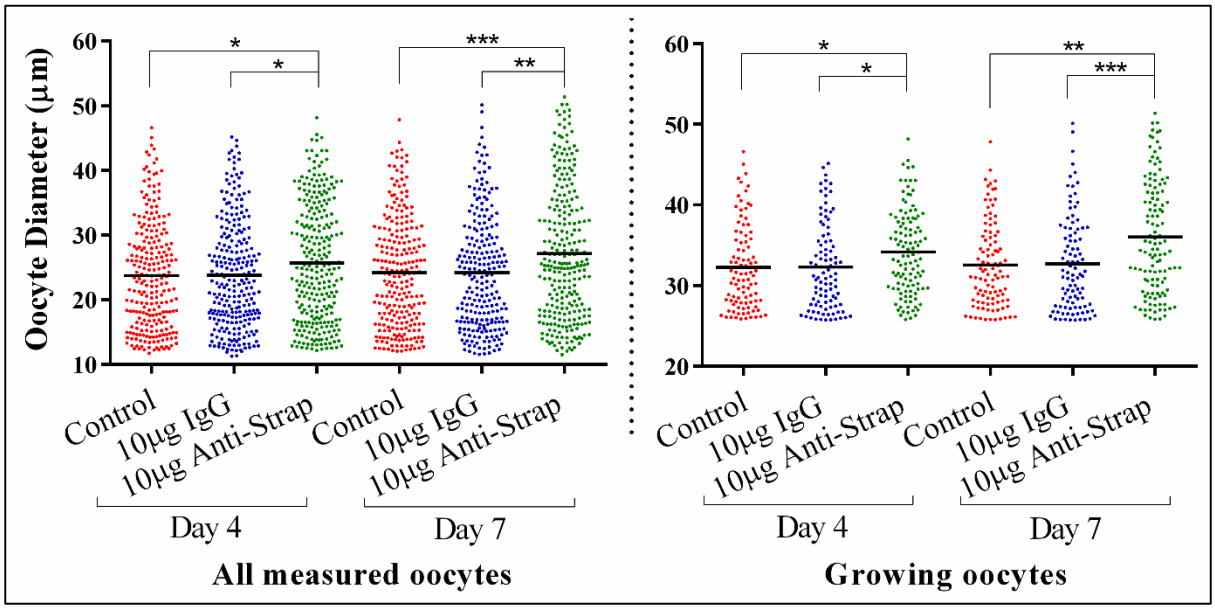

Figure 4.17. Effect of 10µg/ml anti-Strap IgG treatment on oocyte growth. Day 4 ovary fragments were maintained for 7 days in 10µg/ml anti-Strap IgG or 10µg/ml non-immune IgG (10µg/ml IgG) or no IgG (Control). Cultured fragments were imaged after 4 and 7 days exposure to different treatments. All measured oocyte (non-growing, transitional and growing) or only growing oocytes (>25.7µm) were plotted. Variation in the median oocyte diameter between groups at both time points was evaluated using a Kruskal-Wallis and Dunn's multiple comparisons test. *P<0.05, **P<0.01, ***P<0.001.

When the proportion of oocytes in each category (non-growing, transitional, growing) was considered by treatment, there was a reduced proportion of non-growing oocytes in the group treated with 10µg/ml anti-Strap relative to the control and non-immune IgG groups at 4 days (28.15%, 33.88% and 33.33%, respectively; both P<0.001). Although there were no differences in the relative proportions of transitional oocytes, the percentage of growing oocytes was significantly increased in 10µg/ml anti-Strap group relative to the control and non-immune IgG groups (45.55%, 39.67% and 38.04%, respectively; both P<0.001). These effects of 10µg/ml IgG at 4 days were still evident at 7 days (Figure 4.18).

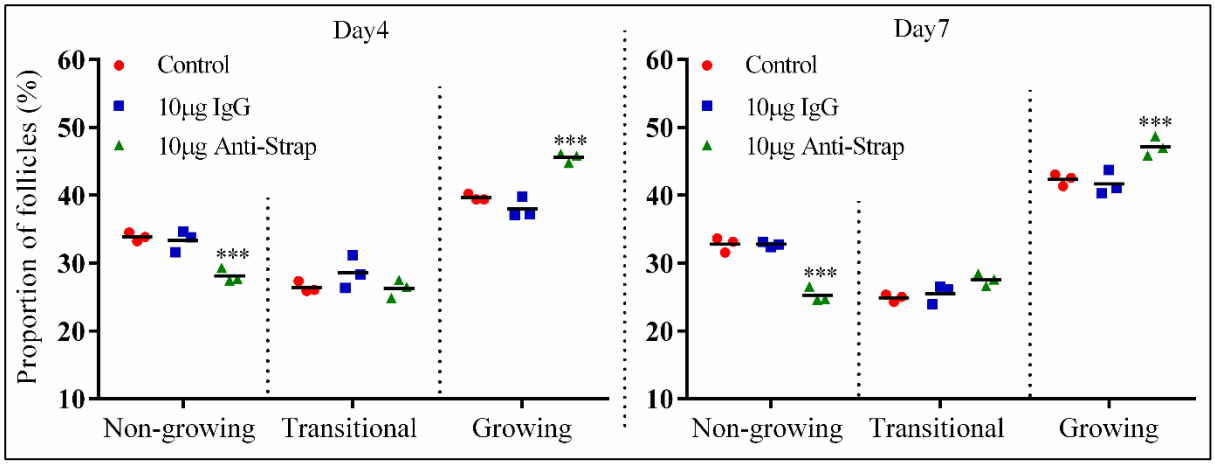

Figure 4.18. Effect of 10µg/ml anti-Strap IgG treatment on oocyte growth in ovary fragment cultures. Graphs show the proportion of oocytes treated with 10µg/ml anti-Strap, 10µg/ml non-immune IgG or control after 4 days or 7 days exposure. Data are presented as mean proportions of oocytes in each stage from three culture plates (n=3). Data were evaluated using ANOVA with a post-hoc Bonferroni multiple comparisons test. ***P<0.001.

Similar to observations with 1µg/ml anti-Strap, Amh staining was more detectable in the 10µg/ml anti-Strap treated group than both control groups, again, consistent with an increase in the proportion of growing follicles with anti-Strap treatment (Figure 4.19).

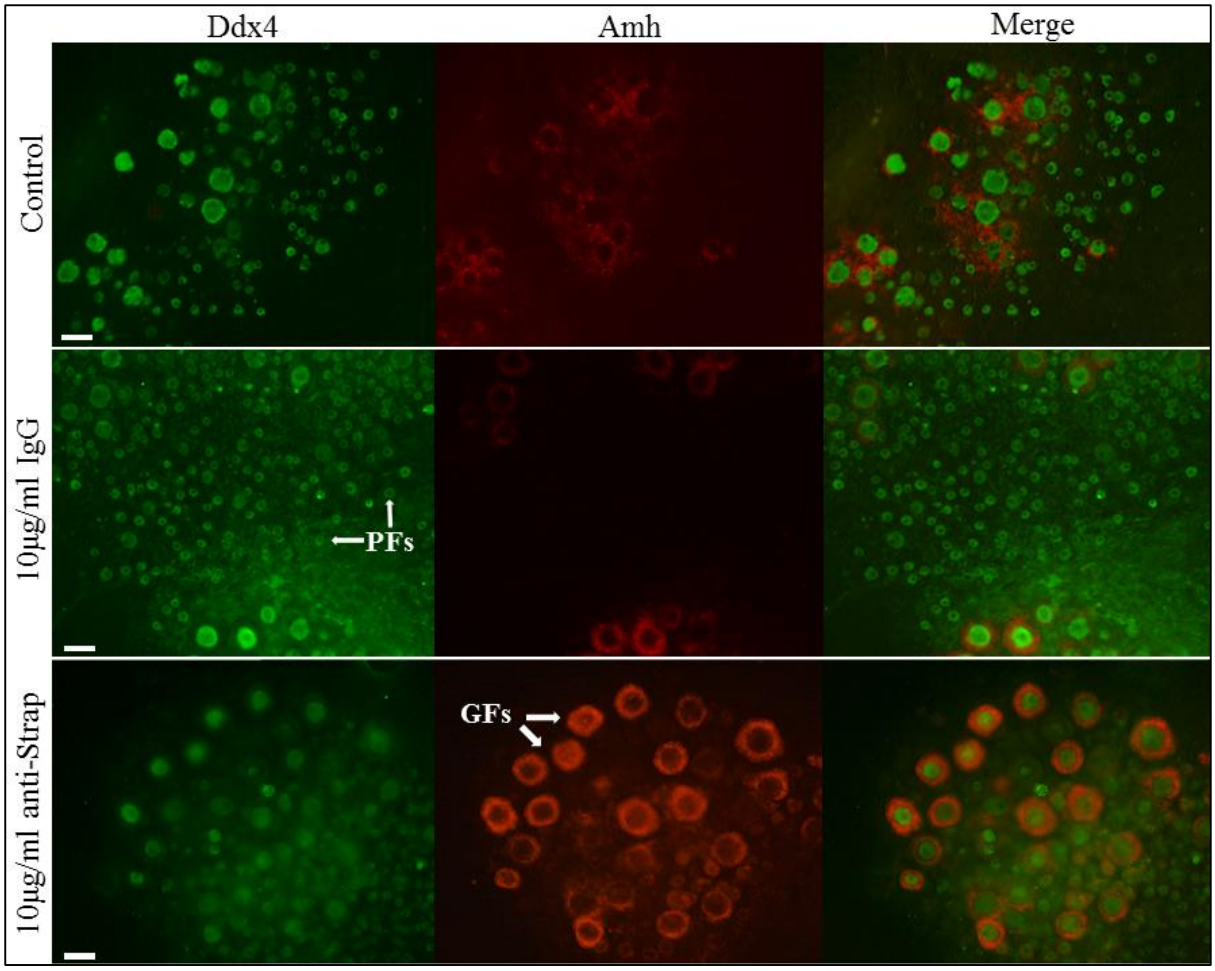

Figure 4.19. Immunofluorescent staining of ovary fragments treated with a high concentration (10µg/ml) of anti-Strap IgG. At the end of culture, fragments were double stained with Ddx4 (green) and Amh (red). GFs: Growing follicles, PFs: primordial follicles. Scale bar= 100µm.

4.4.3. Effect of Strap supplementation on early follicle development

4.4.3.1. Ovary fragments model

The ovary fragments (d4) model was also utilised to identify the effect of rhStrap protein supplementation on primordial follicle growth. In addition to control untreated group, the experiment was designed to culture fragments in 100ng/ml or 200ng/ml rhStrap. After 4 days exposure to rhStrap, there was no difference in the median oocyte diameter of ovaries treated with 100ng/ml rhStrap (23.09µm); however, there was a small, but significant increase in median oocyte diameter in the group treated with 200ng/ml rhStrap compared with control (23.74µm and 22.76µm, respectively; $P<0.05$). This effect was also evident after 7 days ($P<0.05$). When only growing oocytes were considered, there was a significant increase in the median follicle diameter of ovaries treated with 200ng/ml rhStrap vs control after 4 days (33.58µm and 30.79µm, respectively; $P<0.01$).

Both 100ng/ml and 200ng/ml rhStrap caused an increase in the median diameter of growing oocytes after 7 days vs control group (34.17µm; P<0.05 and 34.56µm; P<0.01 vs 31.9µm in control group, respectively) (Figure 4.20).

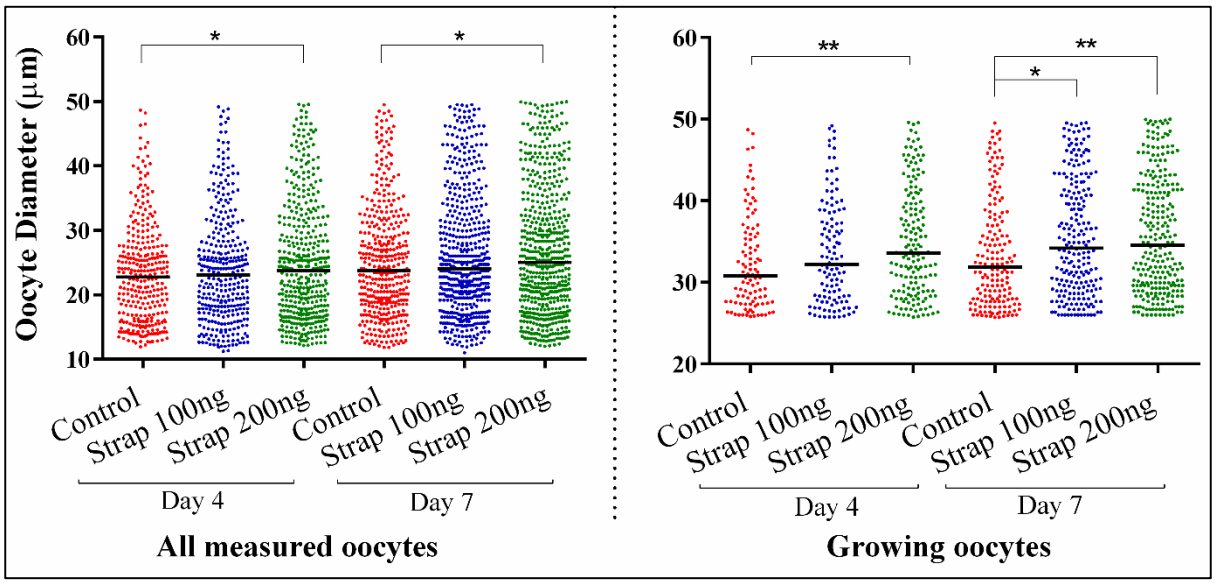

Figure 4.20. Effect of rhStrap on cultured ovary fragments. Day 4 ovary fragments were maintained for 7 days in culture either without treatment (control), 100ng/ml or 200ng/ml rhStrap. Cultured fragments were imaged after 4 and 7 days exposure to different treatments. All measured oocytes (non-growing, transitional and growing) or only growing oocytes (>25.7µm) were plotted. Variation in the median oocyte diameter between groups was evaluated using a Kruskal-Wallis and Dunn's multiple comparisons test. *P<0.05, **P<0.01.

Interestingly, unlike results of *Strap* siRNA and protein inhibition, there was no statistical difference in the proportion of non-growing follicles between treatments at both 4 and 7 days. There was also no differences in the proportions of transitional or growing oocytes (relative to control) in groups exposed to 100ng/ml rhStrap after 4 or 7 days. However, ovary fragments treated by 200ng/ml rhStrap exhibited a reduction in the percentage of transitional oocytes at 4 days (32.8% and 37.8%, respectively; P<0.01 vs control), with a corresponding increase in the proportion of growing oocytes (37.4% and 32.1%, respectively; P<0.01 vs control).

After 7 days, a similar reduction in the proportion of transitional oocytes was found in the 200ng/ml rhStrap treated group vs control (30.1% and 34.5%, respectively; P<0.05) or 100ng/ml group (36.2%, P<0.01). However, there was a significant increase in the proportion of growing oocytes in the 200ng/ml group, relative to the 100ng/ml group (45.5% and 41.7%, respectively; P<0.05) (Figure 4.21).

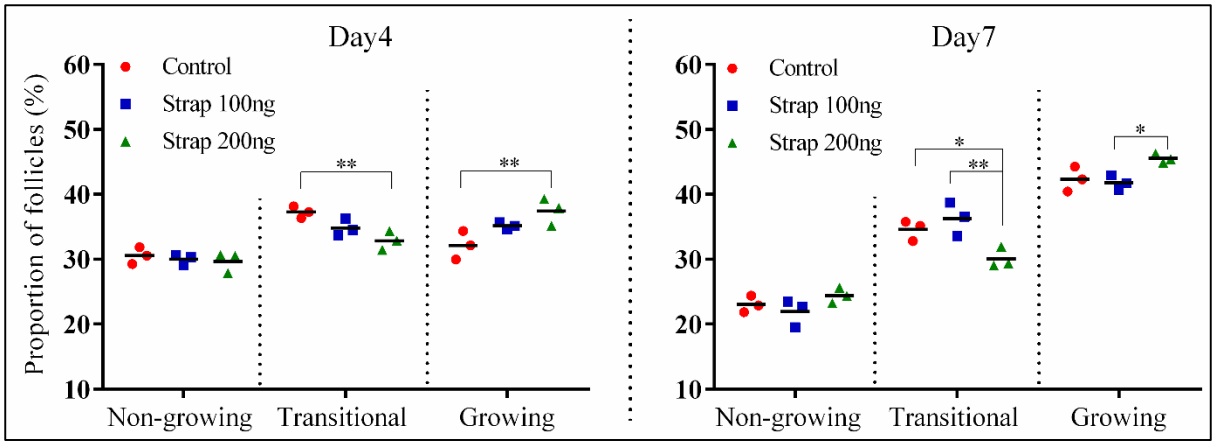

Figure 4.21. Effect of rhStrap treatment on oocyte growth in the ovary fragments culture model. Graphs show the proportion of oocytes in untreated (control), 100ng/ml rhStrap or 200ng/ml rhStrap groups after 4 days or 7 days exposure. Data are presented as mean proportions of oocytes in each stage from three culture plates (n=3). Data were evaluated using ANOVA with a post-hoc Bonferroni multiple comparisons test. *P<0.05, **P<0.01.

Localisation of Amh and Ddx4 in cultured fragments revealed that both rhStrap treated groups included many large growing follicles with relatively more Amh- positive granulosa cells than in control group. Even though, Ddx4 staining revealed the presence of high proportion of non-growing follicles (primordial) in both treated groups (Figure 4.22).

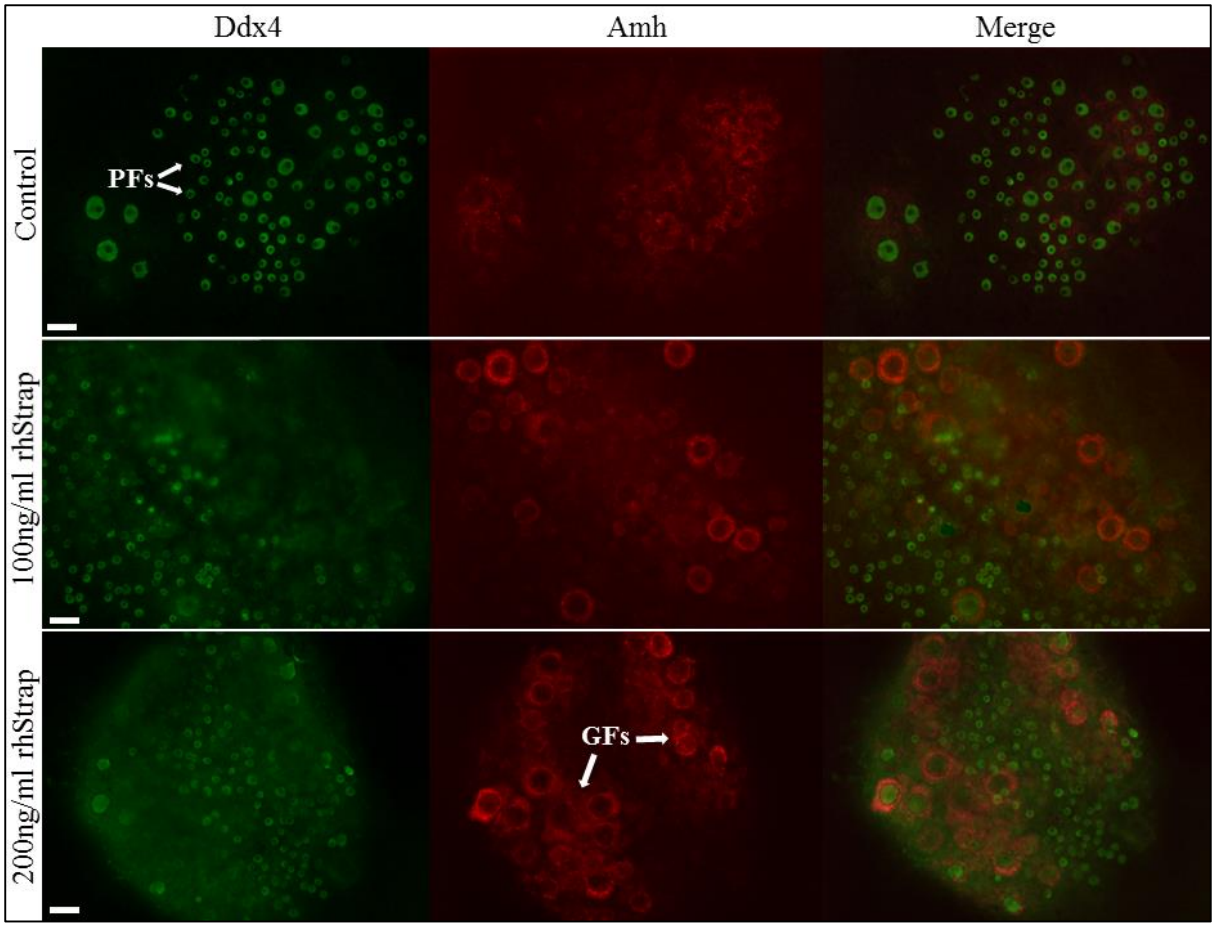

Figure 4.22. Immunofluorescent staining of ovary fragments treated by rhStrap. After 96 hours of culture, ovary fragments were double stained with Ddx4 (green) and Amh (red). GFs: Growing follicles, PFs: primordial follicles. Scale bar= 100µm.

4.4.3.2. Preantral follicle model

Preantral follicles were isolated from d16 ovaries and utilised to evaluate the effect of recombinant human Strap protein (rhStrap) supplementation on follicle growth. Follicles were cultured for 72 hours in the absence or presence of 200ng/ml rhStrap (54 follicles each). Follicle diameters were measured at four-time points (0h, 24h, 48h, and 72h). Some follicles in control and in rhStrap group were excluded from measurements (6 and 10 follicles, respectively) due to morphological changes consistent with degeneration.

In both groups, follicle growth was evaluated by calculating the difference in follicle diameter at each time point relative to the culture starting time point (0h). Thus, the rate of growth for each group was compared. By comparison with untreated follicles, incubation in the presence of 200ng/ml rhStrap caused a significant increase in the mean difference in follicle diameter at 48h (9.2 vs 16.3µm ±95% CI, confidence interval), control and Strap groups, respectively; P<0.01) and 72h (16.8 vs 26.7µm ±95% CI), control and Strap groups, respectively; P<0.001) (Figure 4.23).

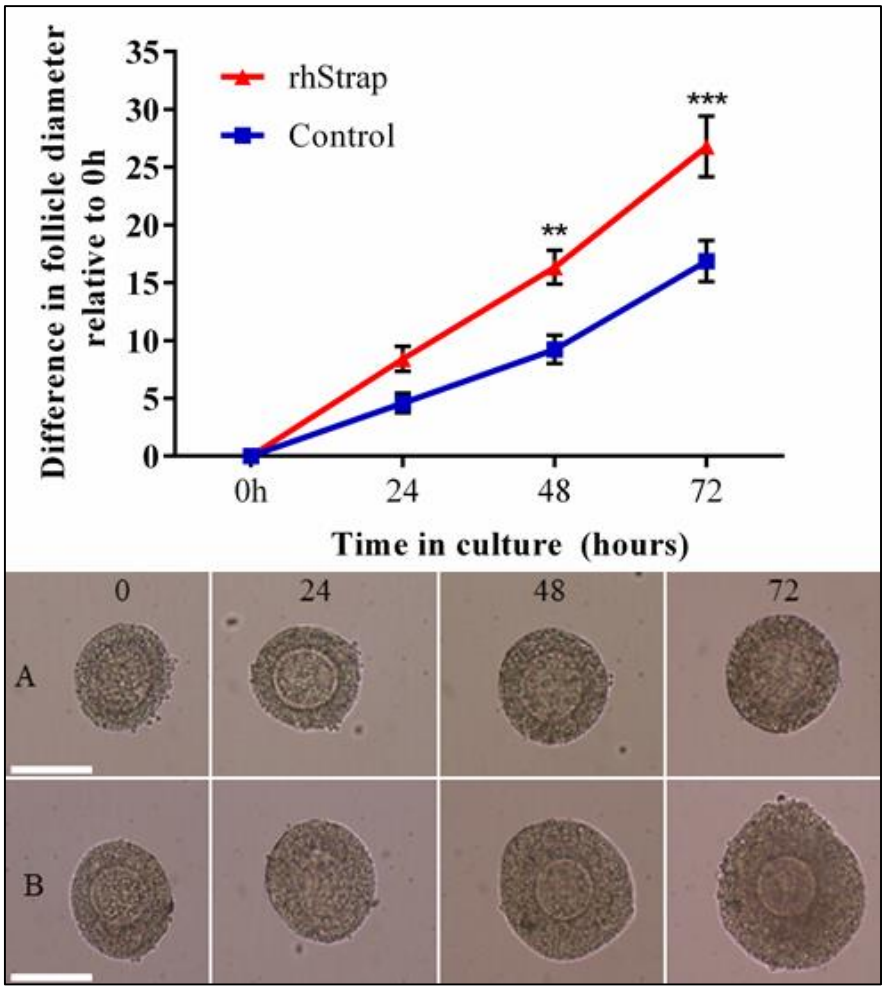

Figure 4.23. Effect of rhStrap treatment on preantral follicle growth *in vitro*. Isolated preantral follicles were cultured for 72h either without treatment (Control n=48 follicles) or with adding 200ng/ml rhStrap (n=44 follicles) to the culture. Follicle diameters were measured every 24h and growth was calculated as the difference in diameter relative to 0h and presented as mean ± SEM at each time point. Data were analysed by a two-way ANOVA with Bonferroni's multiple comparisons test. **P<0.01, ***P<0.001 comparing control vs rhStrap group at 48h and 72h, respectively. Microscope images show examples of cultured preantral follicles from the control group (A) and rhStrap treated group (B). Scale bar= 100µm.

4.5. Discussion

The molecular mechanisms involved in the initial activation and growth regulation of the small gonadotrophin-independent follicles are poorly understood. Many studies have been indicated the essential role of canonical TGFβ signalling pathway (TGFβ/Smad signalling) as intraovarian regulators of follicle development (Li et al., 2008b; Pangas, 2012; Tian et al., 2010). As TGFβ signalling regulates a wide range of cellular activities including proliferation, differentiation, migration, and degeneration (Rahimi and Leof, 2007), dysregulation of signalling results in several reproductive disorders, such as polycystic ovary, early ovarian failure and development of tumours (Hatzirodos et al., 2011; Li, 2015; Pangas et al., 2008).

In other tissues, many Smad inhibitors have been identified to control both duration and strength of signalling (Inoue and Imamura, 2008; Lonn et al., 2009) by various mechanisms including dephosphorisation, ubiquitination and transcriptional co-repressors (Dai et al., 2011; Deheuninck and Luo, 2009; Elliott and Blobe, 2005). Strap is one of these factors that has potential to prevent Smad2/3 phosphorylation by the activated TGFβRI (Datta and Moses, 2000). Previous studies have investigated the impact of Strap in tumourigenesis (Halder et al., 2006; Reiner and Datta, 2011); however, nothing is known about the functional role of Strap in follicle development. In the previous chapter, *Strap* mRNA was detected and its protein was co-localised with Smad2/3 in immature mouse ovaries at different ages; which are densely populated with small (gonadotrophin-independent) follicles. Thus, it was hypothesised that Strap might have a biological role in early follicle growth.

In previous studies, *ex vivo* mouse models have been developed to assess the impact of TGFβ signalling on follicle development (Fenwick et al., 2013; Wang et al., 2014). The present study was designed to determine the effect of modified Strap expression or activity on follicle growth using two different culture models including preantral follicle and d4 ovary fragments culture models. Small interfering RNA (siRNA) and immunoneutralisation by specific antibodies were used for Strap mRNA and protein inhibition, respectively; while supplementation of rhStrap protein was used to enhance the biological function of Strap in both culture model. Intriguingly, this model was amenable to various treatments including siRNA, as well as other macromolecules introduced to the culture media, such as recombinant protein and antibodies.

4.5.1. Ovary fragments culture model

In this model, d4 ovaries, enriched with small non-growing follicles, were sectioned into 6-8 equal sized pieces and utilised to assess the effect of *Strap* siRNA, neutralisation by antibody or protein supplementation on primordial follicle development. Even though this model causes loss of the normal physical architecture of the ovary, it still supports the developmental process and interaction of follicles in the presence of stromal cells. For instance, different stages of follicle growth were identified in cultured fragments and the immunofluorescent staining revealed specific localisation of Amh protein in granulosa cells of growing follicles. Unlike whole ovary culture (Eppig and O'Brien, 1996; Wang et al., 2014), this culture model overcomes several disadvantages of using whole ovaries; for instance, it makes it easier to track and visualise follicle growth under the microscope in real time, and, as cultured fragments flatten out, thus provides more space for follicles to grow.

Intriguingly, this model was amenable to various treatments including siRNA, as well as other macromolecules introduced to the culture media, such as recombinant protein and antibodies. The mechanism that allows the entry of these substances into the cells to interact with target proteins is not clear but may involve non-specific receptor-independent endocytotic processes, such as clathrin-independent endocytosis or micropinocytosis (Maldonado-Baez et al., 2013; Mayor et al., 2014). In addition, fragmentation of the ovary into small pieces provides more accessible surface of the culture media to the ovary tissues. Regardless of the mechanism involved, we observed clear dose-dependent effects of these macromolecules on oocyte growth in this system. Since these outcomes were evaluated in relation to controls indicates that the observed differences were specific to the macromolecule introduced to the system, and may, therefore, be an invaluable model for testing the effects other exogenous compounds on early follicle development *in vitro*.

Consequently, images of cultured fragments can be utilised to identify the effect of treatments by measurement of oocyte diameters and cells can be labelled and visualised in context, e.g. for Amh or Ddx4. A comparable culture model was previously utilised to evaluate the effects of chemotherapeutic treatments on primordial follicles (Maiani et al., 2012). In the study presented here, the effects of all treatments on follicle growth were evaluated by measurements of oocyte diameters. To make these *in vitro* measurements comparable to *in vivo* growth, a novel system of oocyte classification was determined to categorise oocyte growth according to their size, where oocytes were classified as non-growing (<18.3µm), transitional (18.3µm-25.7µm) and growing (>25.7µm) based on morphological characteristics ascertained from microscopic sections. Thus, this model was found to be valid and appropriate to study the effect

of various treatments on early follicle development by providing quantitative data for analysis alongside protein staining.

4.5.2. Effect of Strap downregulation and neutralisation on primordial and preantral follicle growth

The functional impact of Strap on the development of mouse embryos was previously investigated, where deletion of Strap caused prenatal mortality (E10.5-E12.5) due to major congenital abnormalities including defects of the cardiovascular, neural and musculoskeletal system (Chen et al., 2004). Thus, in the present investigation, an ovary fragments culture model was used to assess the impact of *Strap* knockdown on the developmental process of small non-growing follicles (primordial follicles) *in vitro*. At the end of treatment (96 hours), the median oocyte diameters in the *Strap* siRNA treated group were significantly higher than in control groups. Furthermore, exposure to *Strap* siRNA caused a significant decline in the proportion of the non-growing oocytes accompanied with an increase in the proportion of growing oocytes relative to control.

In *Strap* siRNA treatment group, the increased proportion of growing oocytes was accompanied with immunofluorescent staining of many Amh-positive granulosa cells. Similar results were obtained by inhibition of Strap protein bioactivity using 1 or 10μg/ml anti-Strap IgG, where the higher concentration was more effective. These results suggest that Strap is involved in keeping primordial follicles in a quiescent state. The increase in the median follicle diameters in the treated groups (*Strap* siRNA or Anti-Strap IgG) relative to controls indicates that follicles in these groups were activated to grow earlier than in controls. The role of Smad2/3 proteins in small follicles is not clearly understood, but it is assumed that the loss of Strap leads to increased TGFβ signalling. In the present study, it is somewhat surprising that promoting of TGFβ signalling (by inhibition of *Strap* mRNA or protein bioactivity) results in enhanced follicle growth. Previous studies have demonstrated a growth suppressing effect of TGFβ signalling on follicle development (Ding et al., 2010) and tumour progression (Singha et al., 2014). However, the enhanced Smad2/3 pathway (by inhibition of Strap mRNA or protein) might consequently be an essential prerequisite for follicles to initiate growth.

An *in vitro* study indicated that deletion of both Smad2/3 caused a significant decrease in the reproductive efficiency manifested by the failure of the small follicle to grow, ovulation, and improper expansion of cumulus cells (Li et al., 2008b). In addition, in mice at 3 months of age, deletion of exon 8 of Smad3 have significantly more non-growing follicles and fewer growing follicles than wild-type mice (Tomic et al., 2004).

These results suggest that adequate Smad3 expression is important for follicle activation. *Strap* siRNA was also utilised to assess the impact of *Strap* mRNA downregulation on cultured preantral follicle growth. After three days of exposure, the expression of *Strap* mRNA in the treated group was significantly reduced relative to the non-targeting siRNA, however, the reduction was not statistically different relative to control (Figure 4.12). After three days in culture, there was no significant difference in follicle size between *Strap* siRNA group and controls. However, at the first 24h exposure, the mean follicle diameter was significantly greater in control and non-targeting siRNA groups relative to the starting point at 0h, but not in the *Strap* siRNA group. This observation might reflect the short half-life of *Strap* siRNA, as fluorescent microscopy (Figure 4.11) of green non-targeting siRNA treated follicles revealed a decreased fluorescent signal in follicles with time, where the strongest intensity was at 24h of culture. In addition, it might explain the absence of significant difference in *Strap* transcript levels revealed by qPCR between the control and *Strap* knockdown groups.

The difference in follicle size during the first 24h between groups might cause a prolonged TGFβ1-3/Smad2/3 signalling, which has an anti-proliferative impact on cells (Brown et al., 2007). In addition, it might attributes to other biological roles of Strap in cells, as other studies indicated that Strap can regulate a wide range of signalling pathways (Halder et al., 2006; Seong et al., 2005).

4.5.3. Effect of Strap protein on primordial and preantral follicle growth

In contrast to *Strap* siRNA and protein neutralisation, incubation of ovary fragments in media supplemented with exogenous Strap protein (rhStrap) (100 or 200ng/ml) revealed no effect on the proportion of small non- growing oocytes relative to controls. However, a significant increase in the proportions of transitional and growing oocytes was evident in both treated groups relative to control. After 7 days of rhStrap exposure, a significant increase in the median diameter of growing oocytes was determined relative to control. These observations might indicate the essential impact of Strap on the growth of the small growing follicle. In addition, immunofluorescent staining revealed more Amh staining with the increased concentration of rhStrap, suggesting more growing follicle are present; although many non-growing oocytes were stained with Ddx4 in both rhStrap treated groups.

The overall effect of rhStrap on increased follicle size may associate with activation of pathways that can promote cell proliferation such as non-Smad pathway. For instance, in addition to the role of Strap as anti-apoptotic function (Jung et al., 2010), several reports have shown that the presence of Strap can activate the cell proliferative enhancing signals such as ERK/MAPK (Halder et al., 2006), and PDK1 (Seong et al., 2005) (Figure 4.24). In the ovary, it was indicated that activation of such non-canonical pathways can lead to the early depletion of the primordial follicles reserve due to an enhanced primordial follicle activation and follicle growth (John et al., 2008; Reddy et al., 2009; Reddy et al., 2008; Zheng et al., 2012).

In ovary fragments culture, treatment with 200ng/ml rhStrap exhibited more impact on follicle growth than 100ng/ml rhStrap, thus a higher concentration of Strap protein was used to assess its influence in preantral follicle growth. Treated preantral follicles demonstrated a significant increase in size after 48h and 72h of exposure relative to the untreated group. A possible explanation for this effect might relate to the fact that Strap has the potential to control an extensive range of biological activities and intracellular signalling pathways, other than the canonical TGFβ (Reiner and Datta, 2011). For instance, upregulation of Strap has been linked to prompt tumour progression results in the activation of extracellular signal-regulated kinase (ERK) in different cell lines, inhibition of cell cycle suppressor proteins ($p21^{Cip1}$) (Halder et al., 2006). Moreover, Strap can activate 3-phosphoinositide-dependent protein kinase 1 (PDK1), which is responsible for various cellular activities including proliferation, migration, metastasis of a tumour and antagonising of the apoptotic processes induced by tumour necrosis factors-alpha TNF-α (Seong et al., 2005). Furthermore, in the absence of TGFβ signalling, upregulation of Strap enhances the association of PDK1 with R-Smads, Smad4 and Smad7 proteins (Seong et al., 2007). Thus, Strap has the potential to regulate TGFβ signalling and consequently cellular growth by switching off the proliferative suppressor pathway (Smad pathway) and activate the proliferative pathway (non-Smad pathway) (Fleming et al., 2009; Halder et al., 2006).

The non-Smad pathway has been identified as a part of the complex system that regulating early follicle growth (Reddy et al., 2008; Zheng et al., 2012). Thus, the increased size of cultured preantral follicle might be accounted for the effect of rhStrap by activation of cell proliferative pathways. In addition, analysed data from qPCR (Figure 3.7) and protein localisation (Figures 3.11) revealed that expression of Smad2/3 was reduced in the growing preantral follicles, suggesting that reduction in Smad2/3 expression is essential to promote the growth of the preantral follicle.

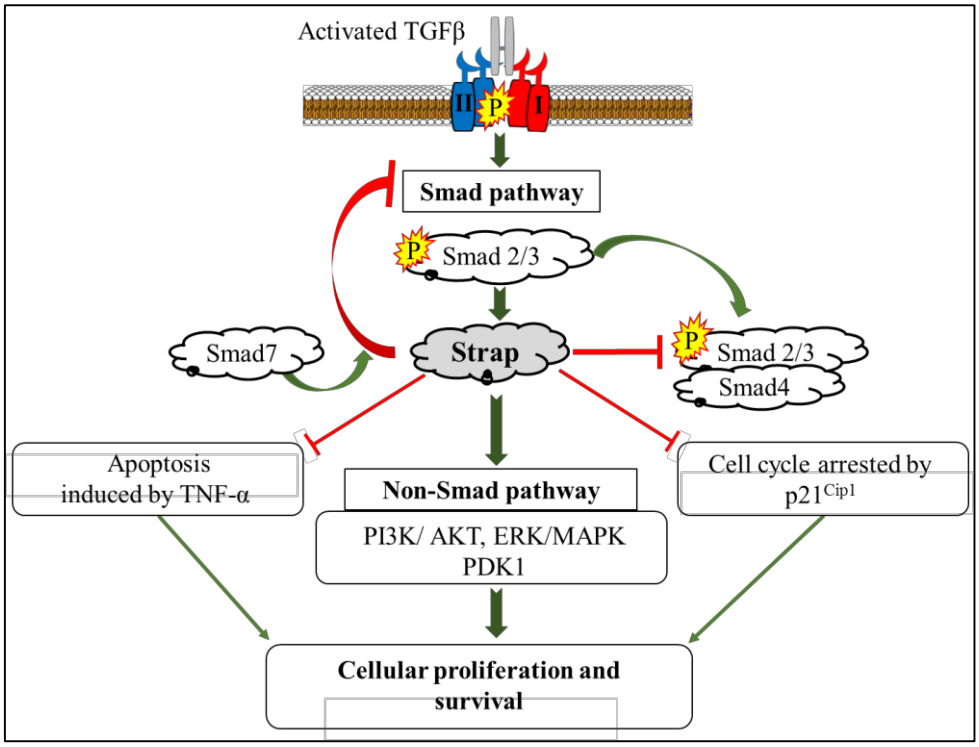

Figure 4.24. Functional role of Strap in the regulation of cell growth. Strap inhibits the anti-proliferative Smad2/3 pathway by recruiting and stabilising Smad7 to the activated TGFβ receptors to prevent phosphorylation of Smad2/3. In addition, Strap blocks the nuclear translocation of the heteromeric complex by interaction with the activated R-Smad and Smad4. Conversely, Strap can promote cellular growth by activating the proliferative Smad-independent pathways accompanied with inhibition $p21^{Cip}$ resulting in progression in the cell cycle. Strap can also prevent cell apoptosis by inhibition of TNF-α (Seong et al., 2005). Thus, generally, Strap functions to enhance both cellular growth and survival by activation of the Smad-independent pathway and overcomes the growth suppression impact of the Smad-dependent pathway by inhibition of Smad2/3 and by blocking the nuclear translocation of activated heteromeric complex.

Even though the ovary fragment culture was useful in these experiments, some drawbacks were apparent. For example, dissection of ovaries into many small pieces makes them unsuitable for imaging during the first 3 days until they have spread on the base of the well. Therefore, treatments should be applied after this times period; however, many of the oocytes would have already begun to grow so many primordial oocytes/follicles will be missed. In addition, if fragments are too large, it will limit the amount of microscope light to pass through the tissue, which consequently affects follicle counting/ measurements and resolution of immuno-staining will be difficult. Although the Amh staining was a valuable protocol to visualise the growing follicles in cultured fragments, it would be preferable to also quantify *Amh* and other genes that associated with follicle growth, such as *Fshr*, *Cyp17a* or *Cyp19a*. Moreover, it is not recommended to extend the culture of ovary fragments beyond 10 days, or more, as tissues will flatten too much and lose the relationships important with the 3-D architecture.

In conclusion, this is the first study that evaluated the effect of different Strap treatments on primordial and preantral follicle development. Strap is capable of regulating follicle development in a growth stage-specific manner demonstrated by a reduction in the number of activated primordial follicle and promote preantral follicle growth; however, it is proposed that the actions of Strap depends on the stage-specific expression of Smad2/3 and might be relevant with non-Smad pathway (Figure 4.25).

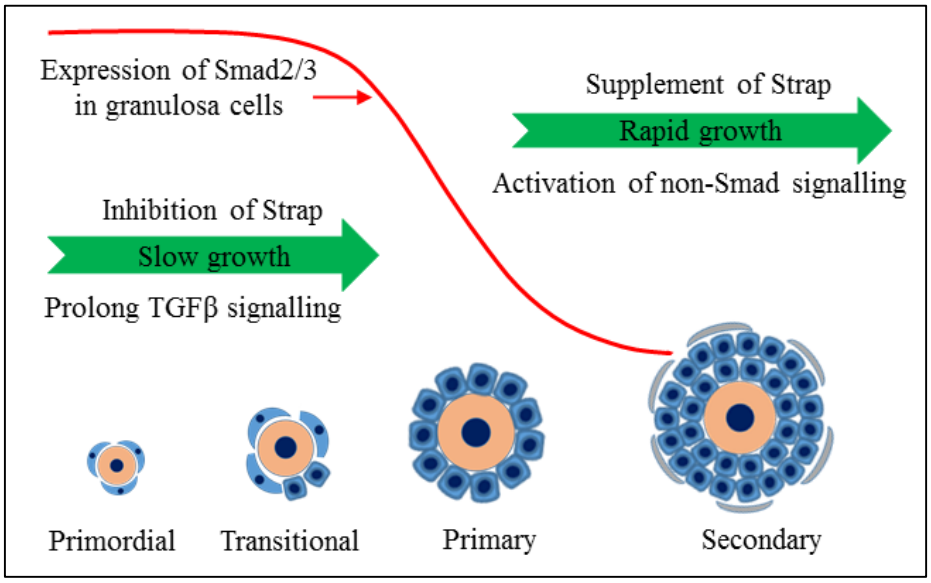

Figure 4.25. Effect of Strap modulation on follicle growth. Granulosa cells of small single-layered follicles, which are relatively slow growing, express Smad2/3. Inhibition of Strap expression or neutralisation of its relative protein caused a reduction in the population of non-growing follicles, which might attribute to the prolonged TGFβ signalling and promote the transition of growth through the early follicle stages. However, supplementation of Strap can drive the non-Smad pathways such as PI3K and MAPK to promote cell proliferation and follicle growth. Further follicle growth is associated with a reduction in Smad2/3, which may be facilitated by the ascribed role of Strap in inhibiting TGFβ signalling.

Chapter 5
Identification and regulation of transmembrane prostate androgen-induced RNA (TMEPAI) in the mouse ovary

5.1. Introduction

In the ovary, the state of follicle dormancy and early follicle development are controlled by complex interactions of locally secreted factors, such as the TGFβ superfamily, which acts to either suppress or activate follicle growth (Kim, 2012). The TGFβ ligands exert their effects through the activation of particular serine/threonine kinase receptors, which eventually activate the R-Smads (Moustakas and Heldin, 2009). After translocation into the nucleus, the biological effects of TGFβ/Smad signalling modulate the transcription of target genes (ten Dijke et al., 2000). TGFβ signalling can regulate gene transcription in two ways including the canonical Smad pathway and non-Smad pathways, such as MAPK, PI3K/AKT, Rho (Derynck and Zhang, 2003; Mu et al., 2012). In addition, the duration and strength of TGFβ signalling can be modified through a self-regulating mechanism; for example, the expression of Smad inhibitors can be induced by increased TGFβ signalling (Quezada et al., 2012; ten Dijke and Hill, 2004).

In prostate cells, Transmembrane prostate androgen induced RNA (Tmepai), also termed Pmepa1 (prostate transmembrane protein androgen induced 1) is modulated by androgens in a duration and dose-specific manner (Xu et al., 2000). Tmepai also has a negative impact on the growth of these cells, and the expression of Tmepai is regulated by androgens through a negative feedback mechanism (Xu et al., 2003). Overexpression of *Tmepai* through androgen signalling causes inhibition of androgen receptors by stimulation of Nedd4, which promotes ubiquitination and proteasome degradation of the androgen receptors (Li et al., 2008a). More recently, other studies have shown that *Tmepai* expression is not only induced by androgens, but also by TGFβ/Smad signalling (Singha et al., 2014; Watanabe et al., 2010), as well as other signalling pathways, such as p53, Wnt, and EGF (Anazawa et al., 2004; Itoh et al., 2003). Tmepai is also overexpressed in tissues affected by various kinds of cancer; for instance lung, breast, colon, pancreas, prostate cancer, and renal cell carcinomas (Brunschwig et al., 2003; Li et al., 2008a; Rae et al., 2001; Singha et al., 2014; Vo Nguyen et al., 2014). The overexpression of Tmepai is associated with the advanced stages of tumour progression, suggesting that Tmepai enhances or permits proliferation of tumorigenic cells (Vo Nguyen et al., 2014).

Interestingly, Tmepai inhibits the TGFβ/Smad signalling pathway through a negative feedback mechanism, where some of the TGFβ ligands (including TGFβ1-3 and Activin) induce the expression of Tmepai. Tmepai then inhibits TGFβ signalling by competing with the Smad anchor of receptor activation (SARA) for interaction with both Smad2 and Smad3 preventing Smad phosphorylation via the activated TGFβ receptor complex (TGFβRI and TGFβRII) (Azami et al., 2015; Watanabe et al., 2010). In addition, Tmepai can block TGFβ signalling by interacting with the activated TGFβRI to enhance the lysosomal degradation of the receptor (Bai et al., 2014). Another study found that Tmepai also inhibits the Smad3/4–c-Myc–p21-signalling pathway leading to an enhanced proliferation of prostate cell tumours (Liu et al., 2011).

In contrast to the inhibitory impact on Smad signalling, Tmepai can activate PI3K/AKT signalling, which is regulated by PTEN. For example, in human breast cancer cells, Tmepai has the potential to block PTEN leading to increased phosphorylation of PI3K/AKT and cellular proliferation, growth and migration (Singha et al., 2014; Xie et al., 2016). Furthermore, deletion of *Tmepai* in breast cancer cells caused elevated expression of PTEN protein accompanied with a reduction in AKT phosphorylation. Conversely, increased *Tmepai* expression by TGFβ treatment in cancer cells leads to decreased PTEN expression and AKT activation (Singha et al., 2014) (Figure 5.1).

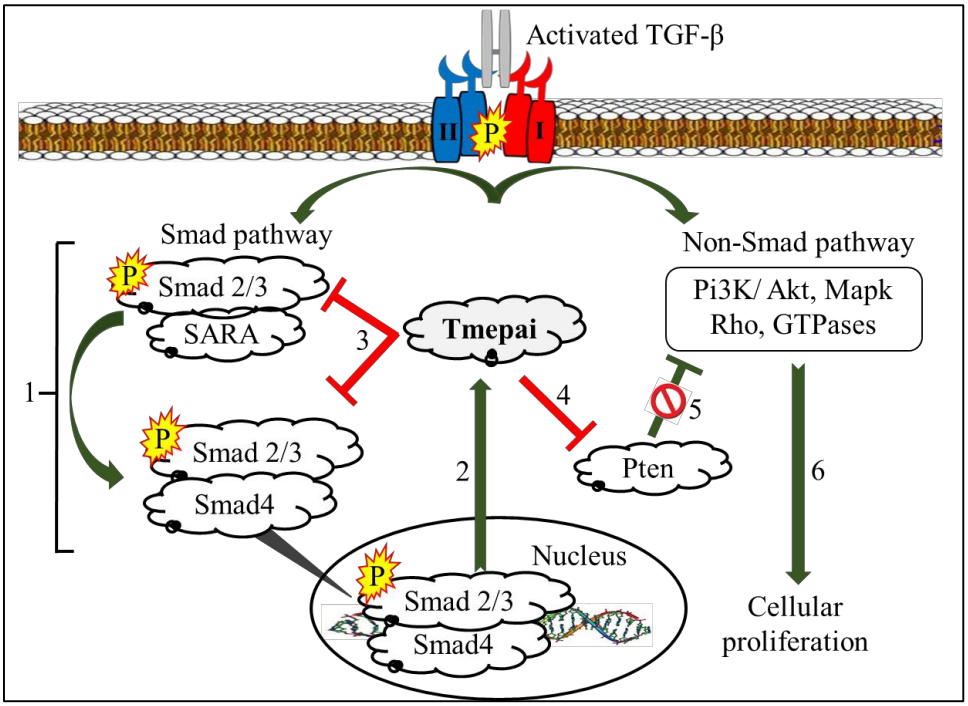

Figure 5.1. Schematic model illustrating the role of Tmepai in regulating TGFβ signalling. TGFβ signalling is initiated by the interaction of activated TGFβ ligand with TGFβ I/II receptors followed by the recruitment of Smad2 and Smad3, which is directed by the cytoplasmic protein SARA to the phosphorylated type I receptor for activation. After activation, Smad2/3 forms a complex with Smad4 to enable their translocation into the nucleus to regulate the transcription of target genes (1). Increased TGFβ signalling causes upregulation of Tmepai expression (2). At this point, Tmepai negatively regulates the duration and intensity of TGFβ/Smad pathway in two ways; firstly, it competes with SARA for association with Smad2 and Smad3 to prevent their activation. Secondly, Tmepai can block the nuclear translocation of the phosphorylated Smad2 and Smad3 (3). Tmepai also causes degradation of PTEN (4), a PI3K/AKT inhibitor, leading to the activation of non-Smad pathways (5) which function to induce cellular proliferation (6). Adapted from (Singha et al., 2014; Watanabe et al., 2010).

In the ovary, expression, regulation and the impact of Tmepai on follicle development has not yet been investigated. Considering the loss of nuclear Smad2/3 with the onset of follicle growth, it is hypothesised that Tmepai may also be detectable in small follicles to account for this change in Smad expression. Furthermore, given that in other cell types, the TGFβ/Smad signalling pathway can regulate Tmepai expression, it is proposed that the expression of this gene is under the control of relevant TGFβ members in small follicles.

The objectives of this chapter are to determine the expression of *Tmepai* mRNA and protein during early follicle development. Then, to evaluate the influence of enhanced TGFβ signalling (by GDF9 supplementation) and receptor inhibition (by SD208) on both the regulation of *Tmepai* expression and preantral follicle growth.

5.2. Materials and methods:

5.2.1. Animals and tissues

Ovaries were dissected from mice of different ages (d4, 8, 16 and adults) as described in 2.1. Ovaries were used for both mRNA and protein expression. In addition, preantral follicles were isolated from d16 ovaries, where similar procedures and materials specified in section 2.2.2 were used for preantral follicle isolation, selection and culture.

5.2.2. Immunohistochemistry

Ovary sections (5µm) from d4, d8, d16 and adult were prepared (section 2.9.1) for colocalisation of Tmepai and Smad2/3 proteins. Goat anti-Tmepai (1µg/ml, Santa Cruz- sc-85829) and Mouse anti-Smad2/3 (0.25µg/ml, Santa Cruz sc-133098) were used for staining according to the protocol described in section 2.9.3. For negative controls, equivalent quantities of non-immune Goat and Mouse IgG (Vector) were utilised to determine non-specific staining in ovary sections. Sections were incubated in a mixture of secondary antibodies including Alexa Fluor 488 Donkey anti-Goat IgG (1:400µl, Molecular probes, A11055) and Alexa Fluor 555 Donkey anti-Mouse IgG (1:400µl, Molecular probes, A31570). Stained tissues (three experiments from three different ovaries) were imaged by a Leica inverted SP5 confocal laser scanning microscope (Leica Microsystems, Wetzlar, Germany).

5.2.3. Preantral follicle culture

Preantral follicle cultures were utilised to identify the effect of a TGFβ ligand (recombinant mouse Gdf9, rmGdf9), an Alk5 inhibitor (SD208) or a combination of both treatments on *Tmepai* expression and follicle growth. This culture model was selected over the ovary fragment model, as both Tmepai quantification and protein staining were higher in the d16 ovary contained many small growing follicles. GDF9 was selected among other TGFβ ligands as it is highly expressed in preantral follicles in the ovary, is known to signal through the TGFβR1 (ALK5 receptor), and is mediated by the Smad2/3 pathway (Shi and Massague, 2003). SD208 is an inhibitor of the TGFβRI kinase receptor and acts by preventing phosphorylation of Smad2/3 (Uhl et al., 2004). Follicles from each single ovary were cultured in wells of four lines (5 follicles per line) of different treatments. The culture media consisted of MEM-α media with supplements (see section 2.2.2). Each single line represents an individual treatment group of (i) untreated control, (ii) 1µM SD208 (Sigma; S7071-5MG) (Wang et al., 2014) (iii) 250ng/ml rmGdf9 (R&D systems; 739-G9) (Fenwick et al., 2013) and a combination of 1µM SD208 with 250ng/ml rmGdf9 (Figure 5.2).

Dimethyl Sulfoxide (DMSO; Sigma- 472301) was used as a solvent for SD208, thus equivalent volumes of DMSO were added to the control and rmGdf9 treatment groups. All plates (11 in total) were cultured at 37°C in the presence of 5% CO_2.

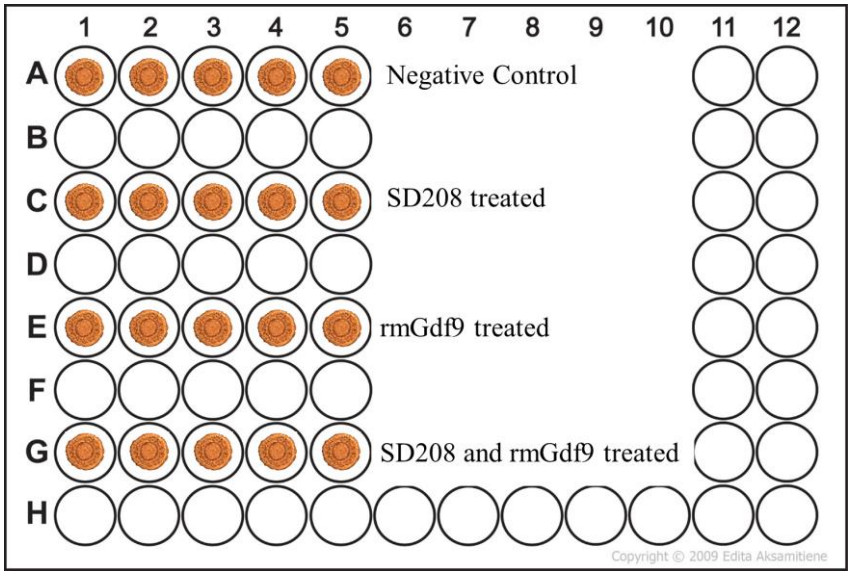

Figure 5.2. The layout of cultured preantral follicles. Eleven plates were prepared, follicles from a single ovary were utilised for each individual plate. Follicles were cultured in four rows where each row consists of five follicles. For RNA extraction, follicles of each particular treatment were collected and were transferred into a single Eppendorf tube.

Total RNA was extracted from cultured preantral follicles after 24h (n= 5 plates) as described in 5.2.2. The remaining six plates were cultured for a total of 72 hours to identify the effect of treatments on follicle growth. Half of the culture media was refreshed after 48 hours of incubation. Follicles were imaged at 0, 24, 48 and 72 hours using light microscopy (Olympus CKX41 with a Nikon camera DS-Fi1). Images were utilised for the measurement of follicle diameters by ImageJ software as described in 2.10.1. At the end of culture (72 hours), follicles were collected, fixed in 10% neutral buffered formalin (Sigma), embedded, sectioned and counterstained with DAPI.

5.2.4. RNA extraction, RT-PCR and qPCR

cDNA of d4, d8, d16 and adult ovaries (n=5 per age group) were prepared (RNA 25ng/µl) and used for gene expression by RT-PCR and qPCR as previously described (2.6 and 2.8, respectively). Total RNA was also extracted from cultured preantral follicles after 24 hours of incubation (n=5 plates), using Qiagen RNeasy Micro Kits (section 2.3). Five cultured follicles from each treatment line were individually pooled and snap frozen in liquid nitrogen and stored at -80ºC.

After extraction, RNA samples were evaluated for integrity and concentration using Agilent 2100 Bioanalyser (Appendix XII). An equivalent concentration of RNA from each sample (12.5ng/µl) was reverse transcribed into cDNA (section 2.4) and tested by RT-PCR for the expression of *Gdf9* as an oocyte-specific internal control. Primers used in PCR reactions, including sequences, annealing temperatures and product sizes for *Tmepai, Gdf9, Strap* and *Smad3* are provided in Table 5.1.

Table 5.1. Oligonucleotide primer sequences used for gene quantification by qPCR.

Gene	Primer sequences (5' →3')	Annealing Temperature	Product size (bp)
Tmepai	F: CTTGTCAAAGGCAGGGTGTC R: CTTTCCAACCAGCCACTTCC	59.0	165
Gdf9	F: TCACCTCTACAATACCGTCCGG R: AGCAAGTGTTCCATGGCAGTC	59.0	139
Strap	F: GGCTACTTTCTGATCAGCGC R: CTGAGACCGCATCCCATACT	59.0	187
Smad3	F: GTCAAAGAACACCGATTCCA R: TCAAGCCACCAGAACAGAAG	58.5	154

Samples were then utilised for quantification of *Tmepai*, *Smad3* and *Strap* by qPCR (section 2.8). *Tmepai* was considered for expression as it is a specific inhibitor of Smad2/3 (Singha et al., 2014) and it has not been expressed in the ovary, yet. As Strap has been identified as a Smad2/3 inhibitor and was the focus of the previous chapter, it was also assayed to identify whether its expression is related to TGFβ signalling in this model. Data from qPCR (ovary and follicle samples) were analysed as fold changes relative to a housekeeping gene (*Atp5b*) using the equation $2^{-\Delta\Delta CT}$ method (Livak and Schmittgen, 2001).

5.2.5. Statistical analysis

Data (CT values) from qPCR were normalised relative to the expression of the internal housekeeping gene (*Atp5b*). Fold changes relative to control were calculated using the $2^{-\Delta\Delta CT}$ equation method, as described in 2.8. Data were statistically analysed using one-way ANOVA with Bonferroni post-hoc test; the differences between groups was considered significant at $P<0.05$. The difference in preantral follicle size between treated groups and control was analysed by one-way ANOVA with Bonferroni post-hoc test of the cultured follicle, *$P<0.05$, **$P<0.01$, ***$P<0.001$ and ****$P<0.001$.

5.3. Results

5.3.1. Expression of *Tmepai* mRNAs in immature and adult ovaries.

Tmepai mRNA was detected in cDNA from mice ovaries at d4, d8, d16 and adult by RT-PCR, stronger bands of expression were detectable in d8 and d16 (Figure 5.3).

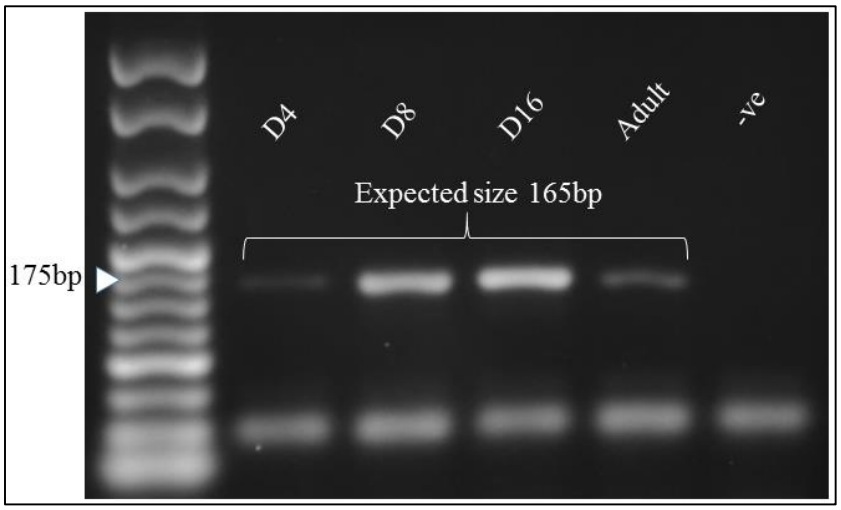

Figure 5.3. Expression of *Tmepai* in ovaries at different ages by RT-PCR. For negative control (-ve), RNase/ DNase free water was added rather than cDNA.

By qPCR analysis, levels of *Tmepai* mRNA were significantly higher in the d16 ovary, which contains a mixture of primordial and growing follicles relative to d4 ovary ($P<0.05$), which contains mostly primordial follicles. However, there was no significant difference in the expression levels of *Tmepai* in d8 or adult ovaries relative to d4. In the same samples, expression levels of *Smad3* revealed a significant decline in the d16 and adult ovaries relative to d4 ($P<0.05$ and $P<0.001$, respectively) (Figure 5.4), which is consistent with findings in chapter 3.

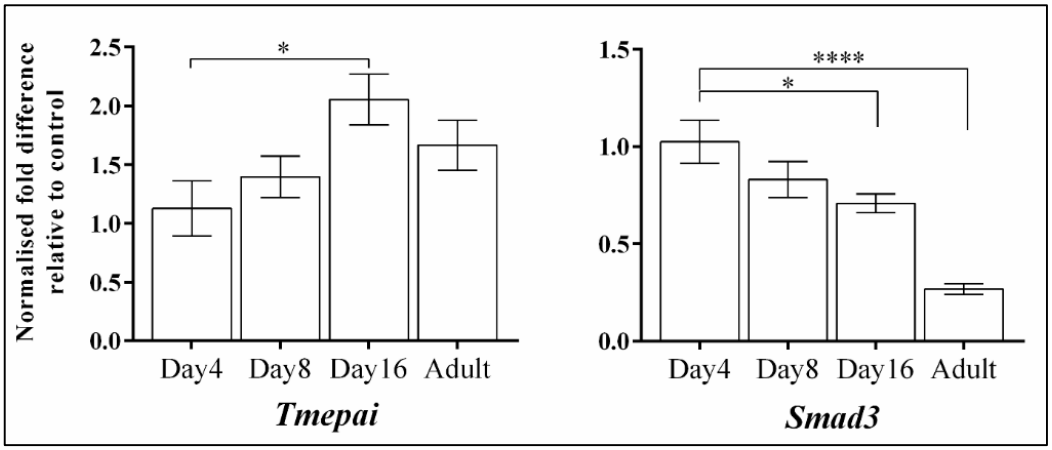

Figure 5.4. Expression levels of *Tmepai* and *Smad3* mRNA in immature and adult ovaries. Data were normalised relative to the expression of the internal housekeeping gene, *Atp5b*, and expressed as fold changes relative to d4 ovary. Statistical differences were assessed using one-way ANOVA with Bonferroni post-hoc test. Data (n=5) are presented as mean ± SEM. *P<0.05, ****P<0.0001.

5.3.2. Colocalisation of Tmepai and Smad2/3 proteins

Immunofluorescent staining was performed to identify the expression pattern of Tmepai protein and the relationship with Smad2/3 expression. In the d4 ovary sections, Tmepai protein was localised in granulosa cells of numerous growing follicles located in the medulla of the ovary. In addition, staining was also observed in some oocytes of primordial follicles located in the peripheral region of the ovary, but not in the stroma. Smad2/3 was localised as previously described (Figure 3.11) in granulosa cells of primordial and growing follicles (Figure 5.5).

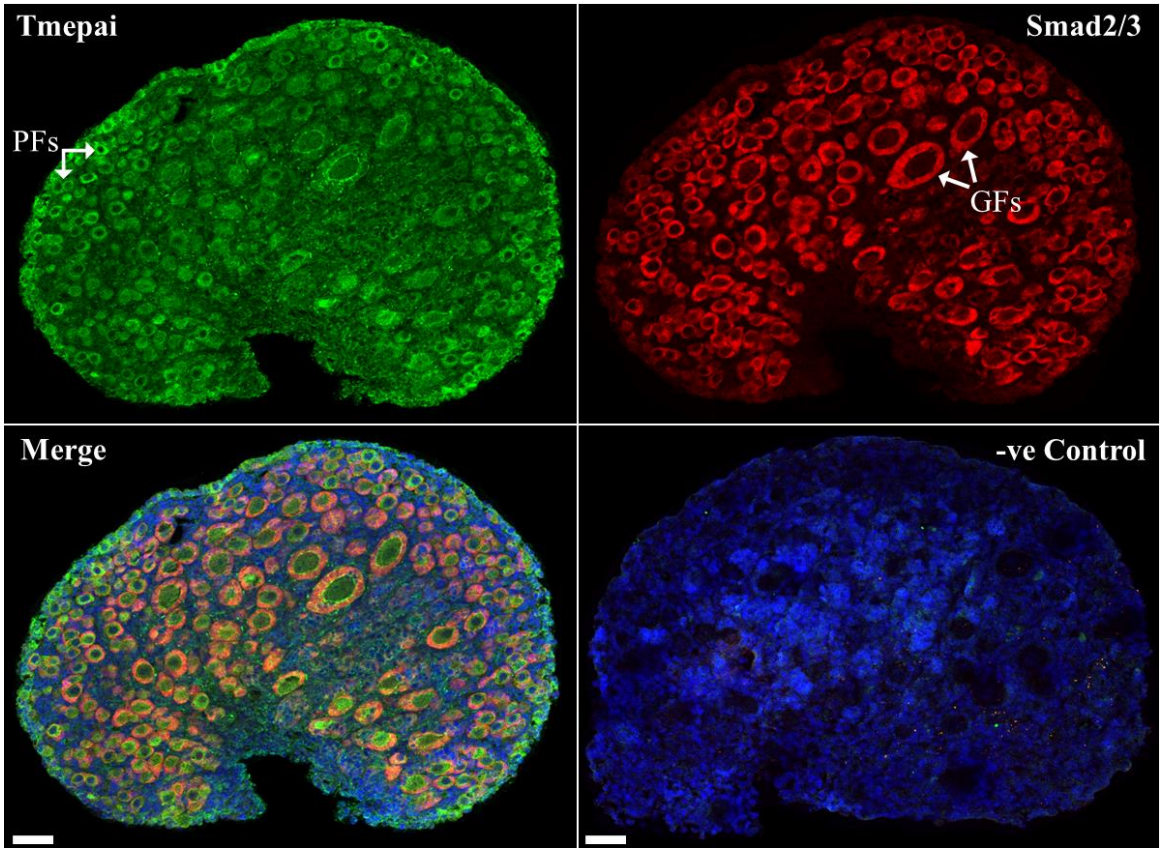

Figure 5.5. Colocalisation of Tmepai and Smad2/3 proteins in d4 ovary. Tmepai (green) was detected in granulosa cells of growing follicles (GFs) located in the medial aspect of the ovary and in some primordial (PFs) located in the cortical area. Smad2/3 proteins (red) were localised with a strong staining in primordial and growing follicles. Tmepai and Smad2/3 were co-localised in growing and numerous non-growing follicles. The negative control section (-ve) was treated with a mixture of non-immune Goat and Mouse IgG's. Nuclei were counterstained with DAPI (blue). Scale bar = 75μm.

High power confocal microscopy of the positively stained growing follicles revealed that Tmepai protein expression is more evident in granulosa cells of follicles that have developed a complete layer of cuboidal granulosa cells. The intensity of staining was stronger in follicles that had begun to develop a second layer of granulosa cells. In single-layered, primary follicles, the localisation of Tmepai protein exhibited a high intensity of staining at the internal surface of granulosa cells close to the oocyte (Figure 5.6).

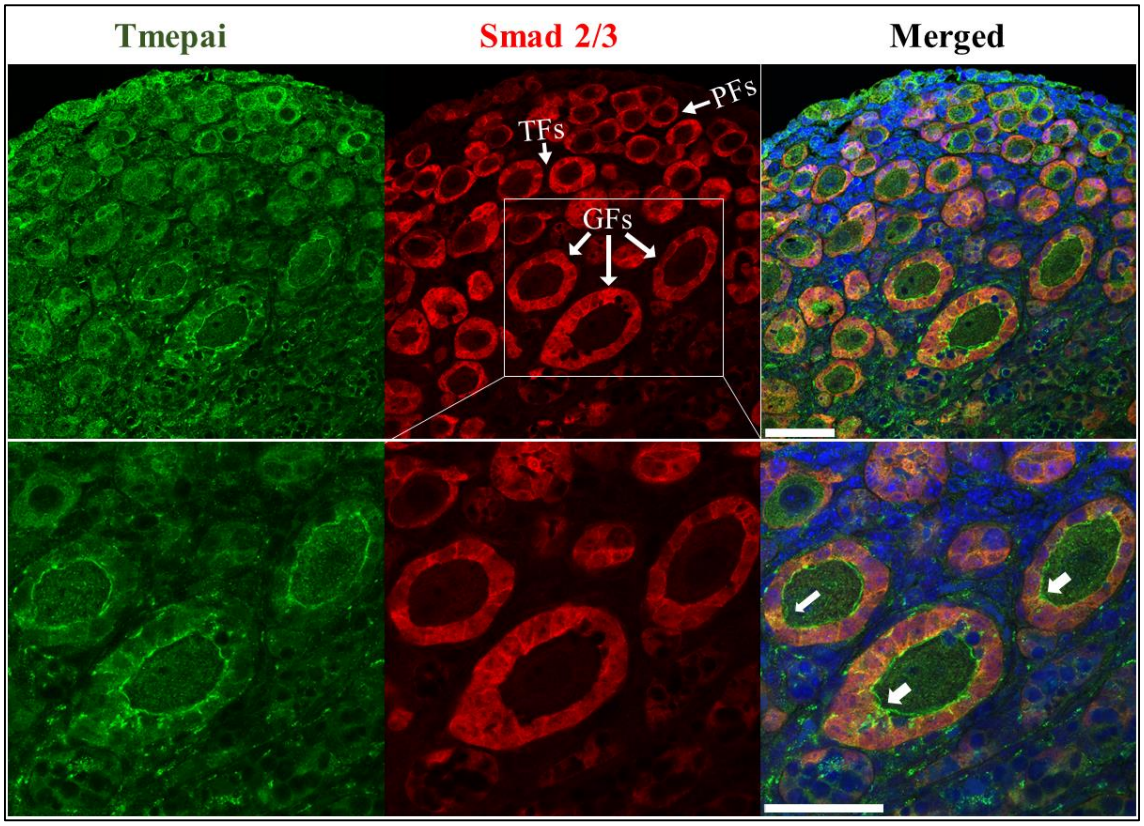

Figure 5.6. High power image of Tmepai and Smad2/3 in the d4 mouse ovary. Tmepai protein (green) was detected with a strong intensity in follicles that had developed a complete layer of cuboidal granulosa cells and also those that had started to develop a second layer of granulosa cells. Smad2/3 was also detected in granulosa cells of these follicles, where this sometimes coincided with the exclusion of Smad2/3 (white arrows). Section was counterstained with DAPI (blue). Scale bar = 75µm.

In the d8 ovary section, as more growing follicles in the medulla are evident, the number of follicles that expressed Tmepai protein was increased. Similar to d4 staining, many of the positively stained follicles were located in the medulla of the ovary. Tmepai-positive follicles also exhibited decreased intensity of Smad2/3 staining. In addition, Tmepai-positive primordial follicles located at the marginal region of the ovary exhibited strong staining for Smad2/3, but a limited number of primordial follicles were positive to Tmepai staining. Similar to the observation in d4 ovary, strong staining for Tmepai has detected granulosa cells of follicles that had started to develop a second layer (Figures 5.7-8).

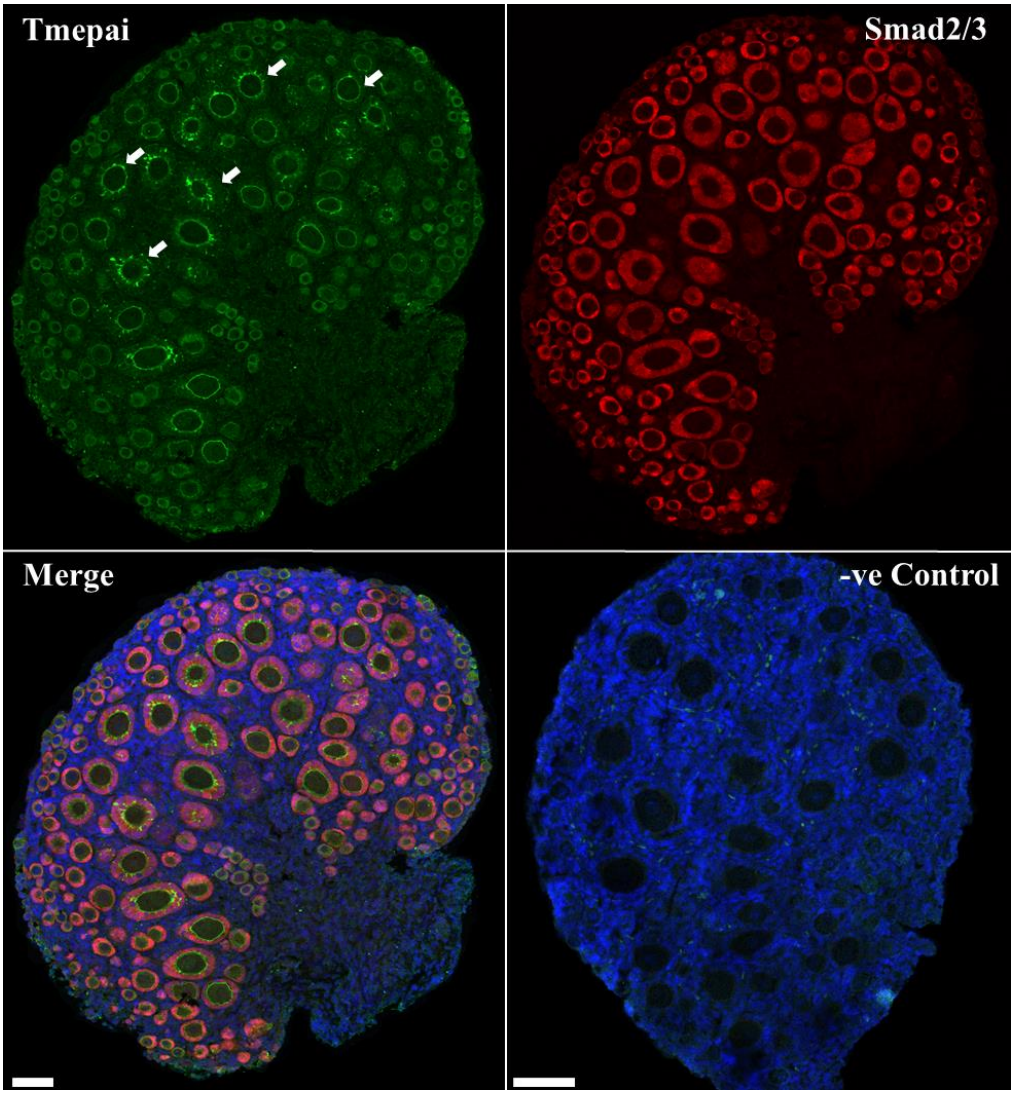

Figure 5.7. Tmepai and Smad2/3 immunolocalisation in the d8 mouse ovary. Tmepai (white arrows, green channel) was detected in granulosa cells of most of the growing follicles situated in the medulla. The intensity of Smad2/3 staining (red) in growing follicles was largely reduced relative to their strong staining in primordial follicles. Proteins were co-localised (yellow) in growing follicles. Negative control (-ve) was treated with a mixture of non-immune Goat and Mouse IgG's. Nuclei were counterstained with DAPI (blue). Scale bar = 75μm.

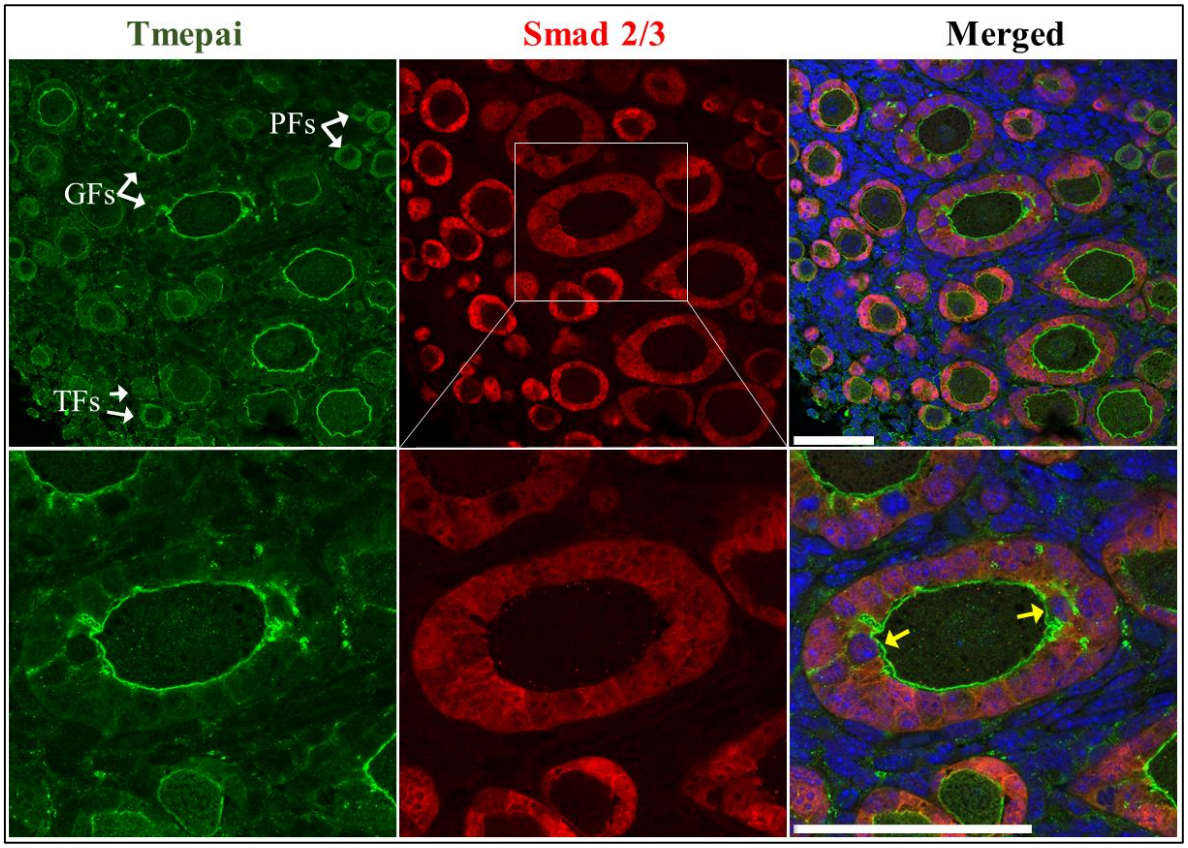

Figure 5.8. High power confocal image of Tmepai and Smad2/3 in the d8 mouse ovary. Tmepai (green) was detected in growing follicles (GFs), with less evident in transitional (TFs) or primordial follicles (PFs). Strong staining for Tmepai was observed in granulosa cells that had begun to form a second layer (yellow arrows). These cells also exhibited relatively reduced nuclear Smad2/3 staining. Section was counterstained with DAPI (blue). Scale bar = 75µm.

The expression pattern of Tmepai was noticeably changed in d16 ovary sections (Figures 5.9-10) where more follicles are starting to grow and more advanced stages of follicle development are apparent than in d4 and d8. Tmepai was precisely localised in granulosa cells of growing preantral follicles that contained more than two layers. These positively stained follicles were mainly located in the cortical region of the ovary, where also Smad2/3 were localised. In addition, the characteristic pattern of Tmepai staining between granulosa cells and oocytes observed in younger ages were not seen in the d16 ovary section. Tmepai was not localised in larger multi-layered follicles located in the medulla of the ovary.

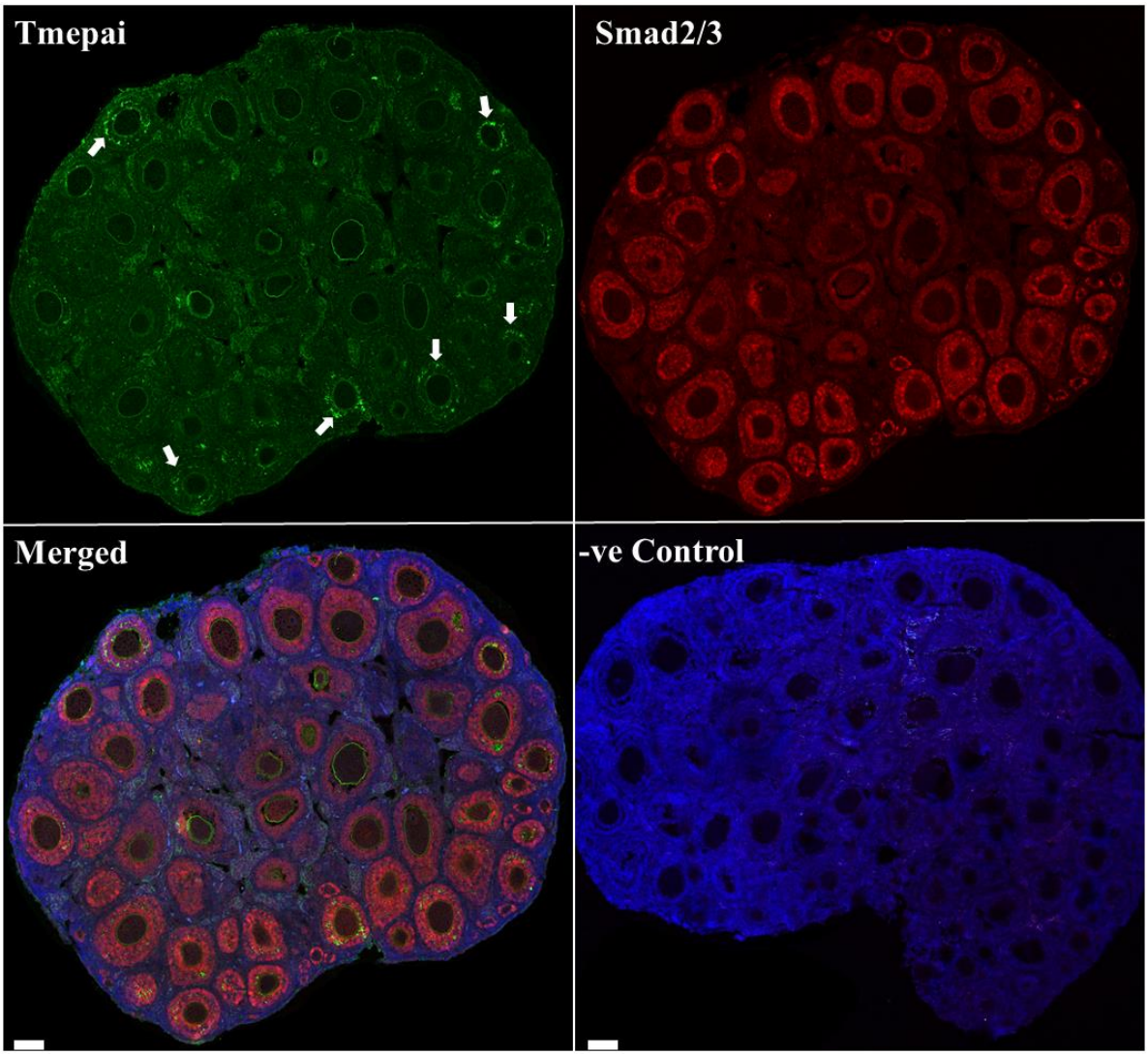

Figure 5.9. Tmepai and Smad2/3 immunolocalisation in the d16 mouse ovary. Tmepai protein was localised in preantral follicles located in the cortical region (white arrows, green channel). Tmepai and Smad2/3 staining were reduced in larger preantral follicles located in the medulla. Negative control was treated with a mixture of non-immune Goat and Mouse IgG's. Nuclei were counter-stained with DAPI (blue). Scale bar = 75μm.

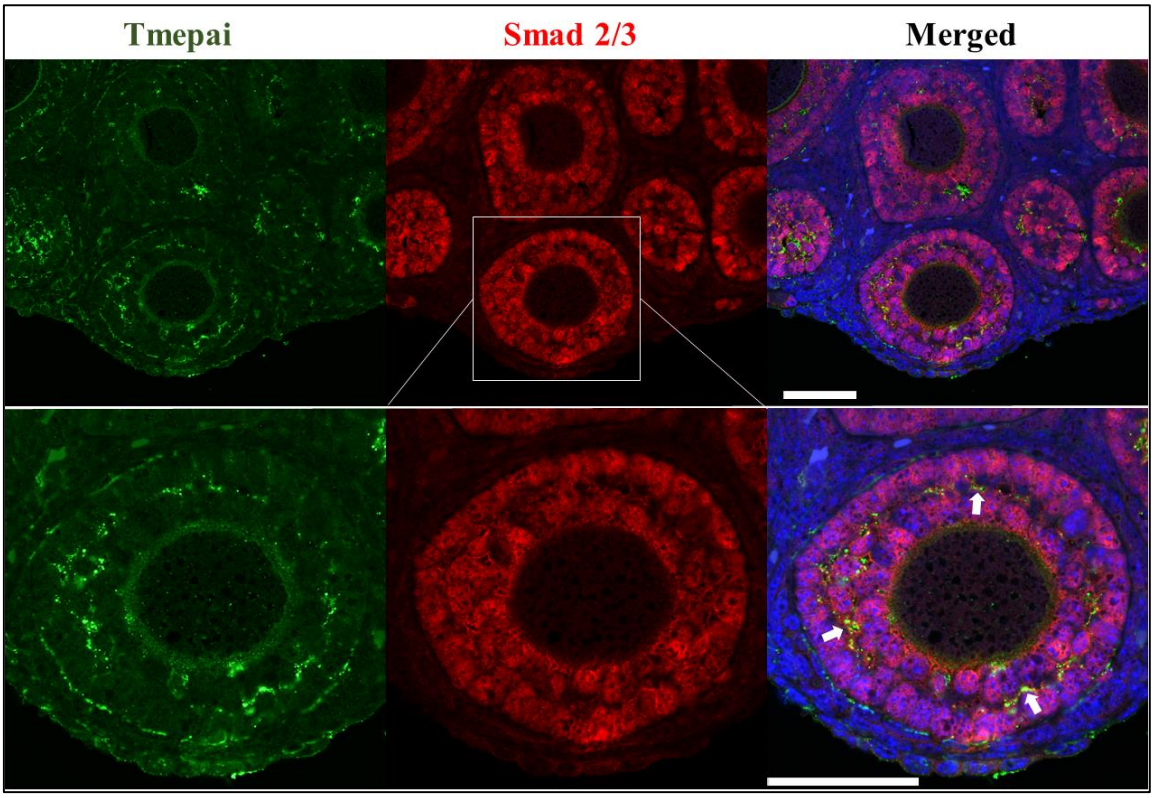

Figure 5.10. Confocal image of Tmepai and Smad2/3 in the secondary follicle. Tmepai protein (green) was localised in preantral follicles containing more than two layers of granulosa cells (white arrows). Smad2/3 staining (red) remained evident in the granulosa cells. Section was counterstained with DAPI. Scale bar = 75μm.

In immature ovaries, as the detection of Tmepai and Smad2/3 were reduced in large growing follicles, adult ovaries containing larger preantral and antral follicles were also stained to confirm this stage-specific expression pattern. Accordingly, Tmepai and Smad2/3 proteins were undetectable in the large preantral or antral follicles that developed more than three layers of granulosa cells; however, both were positively co-localised in earlier stages of follicle growth. (Figures 5.11-12).

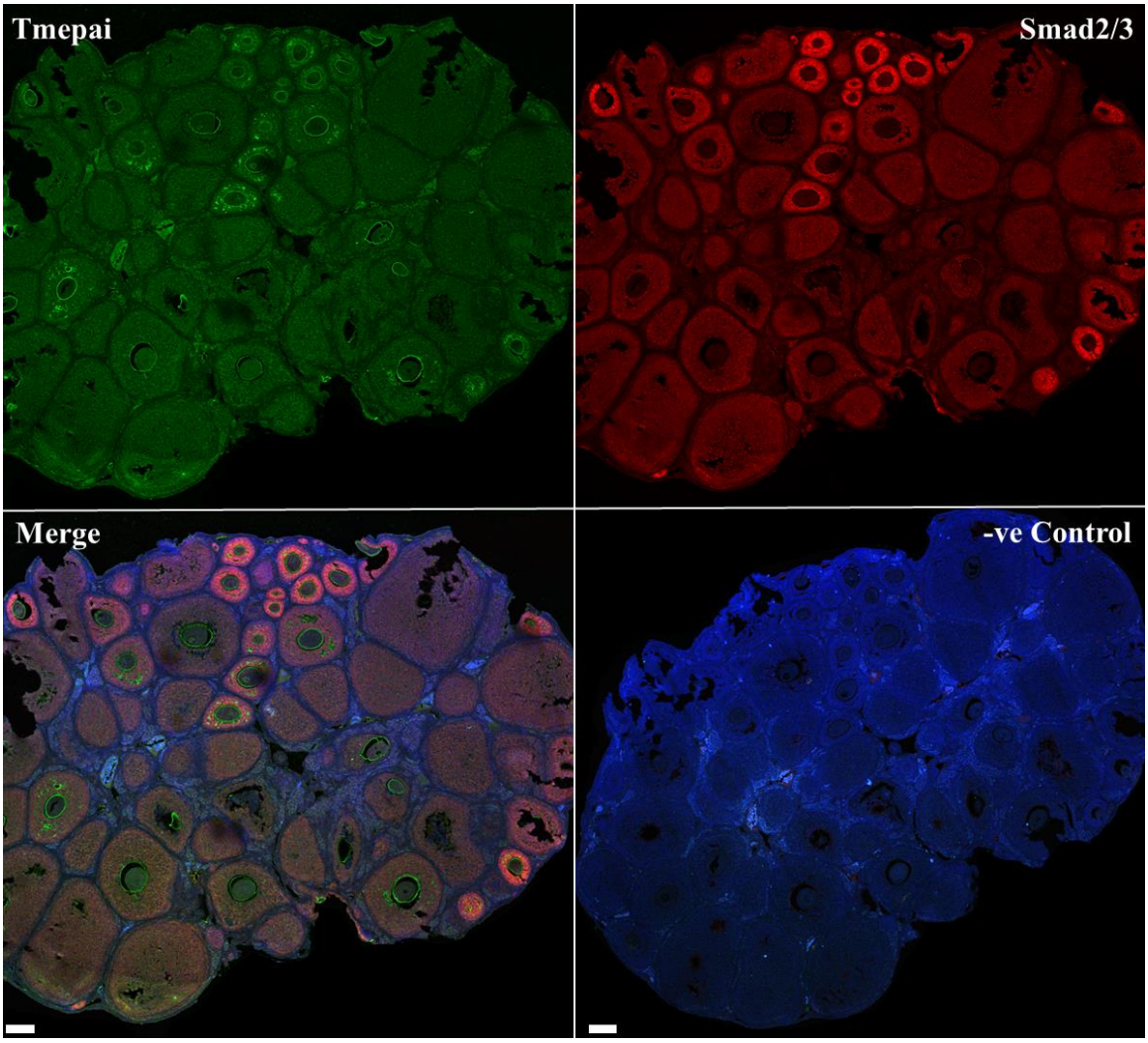

Figure 5.11. Colocalisation of Tmepai and Smad2/3 proteins in adult ovary. Tmepai (green) and Smad2/3 (red) were detectable only in follicles from primary to secondary stages located in both the medulla and cortical regions. However, both proteins were undetectable in more advanced stages. Negative control (-ve) was treated with a mixture of non-immune Goat and Mouse IgG's. Nuclei were counterstained with DAPI (blue). Scale bar = 75μm.

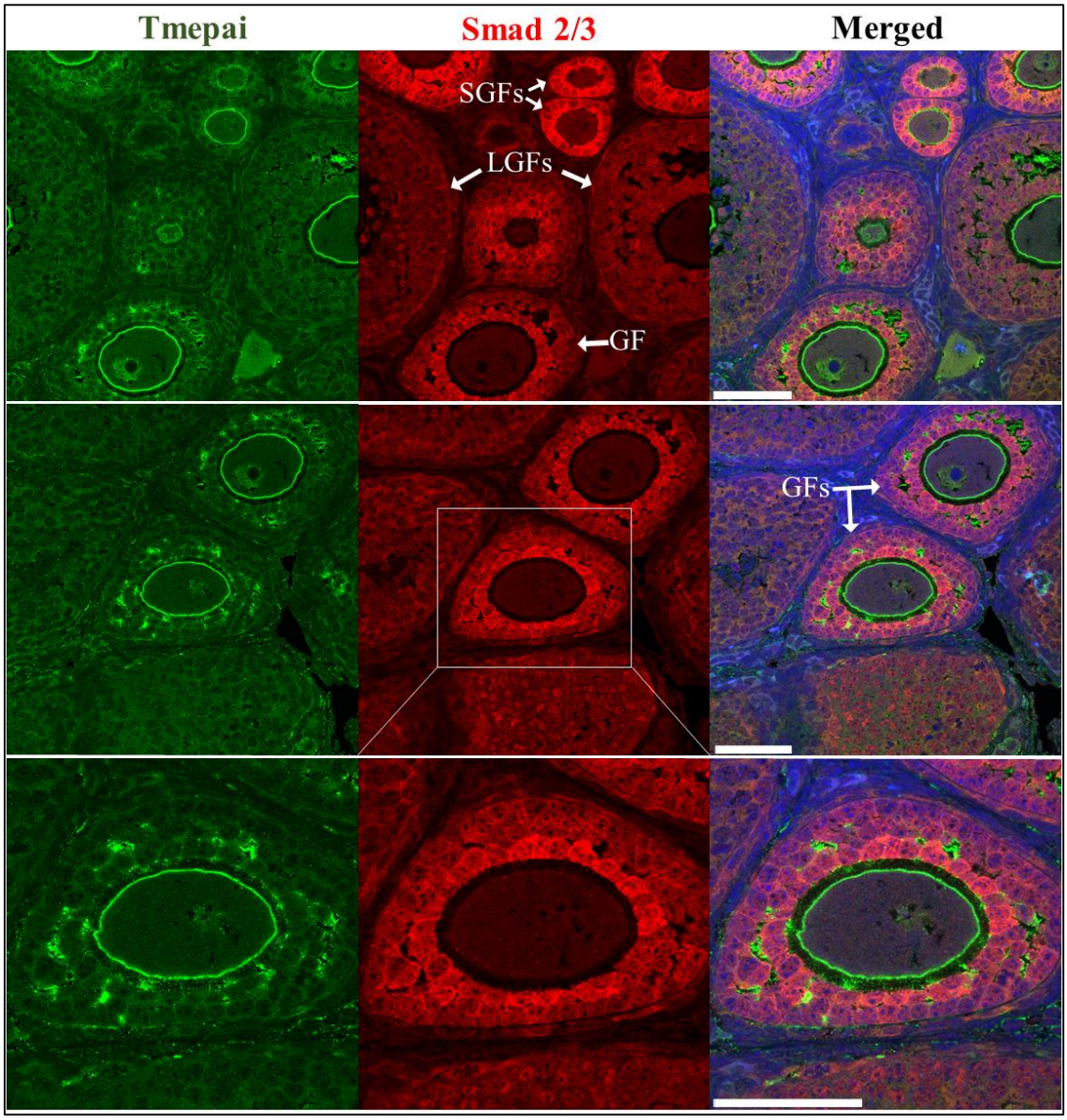

Figure 5.12. High power images of Tmepai and Smad2/3 in adult mouse ovary. Tmepai protein (green) was undetectable in small growing follicles (SGFs) consisting of a complete layer of granulosa cells. Strong staining was observed in growing follicles (GFs), where it colocalised with Smad2/3 (red). Both Tmepai and Smad 2/3 were undetectable in larger growing follicles (LGFs). Section were counterstained with DAPI (blue). Scale bar = 75μm.

5.3.3. Regulation of Tmepai expression in preantral follicles

5.3.3.1. Effect of TGFβRI inhibitor and rmGdf9 on growth of preantral follicles

This experiment was designed to determine whether modification of the TGFβ pathway through the inhibition of TGFβRI receptor or by recombinant protein (rmGdf9) treatment has an impact on preantral follicle growth. Preantral follicles were isolated from d16 mice ovaries and cultured for 72 hours in the presence of SD208 (TGFβRI inhibitor) in the presence or absence of rmGdf9 or rmGdf9 alone and compared with control. Images of a single cultured preantral follicle from each group are shown in Figure 5.13. By comparison with controls, cultured preantral follicles treated with rmGdf9 appeared to increase in size throughout the duration of culture. By comparison, follicles exposed to SD208 with or without rmGdf9 appeared to decrease in size with time, accompanied with an acentric location of the oocyte and a decrease in the size of the granulosa cell layer relative to untreated follicles, which may be indicative of atresia.

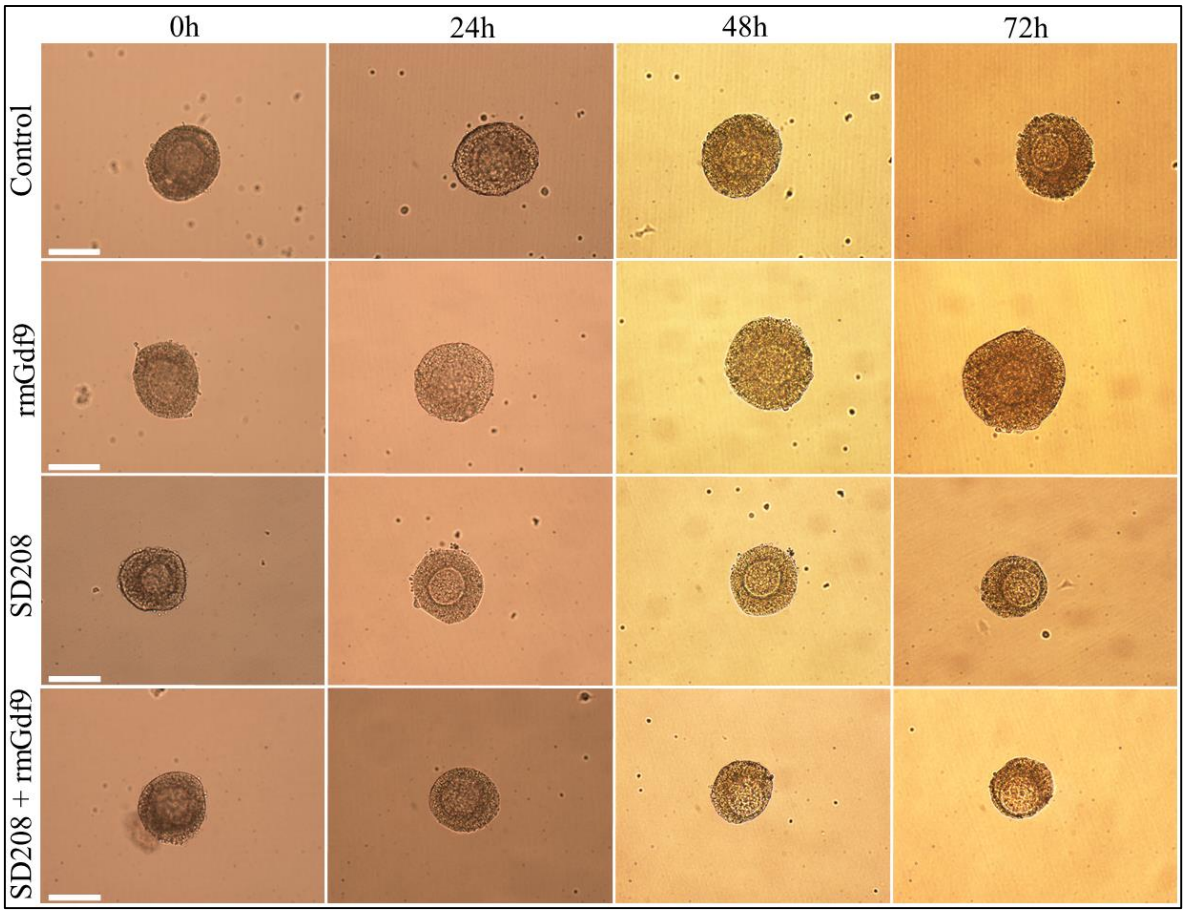

Figure 5.13. Representative images of cultured preantral follicles exposed to TGFβ modifiers. Follicles were incubated in either rmGdf9 (250ng/ml), SD208 (1μM), a combination of both, or control. Follicles were maintained for 72h in culture and images every 24h. Scale bar =100μm.

At the end of culture, some follicles from each group were counterstained with DAPI to show the morphology of the follicles. By comparison with control, follicles treated with rmGdf9 appeared to have more granulosa cell layers. While follicles treated with SD208 with or without rmGdf9 exhibited a reduced number of granulosa cell layers. There was no visual effect on oocytes size between all groups (Figure 5.14).

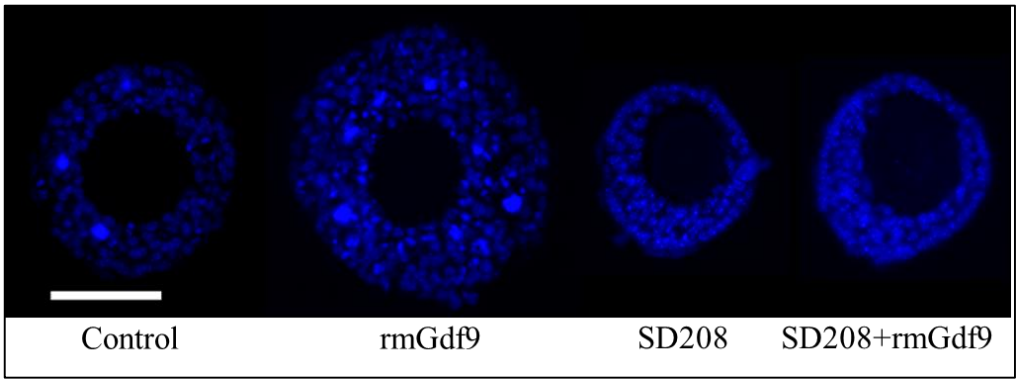

Figure 5.14. Effect of SD208 and rmGdf9 treatments on the morphology of cultured preantral follicles. Paraffin-embedded sections of cultured follicles were fixed, sectioned and counterstained with DAPI (blue). Scale bar =100μm.

To determine the effect of treatments on follicle growth, diameter measurements were made from follicle images at 0h, 24h, 48h and 72h. There was no difference in the mean follicle diameters at 0h of culture between groups (control 134.9μm, rmGdf9 137.1μm, SD208 138.1μm and rmGdf9+SD208 136.1μm). The mean follicle size in the rmGdf9 group was significantly greater than untreated follicles after 24h, 48h, and 72h of exposure ($P<0.05$, $P<0.01$, and $P<0.0001$, respectively). In contrast, treatment with SD208 with and without rmGdf9 caused a significant decrease in the mean follicle size after 24h ($P<0.05$ each) followed by further reduction at 48h and 72h of culture relative to the size of untreated follicles ($P<0.0001$ each) (Figure 5.15).

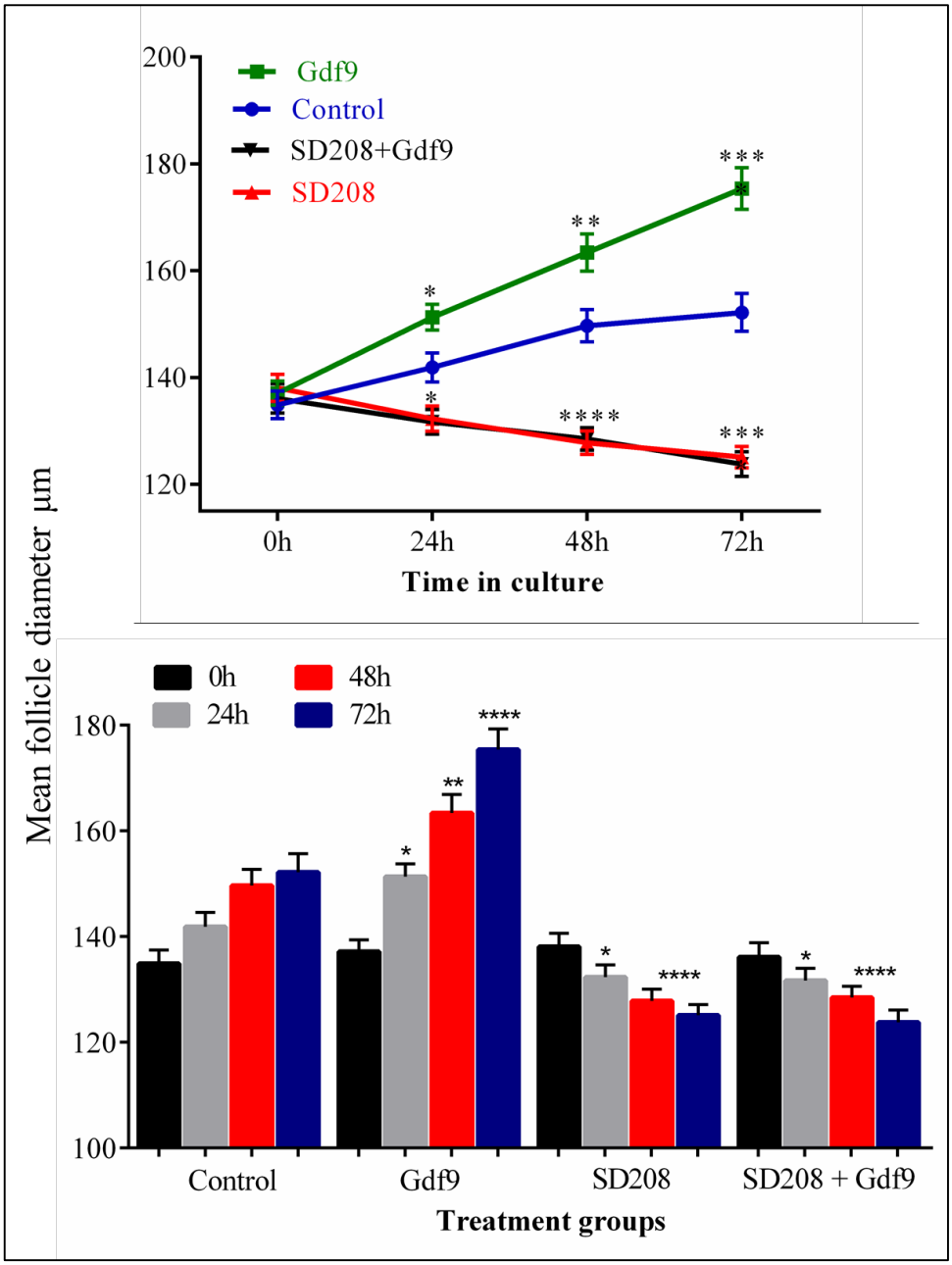

Figure 5.15. Effects of SD208 and rmGdf9 on preantral follicle growth. Preantral follicles were isolated from d16 ovaries and cultured in 96-well plates for 72 hours. Treatment groups included untreated control, rmGdf9, SD208 with or without rmGdf9. Follicles were imaged daily and diameters were measured using ImageJ. Exposure to rmGdf9 caused significant increases in the mean follicle size with time, while, at the same time points, treatment with SD208 (with or without rmGdf9) caused a decrease in mean follicle size relative to control. ANOVA with Bonferroni multiple comparisons test was used for statistical analysis. *P<0.05, ** P<0.01, **** P<0.0001 vs control group. Data (n=30 follicles each group) are presented as mean ± SEM and grouped by time (upper panel) or treatment (lower panel).

5.3.3.2. Gene analysis in cultured preantral follicles

After 24 hours of exposure in different conditions designed to alter TGFβ signalling (Figure 5.1), follicles (n=5) from five plates were collected and cDNA was prepared and analysed for gene expression of *Tmepai, Smad3,* and *Strap* by qPCR. Results showed that expression of *Tmepai* transcript was significantly reduced in the SD208 and SD208 with rmGdf9 treated groups relative to untreated control ($P<0.05$ each). In comparison, treatment with rmGdf9 revealed no significant changes in *Tmepai* expression relative control group ($P=0.7375$). Similarly, there was no changes in the expression levels of *Smad3* or *Strap* in any treatment group relative to control. (Figure 5.16).

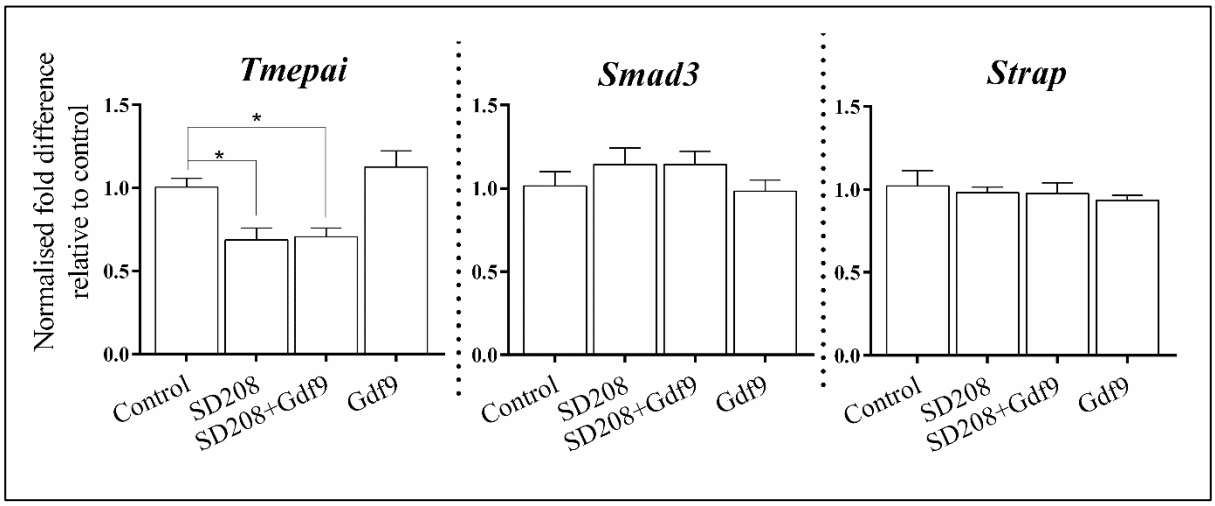

Figure 5.16. Effect of SD208 and rmGdf9 on *Tmepai, Smad3* and *Strap* expression in cultured preantral follicles by qPCR. Data were normalised relative to the expression of the internal housekeeping gene, *Atp5b,* and expressed as fold changes relative to untreated control. Data are represented as mean ± SEM (n=5 samples for each group), *P < 0.05.

5.4. Discussion

In the ovary, dysregulation of TGFβ/Smad signalling is associated with many pathological and reproductive disorders such as polycystic ovary, early ovarian failure, cancer, vascular disorders, and fibrosis (Hatzirodos et al., 2011; Pangas et al., 2006; Shi and Massague, 2003). Thus, in responsive cells including the ovary, both duration and strength of the TGFβ/Smad signalling are regulated by many inhibitory factors (Li, 2015; Moustakas and Heldin, 2009). Tmepai is one of these factors that has the potential to inhibit the Smad2/3 pathway in a self-regulatory feedback mechanism, where its expression is enhanced by some TGFβ ligands (Azami et al., 2015; Watanabe et al., 2010). In this study, we show that Tmepai is detectable in immature and adult mouse ovary in a follicle stage-specific manner and its expression is regulated by modifying TGFβ signalling.

5.4.1. Expression of *Tmepai* mRNA/ protein

Immature mouse ovaries at d4, d8, d16 and from adults were utilised to determine the expression of Tmepai mRNA and protein. In d16 ovary samples, consisting of numerous growing preantral follicles, *Tmepai* was significantly increased relative to d4. However, the expression level of *Smad3* was considerably decreased in the d16 ovary relative to d4. The inverse pattern of expression of *Tmepai* and *Smad3* indicates that Tmepai might be associated with downregulation of *Smad3*. Elevated expression of *Tmepai* in d16 ovaries might be a consequence of the active TGFβ signalling, as the follicle growth at this age is mainly regulated by gonadotrophin-independent signalling (Edson et al., 2009; Kim, 2012; Orisaka et al., 2009). In comparison with d16 ovaries, the decreased level of *Tmepai* expression in adult ovaries might reflect the increased number of advanced preantral/antral follicle stages where the growth of these follicles is largely controlled by hormones (Eppig, 2001; Picton et al., 2003). In the same ovary ages, immunofluorescent colocalisation of Tmepai and Smad2/3 proteins was in agreement with qPCR data. Tmepai protein was localised in a unique expression pattern. Specifically, in the d4 ovary, enriched with primordial follicles, only centrally located growing follicles expressed Tmepai protein in granulosa cells, while primordial follicles revealed positive staining in oocytes. The number of Tmepai positive follicles increased in d8 ovaries, reflecting the fact that more growing follicles are present relative to d4. Interestingly, in both age groups, positively stained follicles were situated in the medulla region of the ovary, whereas, in the d16 ovary, the location of Tmepai positive follicles was inverted, as Tmepai and Smad2/3 were co-localised in growing follicles located close to the ovary surface.

This might be attributed to the fact that in d4 and d8, all growing follicles are in the medulla, whereas in d16 more growing follicles are evident in ovary margin. However, these proteins were undetectable in follicles located in the medulla of the d16 ovary, as these follicles were developed more than three layers of granulosa cells, where Smad1/5/8 is expected to be active (Fenwick et al., 2013). Similarly, in adult ovary section, Tmepai and Smad2/3 were only co-localised in earlier follicle stages, but not in advanced preantral stages and antral follicles. Variation in the location of Tmepai positively stained growing follicles between age groups reflect the programmed recruitment of follicles to initiate the growing process.

In the mouse ovary, a study indicated that follicles in the medulla at the pre-pubertal period represent an early wave of follicles activated to grow shortly after birth, the second wave of primordial follicles located towards the cortex are activated to grow at the later ages (Mork et al., 2012). The expression of Tmepai protein in early growing follicles located in different ovarian regions might be associated with the growth of these different waves. In addition, this observation supports evidence that Tmepai is a specific inhibitor of Smad2/3, but not Smad1/5/8 proteins (Watanabe et al., 2010). Several mechanisms have been suggested for inhibition of Smad2/3 pathway by Tmepai; such as, by competing with SARA for association with Smad2/3 to prevent their activation by the type I receptor, inhibition of the cytoplasmic-nuclear translocation of activated Smad2 and Smad3 (Watanabe et al., 2010), and by lysosomal degradation of TGFβRI thereby preventing Smad2/3 phosphorylation (Bai et al., 2014). In this context, the unique expression pattern of Tmepai in early growing follicles might highlight a controversial issue whether its expression functions to enhance or inhibit follicle growth. Previous studies indicated that TGFβ/Smad signalling activates the non-Smad pathway, such as PI3K, MAPK, ERK, which function to promote cell proliferation; however, the mechanism regulating this process is not clearly defined (Hough et al., 2012; Mu et al., 2012; Xu et al., 2000). Another study raised a question on how TGFβ signalling is altered to promote metastasis through the upregulation of Tmepai expression (Watanabe et al., 2010).

A recent study explained and provided answers for these two questions and indicated that upregulation of Tmepai caused inhibition of the Smad2/3 pathway and induces activation of the non-Smad pathway, which is responsible for cell proliferation and survival, by inhibition of PTEN, an inhibitor of the non-Smad pathway (Singha et al., 2014). In the mouse ovary, inhibition of PTEN caused stimulation of the PI3K pathway and premature activation of primordial follicles followed by premature ovarian failure (Reddy et al., 2008).

Overexpression of Tmepai also inhibits apoptosis through the stimulation of AKT signalling that block the nuclear translocation of the forkhead box protein (FoxO) (Wilkes et al., 2005). In the present study, Tmepai protein was strongly expressed by immunostaining in growing follicles that were developing new granulosa cells. This might indicate that Tmepai has a key role in the proliferation of granulosa cells by switching off the Smad2/3 pathway, accompanied by turning on the non-Smad pathway.

5.4.2. Regulation of *Tmepai* expression and the consequential effect on preantral follicle growth

Enhanced or inhibited TGFβ/Smad signalling has become as a validated protocol to understand mechanisms that regulate cell growth in TGFβ responsive tissues including follicle growth or the development of cancer (DaCosta Byfield et al., 2004; Pangas, 2012). Studies have demonstrated that Tmepai expression is enhanced by TGFβ signalling (Azami et al., 2015; Bai et al., 2014; Liu et al., 2011). For example, in cancer cell culture, inhibition of TGFβ signalling by immunoneutralisation caused a substantial reduction in the expression of *Tmepai* (Vo Nguyen et al., 2014). Therefore, since TGFβ signalling is an important regulator of early follicle development (Kaivo-oja et al., 2006; Li et al., 2008b), it is hypothesised that, in the ovary, Tmepai expression is regulated in the same manner.

To test the hypothesis, cultured preantral follicles were treated with a TGFβRI inhibitor (SD208), exogenous rmGdf9, a combination of both or without any treatment. Gdf9 is a member of the TGFβ superfamily that is exclusively expressed in oocytes, is essential for preantral follicle development, signals through TGFβRI and normally activates Smad2/3 (Knight and Glister, 2006). Thus, Gdf9 was selected in these experiments to assess its role in regulating *Tmepai* expression. SD208 was previously used in mice ovary and brain cells cultures as an effective nontoxic inhibitor of TGFβ superfamily members that signals through a TGFβRI receptor (Uhl et al., 2004; Wang et al., 2014). Follicles were cultured either for 24h and utilised for gene analysis or for 72h and imaged every 24h to determine the effect of treatments on follicle development.

Inhibition of TGFβRI by the exposure to SD208 with or without rmGdf9 demonstrated a significant decrease in *Tmepai* expression level relative to untreated control. However, there were no changes in *Tmepai* level in follicles exposed to rmGdf9 relative to control, indicating that Gdf9 signalling is not essential for *Tmepai* expression or the utilised concentration was not sufficient to increase *Tmepai* expression.

Thus, Tmepai might be regulated by other TGFβ ligands, as a previous investigation in cell line indicated that *Tmepai* expression is primarily induced by TGFβ members and Activin, but not through BMP signalling pathway (Watanabe et al., 2010). As TGFβ1-β3 also signal through the TGFβRI receptor (Lonn et al., 2009; Schmierer and Hill, 2007), it is logical to consider that inhibition of TGFβRI receptor caused inhibition of TGFβ1-β3 signalling, which might consequently downregulate *Tmepai* expression. In the present study, gene expression was analysed in follicles that had been exposed to treatment for 24h; this might be an insufficient period for the induction of *Tmepai* by rmGdf9, or overexpression of *Tmepai* was induced earlier than 24h of exposure.

A previous study in cell culture derived from colon tumour showed that overexpression of *Tmepai* was detectable after two hours of TGFβ exposure and suggested that *Tmepai* can be determined as a unique marker of cellular differentiation and proliferation (Brunschwig et al., 2003). Even though a significant reduction of *Tmepai* in both SD208 treated groups was observed, no changes were detected for *Smad3* in any treatment group. This might indicate the presence of other Smad inhibitors, which function to prevent overexpression of *Smad3*. For example, in various tissues, several factors has been recognised as negative regulators of both duration and strength of TGFβ signalling such as Ppm1a (Chuderland et al., 2012), Strap (Wen et al., 2001), Ski/ SnoN (Deheuninck and Luo, 2009), NEDD4 (Kuratomi et al., 2005), and Smurf1/2 (Inoue and Imamura, 2008).

In the present study, nine Smad2/3 inhibitors were expressed in the immature and adult mouse ovaries (Figure 3.9). These factors might have an effect on the activity of Smad protein, such as phosphorylation, dimerization or translocation rather than the expression of the mRNA. For example, in a cell line, knockdown of *Tmepai* caused a significant increase in Smad2 and Smad3 phosphorylation accompanied with prolonged TGFβ signalling (Watanabe et al., 2010). Unlike *Tmepai, Strap* transcript levels were constant in all treated groups relative to control, suggesting that the expression of *Strap* is stable and is not associated with the disruption of TGFβ signalling. This finding is consistent with a previous data that Strap can interact with TGFβRI and TGFβRII even in the absence of TGFβ signalling (Datta and Moses, 2000). In addition, even though both Tmepai and Strap are Smad2/3 inhibitors, these results provides evidence that the two factors are regulated by different mechanisms.

Regarding the effect of treatments on preantral follicle growth, follicles were maintained in culture for 72h and mean diameter was estimated every 24h. Follicles treated by rmGdf9 were significantly larger after 24hs of culture, followed by a further increase in size after 48 and 72hs relative to the same time points of incubation in the untreated control group. A similar observation of increased follicle size was reported after 24h of treatment by rmGdf9 (250ng/ml), but further increases in follicle size were not evident at later time points (Fenwick et al., 2013). The essential role of Gdf9 in follicle growth was investigated through the study of Gdf9 deletion in the ovary which revealed a reduction in proliferation of granulosa cells, inadequate oocyte development, and failure of theca cell formation (Elvin et al., 1999). Conversely, ovaries exposed to Gdf9 protein showed a significant increase in the transcript level of CYP17 (thecal cells marker) indicated that Gdf9 promotes follicle development (Vitt et al., 2000). Inhibition of TGFβRI receptor in follicles treated by 1μM SD208 with or without rmGdf9 caused a significant decrease in follicle size after 24h followed by a further decrease at 48h and 72h relative to control group. In addition, particularly after 48h and 72h of exposure, treated follicles showed major morphological changes manifested by decreased number of granulosa cell layers accompanied with the loss the central location of the oocyte in the follicle (Figures 5.14-15). These findings highlighted the association of *Tmepai* mRNA reduction with decreased preantral follicle growth. Previous studies have shown that overexpression of *Tmepai* was associated with growth progression and metastasis by activation the non-Smad pathways (Singha et al., 2014; Vo Nguyen et al., 2014).

To exclude the possible cytotoxic effect of the SD208 diluent (DMSO) on follicle growth, an equivalent volume of DMSO was added to control and rmGdf9 groups, thus the reduction in follicle size might be a consequence of TGFβRI inhibition. Another type of TGFβRI inhibitor (SB505124) was previously used in preantral follicle culture, however, follicle size was reduced after 48h of exposure (Fenwick et al., 2013). Variation in response and effects on follicle growth from the present study might refer to the specificity of SD208 to inhibit TGFβRI receptor (Uhl et al., 2004). Another study utilised a different culture model where the impact of 1μM SD208 on follicle growth was investigated on cultured prenatal (18.5dpc) and postnatal (3dpp) mouse ovaries. After 7 days of culture, ovaries demonstrated a significant increase in the population of activated follicles with larger oocytes accompanied with increased granulosa cell proliferation relative to control (Wang et al., 2014).

The difference in the effect of this inhibitor on follicle growth in the present study might reflect the different ovary culture model, which includes only primordial follicles, where Smad2/3 is the dominant pathway. In comparison to the preantral follicle, model used in this study where the expression of Smad2/3 is decreased. To exclude the possibility of toxic effects of SD208 on the exposed preantral follicles, it is recommended to apply a dose response on similar culture model. This could have been evaluated by determining the expression of genes associated with apoptosis such as caspases and p53/63 or using TUNNEL stain to highlight DNA fragmentation. To provide more evidence that *Tmepai* expression is regulating by TGFβ signalling, it might be essential to examine the effects of other TGFβ ligands that signal through the TGFβRI receptor. This study was unable to determine the effect of Tmepai modification on early follicle development, as we could not find appropriate Tmepai products for either protein supplementation or valid antibodies to be in culture models. Attempts were made to co-localise Tmepai or Strap with Smad2/3 proteins in paraffin-embedded sections of preantral follicles exposed to SD208 or rmGdf9; however, images were not included, as staining was inadequate and some of the follicles were lost either during processing for paraffin embedding, sectioning or staining.

In conclusion, this is the first study that has revealed the expression and regulation of Tmepai in the mouse ovary. Tmepai is expressed in a growth stage-specific manner particularly from primary to secondary stages, but not in primordial and advanced stages of follicle growth. Tmepai expression is regulated by TGFβ signalling, but not by GDF9. Downregulation of Tmepai expression was associated with a reduction in follicle size, which implies that normally, the expression of Tmepai in follicles is important for follicle growth, rather than atresia. Further studies are required to assess the direct effect of Tmepai modulation on follicle development using different protocols such as siRNA, immuneneutralisation or exogenous protein supplementation. Since Tmepai functions to inhibit the Smad2/3 pathway and activate the non-Smad pathway, Tmepai might be a key factor implicated in the activation state of early growing follicles.

Chapter 6

Expression and localisation of latent TGFβ binding proteins (Ltbp) in the mouse ovary

6.1. Introduction

Extracellular matrix (ECM) is a complex three-dimensional structure composed of different large molecules including glycoproteins, elastic and collagen fibres found adjacent to cells that have generated it (Hirai et al., 2007; Tsang et al., 2010). The main functions of ECM included supporting, establishing cells into tissues, and regulating cell functions by stimulating intracellular signalling pathways, such as TGFβ, that have an essential role in cell growth or apoptosis (Nagase et al., 2006; Olivieri et al., 2010). Attachment to the ECM is a principle process for the majority of cells to provide regular cell development and maintenance, while, disassociation from ECM or attachment to inadequately structured ECM leads to initiation of cellular death (Marastoni et al., 2008). Recently, it has been suggested that progression of pathological disorders in tissues with a damaged ECM is associated with dysregulated growth factor signalling, such as TGFβ/ Smad signalling, but not due to the destructed ECM (Bourd-Boittin et al., 2011; Robinson et al., 2006).

To this point, most of the studies presented in this thesis have focussed on the intracellular regulators of TGFβ signalling. However, as outlined in Chapter 1, TGFβ signalling can be regulated at many levels, including at the level of ligand processing and extracellular availability. In the mouse ovary, little information is available on the extracellular effectors of the TGFβ/ Smad signalling represented by latent TGFβ binding proteins (Ltbp). Ltbp1-4 are extracellular matrix proteins with high molecular weight (150-220 kDa) belongs to the Ltbp/ fibrillin superfamily (Unsold et al., 2001). Each Ltbp member contains multiple epidermal growth factors (EGF) repeats, which can bind with calcium (Ca^{+2}) to support the Ltbp structure by reducing the effect of proteases (Jovanovic et al., 2008). The other part is the cysteine-rich repeat, called 8-Cysteine, or TGFβ binding protein-like repeats, which are a unique characteristic of Ltbp/fibrillin family (Hyytiainen et al., 2004). All Ltbp members include four cysteine-rich repeats and a repeat that locates on the N-terminal domain called the hybrid repeat as it contains sequences similar to that in both cysteines rich and EGF-like repeats (Hyytiainen et al., 2004; Saharinen et al., 1996). The third cysteine-rich repeat of Ltbp1, 3 and 4 is the site of disulphide binding to the small latent TGFβ complex (SLC). The functional impact of the other two cysteine-rich repeats has not indicated, yet. The N-terminal and C-terminal regions of Ltbp members contain the non-calcium binding EGF-like repeats, which are essential for association with other ECM proteins (Unsold et al., 2001). The N-terminal (amino terminus) of the Ltbp molecule contain a protease-sensitive region (Hinge-region) enriched with proline or glycine and targeted by proteolytic enzymes during dissociation of Ltbp from the ECM at the process of TGFβ activation (Ge and Greenspan, 2006) (Figure 6.1).

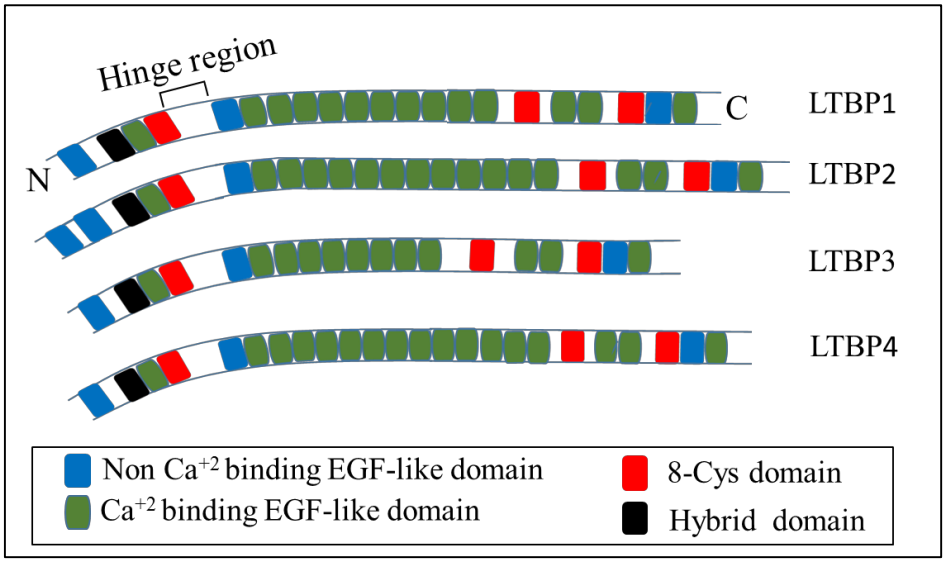

Figure 6.1. Structural differences of latent TGFβ binding proteins members. The N-terminal is a site for the association with the ECM. The N-terminal of all Ltbp members include two (Ltbp1, 3, and 4) or three (Ltbp2) EGF-like repeats (green/blue blocks), one 8-Cys repeat (red block), and a hybrid repeat (black block) that share sequences of both the 8-cysteine repeat and EGF-like repeats, but contains seven cysteines. A protease sensitive region (Hinge region) locates close to the N-terminal domain where dissociation from ECM occurs. While a protease-resistant region is the long central region composed of 8-13 EGF-like repeats. The C-terminal of Ltbp contains the 8-Cys repeat (red block) where the small latent TGFβ complex is associated to Ltbp1, 3 and 4 by disulphide bonds; while in Ltbp2 it provides sites for ECM binding, adapted from (Koli et al., 2001; Todorovic et al., 2005).

The small latent TGFβ complex SLC (includes latency-associated peptide LAP and mature TGFβ; see Figures 1.7-8) binds to a Ltbp to form a large latent TGFβ complex LLC (Annes et al., 2003). Binding of small latent TGFβ complex to Ltbp is an important step to enhance their secretion, accumulation in a particular region in the extracellular matrix, and plays an essential role in the activation of latent TGFβ (Annes et al., 2004; Koli et al., 2001). *Ltbp1* was initially identified in human platelets (Miyazono et al., 1988). Later, *Ltbp2* and *Ltbp3* were characterised according to their sequence similarity to *Ltbp1* (Moren et al., 1994; Yin et al., 1995); while *Ltbp4* was initially identified in the human heart, aorta, uterus, and small intestine (Saharinen et al., 1998). In addition to their tissue specificity, each Ltbp members interacts with a particular TGFβ member. For example, Ltbp1 and Ltbp3 have the potential to form complexes with TGFβ1-3, while Ltbp4 can only associate with TGFβ1 (Penttinen et al., 2002; Saharinen and Keski-Oja, 2000).

Unlike other Ltbp members, Ltbp2 is unable to bind to the LAP part of SLC because its third 8-Cys repeat does not include two amino acids between the cysteines 6 and 7 (Saharinen and Keski-Oja, 2000). In order to enable the initiation of TGFβ signalling, it is essential that the mature TGFβ becomes dissociated from LAP (Koli et al., 2001; Rifkin, 2005). The different mechanisms for dissociation are reviewed in section 1.7.3.

Studies using conditional gene targeting in mice revealed the importance of Ltbp members in different tissues; for example, mice lacking *Ltbp1* exhibit congenital cardiac disorders (Todorovic et al., 2007) and disorders in facial tissue formation (Drews et al., 2008). Deletion of *Ltbp2* leads to early embryonic death (Shipley et al., 2000), while mice lacking *Ltbp3* suffer from bone malformation, particularly affecting long and skull bones accompanied by a reduction in TGFβ signalling (Dabovic et al., 2002).

Animals with reduced *Ltbp4* expression exhibit major lung dysfunction, cardiomyopathy and intestinal cancer due to impaired TGFβ activity (Sterner-Kock et al., 2002). Furthermore, modification in the expression level of a particular Ltbp isoform has no impact on levels of other members (Kretschmer et al., 2011), which implies that each Ltbp isoform is regulated independently from the other members. However, another study suggested *Ltbp4* can substitute for *Ltbp1* in tissues deficient in the latter, as their C-terminal shares the same binding properties to fibrillin, an extracellular microfiber (Isogai et al., 2003).

Since the bioavailability of the TGFβ superfamily members is largely dependent on Ltbp members (Annes et al., 2003; Su et al., 2015), given the proposed requirement for TGFβ signalling in the ovary (Knight and Glister, 2003; Pangas, 2012) and association of fibrillin family with polycystic ovary syndrome (Hatzirodos et al., 2011), it is hypothesised that Ltbps will be detectable in the ovary. The aim of this chapter is to identify the expression levels of *Ltbp1-4 m*RNAs and to determine the staining pattern of Ltbp1 and 4 proteins in ovaries from immature and adult mice.

6.2. Materials

6.2.1. Animals and tissues

Ovaries from mice (d4, 8, 16, and adults) were dissected and manipulated as described in 2.1. Ovaries were used to determine the expression of Ltbps using both RT-PCR/qPCR and immuno-staining. In addition, oocytes were mechanically isolated from d16 ovaries using blunt acupuncture needles (AcuMedic) in drops of isolation media. Isolated oocytes (n=9; Figure 6.2) were pooled in an Eppendorf tube, snap frozen in liquid nitrogen and stored at -80ºC to be used for total RNA extraction and the expression of *Ltbp4* mRNA by RT-PCR.

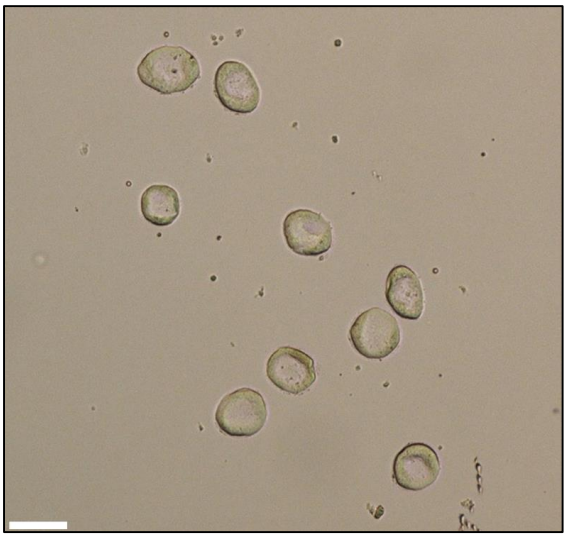

Figure 6.2. Isolated oocytes used for RNA extraction. Intact oocytes were collected with a curved glass pipette and snap frozen in liquid nitrogen. Oocytes were imaged with Olympus CKX41 with a Nikon camera DS-Fi1, Scale bar=50µm.

6.2.2. RNA extraction, RT-PCR and qPCR

Ovaries (n=6 each age group) and an oocyte sample (n=1) were used for total RNA extraction according to manufacturer's instructions of Qiagen RNeasy Micro Kits (QIAGEN, Crawley, UK) (section 2.3). Extracted RNA samples were assessed for concentration and integrity using Agilent Bio-analyser and equivalent amounts of RNA (25ng/µl) were utilised for cDNA synthesis (section 2.4). Primers (*Ltbp1-4*; Table 6.1) were designed to detect mouse transcripts for each candidate gene as described in section 2.5. For gene qualification and quantification, primers were used at a concentration of 500nM for each primer set. The prepared cDNA samples from d4, 8, 16 and adult ovaries were initially checked for the expression of *Gapdh*.

Then, cDNA samples from all age groups were assayed for *Ltbp1-4* by RT-PCR as described in section 2.6. RT-PCR was also used to determine whether *Ltbp4* is detectable in the oocyte sample. In addition to a non-template negative control, cDNA from oocytes sample and adult ovary cDNA was used for the detection of *Gdf9* as a positive control.

To determine the expression levels of *Ltbp1-4* mRNA in the utilised age groups, qPCR reaction mix (20µl) were prepared, two technical replicates for each gene, using 2X SensiFAST SYBR Hi ROX Mix (Bioline). Control groups (non-template) were included for each reaction where nuclease-free water was added instead of cDNA. Thermal cycles included an initial denaturation for 2 minutes at 95°C, followed by cycles of 5 seconds at 95°C, annealing for10 seconds at 59°C, and extension at 72°C for 12 seconds. qPCR data were analysed as fold changes relative to a housekeeping gene (*Atp5b*) using the equation $2^{-\Delta\Delta CT}$ (Livak and Schmittgen, 2001).

Table 6.1. Oligonucleotide primer sequences used to amplify transcripts of *Ltbp1-4*

Gene	Primer Sequence	Annealing Temperature	Product size (bp)
Ltbp1	F: TGAATGCCAAGACCCTAACA R: ACGAGAGGACGGCTACACA	59.3	217
Ltbp2	F: AGACCCTCCCTGACAAAGGT R: ACTTGCTCTTCTGCTGGACT	59.3	152
Ltbp3	F: CCTGGATGGTGTGAGAACCT R: ACTGGAAAGAGCCTGGTGTG	59.9	160
Ltbp4	F: CTGGGCGTTGCGAGAATACA R: CGGGACACACACATAGGAA	60.1	175
Gdf9	F: TCACCTCTACAATACCGTCCGG R: AGCAAGTGTTCCATGGCAGTC	59	139

6.2.3. Immunofluorescent staining

After optimisation with various concentrations of antibodies, Rabbit anti-Ltbp1 and Rabbit anti-Ltbp4 antibodies (Table 6.2) were used for the localisation of Ltbp1 and Ltbp4 proteins in paraffin embedded sections of d4, d8, d16 and adult mouse ovaries. These two Ltbp members were selected for localisation as there is no information about their protein expression in immature ovaries. An equivalent amount of non-immune Rabbit IgG (Vector) was used as a negative control. The same staining protocol described in 2.9.3 was followed. Stained sections were imaged with confocal microscopy using Leica inverted SP5 confocal laser scanning microscope

Table 6.2. Primary and secondary antibodies used for immunofluorescent staining

Primary antibody	Company	Concentration	Secondary antibodies
Ltbp1	Santa Cruz sc-98275	0.25µg/ml	Alexa fluor 555 Donkey anti-Rabbit
Ltbp4	Santa Cruz sc-33144	0.5µg/ml	Alexa fluor 488 Donkey anti-Rabbit

6.2.4. Statistical analysis

For statistical evaluation, qPCR data were statistically analysed using one-way ANOVA with Bonferroni post-hoc test comparisons test. Differences between age groups were considered significant at $P<0.05$. Statistical analyses were performed using Prism (v6.0d; Graphpad) and data were presented as mean ±standard error of the mean (SEM).

6.3. Results

6.3.1. Expression of *Ltbp1-4* mRNAs in immature and adult ovaries

Gapdh was detected in all cDNA from immature (d4, d8, d16) and adult ovaries by RT-PCR. *Ltbp1-4* mRNAs were also expressed in the same ovary ages. *Ltbp1* bands were expressed with similar intensity in all age groups. Strong bands were detectable for *Ltbp2* and *Ltbp4* in d8 and d16 ovary samples, while a clear strong band was also seen for *Ltbp3* in d8, d16 and adult ovaries (Figure 6.3).

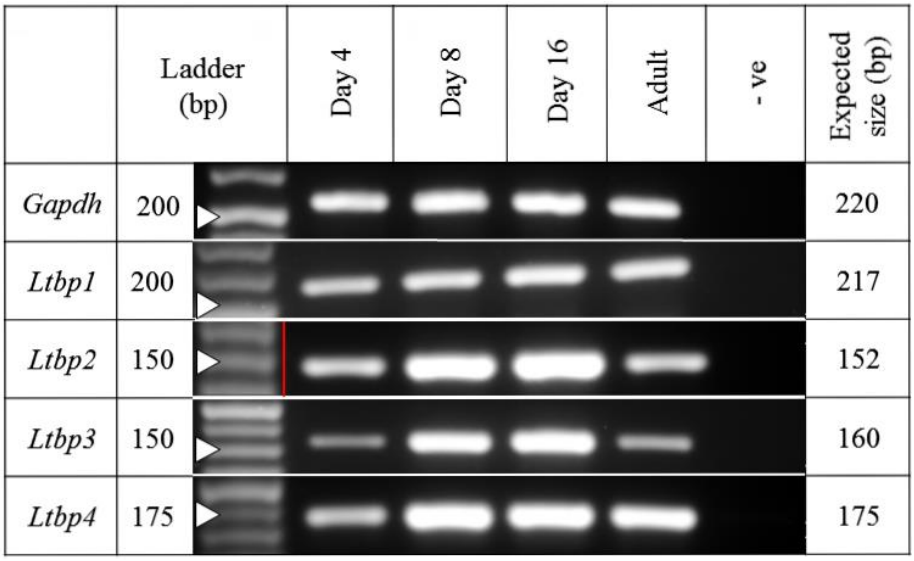

Figure 6.3. RT-PCR gel image showing the expression of *Ltbp1-4* in mice ovary. In addition to *Ltbp1-4*, both positive (*Gapdh*) and negative controls (non-template) were included in the RT-PCR reaction. Red line in *Ltbp2* gel represents to a pasted ladder.

To determine whether steady state transcript levels of *Ltbp1-4* change with age, the expression levels were assessed in ovaries at d4, d8, and d16 by qPCR (n=6). By comparison with d4 ovary, levels of *Ltbp1-4* mRNA were relatively constant and did not vary statistically ($P>0.05$) (Figure 6.4).

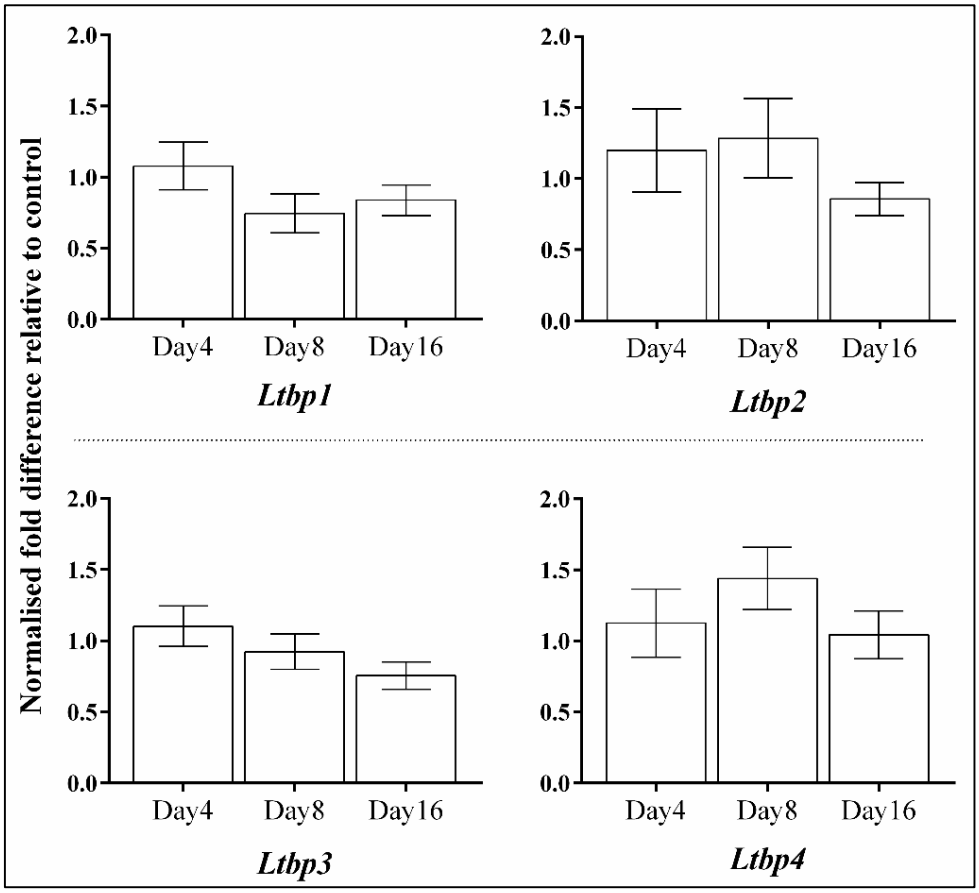

Figure 6.4. Expression levels of *Ltbp1-4* at different ages of immature ovaries. Data were normalised relative to the expression of the internal housekeeping gene, *Atp5b*, and expressed as fold changes relative to day4 ovary. Statistical analysis was assessed using one-way ANOVA with Bonferroni post-hoc test. Data are presented as mean ± SEM (n=6 ovaries per age group).

6.3.2. Localisation of Ltbp1 in immature and adult ovary.

Ovary sections at d4, d8, d16 and from adult mice were used for immunofluorescent localisation of Ltbp1 protein. Results demonstrated that Ltbp1is localised throughout the ovary stroma with a higher intensity in the ovarian surface (Figure 6.5). High power microscopy demonstrated confirmed the positive staining of Ltbp1in epithelial cells and the intensity of staining reduced in stroma beneath the ovarian surface where primordial follicles are situated (Figure 6.6). In agreement with *Ltbp1* gene expression, there was no visual difference in the intensity of staining pattern between the different ages of immature ovaries; however, staining was visually reduced in the adult ovary (Figure 6.7). Ltbp1 protein was undetectable in other ovary components such as follicles or blood vessels.

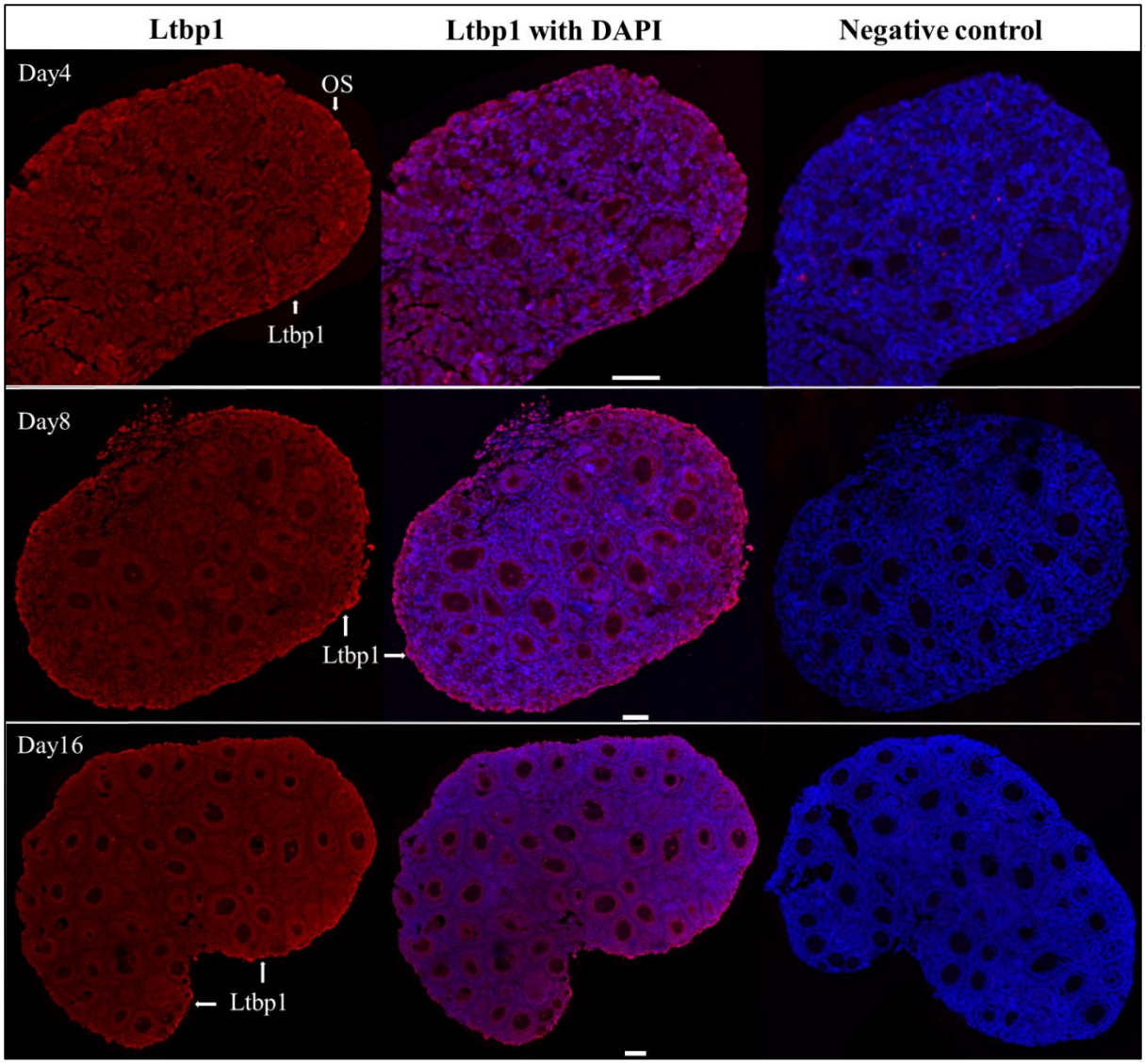

Figure 6.5. Localisation of Ltbp1 protein in immature ovaries. Confocal microscopy revealed that Ltbp1 protein (red) is generally detectable in the stroma cells and being stronger in epithelial cells located at the ovarian surface (OS). There are no visual differences in the staining pattern between the d4, 8, or 16 ovaries. Negative control ovary sections were hybridised with an equivalent concentration of non-immune Rabbit IgG. All ovary sections were incubated with Alexa Donkey anti-Rabbit 555 secondary antibodies. Nuclei were counterstained with DAPI (blue). Scale bar= 50μm.

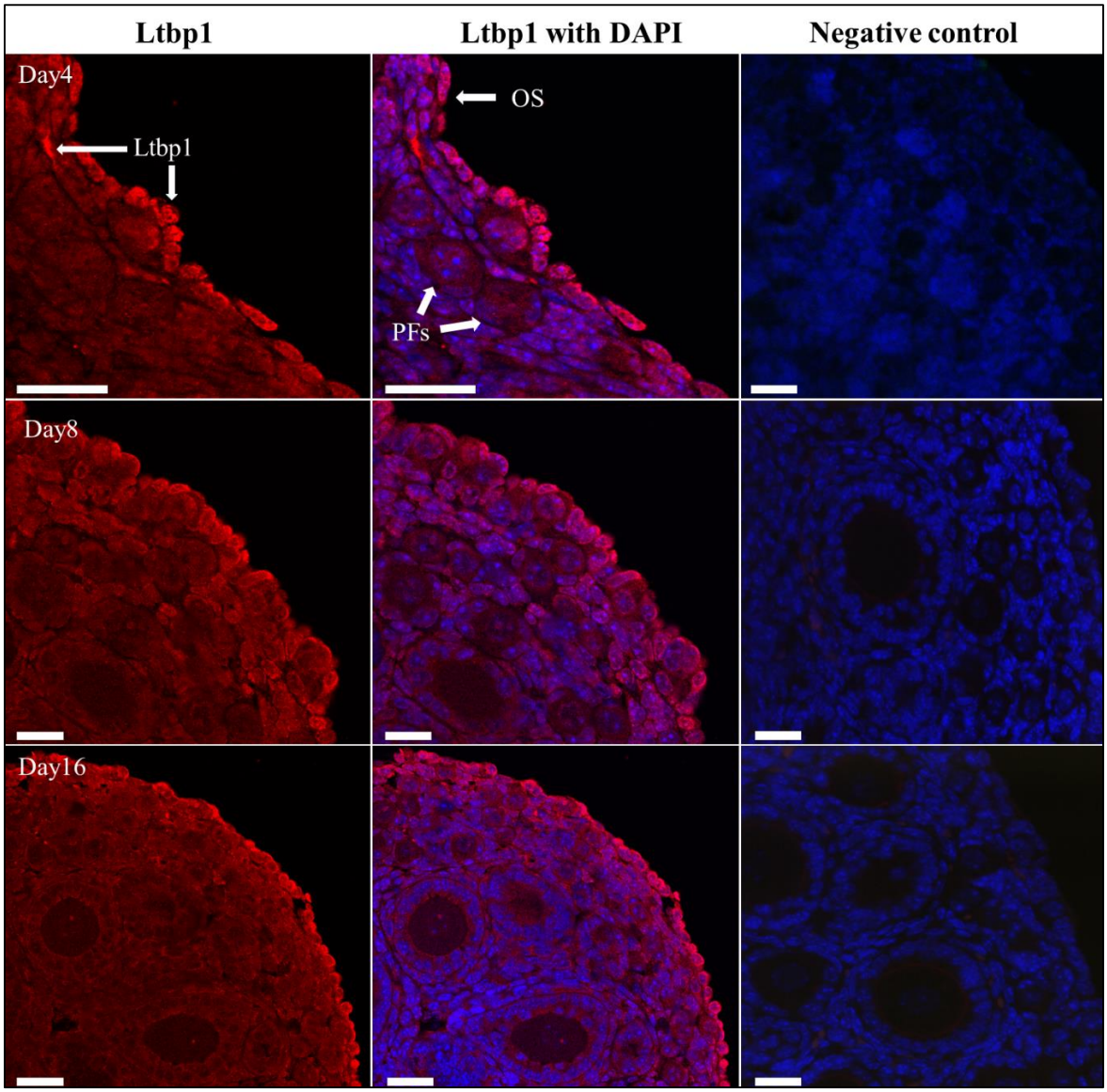

Figure 6.6. High power confocal microscopy for Ltbp1 in immature ovaries. Images show that Ltbp1 protein staining (Red) is evident in stroma and cells located at the ovarian surface (OS) where many primordial follicles (PFs) are present. A similar pattern and staining intensity were revealed in d4, d8 and d16 ovaries. Negative control ovary section was hybridised with an equivalent concentration of non-immune Rabbit IgG and all sections were incubated with Alexa Donkey anti-Rabbit 555 secondary antibodies. Nuclei were counterstained with DAPI (blue). Scale bar =25μm.

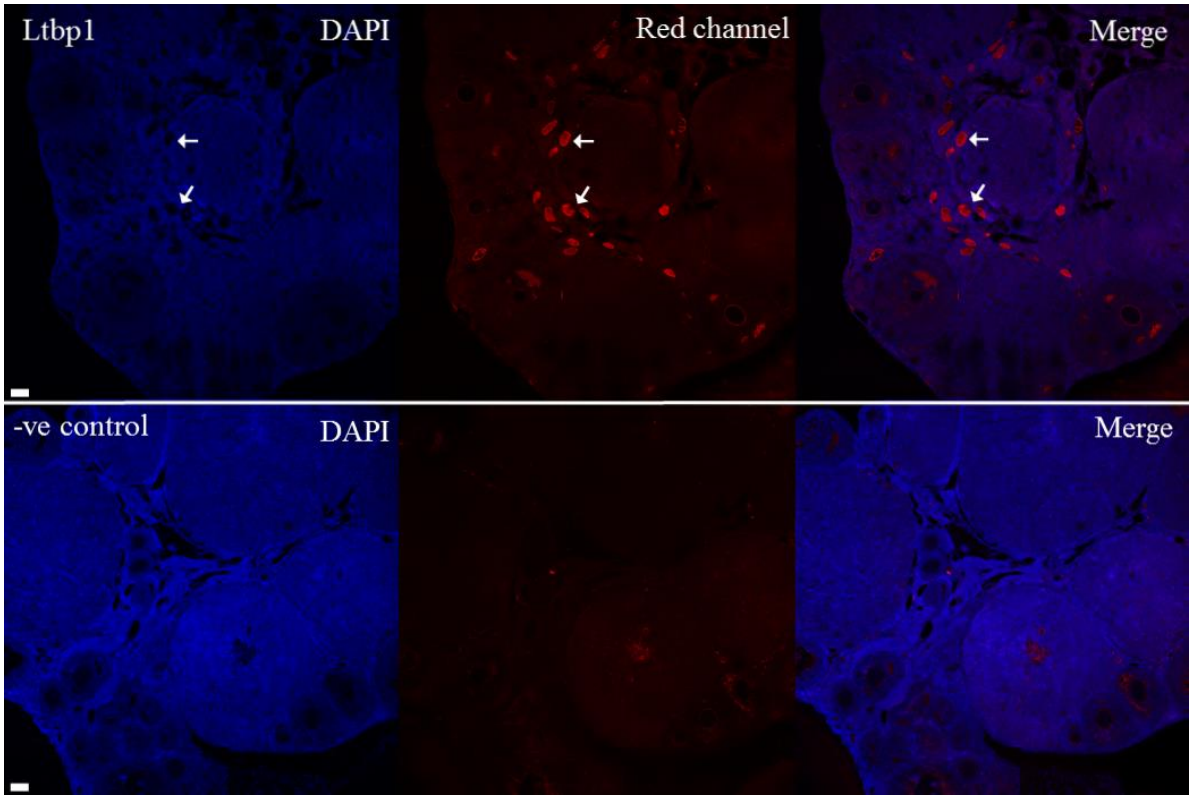

Figure 6.7. Localisation of Ltbp1 protein in the adult ovary. Ltbp1 protein (red, upper row) was undetected in the ovarian surface. Non-specific red spots staining (white arrows) were identified. Negative control (lower row) was hybridised with an equivalent concentration of non-immune Rabbit IgG. All sections were incubated with Alexa Donkey anti-Rabbit 555 secondary antibodies. Nuclei were counterstained with DAPI (blue). Scale bar 50µm.

6.3.3. Localisation of Ltbp4 in immature and adult ovary.

Ltbp4 protein was localised in ovary sections of d4, d8, d16 and adult in a different expression pattern compared to Ltbp1 protein expression. In all ovary ages, Ltbp4 protein was specifically detected in the blood vessels and also, but with reduced intensity in the stroma. In addition, in d4 and d8 and adult sections, Ltbp4 protein was observed with a high intensity of staining in the outer membrane of the oocytes; however, Ltbp4-positve oocyte staining was only detected in numerous oocytes of d16 ovary sections. In immature d4 ovaries, the majority of the Ltbp4-positive oocytes were in growing follicles situated in the medulla (Figure 6.8). Stained sections demonstrated that Ltbp4 protein was visually reduced in d8 (Figure 6.9) and greatly decreased in the d16 ovary (Figure 6.10), where it localised in small distinct foci, compared with d4 ovary. However, the strongest staining pattern of Ltbp4 protein was revealed in the adult ovary (Figure 6.11).

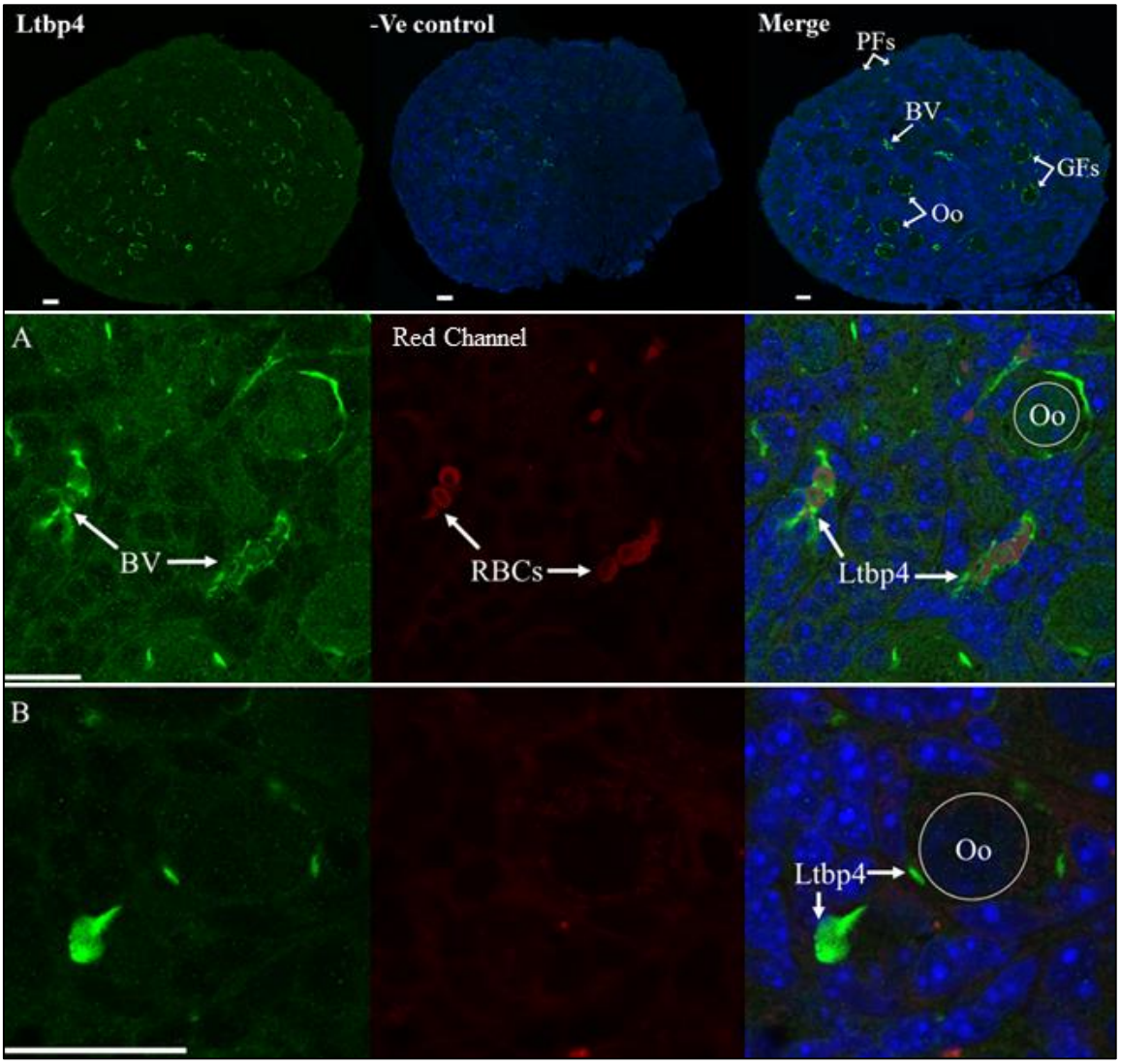

Figure 6.8. Confocal microscopy of Ltbp4 staining in the d4 ovary section. Ltbp4 (green) was not detectable in primordial follicles (PFs) located in the marginal region. In low power images, Staining was evident in large blood vessels (BV) and in oocytes (Oo) of growing follicles (GFs) located in the medulla. High power images demonstrated that Ltbp4 (green) was localised in blood vessels (A; BV) located among several primordial and small growing follicles. Ltbp4 was also detectable in oocytes (circled, Oo) of follicles, where intensity was more evident in the small growing follicles than non-growing primordial follicles (A-B). Positive staining was also evident in extracellular matrix close to a primordial follicle (B) where blood vessels were absence. As red blood cells (RBC) naturally fluoresce, the red channel (middle images) were included to show to visualise RBCs and localise blood vessels.. Negative control was hybridised with an equivalent concentration of non-immune Rabbit IgG non-immune Rabbit IgG. Nuclei were counterstained with DAPI (blue). Scale bar = 25µm.

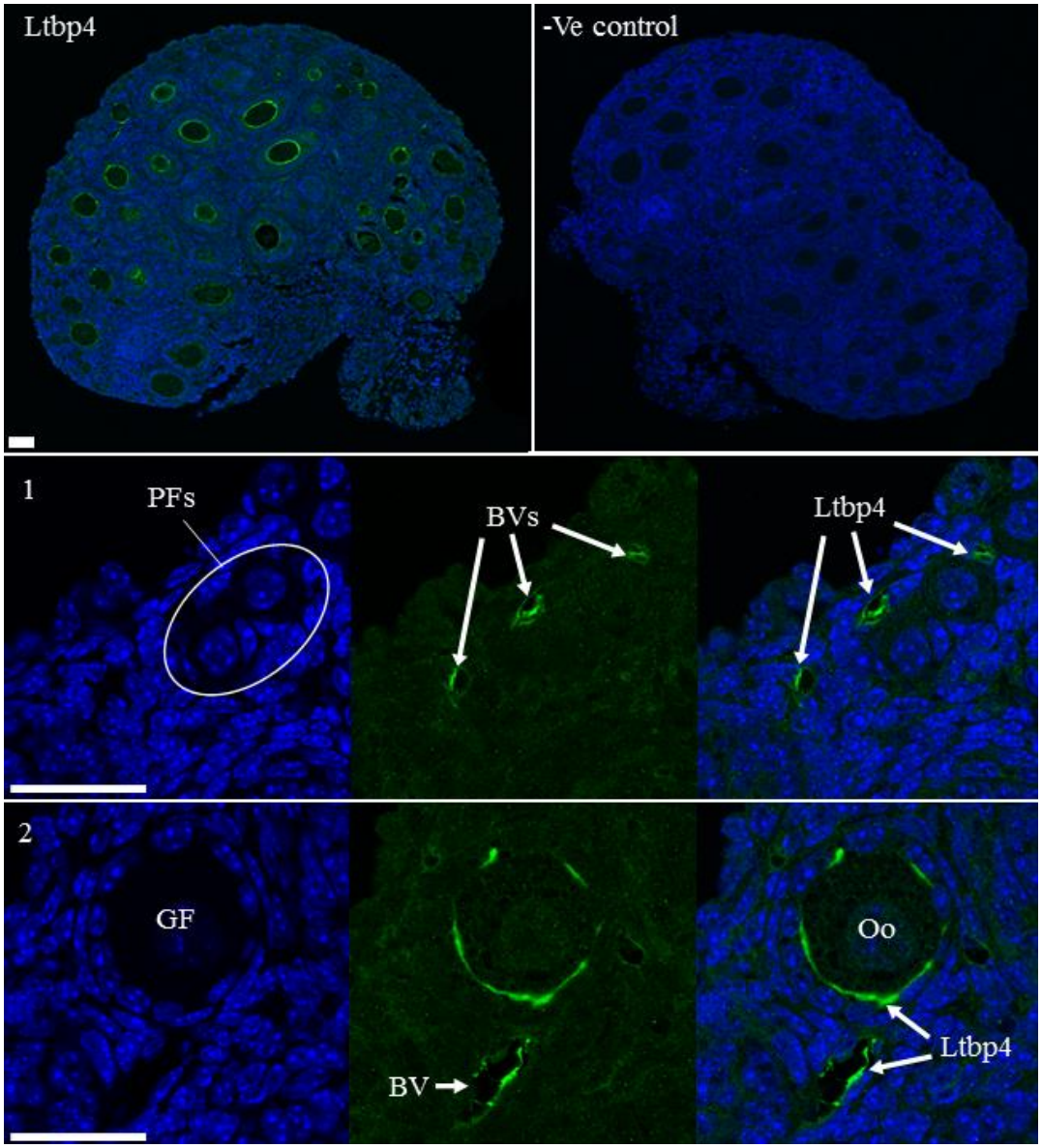

Figure 6.9. Expression of Ltbp4 in the d8 ovary. Ltbp4 (green) was detected in blood vessels (BVs) located close to primordial follicles (PFs, labelled 1) and also near to growing follicles (GF, labelled 2). Positive staining was also evident in oocytes (Oo) of the growing follicles, particularly those located in the medulla, but not in primordial follicles (PFs). Negative control was hybridised with an equivalent concentration of non-immune Rabbit IgG and all sections were incubated with Alexa 488 secondary antibodies. Nuclei were counterstained with DAPI (blue). Scale bar = 25µm.

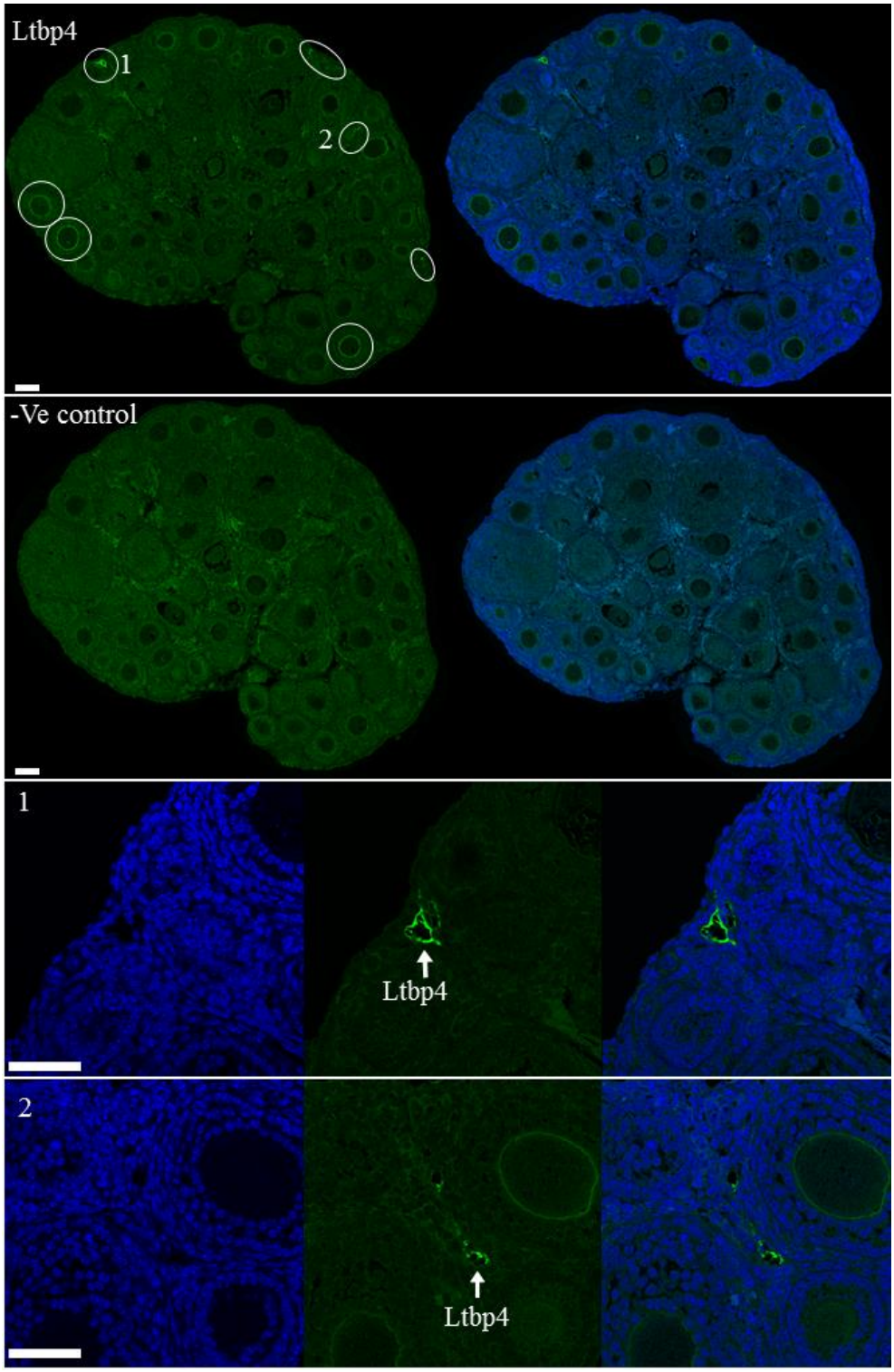

Figure 6.10. Expression of Ltbp4 in the day16 ovary. Ltbp4 protein staining (green) was noticeably reduced where localisation was limited to small regions (encircled) in the ovary section. High power images (1 and 2) showing Ltbp4 positive stain in blood vessels. Negative control was hybridised with an equivalent concentration of non-immune Rabbit IgG and all sections were incubated with Alexa 488 secondary antibodies. Nuclei were counterstained with DAPI (blue). Scale bar= 50µm.

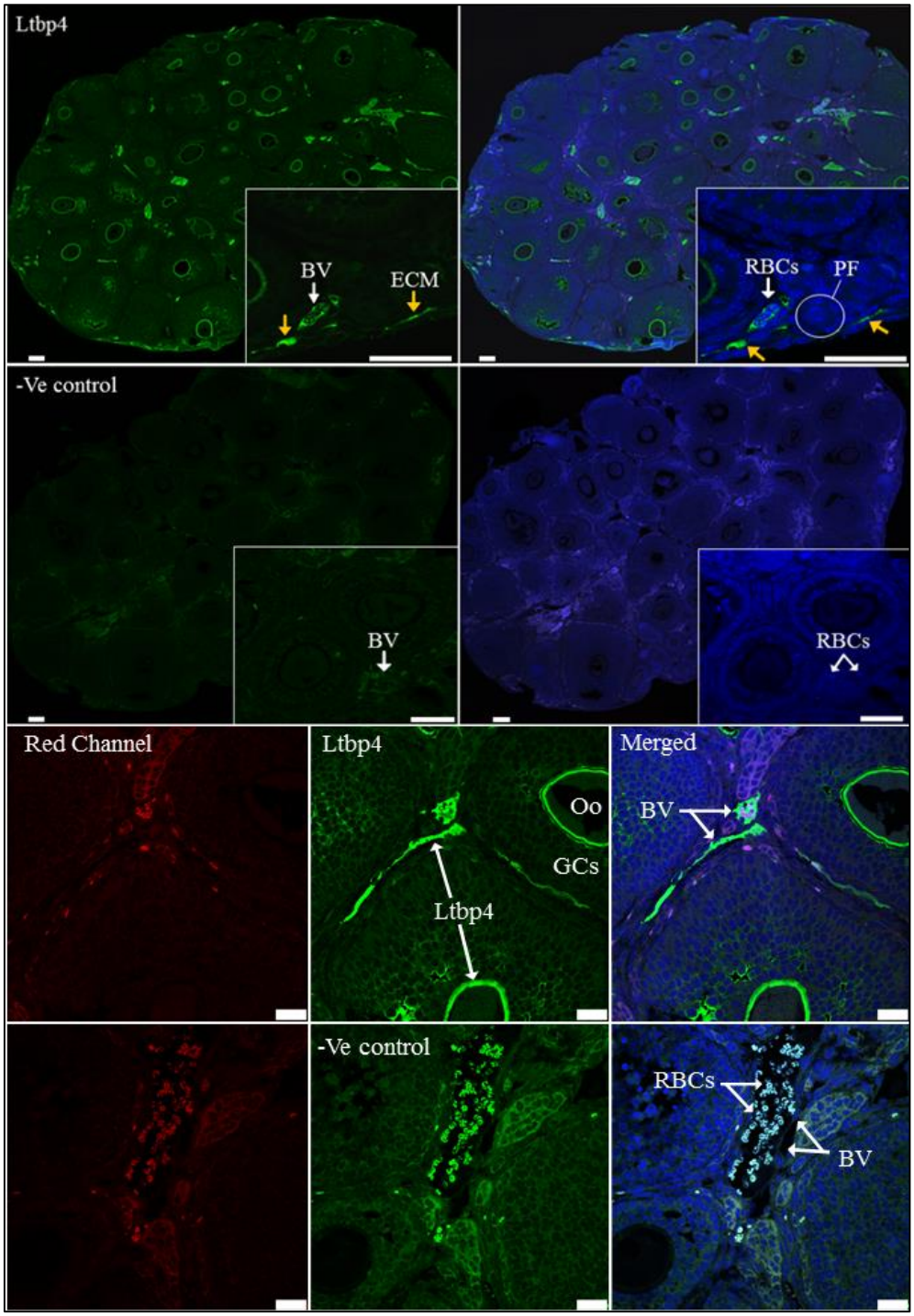

Figure 6.11. Expression of Ltbp4 in adult ovary. The staining intensity of Ltbp4 protein (green) in adult ovary was considerably increased. High power images revealed localisation of Ltbp4 in blood vessels (BV, white arrows) where red blood cells (RBCs) are evident. Ltbp4 was also localised in the stroma (yellow arrows). Positive staining was evident in the oocytes of growing follicles (Oo) but not in granulosa cells (GCs). The red channels were included to determine the endogenous fluorescence and to visualise red blood cells. Negative control was hybridised with an equivalent concentration of non-immune Rabbit IgG. Nuclei were counterstained with DAPI (blue). Scale bar 50μm.

In contrast to the d16 ovary, several oocytes in d4, d8 and adult ovary sections demonstrated positive staining for Ltbp4 protein by immunofluorescence. RT-PCR was therefore performed in a sample of oocytes to identify whether *Ltbp4* mRNA is expressed in these cells. An oocyte-specific gene was expressed in a sample of pooled oocytes; however, *Ltbp4* was not detected in the same sample (Figure 6.12).

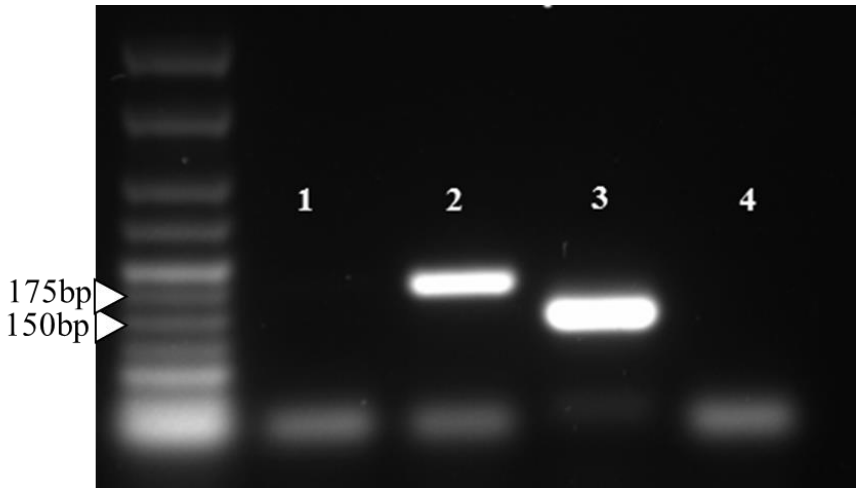

Figure 6.12. RT-PCR gel image presenting the expression of *Ltbp4* in oocyte and adult ovary samples. *Ltbp 4* (175bp) was not detected in oocytes sample (1), while it was expressed in the whole adult ovary (2). *Gdf9* (139bp), an oocyte-specific factor, was detected with a strong band in the same oocyte sample, confirming the validity of the utilised oocyte sample (3). A non-template negative control is also shown (4).

6.4. Discussion

Previous chapters aimed to investigate the expression and role of several intracellular factors that have potential to regulate TGFβ signalling in the mouse ovary. In many tissues, Ltbp members were identified as extracellular elements that regulate the bioavailability of TGFβ (Dabovic et al., 2002; Drews et al., 2008; Hyytiainen et al., 2004). Surprisingly, even though TGFβ signalling is known to play an essential role in follicle development (Kaivo-oja et al., 2006; Pangas, 2012) expression of Ltbp members in the mouse ovary has not been reported. Thus, this part was designed as a small preliminarily study to determine the expression of *Ltbp1-4* mRNA and proteins (Ltbp1 and 4) in mouse ovaries and to relate this with early follicle development. In the present study, transcripts of *Ltbp1-4* were detectable by RT-PCR in immature ovaries at d4, d8, d16 and in adult ovary.

Data from qPCR demonstrated no significant changes in the transcript levels of all *Ltbp* members between different prepubertal ages containing different proportions of non-growing and growing follicles. These results suggest that each individual Ltbp isoform is equally required in the developmental process of immature ovaries. It is possible that the stable expression reflects the activity of these proteins in the extrafollicular compartments, as previous studies indicated the essential role of Ltbp molecules in ECM formation (Rifkin, 2005; Unsold et al., 2001). In addition, early follicle growth at the utilised ages is considered as a gonadotrophin-independent stage (Edson et al., 2009; Orisaka et al., 2009), where TGFβ signalling is essentially required either to enhance or inhibit the growth of small follicle including primordial follicles (Knight and Glister, 2006).

In a previous study, expression of Ltbp1-4 did not differ throughout pregnancy in the human (1^{st}- and 2^{nd}-trimester) and bovine fetal ovaries; however, differences in the expression levels were evident by comparison with adult ovaries. For instance, *Ltbp3* and *Ltbp4* were higher in human ovaries while *Ltbp1* and *Ltbp2* were higher in the cow's ovaries relative to their expression in fetal ovaries (Hatzirodos et al., 2011). This indicates that expression levels of *Ltbp1-4* in the ovary are changeable according to the species and age. In addition, variation in the expression levels between immature and adult ovaries might be associated with the presence of different histological structures in these ovaries; for example, in the adult ovary, advanced stages of follicle growth, ovulated follicles and corpora lutea are evident compared to immature ovaries, which only contain primordial and small preantral follicles.

In the present work, Ltbp1 and Ltbp4 proteins were differentially localised in immature and adult ovary sections. In immature ovaries, Ltbp1 was mainly detected in the surface epithelium and with less intensity of staining in stroma, where primordial follicles are situated. However, Ltbp1 protein was undetectable in adult ovary sections. Reduced Ltbp1 protein in the adult ovary might be a consequence of increased steroid hormones. In monkeys, oral treatment with progesterone caused a reduction in the TGFβ1 expression in the ovarian surface epithelium accompanied with increased apoptosis of these cells (Rodriguez et al., 2002). Thus, since Ltbp1 is responsible for the bioavailability of TGFβ, physiologically, progesterone secreted from corpus luteum might have a relevance in downregulation of Ltbp1 expression in the surface epithelium of adult ovaries.

Localisation of Ltbp1 protein in immature ovaries is consistent with data from qPCR, as no visual difference was observed in the Ltbp1 staining pattern between age groups. Previous studies on adult bovine ovary revealed that Ltbp1 protein is detectable in ovarian tunica albuginea with reduced staining in the stroma underneath the surface epithelium adjacent to primordial and preantral follicles (Hatzirodos et al., 2011; Prodoehl et al., 2009). Functionally, Ltbp1 has the potential to interact with TGFβ1-3, which have anti-proliferative effects on epithelial cells (Singha et al., 2014). In human and bovine ovaries, TGFβ1-3 and their respective receptors (TGFβRI and II) are detectable in the surface epithelium (Henriksen et al., 1995; Nilsson et al., 2001a). Previous studies indicated that reduction in Ltbp1 levels caused downregulation in the bioavailability of extracellular TGFβ1 leading to promotion of the carcinogenic process in epithelial cells (Eklov et al., 1993; Kretschmer et al., 2011). Thus, based on these data, the staining pattern of Ltbp1 in the immature ovary surface might indicate its essential role in secretion and storage of TGFβ1-3 in the ovary surface. This might play an important role in the maintenance and activation of primordial follicles in the marginal region of the immature ovaries.

Ltbp4 protein was mainly localised in blood vessels located close to primordial and growing follicles. In addition, some staining was evident in stroma and the surface of small growing oocytes. In agreement with Ltbp4 protein staining, an oocyte sample from d16 ovary did not express *Ltbp4* mRNA. However, it would be interesting to perform the same analysis on isolated oocytes from d4 and d8 ovaries, particularly if larger growing oocytes could be dissected. Even though there was no change in mRNA expression levels between age groups, the staining intensity of Ltbp4 was decreased in d8 and d16 ovaries relative to d4 ovary; in contrast, the detection of Ltbp4 protein in adult ovary was greatly increased.

The reduction in protein expression in d8 and d16 ovaries might reflect either the dynamic biological activity at these ages manifested by increased number of activated/growing follicles (Palma et al., 2012) or due to the delay in the process of gene translation into protein (Gedeon and Bokes, 2012). However, the increased Ltbp4 protein staining in adult ovary might be due to the presence of the large blood vessels relative to immature ovaries and to the increased demand of tissue for TGFβ signalling, which induces stromal fibroblasts proliferation to produce structural collagens and tissue healing (Govinden and Bhoola, 2003).

This chapter does not included the localisation of Ltbp2 and Ltbp3 proteins; therefore, it would be interesting to identify the expression pattern of these proteins. Isolated oocytes from d16 ovary were used to confirm the expression of *Ltbp4* in oocytes, it was reasonable to use oocytes from adult ovaries, as relative protein staining was more evident by comparison with d16.

In conclusion, this is the first study that aimed to evaluate the expression and localisation of Ltbp members in immature and adult mouse ovaries. Transcripts of *Ltbp1-4* are detectable and their expression levels are constant in the immature ovaries. Immunofluorescent staining indicated that each of Ltbp1 and Ltbp4 proteins has a unique expression site in the ovary.

Ltbp1 appears to be strongly localised at the ovary surface epithelium, while Ltbp4 specifically localised in the blood vessels with evidence of discrete expression in the stroma and oocytes. In the adult ovary, Ltbp1 protein is not detectable while strong staining was detected for Ltbp4. These two different staining patterns suggest that Ltbp1 and 4 have different roles in the ovary development. Further studies are required to specify the localisation of Ltbp2 and Ltbp3 proteins in the immature mouse ovary. Moreover, to identify the molecular role of Ltbp members on the TGFβ signalling and the consequent influence of these factors on early follicle development.

Chapter 7

General Discussion

7.1. Introduction

For decades, even though considerable progress has been made in understanding the mystery of ovarian follicle growth, more investigations are needed to understand the complex molecular mechanisms responsible for primordial follicle activation and early follicle development. The first chapter of this thesis, the literature review, focused on the process of ovarian folliculogenesis and the factors that regulate early follicle growth. Activation of the small quiescent primordial follicle is the initial step where these follicles exhibit an increase in oocyte size, morphological changes in the shape of granulosa cells from flattened to cuboidal, and an increased number of granulosa cells (Hirshfield, 1991). Complex 'gonadotropin-independent' interactions between autocrine and paracrine-secreted factors are responsible for the regulation of the early follicle growth (Kaivo-oja et al., 2006). In this study, particular attention was directed to different levels of the TGFβ superfamily**,** their specific receptors, mediator elements (R-Smads) as well as the intracellular extracellular and regulators.

In many tissues, TGFβ/ Smad signalling is implicated in the regulation of cell proliferation, differentiation, migration, and survival (Rahimi and Leof, 2007). TGFβ signalling is initiated by the formation of a complex between the activated TGFβ ligand and the transmembrane serine-threonine kinase type I and type II receptors. To date, seven TGFβ type I receptors (ALK1-7) and five TGFβ type II receptors (TGFβRII, BMPRII, AMHRII ActRII, and ActRIIB) have been identified (Shi and Massague, 2003; ten Dijke and Hill, 2004). The activated receptors recruit R-Smads for activation by phosphorylation. Once activated, to enhance their nuclear translocation for gene regulation, R-Smads form a heteromeric complex by the associating with Smad4 (Schmierer and Hill, 2007; Shi and Massague, 2003).

TGFβ ligands can signal through either the Smad-dependent or Smad-independent pathways (Derynck and Zhang, 2003). In the ovary, several TGFβ members are expressed in the oocyte, granulosa cells or theca cells, including those that either signal through the Smad2/3 pathway (TGFβ, GDF9, Activin, and inhibin) or Smad1/5/8 (BMPs and AMH) (Drummond et al., 2002; Knight and Glister, 2006).

Although many studies have highlighted the essential role of the TGFβ pathway in early follicle development (Ding et al., 2010; Pangas, 2012; Wang et al., 2014), numerous aspects require further investigation. For example, the impact of attenuated TGFβ signalling on the early follicle development is not clearly understood. In other TGFβ responsive tissues, both duration and strength of TGFβ/ Smad signalling are negatively regulated at different cell levels by numerous intracellular inhibitors (Inoue and Imamura, 2008; Lonn et al., 2009).

Thus, the present study was designed to investigate factors that have the potential to regulate TGFβ/ Smad signalling in the context of the ovary and to specifically determine their impact on early follicle development. Although this thesis was sensibly designed, numerous limitations and shortages were apparent and were specified in each particular chapter. These were mainly a consequence of either technical issues or time limitation. These limitations were specified in each individual chapter. Even though the existence of some limitations, this work provides valuable knowledge on TGFβ/ Smad regulators in relation with different ovary ages.

7.2. TGFβ signalling mediators and many Smad inhibitors are detectable in the ovary

Since TGFβ signalling is active in the ovary (Li et al., 2008b; Pangas, 2012), it was proposed that numerous candidate Smad inhibitors would also be detectable and their expression related to R-Smad expression. Thus, the aim of the first part of this thesis was to determine the expression pattern of R/Co-Smads during early follicle development and to identify candidate Smad inhibitors for further investigation. Immature mouse ovaries at d4, d8 and d16 (and adults) containing increasing density of more advanced stages of follicle growth were utilised. These ages were selected to track the molecular changes in both gene and protein expression during early follicle growth. Although the expression of R-Smads (*Smad1, 2, 3, 5, 8*) in the ovary has been previously described (Fenwick et al., 2013), the present study provides more evidence about the growth stage-specific expression of their mRNA and proteins in three different ages of immature ovaries. In addition, it has confirmed previous data from our lab (Fenwick et al., unpublished work) that the exclusion of Smad2/3 from the nuclei of granulosa cells might be an early sign of primordial follicle activation. As the present work was concerned with early follicle development, ten Smad2/3 inhibitors were selected from the literature, to be analysed for their expression in relation to Smad2/3.

Transcripts of all candidate inhibitors were detected in immature and adult ovaries. Thus, it is interesting to note that in addition to Smad7, a commonly recognised inhibitor of Smad2/3, many other factors exist that could potentially negatively regulate this pathway in the ovary. In other tissues, inhibition of the Smad2/3 pathway by Smad7 can be enhanced by further interaction with other inhibitors such as Strap (Datta and Moses, 2000) or Smurf1/Smurf2 (Liu et al., 2002). The significant reduction in the expression of *Smad3* in d16 ovary relative to d4 might be the result of a cooperative process between Smad7 and some of these inhibitors. Differences in the transcript levels of some candidate genes relative to control (d4) were evident, which may indicate that some of these inhibitors are expressed in a follicle stage-specific manner.

For example, transcripts levels of *Smad7, Smurf1, Smurf2, Ski,* and *Strap* were significantly decreased with age, while no statistical variation was determined in the expression of *Ppm1a*, *Exportin4*, *SnoN* or *RanBP3* at the same age groups. Therefore, a range of isolated follicle samples (primordial to large antral follicles) were utilised to identify whether the expression of the above candidate Smad inhibitors are specifically associated with follicle growth. *Strap*, *Ppm1a,* and *Ski* were expressed in all follicle stages including primordial follicles. For further investigation, Strap and Ppm1a were then selected to relate their protein expression with Smad2/3 and follicle development.

Although Ppm1a protein was previously localised in mature mouse oocytes (Chuderland et al., 2012), the present study was unable to corroborate these findings or detect specific Ppm1a staining in any of the immature ovaries, which may be attributed to the specific antibody used, or the technique used to localise proteins in sections. In contrast, Strap protein was localised in all of the immature ovaries from a range of ages. In particular, the detection of Strap in granulosa cells of small follicles was found to overlap with the expression of cytoplasmic Smad2/3, suggesting a possible role of Strap in the regulation of Smad2/3 and consequently early follicle development. Thus, at this point, the study was directed to identify the functional role of Strap on early follicle growth.

7.3. Consequences of Strap modification on early follicle development

Strap acts as an inhibitor of the Smad2/3 pathway by stabilising Smad7 to the activated TGFβ receptors complex preventing activation of Smad2/3 (Datta et al., 1998; Datta and Moses, 2000). Strap can also interact with activated Smad2/3 to block translocation to the nucleus (Halder et al., 2006). The general hypothesis of this part was to determine whether treatments that affect the expression or action of Strap have a consequence on primordial and preantral follicle development. To test the hypothesis, firstly, the study aimed to identify the effect of *Strap* downregulation by siRNA or Strap protein inhibition by anti-Strap antibodies on primordial and preantral follicles.

Likewise, the effect of exogenous Strap was analysed using recombinant protein supplementation. Both d4 ovary fragments, which mainly contain primordial follicles, and isolated preantral follicle culture models were utilised in the present work. In the d4 ovary model, in order to determine the effect of treatments on follicle growth, a novel oocyte classification protocol was developed where oocytes were assigned as non-growing, transitional or growing according to their diameter and number of granulosa cell layers from histological sections stained with haematoxylin and eosin.

In the d4 ovary fragments model, downregulation of *Strap* expression by *Strap* siRNA or neutralisation of Strap protein by anti-Strap IgG treatments promoted a significant increase in the median oocyte diameters relative to controls. In both experiments, the proportion of non-growing oocytes was significantly reduced alongside an increase in the proportion of growing oocytes relative to controls. Furthermore, cultured ovary fragments exhibited many Amh-positive granulosa cells, suggesting the presence of more growing follicles in the treated groups. To some extent, it is difficult to explain these results as inhibition of Strap expression/function would be expected to increase the duration and strength of TGFβ signalling through the Smad2/3 pathway assuming TGFβ functions as a growth suppressor in this context (Brown et al., 2007).

In human cancer, one study suggested that modulation in the signalling pathway elements might convert the growth suppression effect of the TGFβ to a proliferative effect (Elliott and Blobe, 2005). For example, exposure of cultured cortical human ovarian tissue to a low concentration of Activin caused inhibition of primordial follicle activation, while, treatment with a higher concentration caused an increase in primordial follicle activation (Ding et al., 2010). Thus, in the present work, prolonged TGFβ signalling due to the inhibition of a Smad2/3 inhibitor may enhance the activation process of primordial follicles relative to controls. The importance of R-Smads for follicle development has also been evaluated in knockout mice where deletion of Smad2 and Smad3 resulted in more primordial follicles with a decreased number of growing follicles (Li et al., 2008b; Tomic et al., 2004). Inhibition of a Smad2/3 inhibitor might enhance signalling of other TGFβ superfamily members pathway such as Gdf9 and activin signalling, both of which have a positive impact on primordial and preantral follicle growth in various species (Fenwick et al., 2013; Zhao et al., 2001).

By comparison exposure to *Strap* siRNA in cultured preantral follicles revealed no effect on follicle growth. This suggests that the role of Strap may be follicle stage specific. This assumption was further tested by the incubation of the d4 ovary fragments with a media enriched with rhStrap. After 7 days, a considerable increase in the proportions of transitional and growing oocytes was observed relative to controls. In addition, the median diameter of growing oocytes was greater than in controls supported by Amh staining in granulosa cells. Similarly, in the preantral follicle model, rhStrap promoted the rate of growth relative to controls. These results indicate that Strap has a dual role in the regulation of early follicle development; firstly, in the primordial follicle, it functions to reduce the activation rate and secondly it promotes the growth of the activated follicles.

The molecular mechanism may extend beyond Smad signalling (Reiner and Datta, 2011) since other studies have shown that Strap can activate pathways that function to enhance cell proliferation and survival such as ERK/MAPK (Halder et al., 2006) and PDK1 (Seong et al., 2005). Activation of these pathways is associated with enhanced follicle growth (John et al., 2008; Reddy et al., 2009; Reddy et al., 2008; Zheng et al., 2012). Thus, in addition to inhibiting the antiproliferative impact of the Smad2/3 pathway, Strap supplementation might enhance the growth of growing follicles by activation of non-Smad pathways.

7.4. Tmepai is detectable in the mouse ovary and regulated by TGFβ signalling

Next, another Smad inhibitory factor, Tmepai, was investigated in the context of the ovary since its expression is reported to be induced by androgens (Xu et al., 2000) and it was shown to be overexpressed in advanced stages of cancer where TGFβ signalling was found to further promote its expression (Singha et al., 2014; Watanabe et al., 2010). Tmepai acts to inhibit both androgen and TGFβ signalling in a negative feedback mechanism by blocking their signalling receptors (Bai et al., 2014; Li et al., 2008a). There is no available data on the expression, regulatory mechanisms or role of Tmepai in the ovary. Thus, given the importance of TGFβ signalling and androgens in the ovary, it was proposed that Tmepai might be detectable in the mouse ovary and be regulated by TGFβ signalling.

Tmepai mRNA was detected in immature and adult ovaries and its transcript levels were significantly increased in d16 ovaries, which contain many small preantral follicles. This suggested that the upregulation of Tmepai expression is associated with early stages of follicle growth. Indeed, Tmepai protein was detectable in granulosa cells of small preantral follicles found mainly in d8, d16 and adult ovaries. In contrast, Smad3 mRNA and Smad2/3 protein staining were reduced in d16 ovaries, indicating a possible molecular association between Tmepai and Smad2/3.

Another interesting finding was that Tmepai positive follicles were located in the medulla of the d4 and d8 ovaries, while in the d16 ovaries these follicles were situated in the cortex. This unique pattern of staining provides strong evidence that Tmepai is associated with the stage of follicle development. In the d16 ovary, follicles that had developed more than three layers of granulosa cells were located in the medulla and were negative for Tmepai and for Smad2/3. This might be attributed to the nature of primordial follicle recruitment waves, as in the pre-pubertal period follicles located in the medulla are activated to grow shortly after birth and most of these follicles rapidly degenerate; while, primordial follicles located in the cortical region are activated to grow later (Mork et al., 2012).

High power images revealed that strong staining was obvious in cuboidal granulosa cells that have excluded Smad2/3 from their nuclei. However, at this point, it is unknown whether the expression of Tmepai is associated with enhanced or inhibited follicle growth.

A recent study indicated that Tmepai has the potential to inhibit Smad2/3, a growth suppressor, and can activate the Smad-independent pathways such as PI3K and AKT, which enhances cell proliferation and survival, by inhibition of PTEN (Singha et al., 2014). Thus, in the ovary, expression of Tmepai might be involved with early preantral follicle growth by regulating various pathways. To determine the effect of the TGFβ signalling on *Tmepai* expression and the subsequent impact on the preantral follicle growth, preantral follicles were exposed to a TGFβ receptor inhibitor, a TGFβ ligand (Gdf9) or a mixture of both. After 24h of exposure, receptor inhibition, with or without Gdf9 treatment caused a significant reduction in *Tmepai* expression relative to untreated control. By excluding the possibility of follicle atresia, these results indicate that expression of *Tmepai* depends on the TGFβ ligands that signal through TGFβRI/Alk5 receptor. The reduced *Tmepai* mRNA levels in response to inhibition of TGFβRI might be relevant since these follicles were also decreased in size. Based on the fact that Tmepai has a role in the activation of Smad-independent pathways that promote cell proliferation (Azami et al., 2015; Vo Nguyen et al., 2014), it can therefore be assumed that Tmepai is important for promoting or maintaining early follicle growth.

Preantral follicles exposed to rmGdf9 treatment demonstrated a significant increase in size relative to control. Similar observations have been reported previously (Fenwick et al., 2013; Vitt et al., 2000). Despite this effect on follicle size, Gdf9 did not affect the expression of *Tmepai* transcript levels. These results indicate that Tmepai expression is not regulated by Gdf9 signalling. Although, it is possible that an inappropriate concentration of Gdf9 was used or the time at which the follicles were assayed was inappropriate. In breast cancer and cell line cultures, previous studies indicated that expression of *Tmepai* is regulated through TGFβ signalling in both time and dose-specific manner (Singha et al., 2014; Watanabe et al., 2010).

In the present study, since *Tmepai* levels were significantly reduced by the inhibition of the TGFβRI receptor, it is possible that other TGFβ ligands that signal through these receptors such as TGFβ1-3 and Activin could regulate its expression (Watanabe et al., 2010). Despite the reduction in *Tmepai* expression levels, there were no statistical changes in the *Smad3* levels relative to control. This might reflect the influence of other Smad3 inhibitors in the follicle, where many Smad2/3 inhibitors were identified in the present study.

This section provides new information about the expression and regulation of Tmepai in mouse ovaries. Further work is ongoing to uncover other regulatory factors of Tmepai expression and to determine the impact of Tmepai modification on follicle development.

7.5. Ltbp members are detectable in the mouse ovaries

TGFβ superfamily members are secreted into the ECM as small or large latent TGFβ complexes where their localisation and activation are largely dependent on Ltbp1, 3 and 4 (Hyytiainen et al., 2004; Koli et al., 2004; Su et al., 2015). Deletion of any of these extracellular molecules in mice is associated with varied pathologies from embryonic death to minor morphological mutations mainly caused by a disruption in the bioavailability of TGFβ (Dabovic et al., 2002; Koli et al., 2004; Shipley et al., 2000; Todorovic et al., 2007). Therefore, as the ovary is a TGFβ responsive tissue, it was proposed that Ltbp1-4 would be detectable in the mouse ovary. This study aimed to determine the expression pattern of their mRNA (*Ltbp* 1-4) and protein (Ltbp1 and-4) in immature and adult ovaries.

Transcripts of all *Ltbp* genes were detectable in immature and adult ovaries; however, there were no significant differences in the mRNA expression levels of all *Ltbp* genes between age groups and control. These data suggest a role for all Ltbp members throughout the pre-pubertal period in the mouse ovaries; however, the relationship with follicle development was less clear. In the present study, Ltbp1 and Ltbp4 proteins were localised in varied regions of the mouse ovaries but were not directly associated with follicle (granulosa and theca) cells. In immature ovary sections, Ltbp1 protein was localised with a higher intensity in the ovary surface epithelium and with less staining intensity in the stroma. Ltbp4 was strongly localised in blood vessels and was less evident in the stroma.

The variation in staining pattern suggests that each Ltbp isoform has a specific function in the ovary. For instance, Ltbp1 can regulate the bioavailability of TGFβ1-3, which are known to influence the growth of the epithelial cells, while Ltbp4 might control the growth of endothelial cells, particularly by the regulation of TGFβ1 (Saharinen and Keski-Oja, 2000). In immature ovaries, the majority of primordial follicles are situated in the ovary cortex, thus, the localisation of Ltbp1 in this region might be relevant in terms of regulating signalling in these follicles. Similar observations were reported in bovine ovaries as Ltbp1 was localised in the surface epithelium of adult ovaries, but it was undetectable in fetal ovaries (Hatzirodos et al., 2011; Prodoehl et al., 2009), indicating that expression of Ltbp1 is varied according to the age and animal species.

In the present study, it is interesting to note that Ltbp4 is detectable in blood vessels and stroma close to primordial and growing follicles, proposing a functional role in follicle development. Unlike Ltbp1 protein, the strongest staining of Ltbp4 was observed in adult ovary relative to other age groups, which could be attributed to the increased demand for Ltbp4 due to the presence of larger blood vessels in the adult ovary relative to immature ovaries.

7.6. Impact of the study

It is a fact that females are born with a limited number of primordial follicles resulting in restricted reproductive lifespan. To date, in the human ovary, understanding the role of TGFβ signalling is incomplete, particularly in the process of early follicle growth. Although some variation exists in the regulatory mechanisms responsible for follicle development between humans and mice, many genes associated with follicle activation and growth were initially characterised in the mouse. Therefore, development of a mouse model with modified expression of TGFβ inhibitory factors may provide essential knowledge on the functional role of these factors in both physiological and pathological disorders. Understanding the factors that regulate the ovarian reserve could allow the potential to extend reproductive lifespan and therefore influence disorders such as premature ovarian failure, polycystic ovary syndrome, age-related infertility or toxicant-induced ovarian failure. For example, increasing the activation of primordial follicles by inhibition of a PI3K pathway inhibitor (PTEN) was employed (Reddy et al., 2008) to obtain a sufficient number of growing follicles from ovaries obtained from women with premature ovarian failure (Kawamura et al., 2013). However, using these approaches, the entire reserve will be activated by the treatment. Thus, results in the present study have identified a potential candidate Smad inhibitor that can regulate early follicle growth without global activation of the reserve. In the current study, inhibition of either Strap expression or function caused a significant increase in the recruitment of quiescent follicles to initiate growth. This function of Strap can be employed *in vitro* to increase the number of activated follicles used for maturation techniques and potential fertilisation. These findings might challenge results indicated by other studies of using PTEN inhibitors, as Strap supplementation did not cause massive activation of primordial follicles in treated group; thus, Strap treatment maintained the normal molecular interactions between non-growing and growing follicles. Another study indicated that although bpV(HOpic), a synthetic inhibitor of PTEN, caused substantial promotion in primordial follicle activation; however, the growth of treated preantral follicles was accompanied with an increased rate of follicle atresia (McLaughlin et al., 2014). Strap is a natural protein, not synthetic, and therefore may provide a safer alternative to current synthetic compounds. Taken together, Strap, and other candidates identified in this thesis (e.g. Tmepai) may be clinically important as regulators of maintenance and early follicle growth.

7.7. Future work

Our future work will be also directed to fill the specified gaps, so that, our framework will be approximately completed.

1. In the present study many Smad2/3 inhibitors were detected, thus, further investigations could be conducted to determine their protein localisation and to assess the relative functional role on early follicle development, *in vitro*.
2. Supplementation of Strap promoted an increase in the size of preantral follicles. Therefore, future experiments could focus on evaluating expression levels of numerous genes, which are associated with follicle growth and steroidogeneses such as *Fshr* or *Amh, Cyp11a1* or *Cyp19a*.
3. Further studies are required to assess the direct effects of Tmepai modulation on follicle development using culture models described here along with the different protocols such as siRNA, immunoneutralisation or exogenous protein supplementation.
4. The effect of TGFβ ligands, other than Gdf9, such as TGFβ1-3, ActivinA, and ActivinB could be assessed for their association with Tmepai expression and to be assessed in relation to follicle growth. Ongoing experiments were designed by our lab group to determine the effect of different concentrations of Androgen (dihydrotestosterone DHT) treatments on *Tmepai* expression and preantral follicle growth.
5. Further studies are required to localise Ltbp2 and Ltbp3 proteins in the immature mouse ovary. Moreover, it would be interesting to investigate the effect of molecular modulation of each Ltbp member on TGFβ signalling and the subsequent influence on early follicle development.
6. From the literature, in addition to Smad inhibition, both Strap and Tmepai can activate non-Smad pathway, thus, additional work could also focus on linking these two functions with early follicle growth.

7.8. Conclusions

Overall, the present study provides further evidence that R-Smads are expressed and function in a follicle stage-specific manner. The exclusion of Smad2/3 from the nucleus of granulosa cells was considered as an initial indicator of follicle growth. The detection of a number of Smad2/3 inhibitors in immature and adult ovaries raised the possibility that these factors could regulate early follicle development through regulation of duration and strength of TGFβ signalling (chapter 3). Indeed, modification of Strap expression and function in different culture models provided evidence that Strap can influence early follicle development in a stage- and dose dependent specific manner (chapter 4).

Tmepai is also detectable in immature and adult mouse ovaries in a follicle stage-specific manner. However, unlike Strap, Tmepai expression was limited to follicles that had just initiated growth suggesting a specific role for this protein in follicle growth and its expression is modulated by the functional state of the TGFβR1 receptor (chapter 5).

The extracellular TGFβ-processing Ltbps were also detectable in ovaries, where Ltbp1 protein is more evident in the surface epithelium and stroma, which may represent an important regulator of TGFβ/Smad signalling in nearby primordial and small growing follicles, which are known to present nuclear Smad2/3. Ltbp4 was mainly detectable in the blood vessels, suggests a role in the regulation of endothelial cell development (chapter 6).

To sum up, this study identified the expression of many Smad2/3 inhibitors in immature mouse ovaries. In particular, for the first time, Strap is detected in immature mice ovary and demonstrated a role in the regulation of early follicle growth in a stage-specific manner. Similarly, the detection of Tmepai in small preantral follicles where its expression found to be regulated by TGFβ signalling, this might indicate a relevance role of Tmepai in follicle growth. Ltbp members are detectable in various ovarian compartments. Such studies are essential to understanding molecular factors that regulating early follicle development and might contribute to resolving some physiological and pathological disorders that affecting the mammalian ovary such as early ovarian failure or cancer.

References

1. Abdi, S., Salehnia, M., and Hosseinkhani, S. (2013). Steroid Production and Follicular Development of Neonatal Mouse Ovary during in vitro Culture. International journal of fertility & sterility *7*, 181-186.
2. Abir, R., Fisch, B., Zhang, X.Y., Felz, C., Kessler-Icekson, G., Krissi, H., Nitke, S., and Ao, A. (2009). Keratinocyte growth factor and its receptor in human ovaries from fetuses, girls and women. Molecular human reproduction *15*, 69-75.
3. Accili, D., and Arden, K.C. (2004). FoxOs at the crossroads of cellular metabolism, differentiation, and transformation. Cell *117*, 421-426.
4. Akhurst, R.J., and Hata, A. (2012). Targeting the TGFbeta signalling pathway in disease. Nature reviews Drug discovery *11*, 790-811.
5. Altomare, D.A., Wang, H.Q., Skele, K.L., De Rienzo, A., Klein-Szanto, A.J., Godwin, A.K., and Testa, J.R. (2004). AKT and mTOR phosphorylation is frequently detected in ovarian cancer and can be targeted to disrupt ovarian tumor cell growth. Oncogene *23*, 5853-5857.
6. Anazawa, Y., Arakawa, H., Nakagawa, H., and Nakamura, Y. (2004). Identification of STAG1 as a key mediator of a p53-dependent apoptotic pathway. Oncogene *23*, 7621-7627.
7. Annes, J.P., Chen, Y., Munger, J.S., and Rifkin, D.B. (2004). Integrin alphaVbeta6-mediated activation of latent TGF-beta requires the latent TGF-beta binding protein-1. J Cell Biol *165*, 723-734.
8. Annes, J.P., Munger, J.S., and Rifkin, D.B. (2003). Making sense of latent TGFbeta activation. Journal of cell science *116*, 217-224.
9. Azami, S., Vo Nguyen, T.T., Watanabe, Y., and Kato, M. (2015). Cooperative induction of transmembrane prostate androgen induced protein TMEPAI/PMEPA1 by transforming growth factor-beta and epidermal growth factor signaling. Biochemical and biophysical research communications *456*, 580-585.
10. Bai, S., Shi, X., Yang, X., and Cao, X. (2000). Smad6 as a transcriptional corepressor. J Biol Chem *275*, 8267-8270.
11. Bai, X., Jing, L., Li, Y., Li, Y., Luo, S., Wang, S., Zhou, J., Liu, Z., and Diao, A. (2014). TMEPAI inhibits TGF-beta signaling by promoting lysosome degradation of TGF-beta receptor and contributes to lung cancer development. Cellular signalling *26*, 2030-2039.

12. Bakkebo, M., Huse, K., Hilden, V.I., Forfang, L., Myklebust, J.H., Smeland, E.B., and Oksvold, M.P. (2012). SARA is dispensable for functional TGF-beta signaling. FEBS letters *586*, 3367-3372.
13. Billiar, R.B., St Clair, J.B., Zachos, N.C., Burch, M.G., Albrecht, E.D., and Pepe, G.J. (2004). Localization and developmental expression of the activin signal transduction proteins Smads 2, 3, and 4 in the baboon fetal ovary. Biol Reprod *70*, 586-592.
14. Blanchette, F., Day, R., Dong, W., Laprise, M.H., and Dubois, C.M. (1997). TGFbeta1 regulates gene expression of its own converting enzyme furin. The Journal of clinical investigation *99*, 1974-1983.
15. Bourd-Boittin, K., Bonnier, D., Leyme, A., Mari, B., Tuffery, P., Samson, M., Ezan, F., Baffet, G., and Theret, N. (2011). Protease profiling of liver fibrosis reveals the ADAM metallopeptidase with thrombospondin type 1 motif, 1 as a central activator of transforming growth factor beta. Hepatology (Baltimore, Md) *54*, 2173-2184.
16. Brigstock, D.R. (2002). Regulation of angiogenesis and endothelial cell function by connective tissue growth factor (CTGF) and cysteine-rich 61 (CYR61). Angiogenesis *5*, 153-165.
17. Bristol-Gould, S.K., Kreeger, P.K., Selkirk, C.G., Kilen, S.M., Mayo, K.E., Shea, L.D., and Woodruff, T.K. (2006). Fate of the initial follicle pool: empirical and mathematical evidence supporting its sufficiency for adult fertility. Dev Biol *298*, 149-154.
18. Broekmans, F.J., Soules, M.R., and Fauser, B.C. (2009). Ovarian aging: mechanisms and clinical consequences. Endocr Rev *30*, 465-493.
19. Brown, K.A., Pietenpol, J.A., and Moses, H.L. (2007). A tale of two proteins: differential roles and regulation of Smad2 and Smad3 in TGF-beta signaling. Journal of cellular biochemistry *101*, 9-33.
20. Brown, P.D., Wakefield, L.M., Levinson, A.D., and Sporn, M.B. (1990). Physicochemical activation of recombinant latent transforming growth factor-beta's 1, 2, and 3. Growth factors (Chur, Switzerland) *3*, 35-43.
21. Brunschwig, E.B., Wilson, K., Mack, D., Dawson, D., Lawrence, E., Willson, J.K., Lu, S., Nosrati, A., Rerko, R.M., Swinler, S.*, et al.* (2003). PMEPA1, a transforming growth factor-beta-induced marker of terminal colonocyte differentiation whose expression is maintained in primary and metastatic colon cancer. Cancer research *63*, 1568-1575.
22. Byskov, A.G., Guoliang, X., and Andersen, C.Y. (1997). The cortex-medulla oocyte growth pattern is organized during fetal life: an in-vitro study of the mouse ovary. Molecular human reproduction *3*, 795-800.

23. Canning, J., Takai, Y., and Tilly, J.L. (2003). Evidence for genetic modifiers of ovarian follicular endowment and development from studies of five inbred mouse strains. Endocrinology *144*, 9-12.
24. Castrillon, D.H., Miao, L., Kollipara, R., Horner, J.W., and DePinho, R.A. (2003). Suppression of ovarian follicle activation in mice by the transcription factor Foxo3a. Science *301*, 215-218.
25. Chang, H., and Matzuk, M.M. (2001). Smad5 is required for mouse primordial germ cell development. Mech Dev *104*, 61-67.
26. Chen, Q., Chen, H., Zheng, D., Kuang, C., Fang, H., Zou, B., Zhu, W., Bu, G., Jin, T., Wang, *Z., et al.* (2009). Smad7 is required for the development and function of the heart. J Biol Chem *284*, 292-300.
27. Chen, W.V., Delrow, J., Corrin, P.D., Frazier, J.P., and Soriano, P. (2004). Identification and validation of PDGF transcriptional targets by microarray-coupled gene-trap mutagenesis. Nature genetics *36*, 304-312.
28. Chen, Y., Jefferson, W.N., Newbold, R.R., Padilla-Banks, E., and Pepling, M.E. (2007). Estradiol, progesterone, and genistein inhibit oocyte nest breakdown and primordial follicle assembly in the neonatal mouse ovary in vitro and in vivo. Endocrinology *148*, 3580-3590.
29. Chuderland, D., Dvashi, Z., Kaplan-Kraicer, R., Ben-Meir, D., Shalgi, R., and Lavi, S. (2012). De novo synthesis of protein phosphatase 1A, magnesium dependent, alpha isoform (PPM1A) during oocyte maturation. Cellular & molecular biology letters *17*, 433-445.
30. Da Silva-Buttkus, P., Marcelli, G., Franks, S., Stark, J., and Hardy, K. (2009). Inferring biological mechanisms from spatial analysis: prediction of a local inhibitor in the ovary. Proc Natl Acad Sci U S A *106*, 456-461.
31. Dabovic, B., Chen, Y., Colarossi, C., Zambuto, L., Obata, H., and Rifkin, D.B. (2002). Bone defects in latent TGF-beta binding protein (Ltbp)-3 null mice; a role for Ltbp in TGF-beta presentation. The Journal of endocrinology *175*, 129-141.
32. DaCosta Byfield, S., Major, C., Laping, N.J., and Roberts, A.B. (2004). SB-505124 is a selective inhibitor of transforming growth factor-beta type I receptors ALK4, ALK5, and ALK7. Molecular pharmacology *65*, 744-752.
33. Dai, F., Lin, X., Chang, C., and Feng, X.H. (2009). Nuclear export of Smad2 and Smad3 by RanBP3 facilitates termination of TGF-beta signaling. Dev Cell *16*, 345-357.

34. Dai, F., Shen, T., Li, Z., Lin, X., and Feng, X.H. (2011). PPM1A dephosphorylates RanBP3 to enable efficient nuclear export of Smad2 and Smad3. EMBO Rep *12*, 1175-1181.
35. Dallas, S.L., Sivakumar, P., Jones, C.J., Chen, Q., Peters, D.M., Mosher, D.F., Humphries, M.J., and Kielty, C.M. (2005). Fibronectin regulates latent transforming growth factor-beta (TGF beta) by controlling matrix assembly of latent TGF beta-binding protein-1. J Biol Chem *280*, 18871-18880.
36. Datta, P.K., Chytil, A., Gorska, A.E., and Moses, H.L. (1998). Identification of STRAP, a novel WD domain protein in transforming growth factor-beta signaling. J Biol Chem *273*, 34671-34674.
37. Datta, P.K., and Moses, H.L. (2000). STRAP and Smad7 synergize in the inhibition of transforming growth factor beta signaling. Mol Cell Biol *20*, 3157-3167.
38. Deheuninck, J., and Luo, K. (2009). Ski and SnoN, potent negative regulators of TGF-beta signaling. Cell Res *19*, 47-57.
39. Dennler, S., Huet, S., and Gauthier, J.M. (1999). A short amino-acid sequence in MH1 domain is responsible for functional differences between Smad2 and Smad3. Oncogene *18*, 1643-1648.
40. Derynck, R., Gelbart, W.M., Harland, R.M., Heldin, C.H., Kern, S.E., Massague, J., Melton, D.A., Mlodzik, M., Padgett, R.W., Roberts, A.B.*, et al.* (1996). Nomenclature: vertebrate mediators of TGFbeta family signals (Cell. 1996 Oct 18;87(2):173.).
41. Derynck, R., and Zhang, Y.E. (2003). Smad-dependent and Smad-independent pathways in TGF-beta family signalling. Nature *425*, 577-584.
42. Ding, C.C., Thong, K.J., Krishna, A., and Telfer, E.E. (2010). Activin A inhibits activation of human primordial follicles in vitro. Journal of assisted reproduction and genetics *27*, 141-147.
43. Ding, X., Zhang, X., Mu, Y., Li, Y., and Hao, J. (2013). Effects of BMP4/SMAD signaling pathway on mouse primordial follicle growth and survival via up-regulation of Sohlh2 and c-kit. Mol Reprod Dev *80*, 70-78.
44. Dissen, G.A., Romero, C., Hirshfield, A.N., and Ojeda, S.R. (2001). Nerve growth factor is required for early follicular development in the mammalian ovary. Endocrinology *142*, 2078-2086.
45. Drews, F., Knobel, S., Moser, M., Muhlack, K.G., Mohren, S., Stoll, C., Bosio, A., Gressner, A.M., and Weiskirchen, R. (2008). Disruption of the latent transforming

growth factor-beta binding protein-1 gene causes alteration in facial structure and influences TGF-beta bioavailability. Biochimica et biophysica acta *1783*, 34-48.

46. Drummond, A.E., Dyson, M., Le, M.T., Ethier, J.F., and Findlay, J.K. (2003). Ovarian follicle populations of the rat express TGF-beta signalling pathways. Mol Cell Endocrinol *202*, 53-57.
47. Drummond, A.E., Le, M.T., Ethier, J.F., Dyson, M., and Findlay, J.K. (2002). Expression and localization of activin receptors, Smads, and beta glycan to the postnatal rat ovary. Endocrinology *143*, 1423-1433.
48. Dubois, C.M., Laprise, M.H., Blanchette, F., Gentry, L.E., and Leduc, R. (1995). Processing of transforming growth factor beta 1 precursor by human furin convertase. J Biol Chem *270*, 10618-10624.
49. Durlinger, A.L., Gruijters, M.J., Kramer, P., Karels, B., Ingraham, H.A., Nachtigal, M.W., Uilenbroek, J.T., Grootegoed, J.A., and Themmen, A.P. (2002). Anti-Mullerian hormone inhibits initiation of primordial follicle growth in the mouse ovary. Endocrinology *143*, 1076-1084.
50. Edson, M.A., Nagaraja, A.K., and Matzuk, M.M. (2009). The mammalian ovary from genesis to revelation. Endocr Rev *30*, 624-712.
51. Eklov, S., Funa, K., Nordgren, H., Olofsson, A., Kanzaki, T., Miyazono, K., and Nilsson, S. (1993). Lack of the latent transforming growth factor beta binding protein in malignant, but not benign prostatic tissue. Cancer research *53*, 3193-3197.
52. Elderbroom, J.L., Huang, J.J., Gatza, C.E., Chen, J., How, T., Starr, M., Nixon, A.B., and Blobe, G.C. (2014). Ectodomain shedding of TbetaRIII is required for TbetaRIII-mediated suppression of TGF-beta signaling and breast cancer migration and invasion. Molecular biology of the cell *25*, 2320-2332.
53. Elliott, R.L., and Blobe, G.C. (2005). Role of transforming growth factor Beta in human cancer. Journal of clinical oncology : official journal of the American Society of Clinical Oncology *23*, 2078-2093.
54. Elvin, J.A., Yan, C., Wang, P., Nishimori, K., and Matzuk, M.M. (1999). Molecular characterization of the follicle defects in the growth differentiation factor 9-deficient ovary. Mol Endocrinol *13*, 1018-1034.
55. Eppig, J.J. (2001). Oocyte control of ovarian follicular development and function in mammals. Reproduction *122*, 829-838.
56. Eppig, J.J., and O'Brien, M.J. (1996). Development in vitro of mouse oocytes from primordial follicles. Biol Reprod *54*, 197-207.

57. Ergin, K., Gursoy, E., Basimoglu Koca, Y., Basaloglu, H., and Seyrek, K. (2008). Immunohistochemical detection of insulin-like growth factor-I, transforming growth factor-beta2, basic fibroblast growth factor and epidermal growth factor-receptor expression in developing rat ovary. Cytokine *43*, 209-214.
58. Esparza-Lopez, J., Montiel, J.L., Vilchis-Landeros, M.M., Okadome, T., Miyazono, K., and Lopez-Casillas, F. (2001). Ligand binding and functional properties of betaglycan, a co-receptor of the transforming growth factor-beta superfamily. Specialized binding regions for transforming growth factor-beta and inhibin A. J Biol Chem *276*, 14588-14596.
59. Feng, X.H., and Derynck, R. (1997). A kinase subdomain of transforming growth factor-beta (TGF-beta) type I receptor determines the TGF-beta intracellular signaling specificity. EMBO J *16*, 3912-3923.
60. Fenwick, M.A., Mansour, Y.T., Franks, S., and Hardy, K. (2011). Identification and regulation of bone morphogenetic protein antagonists associated with preantral follicle development in the ovary. Endocrinology *152*, 3515-3526.
61. Fenwick, M.A., Mora, J.M., Mansour, Y.T., Baithun, C., Franks, S., and Hardy, K. (2013). Investigations of TGF-beta signaling in preantral follicles of female mice reveal differential roles for bone morphogenetic protein 15. Endocrinology *154*, 3423-3436.
62. Findlay, J.K., Drummond, A.E., Britt, K.L., Dyson, M., Wreford, N.G., Robertson, D.M., Groome, N.P., Jones, M.E., and Simpson, E.R. (2000). The roles of activins, inhibins and estrogen in early committed follicles. Mol Cell Endocrinol *163*, 81-87.
63. Fink, S.P., Mikkola, D., Willson, J.K., and Markowitz, S. (2003). TGF-beta-induced nuclear localization of Smad2 and Smad3 in Smad4 null cancer cell lines. Oncogene *22*, 1317-1323.
64. Flaws, J.A., Hirshfield, A.N., Hewitt, J.A., Babus, J.K., and Furth, P.A. (2001). Effect of bcl-2 on the primordial follicle endowment in the mouse ovary. Biol Reprod *64*, 1153-1159.
65. Fleming, Y.M., Ferguson, G.J., Spender, L.C., Larsson, J., Karlsson, S., Ozanne, B.W., Grosse, R., and Inman, G.J. (2009). TGF-beta-mediated activation of RhoA signalling is required for efficient (V12)HaRas and (V600E)BRAF transformation. Oncogene *28*, 983-993.
66. Fong, M.Y., and Kakar, S.S. (2009). Ovarian cancer mouse models: a summary of current models and their limitations. J Ovarian Res *2*, 12.

67. Ge, G., and Greenspan, D.S. (2006). BMP1 controls TGFbeta1 activation via cleavage of latent TGFbeta-binding protein. J Cell Biol *175*, 111-120.
68. Gedeon, T., and Bokes, P. (2012). Delayed protein synthesis reduces the correlation between mRNA and protein fluctuations. Biophysical journal *103*, 377-385.
69. Gong, X., and McGee, E.A. (2009). Smad3 is required for normal follicular follicle-stimulating hormone responsiveness in the mouse. Biol Reprod *81*, 730-738.
70. Goto, D., Nakajima, H., Mori, Y., Kurasawa, K., Kitamura, N., and Iwamoto, I. (2001). Interaction between Smad anchor for receptor activation and Smad3 is not essential for TGF-beta/Smad3-mediated signaling. Biochemical and biophysical research communications *281*, 1100-1105.
71. Goto, K., Kamiya, Y., Imamura, T., Miyazono, K., and Miyazawa, K. (2007). Selective inhibitory effects of Smad6 on bone morphogenetic protein type I receptors. J Biol Chem *282*, 20603-20611.
72. Gougeon, A. (1996). Regulation of ovarian follicular development in primates: facts and hypotheses. Endocr Rev *17*, 121-155.
73. Govinden, R., and Bhoola, K.D. (2003). Genealogy, expression, and cellular function of transforming growth factor-beta. Pharmacology & therapeutics *98*, 257-265.
74. Gray, A.M., and Mason, A.J. (1990). Requirement for activin A and transforming growth factor--beta 1 pro-regions in homodimer assembly. Science *247*, 1328-1330.
75. Groppe, J., Hinck, C.S., Samavarchi-Tehrani, P., Zubieta, C., Schuermann, J.P., Taylor, A.B., Schwarz, P.M., Wrana, J.L., and Hinck, A.P. (2008). Cooperative assembly of TGF-beta superfamily signaling complexes is mediated by two disparate mechanisms and distinct modes of receptor binding. Mol Cell *29*, 157-168.
76. Gueripel, X., Benahmed, M., and Gougeon, A. (2004). Sequential gonadotropin treatment of immature mice leads to amplification of transforming growth factor beta action, via upregulation of receptor-type 1, Smad 2 and 4, and downregulation of Smad 6. Biol Reprod *70*, 640-648.
77. Halder, S.K., Anumanthan, G., Maddula, R., Mann, J., Chytil, A., Gonzalez, A.L., Washington, M.K., Moses, H.L., Beauchamp, R.D., and Datta, P.K. (2006). Oncogenic function of a novel WD-domain protein, STRAP, in human carcinogenesis. Cancer research *66*, 6156-6166.
78. Hamamoto, T., Beppu, H., Okada, H., Kawabata, M., Kitamura, T., Miyazono, K., and Kato, M. (2002). Compound disruption of smad2 accelerates malignant progression of intestinal tumors in apc knockout mice. Cancer research *62*, 5955-5961.

79. Hanrahan, J.P., Gregan, S.M., Mulsant, P., Mullen, M., Davis, G.H., Powell, R., and Galloway, S.M. (2004). Mutations in the genes for oocyte-derived growth factors GDF9 and BMP15 are associated with both increased ovulation rate and sterility in Cambridge and Belclare sheep (Ovis aries). Biol Reprod *70*, 900-909.

80. Hansen, K.R., Knowlton, N.S., Thyer, A.C., Charleston, J.S., Soules, M.R., and Klein, N.A. (2008). A new model of reproductive aging: the decline in ovarian non-growing follicle number from birth to menopause. Human reproduction (Oxford, England) *23*, 699-708.

81. Hatzirodos, N., Bayne, R.A., Irving-Rodgers, H.F., Hummitzsch, K., Sabatier, L., Lee, S., Bonner, W., Gibson, M.A., Rainey, W.E., Carr, B.R.*, et al.* (2011). Linkage of regulators of TGF-beta activity in the fetal ovary to polycystic ovary syndrome. FASEB journal : official publication of the Federation of American Societies for Experimental Biology *25*, 2256-2265.

82. Hayashi, H., and Sakai, T. (2012). Biological Significance of Local TGF-beta Activation in Liver Diseases. Frontiers in physiology *3*, 12.

83. He, J., Tegen, S.B., Krawitz, A.R., Martin, G.S., and Luo, K. (2003). The transforming activity of Ski and SnoN is dependent on their ability to repress the activity of Smad proteins. J Biol Chem *278*, 30540-30547.

84. Henriksen, R., Gobl, A., Wilander, E., Oberg, K., Miyazono, K., and Funa, K. (1995). Expression and prognostic significance of TGF-beta isotypes, latent TGF-beta 1 binding protein, TGF-beta type I and type II receptors, and endoglin in normal ovary and ovarian neoplasms. Laboratory investigation; a journal of technical methods and pathology *73*, 213-220.

85. Hirai, M., Horiguchi, M., Ohbayashi, T., Kita, T., Chien, K.R., and Nakamura, T. (2007). Latent TGF-β-binding protein 2 binds to DANCE/fibulin-5 and regulates elastic fiber assembly. The EMBO Journal *26*, 3283-3295.

86. Hirshfield, A.N. (1991). Development of follicles in the mammalian ovary. Int Rev Cytol *124*, 43-101.

87. Hirshfield, A.N. (1992). Heterogeneity of cell populations that contribute to the formation of primordial follicles in rats. Biol Reprod *47*, 466-472.

88. Hough, C., Radu, M., and Dore, J.J. (2012). Tgf-beta induced Erk phosphorylation of smad linker region regulates smad signaling. PLoS One *7*, e42513.

89. Hsueh, A.J., Billig, H., and Tsafriri, A. (1994). Ovarian follicle atresia: a hormonally controlled apoptotic process. Endocr Rev *15*, 707-724.

90. Huang, Z., Wang, D., Ihida-Stansbury, K., Jones, P.L., and Martin, J.F. (2009). Defective pulmonary vascular remodeling in Smad8 mutant mice. Human molecular genetics *18*, 2791-2801.
91. Hunt, P.A., and Hassold, T.J. (2002). Sex matters in meiosis. Science *296*, 2181-2183.
92. Hyytiainen, M., Penttinen, C., and Keski-Oja, J. (2004). Latent TGF-beta binding proteins: extracellular matrix association and roles in TGF-beta activation. Critical reviews in clinical laboratory sciences *41*, 233-264.
93. Ingman, W.V., Robker, R.L., Woittiez, K., and Robertson, S.A. (2006). Null mutation in transforming growth factor beta1 disrupts ovarian function and causes oocyte incompetence and early embryo arrest. Endocrinology *147*, 835-845.
94. Inman, G.J., Nicolas, F.J., and Hill, C.S. (2002). Nucleocytoplasmic shuttling of Smads 2, 3, and 4 permits sensing of TGF-beta receptor activity. Mol Cell *10*, 283-294.
95. Inoue, Y., and Imamura, T. (2008). Regulation of TGF-beta family signaling by E3 ubiquitin ligases. Cancer Sci *99*, 2107-2112.
96. Isogai, Z., Ono, R.N., Ushiro, S., Keene, D.R., Chen, Y., Mazzieri, R., Charbonneau, N.L., Reinhardt, D.P., Rifkin, D.B., and Sakai, L.Y. (2003). Latent transforming growth factor beta-binding protein 1 interacts with fibrillin and is a microfibril-associated protein. J Biol Chem *278*, 2750-2757.
97. Itoh, S., Thorikay, M., Kowanetz, M., Moustakas, A., Itoh, F., Heldin, C.H., and ten Dijke, P. (2003). Elucidation of Smad requirement in transforming growth factor-beta type I receptor-induced responses. J Biol Chem *278*, 3751-3761.
98. Javelaud, D., and Mauviel, A. (2005). Crosstalk mechanisms between the mitogen-activated protein kinase pathways and Smad signaling downstream of TGF-beta: implications for carcinogenesis. Oncogene *24*, 5742-5750.
99. Jeruss, J.S., and Woodruff, T.K. (2009). Preservation of fertility in patients with cancer. The New England journal of medicine *360*, 902-911.
100. Jin, S.Y., Lei, L., Shikanov, A., Shea, L.D., and Woodruff, T.K. (2010). A novel two-step strategy for in vitro culture of early-stage ovarian follicles in the mouse. Fertility and sterility *93*, 2633-2639.
101. John, G.B., Gallardo, T.D., Shirley, L.J., and Castrillon, D.H. (2008). Foxo3 is a PI3K-dependent molecular switch controlling the initiation of oocyte growth. Dev Biol *321*, 197-204.
102. Johnson, J., Bagley, J., Skaznik-Wikiel, M., Lee, H.J., Adams, G.B., Niikura, Y., Tschudy, K.S., Tilly, J.C., Cortes, M.L., Forkert, R.*, et al.* (2005). Oocyte generation in

adult mammalian ovaries by putative germ cells in bone marrow and peripheral blood. Cell *122*, 303-315.

103. Johnson, J., Canning, J., Kaneko, T., Pru, J.K., and Tilly, J.L. (2004). Germline stem cells and follicular renewal in the postnatal mammalian ovary. Nature *428*, 145-150.
104. Jones, R.L., and Pepling, M.E. (2013). KIT signaling regulates primordial follicle formation in the neonatal mouse ovary. Dev Biol *382*, 186-197.
105. Jovanovic, J., Iqbal, S., Jensen, S., Mardon, H., and Handford, P. (2008). Fibrillin-integrin interactions in health and disease. Biochemical Society transactions *36*, 257-262.
106. Jung, H., Seong, H.A., Manoharan, R., and Ha, H. (2010). Serine-threonine kinase receptor-associated protein inhibits apoptosis signal-regulating kinase 1 function through direct interaction. J Biol Chem *285*, 54-70.
107. Kaivo-oja, N., Jeffery, L.A., Ritvos, O., and Mottershead, D.G. (2006). Smad signalling in the ovary. Reproductive biology and endocrinology : RB&E *4*, 21.
108. Kawamura, K., Cheng, Y., Suzuki, N., Deguchi, M., Sato, Y., Takae, S., Ho, C.H., Kawamura, N., Tamura, M., Hashimoto, S.*, et al.* (2013). Hippo signaling disruption and Akt stimulation of ovarian follicles for infertility treatment. Proc Natl Acad Sci U S A *110*, 17474-17479.
109. Kerr, B., Garcia-Rudaz, C., Dorfman, M., Paredes, A., and Ojeda, S.R. (2009). NTRK1 and NTRK2 receptors facilitate follicle assembly and early follicular development in the mouse ovary. Reproduction *138*, 131-140.
110. Kerr, J.B., Brogan, L., Myers, M., Hutt, K.J., Mladenovska, T., Ricardo, S., Hamza, K., Scott, C.L., Strasser, A., and Findlay, J.K. (2012). The primordial follicle reserve is not renewed after chemical or gamma-irradiation mediated depletion. Reproduction *143*, 469-476.
111. Kezele, P., Nilsson, E., and Skinner, M.K. (2002). Cell-cell interactions in primordial follicle assembly and development. Front Biosci *1*, d1990-1996.
112. Kezele, P., and Skinner, M.K. (2003). Regulation of ovarian primordial follicle assembly and development by estrogen and progesterone: endocrine model of follicle assembly. Endocrinology *144*, 3329-3337.
113. Kim, H., Yamanouchi, K., and Nishihara, M. (2006). Expression of ski in the granulosa cells of atretic follicles in the rat ovary. The Journal of reproduction and development *52*, 715-721.

114. Kim, J.Y. (2012). Control of ovarian primordial follicle activation. Clin Exp Reprod Med *39*, 10-14.
115. Kimura, N., Matsuo, R., Shibuya, H., Nakashima, K., and Taga, T. (2000). BMP2-induced apoptosis is mediated by activation of the TAK1-p38 kinase pathway that is negatively regulated by Smad6. J Biol Chem *275*, 17647-17652.
116. Knight, P.G., and Glister, C. (2001). Potential local regulatory functions of inhibins, activins and follistatin in the ovary. Reproduction *121*, 503-512.
117. Knight, P.G., and Glister, C. (2003). Local roles of TGF-beta superfamily members in the control of ovarian follicle development. Anim Reprod Sci *78*, 165-183.
118. Knight, P.G., and Glister, C. (2006). TGF-beta superfamily members and ovarian follicle development. Reproduction *132*, 191-206.
119. Koli, K., Saharinen, J., Hyytiainen, M., Penttinen, C., and Keski-Oja, J. (2001). Latency, activation, and binding proteins of TGF-beta. Microscopy research and technique *52*, 354-362.
120. Koli, K., Wempe, F., Sterner-Kock, A., Kantola, A., Komor, M., Hofmann, W.K., von Melchner, H., and Keski-Oja, J. (2004). Disruption of LTBP-4 function reduces TGF-beta activation and enhances BMP-4 signaling in the lung. J Cell Biol *167*, 123-133.
121. Komatsu, K., Koya, T., Wang, J., Yamashita, M., Kikkawa, F., and Iwase, A. (2015). Analysis of the Effect of Leukemia Inhibitory Factor on Follicular Growth in Cultured Murine Ovarian Tissue. Biol Reprod *93*, 18.
122. Kretschmer, C., Conradi, A., Kemmner, W., and Sterner-Kock, A. (2011). Latent transforming growth factor binding protein 4 (LTBP4) is downregulated in mouse and human DCIS and mammary carcinomas. Cellular oncology (Dordrecht) *34*, 419-434.
123. Kretzschmar, M., Doody, J., Timokhina, I., and Massague, J. (1999). A mechanism of repression of TGFbeta/ Smad signaling by oncogenic Ras. Genes Dev *13*, 804-816.
124. Kuratomi, G., Komuro, A., Goto, K., Shinozaki, M., Miyazawa, K., Miyazono, K., and Imamura, T. (2005). NEDD4-2 (neural precursor cell expressed, developmentally down-regulated 4-2) negatively regulates TGF-beta (transforming growth factor-beta) signalling by inducing ubiquitin-mediated degradation of Smad2 and TGF-beta type I receptor. Biochem J *386*, 461-470.
125. Kyriakides, T.R., and Maclauchlan, S. (2009). The role of thrombospondins in wound healing, ischemia, and the foreign body reaction. Journal of cell communication and signaling *3*, 215-225.

126. Lawson, K.A., and Hage, W.J. (1994). Clonal analysis of the origin of primordial germ cells in the mouse. Ciba Found Symp *182*, 68-84.
127. Lee, W.S., Yoon, S.J., Yoon, T.K., Cha, K.Y., Lee, S.H., Shimasaki, S., Lee, S., and Lee, K.A. (2004). Effects of bone morphogenetic protein-7 (BMP-7) on primordial follicular growth in the mouse ovary. Mol Reprod Dev *69*, 159-163.
128. Lei, L., and Spradling, A.C. (2016). Mouse oocytes differentiate through organelle enrichment from sister cyst germ cells. Science *352*, 95-99.
129. Li, H., Xu, L.L., Masuda, K., Raymundo, E., McLeod, D.G., Dobi, A., and Srivastava, S. (2008a). A feedback loop between the androgen receptor and a NEDD4-binding protein, PMEPA1, in prostate cancer cells. J Biol Chem *283*, 28988-28995.
130. Li, Q. (2015). Inhibitory SMADs: potential regulators of ovarian function. Biol Reprod *92*, 50.
131. Li, Q., Pangas, S.A., Jorgez, C.J., Graff, J.M., Weinstein, M., and Matzuk, M.M. (2008b). Redundant roles of SMAD2 and SMAD3 in ovarian granulosa cells in vivo. Mol Cell Biol *28*, 7001-7011.
132. Lin, H.K., Bergmann, S., and Pandolfi, P.P. (2004). Cytoplasmic PML function in TGF-beta signalling. Nature *431*, 205-211.
133. Lin, X., Duan, X., Liang, Y.Y., Su, Y., Wrighton, K.H., Long, J., Hu, M., Davis, C.M., Wang, J., Brunicardi, F.C.*, et al.* (2006). PPM1A functions as a Smad phosphatase to terminate TGFbeta signaling. Cell *125*, 915-928.
134. Liu, R., Zhou, Z., Huang, J., and Chen, C. (2011). PMEPA1 promotes androgen receptor-negative prostate cell proliferation through suppressing the Smad3/4-c-Myc-p21 Cip1 signaling pathway. The Journal of pathology *223*, 683-694.
135. Liu, X., Nagarajan, R.P., Vale, W., and Chen, Y. (2002). Phosphorylation regulation of the interaction between Smad7 and activin type I receptor. FEBS letters *519*, 93-98.
136. Livak, K.J., and Schmittgen, T.D. (2001). Analysis of relative gene expression data using real-time quantitative PCR and the 2(-Delta Delta C(T)) Method. Methods (San Diego, Calif) *25*, 402-408.
137. Loeys, B.L., Gerber, E.E., Riegert-Johnson, D., Iqbal, S., Whiteman, P., McConnell, V., Chillakuri, C.R., Macaya, D., Coucke, P.J., De Paepe, A.*, et al.* (2010). Mutations in fibrillin-1 cause congenital scleroderma: stiff skin syndrome. Science translational medicine *2*, 23ra20.
138. Lonn, P., Moren, A., Raja, E., Dahl, M., and Moustakas, A. (2009). Regulating the stability of TGFbeta receptors and Smads. Cell Res *19*, 21-35.

139. Maiani, E., Di Bartolomeo, C., Klinger, F.G., Cannata, S.M., Bernardini, S., Chateauvieux, S., Mack, F., Mattei, M., De Felici, M., Diederich, M., *et al.* (2012). Reply to: Cisplatin-induced primordial follicle oocyte killing and loss of fertility are not prevented by imatinib. Nature medicine *18*, 1172-1174.
140. Maldonado-Baez, L., Williamson, C., and Donaldson, J.G. (2013). Clathrin-independent endocytosis: a cargo-centric view. Experimental cell research *319*, 2759-2769.
141. Marastoni, S., Ligresti, G., Lorenzon, E., Colombatti, A., and Mongiat, M. (2008). Extracellular matrix: a matter of life and death. Connective tissue research *49*, 203-206.
142. Matzuk, M.M., Finegold, M.J., Su, J.G., Hsueh, A.J., and Bradley, A. (1992). Alpha-inhibin is a tumour-suppressor gene with gonadal specificity in mice. Nature *360*, 313-319.
143. Mayor, S., Parton, R.G., and Donaldson, J.G. (2014). Clathrin-independent pathways of endocytosis. Cold Spring Harbor perspectives in biology *6*.
144. McGee, E.A., and Hsueh, A.J. (2000). Initial and cyclic recruitment of ovarian follicles. Endocr Rev *21*, 200-214.
145. McGrath, S.A., Esquela, A.F., and Lee, S.J. (1995). Oocyte-specific expression of growth/differentiation factor-9. Mol Endocrinol *9*, 131-136.
146. McLaren, A. (2000). Germ and somatic cell lineages in the developing gonad. Mol Cell Endocrinol *163*, 3-9.
147. McLaughlin, M., Kinnell, H.L., Anderson, R.A., and Telfer, E.E. (2014). Inhibition of phosphatase and tensin homologue (PTEN) in human ovary in vitro results in increased activation of primordial follicles but compromises development of growing follicles. Molecular human reproduction *20*, 736-744.
148. McMullen, M.L., Cho, B.N., Yates, C.J., and Mayo, K.E. (2001). Gonadal pathologies in transgenic mice expressing the rat inhibin alpha-subunit. Endocrinology *142*, 5005-5014.
149. Miyazono, K., Hellman, U., Wernstedt, C., and Heldin, C.H. (1988). Latent high molecular weight complex of transforming growth factor beta 1. Purification from human platelets and structural characterization. J Biol Chem *263*, 6407-6415.
150. Miyazono, K., Kusanagi, K., and Inoue, H. (2001). Divergence and convergence of TGF-beta/BMP signaling. J Cell Physiol *187*, 265-276.

151. Miyazono, K., Olofsson, A., Colosetti, P., and Heldin, C.H. (1991). A role of the latent TGF-beta 1-binding protein in the assembly and secretion of TGF-beta 1. EMBO J *10*, 1091-1101.
152. Moren, A., Olofsson, A., Stenman, G., Sahlin, P., Kanzaki, T., Claesson-Welsh, L., ten Dijke, P., Miyazono, K., and Heldin, C.H. (1994). Identification and characterization of LTBP-2, a novel latent transforming growth factor-beta-binding protein. J Biol Chem *269*, 32469-32478.
153. Morgan, S., Campbell, L., Allison, V., Murray, A., and Spears, N. (2015). Culture and co-culture of mouse ovaries and ovarian follicles. Journal of visualized experiments : JoVE.
154. Mori, S., Matsuzaki, K., Yoshida, K., Furukawa, F., Tahashi, Y., Yamagata, H., Sekimoto, G., Seki, T., Matsui, H., Nishizawa, M.*, et al.* (2004). TGF-beta and HGF transmit the signals through JNK-dependent Smad2/3 phosphorylation at the linker regions. Oncogene *23*, 7416-7429.
155. Mork, L., Maatouk, D.M., McMahon, J.A., Guo, J.J., Zhang, P., McMahon, A.P., and Capel, B. (2012). Temporal differences in granulosa cell specification in the ovary reflect distinct follicle fates in mice. Biol Reprod *86*, 37.
156. Moustakas, A., and Heldin, C.H. (2008). Dynamic control of TGF-beta signaling and its links to the cytoskeleton. FEBS letters *582*, 2051-2065.
157. Moustakas, A., and Heldin, C.H. (2009). The regulation of TGFbeta signal transduction. Development *136*, 3699-3714.
158. Moustakas, A., Souchelnytskyi, S., and Heldin, C.H. (2001). Smad regulation in TGF-beta signal transduction. Journal of cell science *114*, 4359-4369.
159. Mu, Y., Gudey, S.K., and Landstrom, M. (2012). Non-Smad signaling pathways. Cell and tissue research *347*, 11-20.
160. Nagase, H., Visse, R., and Murphy, G. (2006). Structure and function of matrix metalloproteinases and TIMPs. Cardiovascular research *69*, 562-573.
161. Nehra, D., Le, H.D., Fallon, E.M., Carlson, S.J., Woods, D., White, Y.A., Pan, A.H., Guo, L., Rodig, S.J., Tilly, J.L.*, et al.* (2012). Prolonging the female reproductive lifespan and improving egg quality with dietary omega-3 fatty acids. Aging cell *11*, 1046-1054.
162. Nilsson, E., Doraiswamy, V., Parrott, J.A., and Skinner, M.K. (2001a). Expression and action of transforming growth factor beta (TGFbeta1, TGFbeta2, TGFbeta3) in normal

bovine ovarian surface epithelium and implications for human ovarian cancer. Mol Cell Endocrinol *182*, 145-155.

163. Nilsson, E., Parrott, J.A., and Skinner, M.K. (2001b). Basic fibroblast growth factor induces primordial follicle development and initiates folliculogenesis. Mol Cell Endocrinol *175*, 123-130.
164. Nilsson, E.E., Doraiswamy, V., and Skinner, M.K. (2003). Transforming growth factor-beta isoform expression during bovine ovarian antral follicle development. Mol Reprod Dev *66*, 237-246.
165. Nilsson, E.E., Kezele, P., and Skinner, M.K. (2002). Leukemia inhibitory factor (LIF) promotes the primordial to primary follicle transition in rat ovaries. Mol Cell Endocrinol *188*, 65-73.
166. Nilsson, E.E., and Skinner, M.K. (2003). Bone morphogenetic protein-4 acts as an ovarian follicle survival factor and promotes primordial follicle development. Biol Reprod *69*, 1265-1272.
167. Nunes, I., Gleizes, P.E., Metz, C.N., and Rifkin, D.B. (1997). Latent transforming growth factor-beta binding protein domains involved in activation and transglutaminase-dependent cross-linking of latent transforming growth factor-beta. J Cell Biol *136*, 1151-1163.
168. Oktay, K., and Oktem, O. (2007). Regeneration of oocytes after chemotherapy: connecting the evidence from mouse to human. Journal of clinical oncology : official journal of the American Society of Clinical Oncology *25*, 3185-3187.
169. Olivieri, J., Smaldone, S., and Ramirez, F. (2010). Fibrillin assemblies: extracellular determinants of tissue formation and fibrosis. Fibrogenesis & tissue repair *3*, 24.
170. Orisaka, M., Tajima, K., Tsang, B.K., and Kotsuji, F. (2009). Oocyte-granulosa-theca cell interactions during preantral follicular development. J Ovarian Res *2*, 1757-2215.
171. Otsuka, F., Moore, R.K., and Shimasaki, S. (2001). Biological function and cellular mechanism of bone morphogenetic protein-6 in the ovary. J Biol Chem *276*, 32889-32895.
172. Palma, G.A., Arganaraz, M.E., Barrera, A.D., Rodler, D., Mutto, A.A., and Sinowatz, F. (2012). Biology and biotechnology of follicle development. ScientificWorldJournal *938138*, 22.
173. Pangas, S.A. (2012). Regulation of the ovarian reserve by members of the transforming growth factor beta family. Mol Reprod Dev *79*, 666-679.

174. Pangas, S.A., Li, X., Robertson, E.J., and Matzuk, M.M. (2006). Premature luteinization and cumulus cell defects in ovarian-specific Smad4 knockout mice. Mol Endocrinol *20*, 1406-1422.

175. Pangas, S.A., Li, X., Umans, L., Zwijsen, A., Huylebroeck, D., Gutierrez, C., Wang, D., Martin, J.F., Jamin, S.P., Behringer, R.R.*, et al.* (2008). Conditional deletion of Smad1 and Smad5 in somatic cells of male and female gonads leads to metastatic tumor development in mice. Mol Cell Biol *28*, 248-257.

176. Pangas, S.A., and Matzuk, M.M. (2004). Genetic models for transforming growth factor beta superfamily signaling in ovarian follicle development. Mol Cell Endocrinol *225*, 83-91.

177. Pangas, S.A., Saudye, H., Shea, L.D., and Woodruff, T.K. (2003). Novel approach for the three-dimensional culture of granulosa cell-oocyte complexes. Tissue engineering *9*, 1013-1021.

178. Parrott, J.A., and Skinner, M.K. (2000). Kit ligand actions on ovarian stromal cells: effects on theca cell recruitment and steroid production. Mol Reprod Dev *55*, 55-64.

179. Penttinen, C., Saharinen, J., Weikkolainen, K., Hyytiainen, M., and Keski-Oja, J. (2002). Secretion of human latent TGF-beta-binding protein-3 (LTBP-3) is dependent on co-expression of TGF-beta. Journal of cell science *115*, 3457-3468.

180. Pepling, M.E. (2006). From primordial germ cell to primordial follicle: mammalian female germ cell development. Genesis *44*, 622-632.

181. Pepling, M.E. (2012). Follicular assembly: mechanisms of action. Reproduction *143*, 139-149.

182. Pepling, M.E., and Spradling, A.C. (2001). Mouse ovarian germ cell cysts undergo programmed breakdown to form primordial follicles. Dev Biol *234*, 339-351.

183. Persson, U., Izumi, H., Souchelnytskyi, S., Itoh, S., Grimsby, S., Engstrom, U., Heldin, C.H., Funa, K., and ten Dijke, P. (1998). The L45 loop in type I receptors for TGF-beta family members is a critical determinant in specifying Smad isoform activation. FEBS letters *434*, 83-87.

184. Pesce, M., and De Felici, M. (1994). Apoptosis in mouse primordial germ cells: a study by transmission and scanning electron microscope. Anatomy and embryology *189*, 435-440.

185. Pesce, M., Klinger, F.G., and De Felici, M. (2002). Derivation in culture of primordial germ cells from cells of the mouse epiblast: phenotypic induction and growth control by Bmp4 signalling. Mech Dev *112*, 15-24.

186. Picton, H.M., Danfour, M.A., Harris, S.E., Chambers, E.L., and Huntriss, J. (2003). Growth and maturation of oocytes in vitro. Reprod Suppl *61*, 445-462.
187. Prodoehl, M.J., Irving-Rodgers, H.F., Bonner, W.M., Sullivan, T.M., Micke, G.C., Gibson, M.A., Perry, V.E., and Rodgers, R.J. (2009). Fibrillins and latent TGFbeta binding proteins in bovine ovaries of offspring following high or low protein diets during pregnancy of dams. Mol Cell Endocrinol *307*, 133-141.
188. Prokova, V., Mavridou, S., Papakosta, P., and Kardassis, D. (2005). Characterization of a novel transcriptionally active domain in the transforming growth factor beta-regulated Smad3 protein. Nucleic acids research *33*, 3708-3721.
189. Qin, B.Y., Lam, S.S., Correia, J.J., and Lin, K. (2002). Smad3 allostery links TGF-beta receptor kinase activation to transcriptional control. Genes Dev *16*, 1950-1963.
190. Quezada, M., Wang, J., Hoang, V., and McGee, E.A. (2012). Smad7 is a transforming growth factor-beta-inducible mediator of apoptosis in granulosa cells. Fertility and sterility *97*, 1452-1459 e1451-1456.
191. Rae, F.K., Hooper, J.D., Nicol, D.L., and Clements, J.A. (2001). Characterization of a novel gene, STAG1/PMEPA1, upregulated in renal cell carcinoma and other solid tumors. Molecular carcinogenesis *32*, 44-53.
192. Rahimi, R.A., and Leof, E.B. (2007). TGF-beta signaling: a tale of two responses. Journal of cellular biochemistry *102*, 593-608.
193. Reddy, P., Adhikari, D., Zheng, W., Liang, S., Hamalainen, T., Tohonen, V., Ogawa, W., Noda, T., Volarevic, S., Huhtaniemi, I.*, et al.* (2009). PDK1 signaling in oocytes controls reproductive aging and lifespan by manipulating the survival of primordial follicles. Human molecular genetics *18*, 2813-2824.
194. Reddy, P., Liu, L., Adhikari, D., Jagarlamudi, K., Rajareddy, S., Shen, Y., Du, C., Tang, W., Hamalainen, T., Peng, S.L.*, et al.* (2008). Oocyte-specific deletion of Pten causes premature activation of the primordial follicle pool. Science *319*, 611-613.
195. Reiner, J.E., and Datta, P.K. (2011). TGF-beta-dependent and -independent roles of STRAP in cancer. Frontiers in bioscience (Landmark edition) *16*, 105-115.
196. Reynaud, K., Cortvrindt, R., Smitz, J., Bernex, F., Panthier, J.J., and Driancourt, M.A. (2001). Alterations in ovarian function of mice with reduced amounts of KIT receptor. Reproduction *121*, 229-237.
197. Rifkin, D.B. (2005). Latent transforming growth factor-beta (TGF-beta) binding proteins: orchestrators of TGF-beta availability. J Biol Chem *280*, 7409-7412.

198. Robinson, P.N., Arteaga-Solis, E., Baldock, C., Collod-Beroud, G., Booms, P., De Paepe, A., Dietz, H.C., Guo, G., Handford, P.A., Judge, D.P., *et al.* (2006). The molecular genetics of Marfan syndrome and related disorders. Journal of medical genetics *43*, 769-787.
199. Rodriguez, G.C., Nagarsheth, N.P., Lee, K.L., Bentley, R.C., Walmer, D.K., Cline, M., Whitaker, R.S., Isner, P., Berchuck, A., Dodge, R.K., *et al.* (2002). Progestin-induced apoptosis in the Macaque ovarian epithelium: differential regulation of transforming growth factor-beta. Journal of the National Cancer Institute *94*, 50-60.
200. Ross, S., and Hill, C.S. (2008). How the Smads regulate transcription. The international journal of biochemistry & cell biology *40*, 383-408.
201. Saharinen, J., Hyytiainen, M., Taipale, J., and Keski-Oja, J. (1999). Latent transforming growth factor-beta binding proteins (LTBPs)--structural extracellular matrix proteins for targeting TGF-beta action. Cytokine Growth Factor Rev *10*, 99-117.
202. Saharinen, J., and Keski-Oja, J. (2000). Specific sequence motif of 8-Cys repeats of TGF-beta binding proteins, LTBPs, creates a hydrophobic interaction surface for binding of small latent TGF-beta. Molecular biology of the cell *11*, 2691-2704.
203. Saharinen, J., Taipale, J., and Keski-Oja, J. (1996). Association of the small latent transforming growth factor-beta with an eight cysteine repeat of its binding protein LTBP-1. EMBO J *15*, 245-253.
204. Saharinen, J., Taipale, J., Monni, O., and Keski-Oja, J. (1998). Identification and characterization of a new latent transforming growth factor-beta-binding protein, LTBP-4. J Biol Chem *273*, 18459-18469.
205. Saitou, M., and Yamaji, M. (2012). Primordial germ cells in mice. Cold Spring Harbor perspectives in biology *4*.
206. Scaramuzzi, R.J., Baird, D.T., Campbell, B.K., Driancourt, M.A., Dupont, J., Fortune, J.E., Gilchrist, R.B., Martin, G.B., McNatty, K.P., McNeilly, A.S., *et al.* (2011). Regulation of folliculogenesis and the determination of ovulation rate in ruminants. Reproduction, fertility, and development *23*, 444-467.
207. Schindler, R., Nilsson, E., and Skinner, M.K. (2010). Induction of ovarian primordial follicle assembly by connective tissue growth factor CTGF. PLoS One *5*, 0012979.
208. Schmidt, D., Ovitt, C.E., Anlag, K., Fehsenfeld, S., Gredsted, L., Treier, A.C., and Treier, M. (2004). The murine winged-helix transcription factor Foxl2 is required for granulosa cell differentiation and ovary maintenance. Development *131*, 933-942.

209. Schmierer, B., and Hill, C.S. (2005). Kinetic analysis of Smad nucleocytoplasmic shuttling reveals a mechanism for transforming growth factor beta-dependent nuclear accumulation of Smads. Mol Cell Biol *25*, 9845-9858.
210. Schmierer, B., and Hill, C.S. (2007). TGFbeta-SMAD signal transduction: molecular specificity and functional flexibility. Nat Rev Mol Cell Biol *8*, 970-982.
211. Sekelsky, J.J., Newfeld, S.J., Raftery, L.A., Chartoff, E.H., and Gelbart, W.M. (1995). Genetic characterization and cloning of mothers against dpp, a gene required for decapentaplegic function in Drosophila melanogaster. Genetics *139*, 1347-1358.
212. Seong, H.A., Jung, H., Choi, H.S., Kim, K.T., and Ha, H. (2005). Regulation of transforming growth factor-beta signaling and PDK1 kinase activity by physical interaction between PDK1 and serine-threonine kinase receptor-associated protein. J Biol Chem *280*, 42897-42908.
213. Seong, H.A., Jung, H., Kim, K.T., and Ha, H. (2007). 3-Phosphoinositide-dependent PDK1 negatively regulates transforming growth factor-beta-induced signaling in a kinase-dependent manner through physical interaction with Smad proteins. J Biol Chem *282*, 12272-12289.
214. Shi, W., Sun, C., He, B., Xiong, W., Shi, X., Yao, D., and Cao, X. (2004). GADD34-PP1c recruited by Smad7 dephosphorylates TGFbeta type I receptor. J Cell Biol *164*, 291-300.
215. Shi, Y., and Massague, J. (2003). Mechanisms of TGF-beta signaling from cell membrane to the nucleus. Cell *113*, 685-700.
216. Shimasaki, S., Moore, R.K., Otsuka, F., and Erickson, G.F. (2004). The bone morphogenetic protein system in mammalian reproduction. Endocr Rev *25*, 72-101.
217. Shipley, J.M., Mecham, R.P., Maus, E., Bonadio, J., Rosenbloom, J., McCarthy, R.T., Baumann, M.L., Frankfater, C., Segade, F., and Shapiro, S.D. (2000). Developmental expression of latent transforming growth factor beta binding protein 2 and its requirement early in mouse development. Mol Cell Biol *20*, 4879-4887.
218. Singha, P.K., Pandeswara, S., Geng, H., Lan, R., Venkatachalam, M.A., and Saikumar, P. (2014). TGF-beta induced TMEPAI/PMEPA1 inhibits canonical Smad signaling through R-Smad sequestration and promotes non-canonical PI3K/Akt signaling by reducing PTEN in triple negative breast cancer. Genes & cancer *5*, 320-336.
219. Spears, N., Molinek, M.D., Robinson, L.L., Fulton, N., Cameron, H., Shimoda, K., Telfer, E.E., Anderson, R.A., and Price, D.J. (2003). The role of neurotrophin receptors in female germ-cell survival in mouse and human. Development *130*, 5481-5491.

220. Sterner-Kock, A., Thorey, I.S., Koli, K., Wempe, F., Otte, J., Bangsow, T., Kuhlmeier, K., Kirchner, T., Jin, S., Keski-Oja, J.*, et al.* (2002). Disruption of the gene encoding the latent transforming growth factor-beta binding protein 4 (LTBP-4) causes abnormal lung development, cardiomyopathy, and colorectal cancer. Genes Dev *16*, 2264-2273.
221. Su, C.T., Huang, J.W., Chiang, C.K., Lawrence, E.C., Levine, K.L., Dabovic, B., Jung, C., Davis, E.C., Madan-Khetarpal, S., and Urban, Z. (2015). Latent transforming growth factor binding protein 4 regulates transforming growth factor beta receptor stability. Human molecular genetics *24*, 4024-4036.
222. Sun, Y., Lowther, W., Kato, K., Bianco, C., Kenney, N., Strizzi, L., Raafat, D., Hirota, M., Khan, N.I., Bargo, S.*, et al.* (2005). Notch4 intracellular domain binding to Smad3 and inhibition of the TGF-beta signaling. Oncogene *24*, 5365-5374.
223. Taipale, J., Koli, K., and Keski-Oja, J. (1992). Release of transforming growth factor-beta 1 from the pericellular matrix of cultured fibroblasts and fibrosarcoma cells by plasmin and thrombin. J Biol Chem *267*, 25378-25384.
224. Tanwar, P.S., O'Shea, T., and McFarlane, J.R. (2008). In vivo evidence of role of bone morphogenetic protein-4 in the mouse ovary. Anim Reprod Sci *106*, 232-240.
225. Tazat, K., Hector-Greene, M., Blobe, G.C., and Henis, Y.I. (2015). TbetaRIII independently binds type I and type II TGF-beta receptors to inhibit TGF-beta signaling. Molecular biology of the cell *26*, 3535-3545.
226. ten Dijke, P., and Hill, C.S. (2004). New insights into TGF-beta-Smad signalling. Trends Biochem Sci *29*, 265-273.
227. ten Dijke, P., Miyazono, K., and Heldin, C.H. (2000). Signaling inputs converge on nuclear effectors in TGF-beta signaling. Trends Biochem Sci *25*, 64-70.
228. Thompson, T.B., Lerch, T.F., Cook, R.W., Woodruff, T.K., and Jardetzky, T.S. (2005). The structure of the follistatin:activin complex reveals antagonism of both type I and type II receptor binding. Dev Cell *9*, 535-543.
229. Tian, X., Halfhill, A.N., and Diaz, F.J. (2010). Localization of phosphorylated SMAD proteins in granulosa cells, oocytes and oviduct of female mice. Gene expression patterns : GEP *10*, 105-112.
230. Tilly, J.L. (2003). Ovarian follicle counts--not as simple as 1, 2, 3. Reproductive biology and endocrinology : RB&E *1*, 11.
231. Tingen, C.M., Bristol-Gould, S.K., Kiesewetter, S.E., Wellington, J.T., Shea, L., and Woodruff, T.K. (2009). Prepubertal primordial follicle loss in mice is not due to classical apoptotic pathways. Biol Reprod *81*, 16-25.

232. Todorovic, V., Frendewey, D., Gutstein, D.E., Chen, Y., Freyer, L., Finnegan, E., Liu, F., Murphy, A., Valenzuela, D., Yancopoulos, G.*, et al.* (2007). Long form of latent TGF-beta binding protein 1 (Ltbp1L) is essential for cardiac outflow tract septation and remodeling. Development *134*, 3723-3732.

233. Todorovic, V., Jurukovski, V., Chen, Y., Fontana, L., Dabovic, B., and Rifkin, D.B. (2005). Latent TGF-beta binding proteins. The international journal of biochemistry & cell biology *37*, 38-41.

234. Tomic, D., Brodie, S.G., Deng, C., Hickey, R.J., Babus, J.K., Malkas, L.H., and Flaws, J.A. (2002). Smad 3 may regulate follicular growth in the mouse ovary. Biol Reprod *66*, 917-923.

235. Tomic, D., Miller, K.P., Kenny, H.A., Woodruff, T.K., Hoyer, P., and Flaws, J.A. (2004). Ovarian follicle development requires Smad3. Mol Endocrinol *18*, 2224-2240.

236. Tremblay, K.D., Dunn, N.R., and Robertson, E.J. (2001). Mouse embryos lacking Smad1 signals display defects in extra-embryonic tissues and germ cell formation. Development *128*, 3609-3621.

237. Tsang, K.Y., Cheung, M.C., Chan, D., and Cheah, K.S. (2010). The developmental roles of the extracellular matrix: beyond structure to regulation. Cell and tissue research *339*, 93-110.

238. Tsukazaki, T., Chiang, T.A., Davison, A.F., Attisano, L., and Wrana, J.L. (1998). SARA, a FYVE domain protein that recruits Smad2 to the TGFbeta receptor. Cell *95*, 779-791.

239. Turley, R.S., Finger, E.C., Hempel, N., How, T., Fields, T.A., and Blobe, G.C. (2007). The type III transforming growth factor-beta receptor as a novel tumor suppressor gene in prostate cancer. Cancer research *67*, 1090-1098.

240. Uda, M., Ottolenghi, C., Crisponi, L., Garcia, J.E., Deiana, M., Kimber, W., Forabosco, A., Cao, A., Schlessinger, D., and Pilia, G. (2004). Foxl2 disruption causes mouse ovarian failure by pervasive blockage of follicle development. Human molecular genetics *13*, 1171-1181.

241. Uhl, M., Aulwurm, S., Wischhusen, J., Weiler, M., Ma, J.Y., Almirez, R., Mangadu, R., Liu, Y.W., Platten, M., Herrlinger, U.*, et al.* (2004). SD-208, a novel transforming growth factor beta receptor I kinase inhibitor, inhibits growth and invasiveness and enhances immunogenicity of murine and human glioma cells in vitro and in vivo. Cancer research *64*, 7954-7961.

242. Uhlenhaut, N.H., and Treier, M. (2011). Forkhead transcription factors in ovarian function. Reproduction *142*, 489-495.
243. Unsold, C., Hyytiainen, M., Bruckner-Tuderman, L., and Keski-Oja, J. (2001). Latent TGF-beta binding protein LTBP-1 contains three potential extracellular matrix interacting domains. Journal of cell science *114*, 187-197.
244. Vitt, U.A., McGee, E.A., Hayashi, M., and Hsueh, A.J. (2000). In vivo treatment with GDF-9 stimulates primordial and primary follicle progression and theca cell marker CYP17 in ovaries of immature rats. Endocrinology *141*, 3814-3820.
245. Vo Nguyen, T.T., Watanabe, Y., Shiba, A., Noguchi, M., Itoh, S., and Kato, M. (2014). TMEPAI/PMEPA1 enhances tumorigenic activities in lung cancer cells. Cancer Sci *105*, 334-341.
246. Wang, J., and Roy, S.K. (2004). Growth differentiation factor-9 and stem cell factor promote primordial follicle formation in the hamster: modulation by follicle-stimulating hormone. Biol Reprod *70*, 577-585.
247. Wang, S., Yang, S., Lai, Z., Ding, T., Shen, W., Shi, L., Jiang, J., Ma, L., Tian, Y., Du, X.*, et al.* (2013). Effects of culture and transplantation on follicle activation and early follicular growth in neonatal mouse ovaries. Cell and tissue research *354*, 609-621.
248. Wang, Y., and Ge, W. (2003). Spatial expression patterns of activin and its signaling system in the zebrafish ovarian follicle: evidence for paracrine action of activin on the oocytes. Biol Reprod *69*, 1998-2006.
249. Wang, Z.P., Mu, X.Y., Guo, M., Wang, Y.J., Teng, Z., Mao, G.P., Niu, W.B., Feng, L.Z., Zhao, L.H., and Xia, G.L. (2014). Transforming growth factor-beta signaling participates in the maintenance of the primordial follicle pool in the mouse ovary. J Biol Chem *289*, 8299-8311.
250. Watanabe, Y., Itoh, S., Goto, T., Ohnishi, E., Inamitsu, M., Itoh, F., Satoh, K., Wiercinska, E., Yang, W., Shi, L.*, et al.* (2010). TMEPAI, a transmembrane TGF-beta-inducible protein, sequesters Smad proteins from active participation in TGF-beta signaling. Mol Cell *37*, 123-134.
251. Weenen, C., Laven, J.S., Von Bergh, A.R., Cranfield, M., Groome, N.P., Visser, J.A., Kramer, P., Fauser, B.C., and Themmen, A.P. (2004). Anti-Mullerian hormone expression pattern in the human ovary: potential implications for initial and cyclic follicle recruitment. Molecular human reproduction *10*, 77-83.

252. Wen, J., Xie, J., Liu, S., and Gui, J. (2001). Differential expression and characterization analysis of a new gene with WD domains in fish oogenesis. Science in China Series C, Life sciences / Chinese Academy of Sciences *44*, 541-553.
253. White, Y.A., Woods, D.C., Takai, Y., Ishihara, O., Seki, H., and Tilly, J.L. (2012). Oocyte formation by mitotically active germ cells purified from ovaries of reproductive-age women. Nature medicine *18*, 413-421.
254. Wicks, S.J., Lui, S., Abdel-Wahab, N., Mason, R.M., and Chantry, A. (2000). Inactivation of smad-transforming growth factor beta signaling by Ca(2+)-calmodulin-dependent protein kinase II. Mol Cell Biol *20*, 8103-8111.
255. Wilkes, M.C., Mitchell, H., Penheiter, S.G., Dore, J.J., Suzuki, K., Edens, M., Sharma, D.K., Pagano, R.E., and Leof, E.B. (2005). Transforming growth factor-beta activation of phosphatidylinositol 3-kinase is independent of Smad2 and Smad3 and regulates fibroblast responses via p21-activated kinase-2. Cancer research *65*, 10431-10440.
256. Wrighton, K.H., Lin, X., and Feng, X.H. (2009). Phospho-control of TGF-beta superfamily signaling. Cell Res *19*, 8-20.
257. Wu, G., Chen, Y.G., Ozdamar, B., Gyuricza, C.A., Chong, P.A., Wrana, J.L., Massague, J., and Shi, Y. (2000). Structural basis of Smad2 recognition by the Smad anchor for receptor activation. Science *287*, 92-97.
258. Xie, C.Y., Kong, J.R., Zhao, C.S., Xiao, Y.C., Peng, T., Liu, Y., and Wang, W.N. (2016). Molecular characterization and function of a PTEN gene from Litopenaeus vannamei after Vibrio alginolyticus challenge. Developmental and comparative immunology *59*, 77-88.
259. Xu, J., Oakley, J., and McGee, E.A. (2002a). Stage-specific expression of Smad2 and Smad3 during folliculogenesis. Biol Reprod *66*, 1571-1578.
260. Xu, L., Kang, Y., Col, S., and Massague, J. (2002b). Smad2 nucleocytoplasmic shuttling by nucleoporins CAN/Nup214 and Nup153 feeds TGFbeta signaling complexes in the cytoplasm and nucleus. Mol Cell *10*, 271-282.
261. Xu, L., Yao, X., Chen, X., Lu, P., Zhang, B., and Ip, Y.T. (2007). Msk is required for nuclear import of TGF-{beta}/BMP-activated Smads. J Cell Biol *178*, 981-994.
262. Xu, L.L., Shanmugam, N., Segawa, T., Sesterhenn, I.A., McLeod, D.G., Moul, J.W., and Srivastava, S. (2000). A novel androgen-regulated gene, PMEPA1, located on chromosome 20q13 exhibits high level expression in prostate. Genomics *66*, 257-263.
263. Xu, L.L., Shi, Y., Petrovics, G., Sun, C., Makarem, M., Zhang, W., Sesterhenn, I.A., McLeod, D.G., Sun, L., Moul, J.W.*, et al.* (2003). PMEPA1, an androgen-regulated

NEDD4-binding protein, exhibits cell growth inhibitory function and decreased expression during prostate cancer progression. Cancer research *63*, 4299-4304.

264. Xu, W.W., Kong, X.B., An, L.G., and Zhang, C. (2009). Relationship between SnoN expression and mouse follicular development, atresia, and luteinization. Zoological science *26*, 66-73.
265. Yamaguchi, T., Kurisaki, A., Yamakawa, N., Minakuchi, K., and Sugino, H. (2006). FKBP12 functions as an adaptor of the Smad7-Smurf1 complex on activin type I receptor. J Mol Endocrinol *36*, 569-579.
266. Yamamoto, S., Konishi, I., Nanbu, K., Komatsu, T., Mandai, M., Kuroda, H., Matsushita, K., and Mori, T. (1997). Immunohistochemical localization of basic fibroblast growth factor (bFGF) during folliculogenesis in the human ovary. Gynecological endocrinology : the official journal of the International Society of Gynecological Endocrinology *11*, 223-230.
267. Yan, C., Wang, P., DeMayo, J., DeMayo, F.J., Elvin, J.A., Carino, C., Prasad, S.V., Skinner, S.S., Dunbar, B.S., Dube, J.L.*, et al.* (2001). Synergistic roles of bone morphogenetic protein 15 and growth differentiation factor 9 in ovarian function. Mol Endocrinol *15*, 854-866.
268. Yan, X., and Chen, Y.G. (2011). Smad7: not only a regulator, but also a cross-talk mediator of TGF-beta signalling. Biochem J *434*, 1-10.
269. Yang, F., Chung, A.C., Huang, X.R., and Lan, H.Y. (2009). Angiotensin II induces connective tissue growth factor and collagen I expression via transforming growth factor-beta-dependent and -independent Smad pathways: the role of Smad3. Hypertension *54*, 877-884.
270. Yao, X., Chen, X., Cottonham, C., and Xu, L. (2008). Preferential utilization of Imp7/8 in nuclear import of Smads. J Biol Chem *283*, 22867-22874.
271. Yin, W., Smiley, E., Germiller, J., Mecham, R.P., Florer, J.B., Wenstrup, R.J., and Bonadio, J. (1995). Isolation of a novel latent transforming growth factor-beta binding protein gene (LTBP-3). J Biol Chem *270*, 10147-10160.
272. Yu, Q., and Stamenkovic, I. (2000). Cell surface-localized matrix metalloproteinase-9 proteolytically activates TGF-beta and promotes tumor invasion and angiogenesis. Genes Dev *14*, 163-176.
273. Zacchigna, L., Vecchione, C., Notte, A., Cordenonsi, M., Dupont, S., Maretto, S., Cifelli, G., Ferrari, A., Maffei, A., Fabbro, C.*, et al.* (2006). Emilin1 links TGF-beta maturation to blood pressure homeostasis. Cell *124*, 929-942.

274. Zhang, H., Adhikari, D., Zheng, W., and Liu, K. (2013). Combating ovarian aging depends on the use of existing ovarian follicles, not on putative oogonial stem cells. Reproduction *146*, R229-233.
275. Zhang, S., Fei, T., Zhang, L., Zhang, R., Chen, F., Ning, Y., Han, Y., Feng, X.H., Meng, A., and Chen, Y.G. (2007). Smad7 antagonizes transforming growth factor beta signaling in the nucleus by interfering with functional Smad-DNA complex formation. Mol Cell Biol *27*, 4488-4499.
276. Zhang, Y., Chang, C., Gehling, D.J., Hemmati-Brivanlou, A., and Derynck, R. (2001). Regulation of Smad degradation and activity by Smurf2, an E3 ubiquitin ligase. Proc Natl Acad Sci U S A *98*, 974-979.
277. Zhang, Y.E. (2009). Non-Smad pathways in TGF-beta signaling. Cell Res *19*, 128-139.
278. Zhao, J., Taverne, M.A., van der Weijden, G.C., Bevers, M.M., and van den Hurk, R. (2001). Effect of activin A on in vitro development of rat preantral follicles and localization of activin A and activin receptor II. Biol Reprod *65*, 967-977.
279. Zheng, W., Nagaraju, G., Liu, Z., and Liu, K. (2012). Functional roles of the phosphatidylinositol 3-kinases (PI3Ks) signaling in the mammalian ovary. Mol Cell Endocrinol *356*, 24-30.
280. Zheng, W., Zhang, H., Gorre, N., Risal, S., Shen, Y., and Liu, K. (2014). Two classes of ovarian primordial follicles exhibit distinct developmental dynamics and physiological functions. Human molecular genetics *23*, 920-928.
281. Zhu, J., Lin, S.J., Zou, C., Makanji, Y., Jardetzky, T.S., and Woodruff, T.K. (2012). Inhibin alpha-subunit N terminus interacts with activin type IB receptor to disrupt activin signaling. J Biol Chem *287*, 8060-8070.
282. Zhu, Y., Richardson, J.A., Parada, L.F., and Graff, J.M. (1998). Smad3 mutant mice develop metastatic colorectal cancer. Cell *94*, 703-714.
283. Zou, K., Yuan, Z., Yang, Z., Luo, H., Sun, K., Zhou, L., Xiang, J., Shi, L., Yu, Q., Zhang, Y*., et al.* (2009). Production of offspring from a germline stem cell line derived from neonatal ovaries. Nature cell biology *11*, 631-636.

Appendices

I. TGFβ signalling through Smad pathway

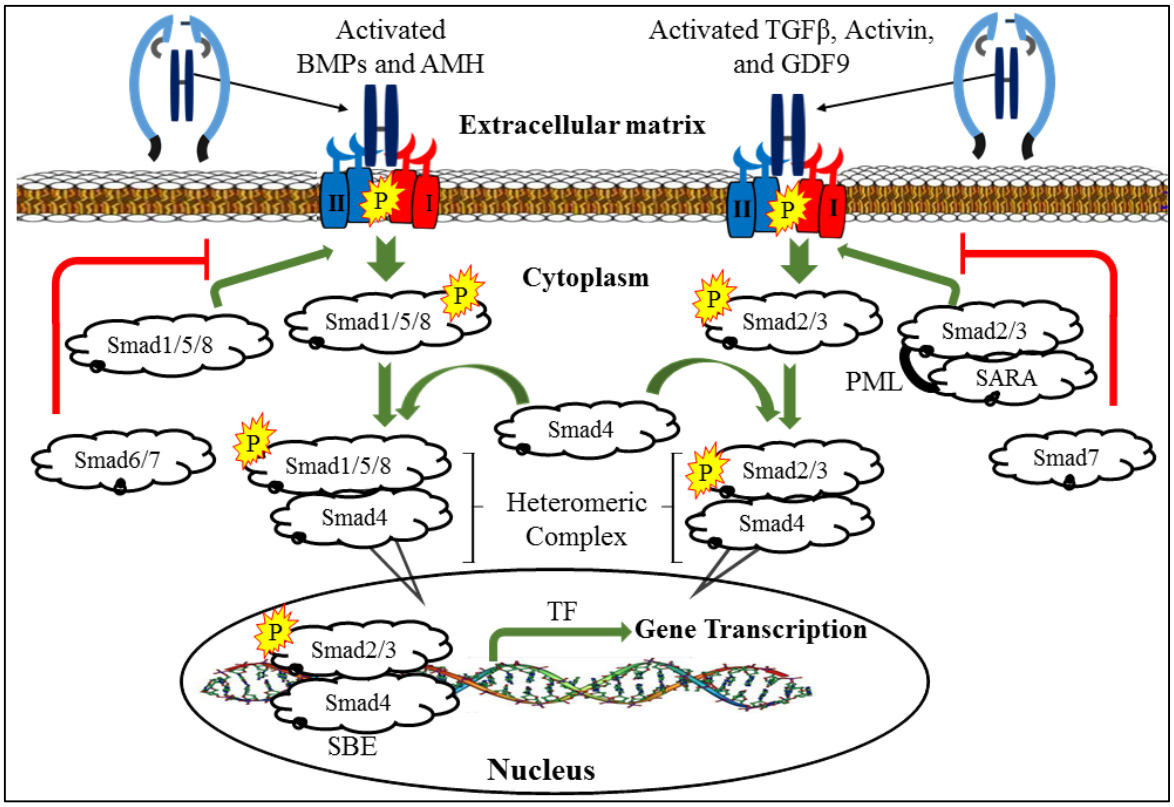

I.1. At the cell surface, TGFβ ligand stimulates type II receptor, which in turns stimulates type I receptors by phosphorylation. In Smad2/3 pathway, but not Smad1/5/8 pathway, the phosphorylated Type I receptor recruits R-Smad which directing by SARA protein to the activated receptor, where the association between Smad2/3 and SARA is enhanced by a TGFβ induced cytoplasmic protein (PML). Then, heteromeric complex forms via the interaction of R-Smad with Smad4. Through nuclear import, this complex interact to the Smad-binding elements (SBE) of the targeting gene. The regulation of gene transcription occurs by interaction with transcriptional co-activators or co-repressors. TGFβ/Smad2/3 signalling is terminating by Smad7, while Smad1/5/8 pathway can antagonise by both Smad6 and Smad7.

II. Equipment

Equipment	Company
96-well plate	Nunclon
acupuncture needles	AcuMedic
Centrifuge- accuspin 3R	Fisher Scientific
Agilent 2100 Bioanalyser	Agilent G2938B
Culture plates of 24-wells	Corning Costar- Sigma-Aldrich
Edge pen	Vector Laboratories
Electrophoresis (Power Pac™ HC)	Bio Rad- Singapore
Flow hood with a dissecting microscope	Leica
inverted Widefield fluorescence microscope Leica DMI4000B	Leica
Leica inverted SP5 confocal laser scanning microscope	Leica Microsystems, Wetzlar, Germany
Manual processing microtome	Reichert-Jung
Olympus CKX41 with a Nikon camera DS-Fi1	Olympus
Olympus IX73 inverted microscope	Olympus
Superfrost Plus Microscope Slides	Thermo scientific
Stage micrometre Graticules	PYSER-SGI
Thermal cycler	Geneflow
Ultraviolet transilluminator	Geneflow

III. Chemicals and reagents

Chemical agents	Company
10X TAE Buffer	Gibco
2X SensiFAST SYBR Hi ROX Mix	Bioline
384- well plate	Applied Biosystems Inc
Agarose gel	Bioline/ Bioproducts, AGD1
Applied Biosystems 7900HT Fast instrument	Applied Biosystems Inc
Aqueous eosin 1%	Diagnostics
Bovine serum albumen	Vector Laboratories
CAS-Block	Invitrogen
Citrate Buffer	Sigma- Aldrich
DNase I	Qiagen; West Sussex, UK
DPX (Xylene, Dibutylphtalate)	Merck
Ethanol	Fisher Scientific, UK
Fetal bovine serum FBS	ThermoFisher
GelRed ^{TM} Nucleic Acid Gel Stain	Biotium
Hematoxylin gills II stain	Surgipath
Histochoice Clearing agent	Sigma- Aldrich
Hyper Ladder	Bioline
Insulin-Transferrin-Selenium (ITS)	Sigma
KAPA SYBR Green	KAPA Biosystems, KK4602
Leibovitz's L-15 medium 1x Gibco	Life Technologies
Leibovitz's media L15	Gibco
L-Glutathione reduced 99%	Sigma- Aldrich

Low gelling temperature agarose	Sigma
MyTag^{TM} Red Mix	Bioline
Neutral Buffered Formalin Solution 10x	Sigma- Aldrich
Non-immune mouse IgG or Rabbit IgG	Vector
Nuclear fast red stain	Sigma
Optical adhesive cover	Applied Biosystems Inc
Penicillin	Sigma PENK
Prolong Gold antifade reagent with Dapi	Invitrogen
Qiagen RNeasy Micro Kits	QIAGEN, Crawley, UK
RNase/DNase free water (10ml)	Qiagen
ROX dye	KAPA Biosystems
Sodium phosphate dibasic	Sigma- Aldrich
Sodium phosphate monobasic	Sigma- Aldrich
Streptomycin sulphate	Sigma
Superscript III First strand synthesis system	Invitrogen
Tris (Hydroxymethyle) aminomethane (mw 121.14)	BDH Prolabo
Triton	Sigma
Vectashield ABC Kit PK- 6100	Vector Laboratories
β- Mercaptoethanol 98%	Sigma- Aldrich

IV. Buffer and solution recipes

Buffer\ Solution	Preparation and composition
100ml of 1X TAE buffer,	10ml of 10X TAE was added to 90ml of dH2O
2% agarose gel solution	Two grams of agarose powder added to 100ml TAE 1X
70% ethanol 80% ethanol 95% ethanol	30 ml of ddH2O added to 70 ml of ethanol (96–100%). 20 ml of ddH2O added to 80ml of ethanol (96–100%). 5 ml of ddH2O added to 95 ml of ethanol (96–100%).
Bovine serum albumin BSA 4%	0.2 grams of BSA powder in 5 ml PBS
Citrate Buffer (0.01M Citric Acid	Citric acid (anhydrous) ------- 1.92 g Distilled water ---------- 1000 ml Mixed to dissolve, and pH was adjusted to 6.0.
DNase I stock solution	Lyophilized DNase I dissolved in 550µl of RNase/ DNase free water, stored at –20°C.
L-Glutathione –Tris solution	Tris 50mM (0.605g) dissolved in 70ml of H2O, pH was adjusted to 8.0 by concentrated HCL before the addition of glutathione 10mM (0.307g), and a final volume of 10 ml was completed by water.
Phosphate Buffered Saline (0.1 M)	Sodium phosphate dibasic Na2HPO4…….. 10.9 g Sodium phosphate monobasic NaH2PO4….. 3.2 g NaCl ……... 90 g Mixed to dissolve and brought to a final volume of 1000 ml with distilled water. Adjusted to pH 7.4. Stored at room temperature, for working solution, diluted at 1:10.
Working solution of DNase I	10µl DNase I stock solution added to 70µl buffer RDD to make a final volume of 80µl per a sample, stored at -20°C.
working solution of poly A RNA (4ng/µl)	5 µl of poly A RNA stock solution (310ng /ml) added to 34µl RLT buffer. Then, 12µl of the previous solution added to 108µl buffer RLT.
Working solution of RPE buffer	44ml of ethanol (96–100%) added to RPE Buffer volume (11 ml).
β- Mercaptoethanol (β-ME) - RLT buffer	10µl β-ME added to 1ml RLT buffer

V. Immunofluorescence staining and troubleshooting

1. Antibodies used in this study were selected from supplier's web sites stated that the desired antibody is suitable for immunohistochemistry staining. In addition, most of these suppliers provided publications in which antibodies have been used and/or images of staining were included. This provided essential detail on the concentration used, specific localisation of their target proteins within the tissue or cell compartments.
2. To ensure consistency for all staining, solutions including Histochoice and ethanol were periodically refreshed.
3. Other antigen retrieval buffer was used such as Tris (MW 121.14 BDH PROLABO) and urea (BDH ANALAR 5%). Tris-urea buffer was prepared as following:

- 800 ml H2O
- 12.11 grams Tris.
- 50 grams urea.
- Adjust PH to 10.0.
- Add 200 ml of H2O to prepare 1liter

4. Alternative blocking approach was used such as bovine serum albumin block (BSA 4% in PBS) for 20 minutes rather than CAS block for 10 minutes.
5. To optimise dilutions used for primary antibodies where optimum dilutions were not included in their data sheath, a wide range of serial dilution were used (1:100, 1:200, 1:400, 1:800, 1:1600).
6. Slides stained with primary antibodies were differentially incubated either at room temperature for 1hours or overnight at 4°C.
7. To ensure consistency of staining, freshly embedded and sectioned ovary sections (d4, d8, d16 and adults) were used.
8. Ovary sections from mice of other ages including d21 and d26 were used as controls.
9. In addition to use a positive control of a well-known working antibody (Ddx4), sections of heart, kidney and uterus tissues (where Ppm1a is highly expressed) were used along with ovary sections stained for Ppm1a.
10. For colocalisation of two antibodies (double staining), two protocols were tested to determine whether primary antibodies to be added individually or together:

    - Ovary sections were incubated overnight at 4°C with the first primary antibody, while the second primary antibody was added next day for 1hour at room temperature and

vice versa. At the end of incubation, secondary antibodies were added either individually or both together for 45 minutes.

- Both primary antibodies were added together on the section followed by incubation with secondary antibodies for both primary antibodies.

11. To troubleshoot an extensive unspecific background staining of primary/secondary antibodies:
    - Slides were incubated with CAS for a longer period (20 minutes).
    - Prolong time of washing with PBS to 15 minutes x3.
    - Washing with 0.5% Tween solution of with PBS.
    - Less concentrated solutions of primary antibodies were used.
    - Reduce the incubation time of secondary antibodies to 30 minutes.
12. For each particular experiment, to eliminate technical errors, stained sections and controls (positive and negative) were imaged using same exposure and gain.
13. Before being used for staining, paraffin embedded ovary sections were visualised with fluorescent microscope using all channels to ensure that no auto-fluorescence background signal are produced.

VI. Immunofluorescent localisation of Smad2/3 and Smad1/5/8 in the preantral follicle

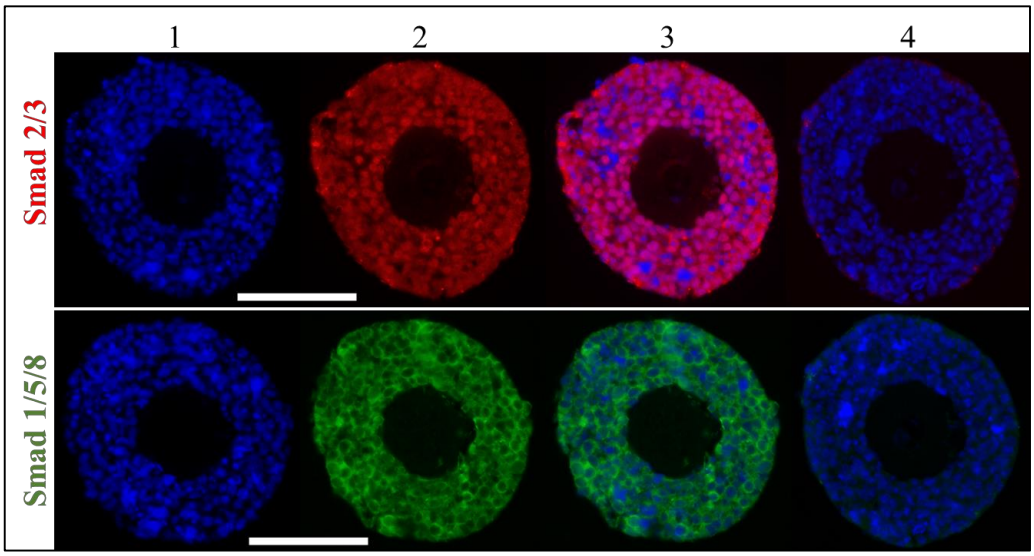

VI.1. Preantral follicle sections used to assess immunofluorescent staining protocol. Smad2/3 (2-3, red; 0.25µg/ml, Santa Cruz sc-133098) was lightly localised in the granulosa cells; while, Smad1/5/8 (2-3, green; 0.5µg/ml, Santa Cruz sc-6031-R) were detected with high intensity of staining in granulosa cells. Negative controls were treated with non-immune mouse IgG (4, above row) or Rabbit IgG (4, down row). Slides were incubated with Alexa Donkey anti-Mouse 555 or Donkey anti-Rabbit 588 antibodies, respectively. Nuclei (blue) were contrastained with DAPI (1). Images were taken with Olympus IX73 inverted microscope. Scale bar = 100µm.

VII. Protocol used for oocyte measurement in ovary section

ImageJ was used for calculation of oocyte diameters in ovary sections stained by haematoxylin and Eosin stain. Ovary sections from d4 (n=5), d8 (n=8), d13 (n=5), d16 (n=7) were used to provide a model for oocytes classification to be utilised for evaluation the effect of different treatment on follicle development. The morphology represented by a number of granulosa cells layers surrounding the oocyte was to identify the growing state of follicles. A single oocyte that surrounded by a monolayer of undeveloped flat cells was considered non-growing follicle. Follicles containing one layer of granulosa cells that included both cuboidal and flat cells accounted as a transitional oocyte. Large oocyte with at least one complete layer of cuboidal granulosa cells classified as growing oocyte. Only clearly presented oocytes were included in measurements.

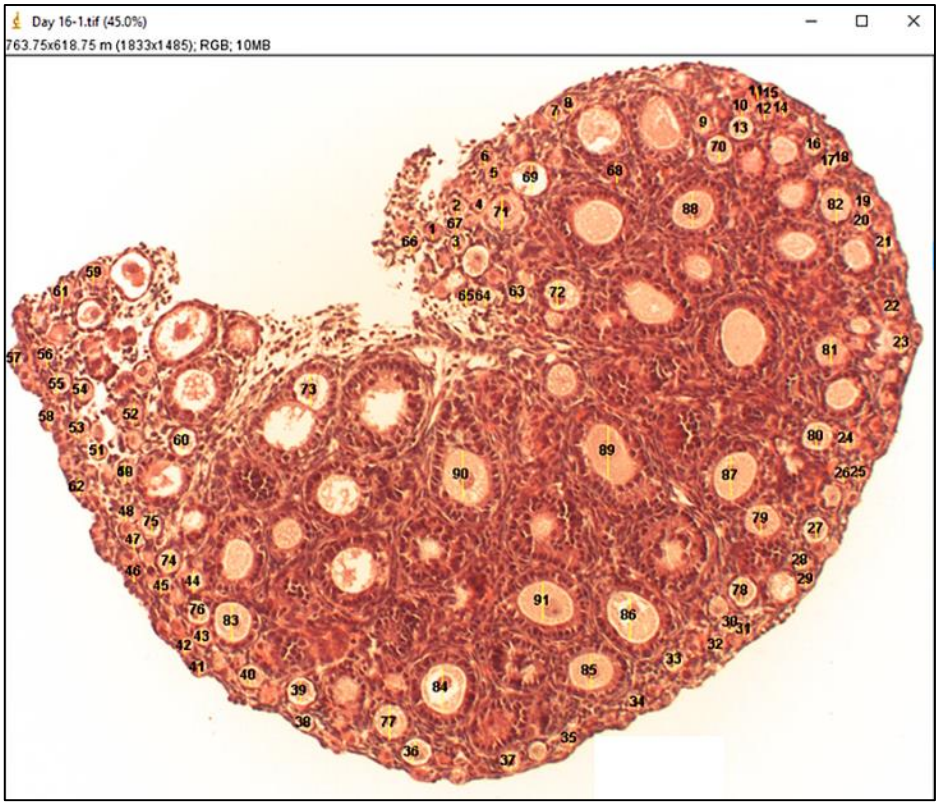

VII.1. An example of oocyte measurement in a day 16 ovary section stained by haematoxylin and eosin stain.

VIII. Isolated oocyte and follicle samples used for RNA extraction

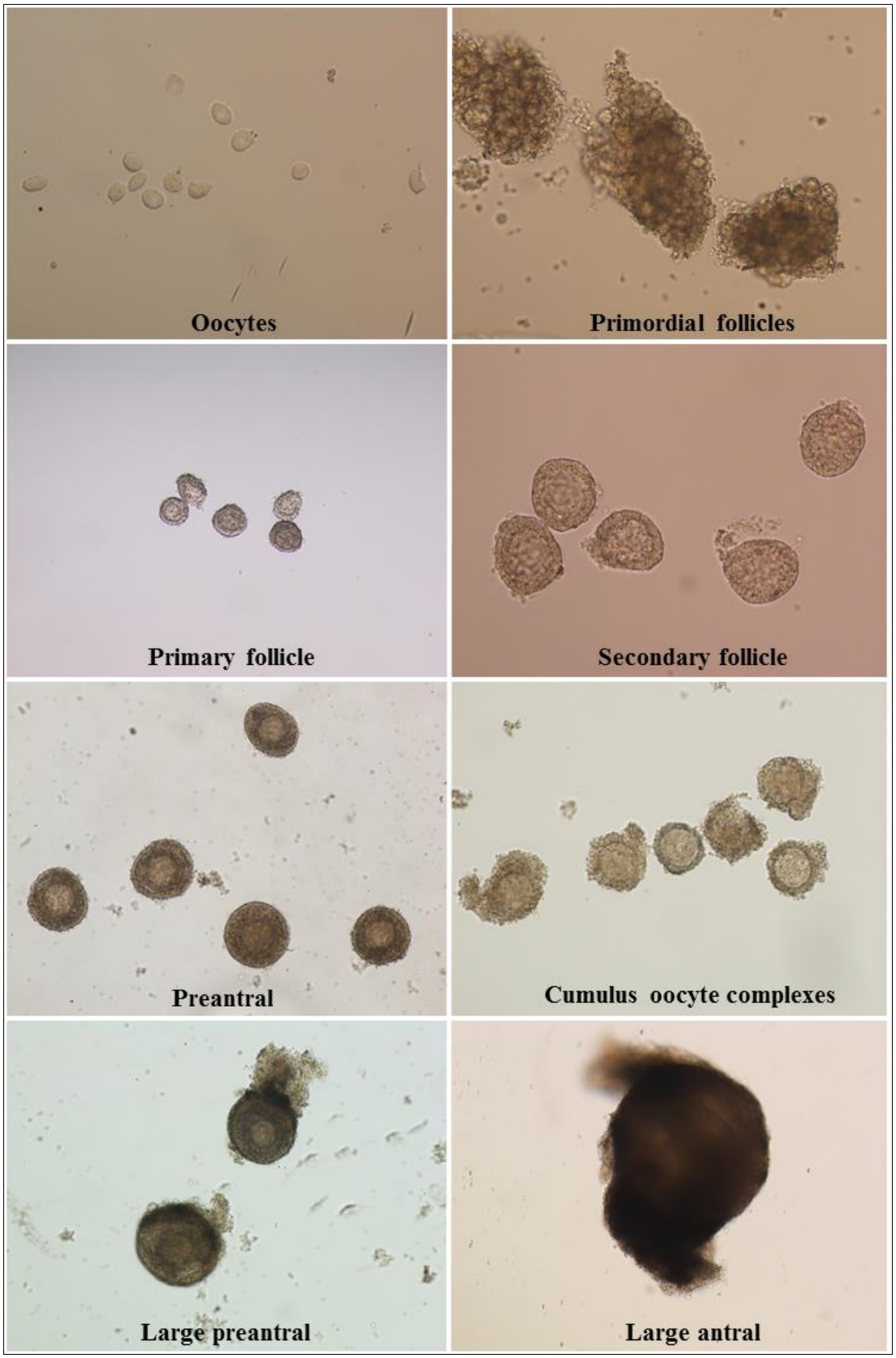

IX. Illustrate RT-PCR results for the expression of control genes in various follicles stages. Symbol: - not expressed; + weak band; ++ moderate band; and +++ strong band.

Genes	Primordial	Primary	Secondary	Pre-antral	Large pre-antral	Large antral	COCX	Oocytes	- ve control
Gabpdh	+	++	++	+++	+++	+++	++	+	-
Amh	+	+++	+++	+++	+	-	+	-	-
Amhr2	+	++	++	++	+	-	-	-	-
Gdf9	++	+++	+++	+++	-	-	++	+++	-
Fshr	-	++	++	++	++	-	++	-	-
Cyp17a	-	-	-	++	+++	++	-	-	-
Kl1	-	++	++	++	++	++	-	-	-
Kl2	-	++	++	+++	++	++	-	-	-

X. Illustrate RT-PCR results for the expression of Smad inhibitors in various follicles stages. Symbol - not expressed; + weak band; ++ moderate band; and +++ strong band.

Genes	Primordial	Primary	Secondary	Pre-antral	Large pre-antral	Large antral	COCX	Oocytes	- ve control
Gapdh	+	+	+	++	++	++	+	+	-
Strap	+	+	++	++	++	+++	++	+++	-
Ppm1a	+	+	++	++	++	++	+	+	-
Ski	-	+	+	++	++	++	+	-	-
SnoN	-	+	+	+	+	+	-	-	-
Ranbp3	-	+	+	+	+	+	-	+	-
Exportin4	-	-	+	+	+	+	-	+	-
Smad7	-	-	++	++	++	+	+	+	-
Smurf1	-	-	-	+	+	+	+	-	-
Smurf2	-	-	+	+	+	+	-	-	-

XI. Optimising culture media for *Strap* siRNA treatment

The aim of this experiment was to determine whether to use the Accell delivery media for the experiment of *Strap* siRNA with or without supplements. Preantral follicles were isolated from d16 mouse ovaries, as described in 2.2.2. The experiment was designed to include three treatment groups, where each group included 21 preantral follicles. For each 96 wells plate (n=3) three lines of treatments were prepared (each line included 7 follicles). Follicles in the first group were cultured in 100µl MEM-α (Gibco) with supplements, the second and third groups included Accell media with or without supplements, respectively, Figure XI-1.

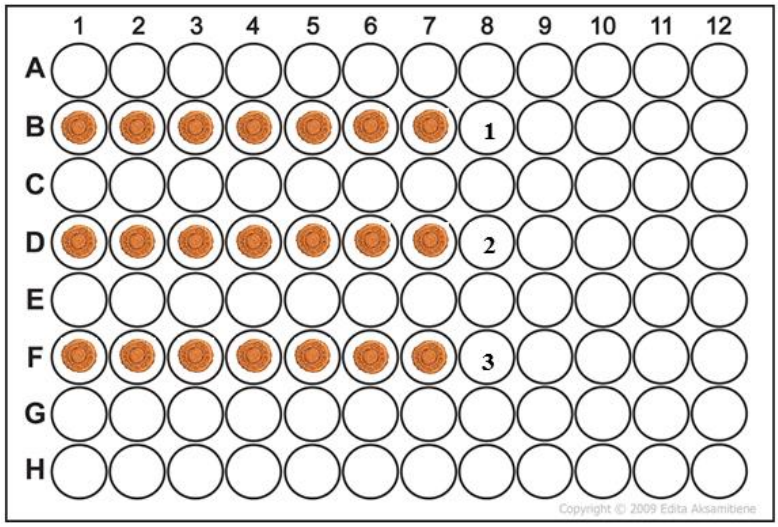

Figure XI.1. An example of 96 wells plates for culture optimisation. Three plates were prepared to identify the effect of adding growth supplements to Accell delivery media on follicle growth. Follicles were cultured in three rows where each row consists of seven follicles (a single follicle in each well). Treatment groups included MEM-α medium with supplements (1), accell delivery with and without supplements (2, 3 respectively). Plates were incubated for three days at 37°C in the presence of 5% CO_2.

The supplement consists of 0.1% (w/v) BSA (Sigma), 75µg/ml penicillin (Sigma), 100µg/ml streptomycin sulphate (Sigma) and insulin-transferrin-sodium selenite ITS (5µg/ml, 5µg/ml, 5ng/ml, respectively; Sigma). All plates were cultured at 37°C in the presence of 5% CO_2. Half of the culture medium was replaced after 48 hours of incubation. Follicles were regularly imaged at time points of 0, 24, 48 and 72 hours using light microscopy (Olympus CKX41 with a Nikon camera DS-Fi1). Images were obtained for the measurement of follicle diameter by ImageJ software. Two measurements were taken from the basal lamina of the follicle, excluding theca cells layer. The two measurements were averaged and were presented as mean follicle diameter, see 2.10.1.

After 72h in culture, even though the mean follicles in Accell delivery with supplements group was greater than other groups, there was no significant difference in follicle size between groups (Figure XI-2). Thus, a decision was made that growth supplements to be added to the Accell delivery for *Strap* siRNA experiment.

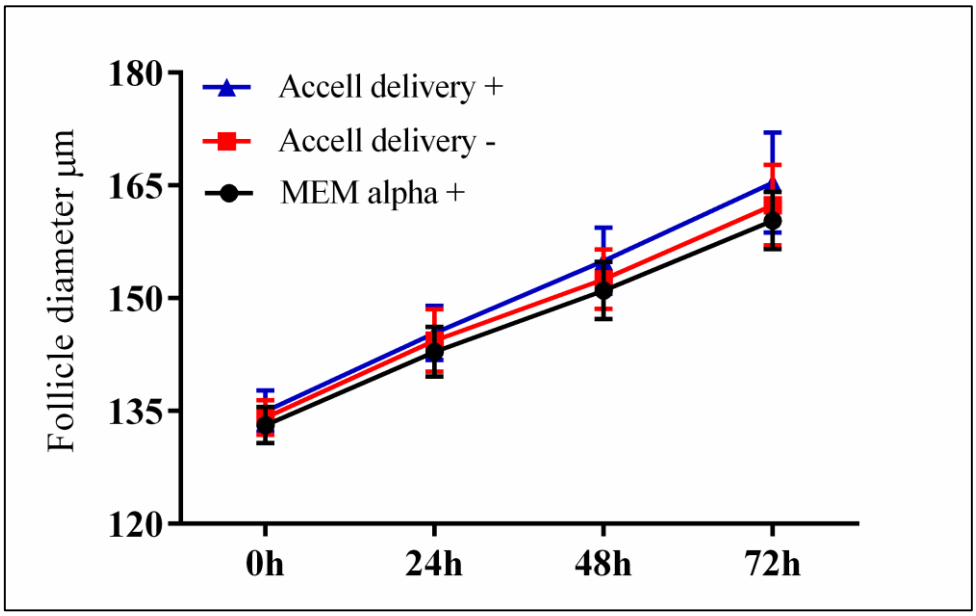

Figure XI-2. Effect of different culture media on preantral follicle growth. The aim of this experiment was to optimise Accell delivery media to be used for *Strap* knockdown either with or without supplements at different time points. Even though follicle diameter revealed no significant difference in follicle growth between groups. The mean diameter of follicles cultured in Accell delivery media with supplements was greater (165.3µm) than those cultured in Accell delivery without supplements (162.3µm) or in MEM-α medium with supplements (160.3µm). Follicle diameters were presented as mean ± SEM (n=21 follicles for each group), data were statistically analysed using Kruskal-Wallis and Dunn's multiple comparisons test $P<0.05$.

XII. Agilent Bioanalyser and expression of *Gdf9* in cultured preantral follicle samples by RT-PCR.

All of the tested RNA samples (5 samples for each group where each sample included 5 follicles) were considered as good quality and valid for further gene analysis. Treatment groups included C: control; G: Gdf9; SD: SD208 and S+G: a mixture of SD208 and Gdf9 groups.

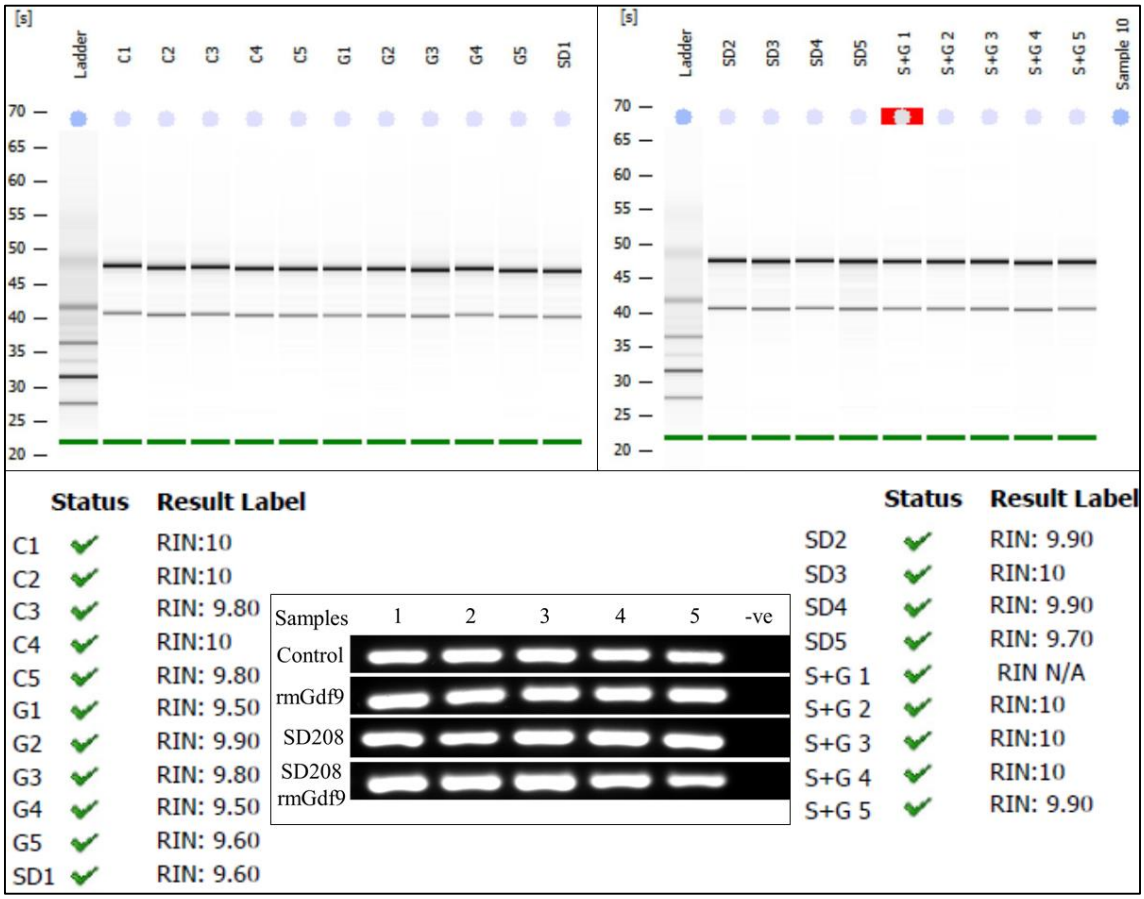

XII.1. Evaluation of extracted RNA using Agilent Bioanalyser and expression of *Gdf9* in cultured preantral follicle samples by RT-PCR.